32

Steel Design Guide

Design of Modular Steel-Plate Composite Walls for Safety-Related Nuclear Facilities

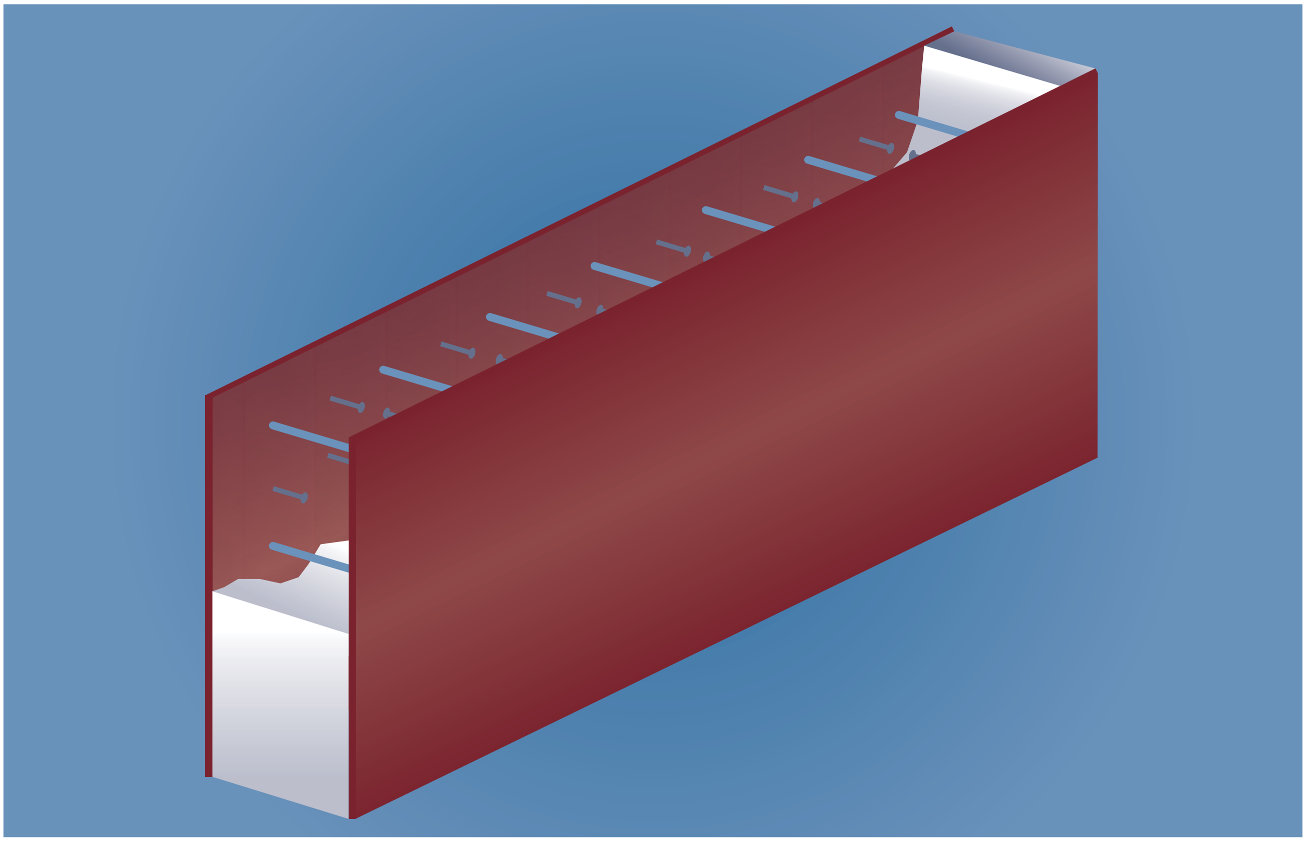

32

Steel Design Guide

Design of Modular Steel-Plate Composite Walls for Safety-Related Nuclear Facilities

Saahastaranshu R. Bhardwaj

Amit H. Varma

AMERICAN INSTITUTE OF STEEL CONSTRUCTION

© AISC 2017

by

American Institute of Steel Construction

All rights reserved. This book or any part thereof
must not be reproduced in any form without the
written permission of the publisher.
The AISC logo is a registered trademark of AISC.

The information presented in this publication has been prepared following recognized principles of design and construction. While it is believed to be accurate, this information should not be used or relied upon for any specific application without competent professional examination and verification of its accuracy, suitability and applicability by a licensed engineer or architect. The publication of this information is not a representation or warranty on the part of the American Institute of Steel Construction, its officers, agents, employees or committee members, or of any other person named herein, that this information is suitable for any general or particular use, or of freedom from infringement of any patent or patents. All representations or warranties, express or implied, other than as stated above, are specifically disclaimed. Anyone making use of the information presented in this publication assumes all liability arising from such use.

Caution must be exercised when relying upon standards and guidelines developed by other bodies and incorporated by reference herein since such material may be modified or amended from time to time subsequent to the printing of this edition. The American Institute of Steel Construction bears no responsibility for such material other than to refer to it and incorporate it by reference at the time of the initial publication of this edition.

Printed in the United States of America

Authors

Saahastaranshu R. Bhardwaj is a Ph.D. candidate in the Lyles School of Civil Engineering at Purdue University. Mr. Bhardwaj assisted Dr. Varma with the writing, editing and formatting of the steel-plate composite wall design provisions and commentary in Appendix N9 of ANSI/AISC N690. Mr. Bhardwaj and Dr. Varma collaborated with several industry practitioners to develop the design examples presented in this Guide.

Amit H. Varma, Ph.D, is a Professor in the Lyles School of Civil Engineering and a University Faculty Scholar at Purdue University. Dr. Varma served as the Vice Chair of AISC Task Committee 12, Nuclear Facilities Design, that developed the supplement to the AISC *Specification for Safety-Related Steel Structures for Nuclear Facilities,* ANSI/AISC N690 (AISC, 2015) for modular composite construction. He is currently a member of the AISC Committee on Specifications (COS), AISC Task Committee 5, Composite Design, and the Chair of the AISI/AISC Fire Committee. He served as the Chair of the SEI/ACI Committee of Composite Construction from 2010 to 2016.

Acknowledgments

This Design Guide would be incomplete and inadequate without valuable input from the following individuals. The authors would like to thank Dr. Sanjeev Malushte for his significant intellectual and engineering contributions to the completion of the Supplement to ANSI/AISC N690 and this Design Guide. The copyright images in the Design Guide are reprinted with the permission of Westinghouse Electric Company, LLC, and its contribution is appreciated. The authors are also grateful to the following reviewers of the document for their valuable comments.

Taha Alshawaf
Steve Ashton
Michel Bruneau
Shu-Jin Fang
Lou Geschwindner
Jay Harris
Chris Hewitt
Mark Holland
Ron Janowiak
Wonki Kim
Davis Parsons
Matthew Van Liew
Derek Winkler

Preface

This Guide is intended to facilitate the design of steel-plate composite (SC) walls for safety-related nuclear facilities and is to be used in conjunction with ANSI/AISC N690. The Guide discusses the behavior and design of SC walls subjected to various demands, including both individual and combined force demands. The detailing, analysis and design of SC walls and connections are based on the provisions in Appendix N9 of ANSI/AISC N690. The design of SC walls and connections is illustrated in a design example in Appendix A.

TABLE OF CONTENTS

CHAPTER 1 INTRODUCTION 1

1.1 BACKGROUND 1
1.2 ADVANTAGES OF SC WALLS 3
    1.2.1 Resilience and Sustainability Aspects of SC Construction 4
1.3 LIMITATIONS OF SC WALLS. 9
1.4 APPENDIX N9 TO ANSI/AISC N690 10

CHAPTER 2 SCOPE AND LAYOUT. 11

2.1 DESIGN EXAMPLE. 11

CHAPTER 3 MINIMUM REQUIREMENTS. 13

CHAPTER 4 FACEPLATE SLENDERNESS REQUIREMENT. 15

CHAPTER 5 STEEL ANCHOR DETAILING 17

5.1 CLASSIFICATION OF STEEL ANCHORS . . .17
5.2 SPACING OF STEEL ANCHORS 17
    5.2.1 Development Length 17
    5.2.2 Interfacial Shear 19

CHAPTER 6 TIE DETAILING. 21

6.1 CLASSIFICATION AND SPACING OF TIES 21
    6.1.1 Transfer Length 21
6.2 REQUIRED TENSILE STRENGTH OF TIES 23

CHAPTER 7 MODELING PARAMETERS FOR ANALYSIS 27

7.1 LOADS AND LOAD COMBINATIONS. 27
7.2 GEOMETRIC AND MATERIAL PROPERTIES FOR ANALYSIS 27
7.3 STIFFNESS VALUES FOR THE MODEL 28
    7.3.1 Effective Flexural Stiffness 28
    7.3.2 Effective In-Plane Shear Stiffness. 29
7.4 MODELING THE OPENINGS 31
    7.4.1 Design and Detailing Requirements Around Small Openings 31
    7.4.2 Design and Detailing Requirements Around Large Openings 32
    7.4.3 Bank of Small Openings. 33
7.5 ANALYSIS INVOLVING ACCIDENT THERMAL LOADS 33
7.6 INTERIOR AND CONNECTION REGIONS. 35
7.7 REQUIRED STRENGTH DETERMINATION 36

CHAPTER 8 INDIVIDUAL DESIGN AVAILABLE STRENGTHS. 37

8.1 UNIAXIAL TENSILE STRENGTH. 37
8.2 COMPRESSIVE STRENGTH 37
8.3 OUT-OF-PLANE FLEXURAL STRENGTH 38
8.4 IN-PLANE SHEAR STRENGTH 38
8.5 OUT-OF-PLANE SHEAR STRENGTH 39

CHAPTER 9 INTERACTION OF DESIGN AVAILABLE STRENGTHS 43

9.1 INTERACTION OF OUT-OF-PLANE SHEAR FORCES. 43
9.2 IN-PLANE FORCES AND OUT-OF-PLANE MOMENTS. 43

CHAPTER 10 DEMAND CAPACITY RATIOS AND INTERACTION SURFACES 49

CHAPTER 11 DESIGN OF SC WALL CONNECTION. 51

11.1 CONNECTION DEMAND TYPES 52
11.2 FORCE TRANSFER MECHANISM 52
11.3 CONNECTION DESIGN PHILOSOPHY AND REQUIRED STRENGTH 52
    11.3.1 Full-Strength Connection Design 52
    11.3.2 Overstrength Connection Design 54
    11.3.3 Connection Evaluation for Combined Forces 54
11.4 CONNECTION AVAILABLE STRENGTH. . . .54
    11.4.1 Connector Available Strength 54
11.5 SC WALL-TO-BASEMAT ANCHORAGE CONNECTION 55
    11.5.1 Single Base Plate Connection 55
    11.5.2 Split Base Plate Connection 58
    11.5.3 Rebar SC Wall-to-Basemat Connection 58
11.6 SC WALL-TO-WALL JOINT CONNECTION 60
11.7 RC SLAB-TO-SC WALL JOINT CONNECTION 61

CHAPTER 12 IMPACTIVE AND IMPULSIVE LOADS 69

CHAPTER 13 FABRICATION, ERECTION AND CONSTRUCTION REQUIREMENTS 73

13.1 DIMENSIONAL TOLERANCES FOR FABRICATION 73

CHAPTER 14 QUALITY ASSURANCE AND QUALITY CONTROL REQUIREMENTS . . 77

APPENDIX A: DESIGN EXAMPLE. 79

SYMBOLS 129

ACRONYMS AND ABBREVIATIONS. 135

REFERENCES. 137

Chapter 1
Introduction

Nuclear structures involve heavy concrete construction to provide adequate radiation shielding and resistance to severe and extreme loads. This results in longer construction durations and large field labor requirements. Generic modular construction, especially modular steel-plate composite (SC) construction, can minimize schedule and labor requirements. In SC construction, concrete walls are reinforced with two steel faceplates attached to concrete using steel anchors, such as steel headed stud anchors, and connected to each other using steel tie bars. Figure 1-1 illustrates a typical SC wall section. Steel anchors ensure composite behavior of faceplates and concrete. Ties provide structural integrity, prevent delamination of the plain concrete core, and serve as shear reinforcement. The SC walls may have sleeves for penetrations and embed plates for commodity attachments.

The behavior of SC walls under axial tension and compression (Zhang et al., 2014), out-of-plane flexure (Sener et al., 2015b), and out-of-plane shear (Sener and Varma, 2014; Sener et al., 2016) is similar to that of reinforced concrete (RC) walls. However, behavior of SC walls under in-plane shear (Seo et al., 2016; Varma et al., 2011e; Ozaki et al., 2004), combined in-plane forces, and out-of-plane moments (Varma et al., 2014) can be significantly different from that of RC walls. Additionally, specific limit states such as faceplate local buckling (Zhang et al., 2014), interfacial shear failure (Sener and Varma, 2014; Sener et al., 2016) between the faceplates and concrete infill, and section delamination through the concrete infill (Bhardwaj et al., 2017) need to be adequately considered in the design of SC walls. These limit states are discussed in Chapters 3 through 6, along with section detailing provisions to prevent them from limiting the design.

1.1 BACKGROUND

The initial application of SC walls was in non-nuclear commercial projects to resist extreme events in large concrete structures. SC walls were expected to provide better resistance to extreme blast and earthquake events. Other non-nuclear applications of SC walls included submerged tube tunnels (Narayanan et al., 1987), offshore oil rigs (Adams and Zimmerman, 1987), and ship building (Dai and Liew, 2006). The need for construction schedule reduction and better constructability and performance aspects of SC walls in comparison to RC walls led to the consideration of their use in safety-related nuclear facilities (Schlaseman and Russell, 2004).

Some of the early studies on nuclear power plant type structures composed of SC walls were conducted in Japan. For example, the seismic behavior of a containment internal structure (CIS) composed entirely of SC walls was evaluated experimentally by testing a $\frac{1}{10}$-scale model of the entire structure by Akiyama et al. (1989). The structure was subjected to a cyclic loading history with load control cycles in the elastic range and displacement control cycles in the inelastic range. The cyclic response of the structure included events such as concrete cracking, steel yielding, local buckling, shear buckling, and eventual fracture failure of the steel plates. The cyclic lateral load displacement responses and hysteresis loops indicated that the structure had excellent stiffness, strength and ductility. The equivalent viscous damping factor, obtained from the hysteresis loops, was about 5% before steel yielding, and increased significantly thereafter due to yielding and inelasticity. Sener et al. (2015a) recently developed and verified a 3D nonlinear inelastic finite element model of the $\frac{1}{10}$-scale test structure. They used the model to predict, further evaluate and gain insight into the seismic response of the SC structure. Both the experimental and numerical results confirmed that the seismic response including the stiffness, strength and drift capacity were governed by the in-plane shear behavior and corresponding concrete cracking and yielding of the steel plates of the SC walls. The lateral load ultimate strength was governed by the in-plane shear strength and failure of the SC walls parallel to the lateral loading direction. The final fracture occurred in regions where transverse shear reinforcement—web plates—in the SC walls were discontinued abruptly. The overturning moment at the base also contributed to inelastic deformations with extensive concrete cracking and yielding in the SC walls at the exterior outer regions of the CIS.

Akiyama et al. (1989) compared the cyclic response of the SC structure with that of an equivalent RC structure that had been tested earlier using a similar size model by Kato et al. (1987). Akiyama et al. concluded: (1) The ultimate strength of the SC structure was much higher than the corresponding RC structure due to the significant contribution of the steel plates; (2) cyclic loading causes some stiffness degradation in the elastic range due to concrete cracking, and this degradation was about 30% for the SC structure as compared to about 65% for the RC structure; and (3) the SC structure was more ductile as the corresponding RC structure lost capacity rapidly after peak load due to shear failure. It is important to note that these conclusions were limited to specific SC and RC structures that were tested by Akiyama et al. and Kato et al., and the corresponding design, reinforcing and connection details. These conclusions cannot be generalized, but they motivated extensive research and studies in

Japan, China, South Korea, the United States and Europe to establish rational design provisions, codes and standards for SC structures.

Significant research on the behavior of SC walls for various loading conditions, both in-plane and out-of-plane, has been performed in Japan (Takeuchi et al., 1998; Takeuchi et al., 1999; Ozaki et al., 2000; Ozaki et al., 2001; Ozaki et al., 2004; Mizuno et al., 2005), China (Song et al., 2014; Leng et al., 2015a; Leng et al., 2015b), and South Korea (Moon et al., 2007; Moon et al., 2008; Kim and Kim, 2008; Lee et al., 2008; Lee et al., 2009; Hong et al., 2009). The research in Japan and South Korea has been the basis for design standards for SC construction in Japan (JEAG, 2005) and South Korea (KSSC, 2010), respectively.

In the United States, extensive research has been conducted over the past decade to evaluate the behavior of SC walls and connections and to develop consensus design standards, such as the AISC *Specification for Safety-Related Steel Structures for Nuclear Facilities* including Supplement No. 1 (AISC, 2015), hereafter referred to as ANSI/AISC N690. For example,

- The behavior of SC walls subjected to accident thermal and mechanical loading was evaluated by Booth et al. (2007), Varma et al. (2009), Varma et al. (2013), and Booth et al. (2015a).
- The out-of-plane shear behavior and design of SC walls was evaluated by Varma et al. (2011c), Sener and Varma (2014), and Sener et al. (2016). The out-of-plane flexure behavior of SC walls was analyzed by Sener et al. (2015a).
- The in-plane behavior and design of SC walls was evaluated by Varma et al. (2011e), Seo et al. (2016), and Kurt et al. (2016a).
- The local buckling behavior of steel faceplates in SC walls and the composite action between steel plates and concrete infill was evaluated by Varma et al. (2013), Zhang (2014), Zhang et al. (2014), Zhang (2014), and Bhardwaj and Varma (2016).
- The behavior and design of SC walls subjected to combined in-plane forces and out-of-plane flexure was presented by Varma et al. (2011b; 2014).
- The missile impact behavior and design of SC walls was evaluated by Bruhl et al. (2015a; 2015b). The effects of impulsive loading on the design of SC walls was also evaluated by Bruhl and Varma (2015; 2016).

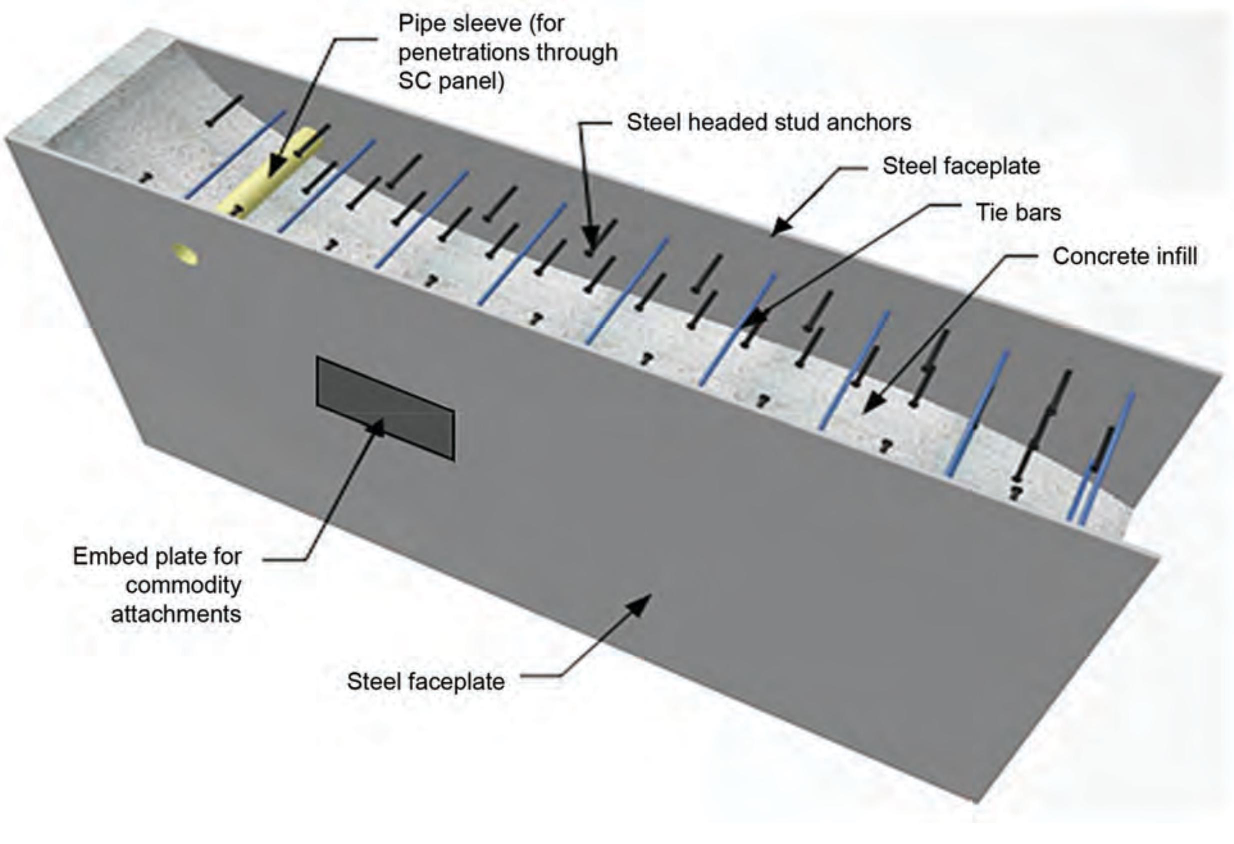
Pipe sleeve (for penetrations through SC panel)
Steel headed stud anchors
Steel faceplate
Tie bars
Concrete infill
Embed plate for commodity attachments
Steel faceplate

Fig. 1-1. Typical SC wall configuration (AISC, 2015).

- The behavior and design of non-contact lap splices between the steel plates of SC walls and rebar of RC components were evaluated by Varma et al. (2011d), and Seo and Varma (2017). The direct shear strength of rebar coupler anchor systems for SC walls was evaluated by Kurt et al. (2016b).
- The behavior, design and shear strength of SC wall-to-wall T-joints and corner or L-joints were evaluated by Seo et al. (2013), Seo (2014), and Seo and Varma (2015).
- The design and detailing of faceplates, steel anchors and ties of SC walls to prevent local buckling, interfacial shear failure, and section delamination failure were presented in Bhardwaj et al. (2017). This paper also presented the design of steel anchors and ties to account for the effect of combined shear forces.
- The lateral load capacity of SC walls with boundary elements was evaluated by Booth et al. (2015c). The lateral load capacity of SC walls without boundary elements was evaluated by Epackachi et al. (2015), Kurt et al. (2016a), and Bhardwaj et al. (2015a).

SC walls are being increasingly used in nuclear facilities. GE Hitachi Nuclear Energy and Toshiba have used SC walls for advanced boiling water reactor (ABWR) Kashiwazaki-Kariwa Units 6 and 7 in Japan. These units were opened in 1996 and 1997. Tokyo Electric Power Company (TEPCO) used SC walls in ABWR Fukushima 7 and 8 units. These units began commercial operation in 2007 and 2008. Westinghouse Electric Corporation (WEC) has incorporated SC modules for walls and floors of its AP1000 plant internal structures. A typical wall module panel for the AP1000 plant containment internal structure is shown in Figure 1-2. Figure 1-3 presents a preassembled internal structure SC module. WEC also extended the use of SC modules to the AP1000 shield building to make it resilient against aircraft impact, a stipulated beyond design basis event. Construction of several AP1000 units is under way in the United States (South Carolina and Georgia) and China (Sanmen and Haiyang). Korea Hydro and Nuclear Power (KHNP) is incorporating SC construction in its advanced pressurized reactor (APR+) standard plant. Mitsubishi Heavy Industries (MHI) is doing the same for its advanced pressurized water reactor (APWR) standard plant. The use of SC construction in small modular reactors (SMR) is also currently being explored. Commercial applications of SC wall piers—known as composite plate shear walls—with and without boundary elements, are also being considered in building construction.

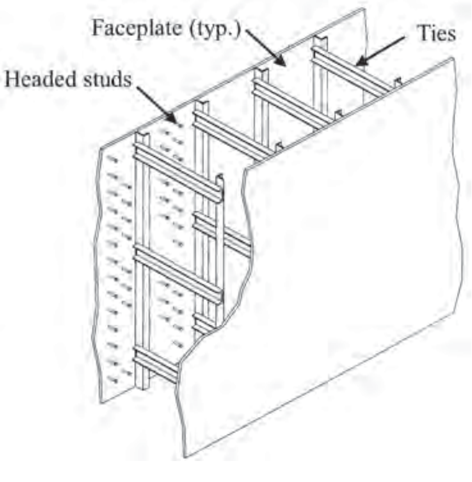

Fig. 1-2. Typical structural wall module in AP1000 plant (DCD, 2011) (©Westinghouse Electric Company, LC. All rights reserved).

1.2 ADVANTAGES OF SC WALLS

SC construction has numerous advantages over RC construction. The presence of faceplates in SC walls eliminates the need for rebar and formwork. The use of faceplates facilitates fabrication of large empty modules in the shop. These modules can then be shipped to the site and assembled in the field. Figure 1-4 presents the comparison between modular RC and SC construction. The schedule contraction achieved by modular SC construction is illustrated in Figure 1-5. Figure 1-6 presents fabrication, lifting and erection operations for some modules for AP1000 in China and the United States (WEC-Sanmen Project and Vogtle Project). The figures illustrate the extent of schedule and modularity contraction achieved by SC construction.

Steel faceplates in SC walls provide better shielding behavior. Compared to RC walls, the faceplates act as a barrier to incident radiation and reduce the intensity of radiation passing through to the concrete infill. The improved performance enables up to a 10% reduction in wall thickness due to reduction in the volume of concrete required for radiation shielding. SC walls do not have problems associated with rebar congestion or moisture loss due to evaporation. Faceplates in SC walls prevent moisture loss thus eliminating the need for concrete curing. With proper use of concrete lifts, the quality of placed concrete is generally superior to that in RC construction. Existence of faceplates makes it easier to incorporate major attachments, such as large bore pipe supports during the initial construction. Additional minor attachments can also be easily handled during the service life of the structure. Similarly, the walls can be detailed during construction to accommodate any penetrations. The SC walls have improved resistance to out-of-plane loads, such as bending and shear, that may be due to seismic or accident thermal events. The faceplates also provide better leak-tightness behavior, which reduces the loss of stored water. The leak-tightness also protects the concrete during the service life of the structure.

1.2.1 Resilience and Sustainability Aspects of SC Construction

SC construction has natural benefits in terms of resilience and sustainability of the structure. The resilience performance of SC walls can be improved as discussed in the following (Malushte and Varma, 2015).

(a) Missile and blast loads: The presence of faceplates leads to increased blast and missile resistance. This resistance is further improved by higher strength faceplates with closer tie spacing.

(b) External hazard (environmental) or abnormal loads: SC construction typically results in increased strength and ductility, leading to higher margins against design basis external hazard loads—for example, environmental hazards, such as seismic or tornado wind events. This benefit is best realized if full-strength connections—connections stronger than the wall capacities—are used to join SC elements with other connected members, such as a basemat, and the reinforcement ratio is kept between 0.02 and 0.04.

(c) Accident thermal loads: The accident thermal load, resulting from a loss-of-coolant or main steam break event, leads to exposure to elevated temperature for sustained duration. This loading poses a unique challenge to SC members because the faceplate is immediately exposed to the elevated temperature due to there being no concrete cover. A seismic event could occur during such extended exposure, which could be a beyond design basis (BDB) consideration. Performance in these scenarios is improved by using full-strength connections, steel or fiber reinforced concrete, or fire-resistant steel plates.

(d) Exposure to fire: The faceplate that is exposed to fire loses strength and stiffness; however, similar to RC construction, the bulk of the concrete and the opposite

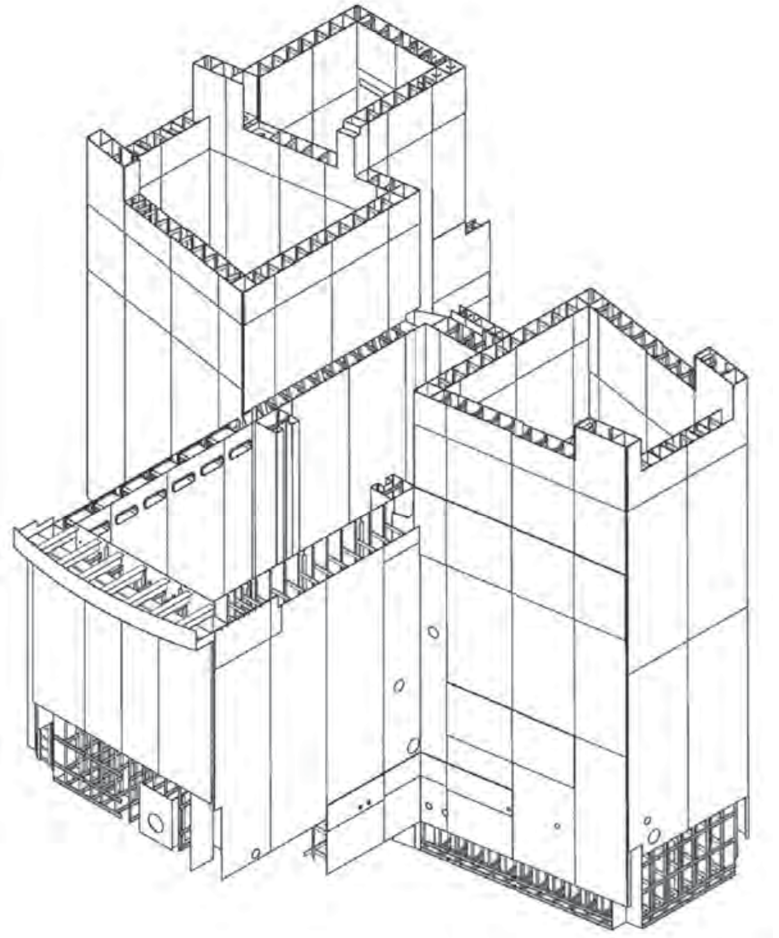

Fig. 1-3. Example of large preassembled module in AP1000 plant (DCD, 2011) (©Westinghouse Electric Company, LC. All rights reserved).

faceplate maintain good strength and stiffness. As such, SC structures have better fire resistance than pure steel structures. Fire resistance of SC walls is potentially lower than RC structures; however, the fire resistance is enhanced if a suitable fire protection coating is applied to the faceplate(s) or fire-resistant steel is used. The member strength and stiffness during fire exposure is also improved by embedding another steel plate within the concrete, that is, between the faceplates. ANSI/AISC N690 does not currently cover SC walls with embedded steel plates.

(e) Durability and long service life: The faceplates improve leak-tightness of concrete. However, just like any steel structure, the exposed steel surfaces need to be protected from corrosion. The protection scheme will depend on the service environment; for example, interior versus exterior walls and underground walls.

Advantages and considerations of sustainability of SC structures include (Varma et al., 2015):

(a) Field labor force reduction: SC construction requires a smaller field labor force compared to conventional RC construction because of elimination of activities related to formwork, rebar erection and curing. As in any modular construction, the degree of field labor reduction depends on the extent of modularization and the size of the modules. Use of automated welding techniques can help further in this regard. Reduction in field labor results in a significant reduction in the carbon footprint associated with mobilization, demobilization, and daily coordination between crafts.

(b) Reduction of water usage: SC construction does not have rebar congestion issues, therefore, the amount of water used in the concrete mix design can be reduced without sacrificing placement quality. Additionally, the water use associated with concrete curing is eliminated.

(c) Use of green concrete or cement substitutes: Cement is an energy-intensive ingredient of concrete. Green concrete mixes—those replacing cementitious materials

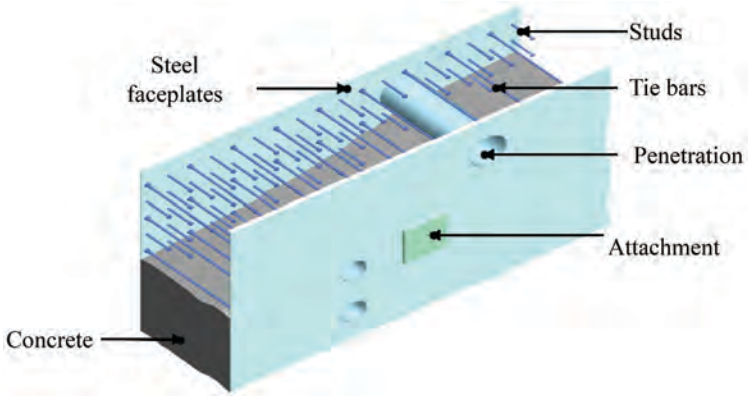

(a) Modular SC Wall

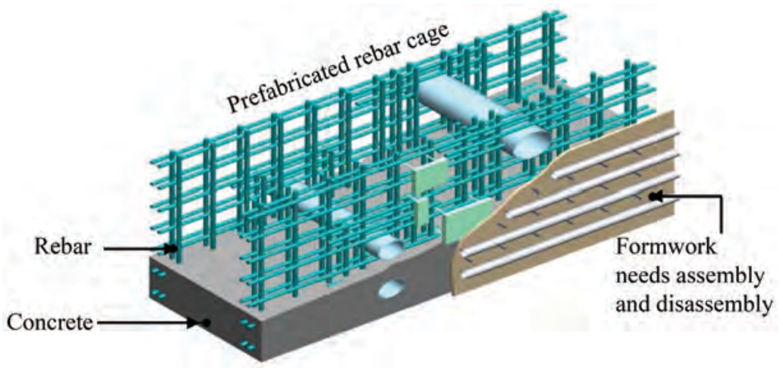

(b) Modular RC Wall

Fig. 1-4. Typical modular SC and RC wall configurations (Schlaseman and Russell, 2004).

with naturally occurring cement substitutes, such as fly ash, pozzolan or slag—are always desirable from a sustainability standpoint. Unlike the schedule impact due to the slow-setting pace of cement substitutes in RC construction, this issue is easily handled in SC construction by ensuring that the faceplates are adequately designed as permanent formwork.

(d) Prolonged service life: SC structures will have a long service life provided the potential for steel plate corrosion is addressed. Depending on the application—underground wall, exterior wall exposed to atmosphere, or walls exposed to water—certain types of stainless steel can be used advantageously. Compared to surface treatment options, such as cathodic protection or surface coatings, the stainless steel option may be the most cost efficient in the long term.

(e) Surface decontamination: The ability to decontaminate the exposed surfaces and the effort required to do so is an important consideration in any nuclear facility. The presence of faceplates provides an easy decontamination process during the service life and after decommissioning. Faceplate surface treatment and material selection can be especially important based on ease of decontamination. This is a sustainability consideration in terms of controlling potential spread of radioactive materials.

(f) Potential for recycling: Unlike rebar in RC construction, the steel faceplates can be more easily removed and recycled. Also, the concrete can be pulverized and used in rubblized pavement construction.

(g) Reduced energy use during construction: SC construction has reduced the need for concrete compaction—consolidation using vibrators—because there is no congestion due to rebar. Self-consolidating concrete can be used for hard to reach areas under penetrations. Additionally, options for field bolting can be maximized to reduce energy consumption during construction.

(h) Material savings in steel and concrete quantity: Because of higher strength and radiation shield capability, SC member design can be optimized for a reduced amount of steel and concrete versus comparable RC members. This aspect has to be investigated during the design phase. The quantity reductions have obvious sustainability implications.

(i) Elimination of water-stops and rebar accessories: Compared to conventional RC construction, SC construction has a reduced need for water-stops—because of its inherent leaktightness—and accessories such as rebar chairs. This results in a reduction of the rubber and plastic-based materials, which is good in terms of sustainability.

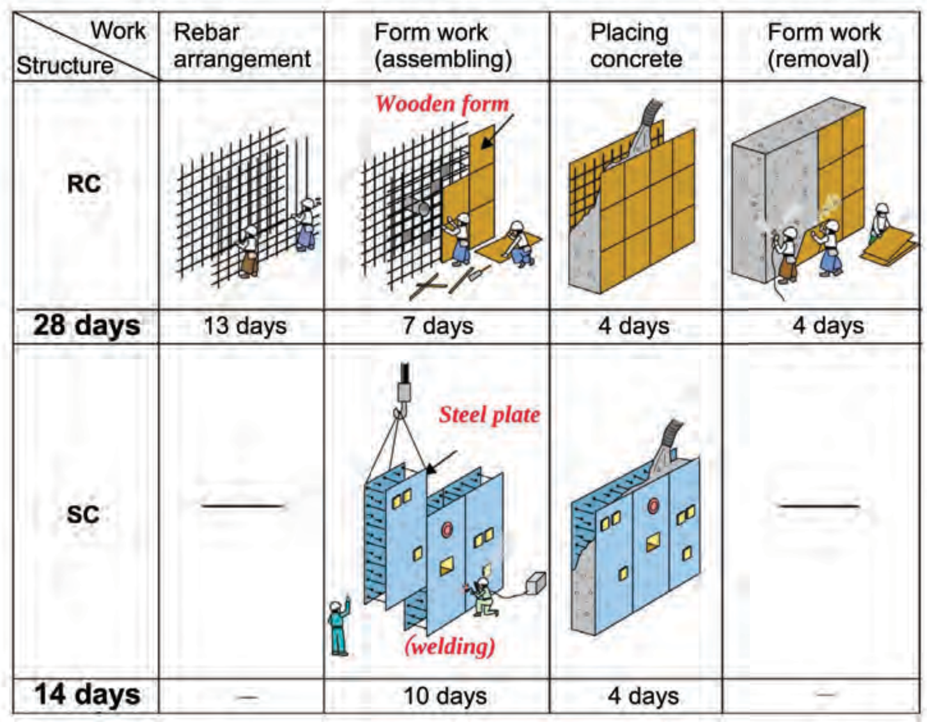

Fig. 1-5. Schedule contraction by means of SC construction (Schlaseman and Russell, 2004).

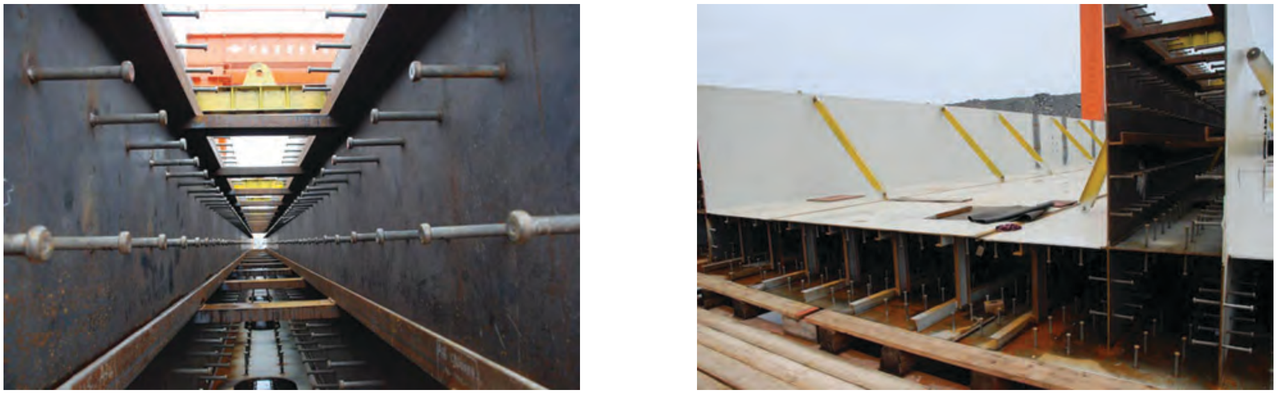

(a) Tie bar and stud layout
(©2009 Sanmen Nuclear Power Company Ltd.
All rights reserved)

(b) Panel section ready to be transported
(©2009 Sanmen Nuclear Power Company Ltd.
All rights reserved)

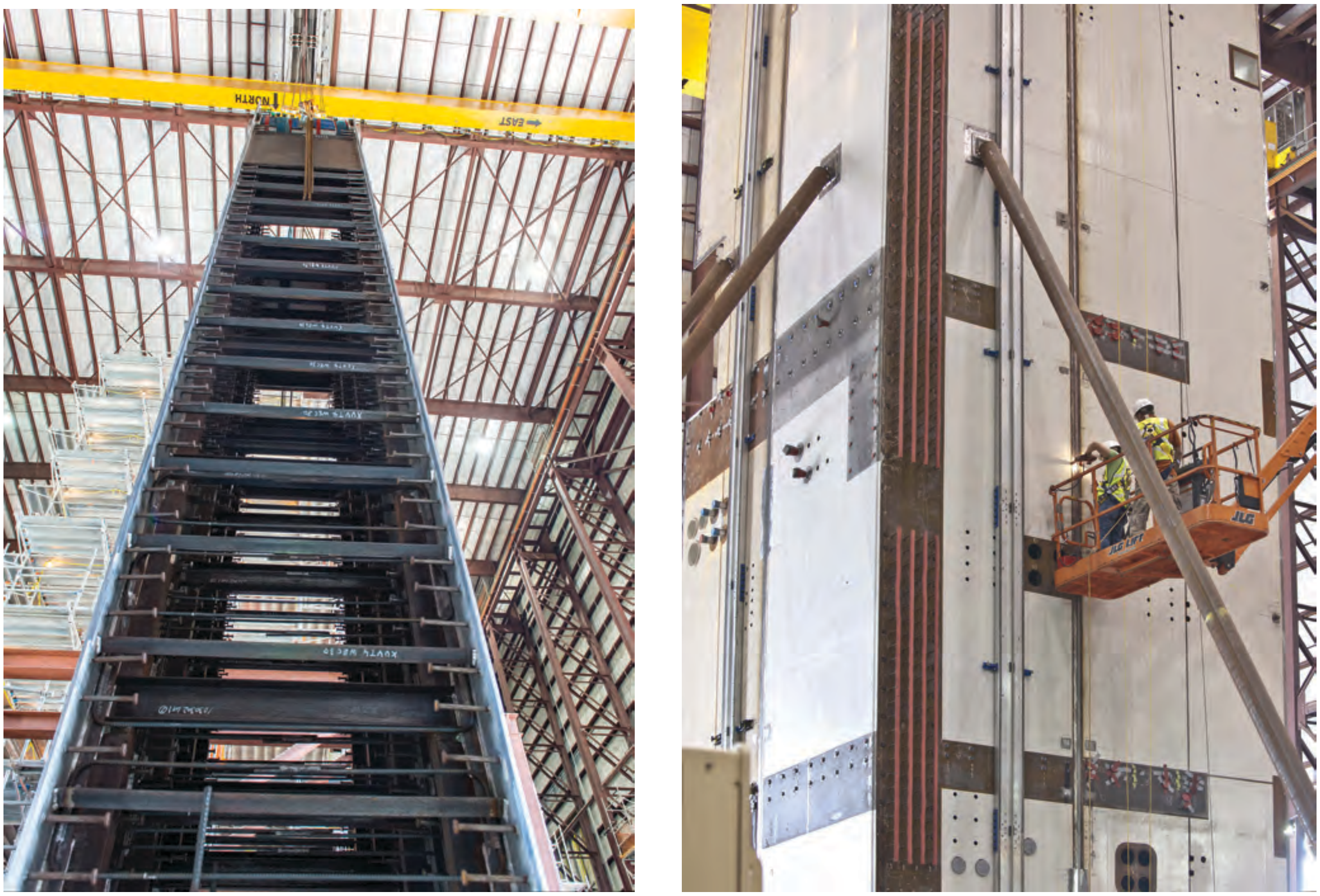

(c) Sub-module wall

(d) Welding of a sub-module

Fig. 1-6. Fabrication, lifting and erection operations for AP1000 modules in China and the United States.

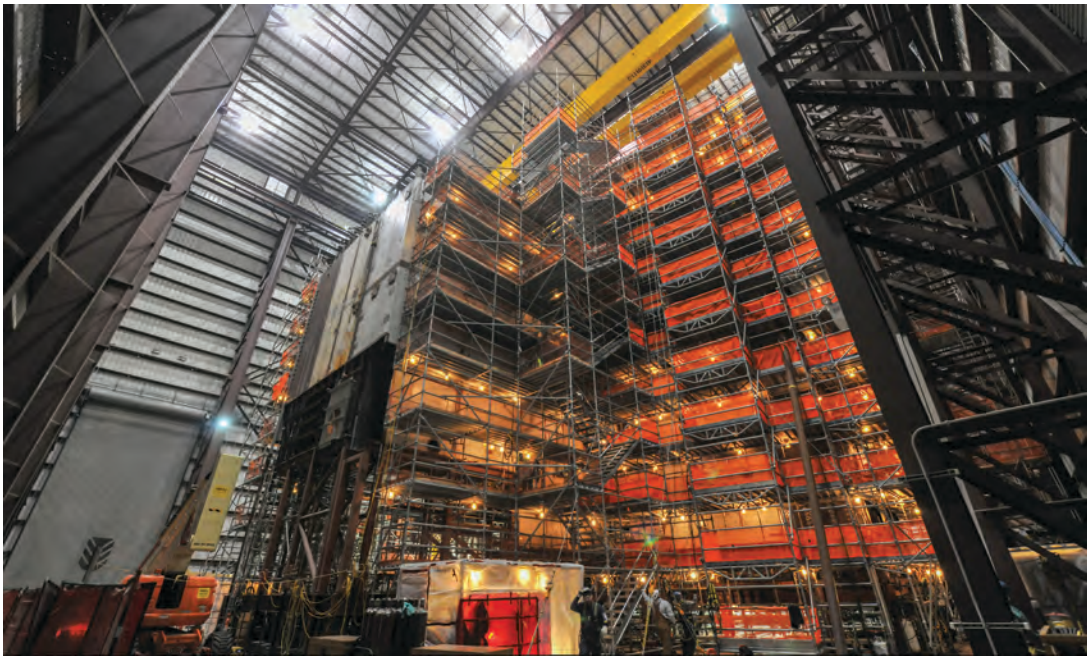

(e) Module inside the fabrication yard

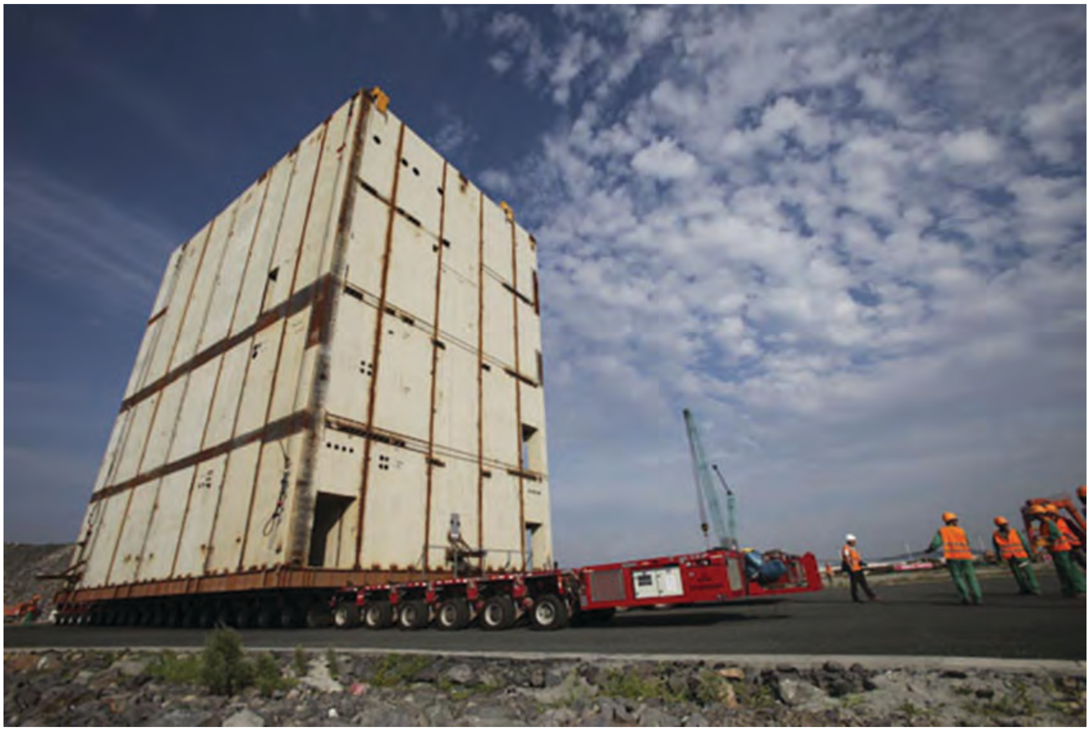

(f) Module being transported (©2009 Sanmen Nuclear Power Company Ltd. All rights reserved)

Fig. 1-6. Fabrication, lifting and erection operations for AP1000 modules in China and the United States (continued).

(j) Increased potential for modular attachment of supported commodities: SC modules can be designed to further enhance the ability to support or attach piping, equipment components and structural components, such as for floors or platforms. The integrated SC module is assembled in the fabrication yard with these components. This will lead to further reduction in the associated labor forces and energy use on site, in addition to the resulting schedule contraction.

1.3 LIMITATIONS OF SC WALLS

SC construction has some potential limitations in comparison with RC construction. SC walls have reinforcement—steel faceplates—exposed to the atmosphere. This renders the reinforcement susceptible to corrosion in harsh environments. Additionally, SC walls are expected to experience higher strength demands due to accident thermal loads and fire events. Because the use of SC construction is relatively new, there may be some fabrication and construction tolerance issues. Modular SC walls involve significant

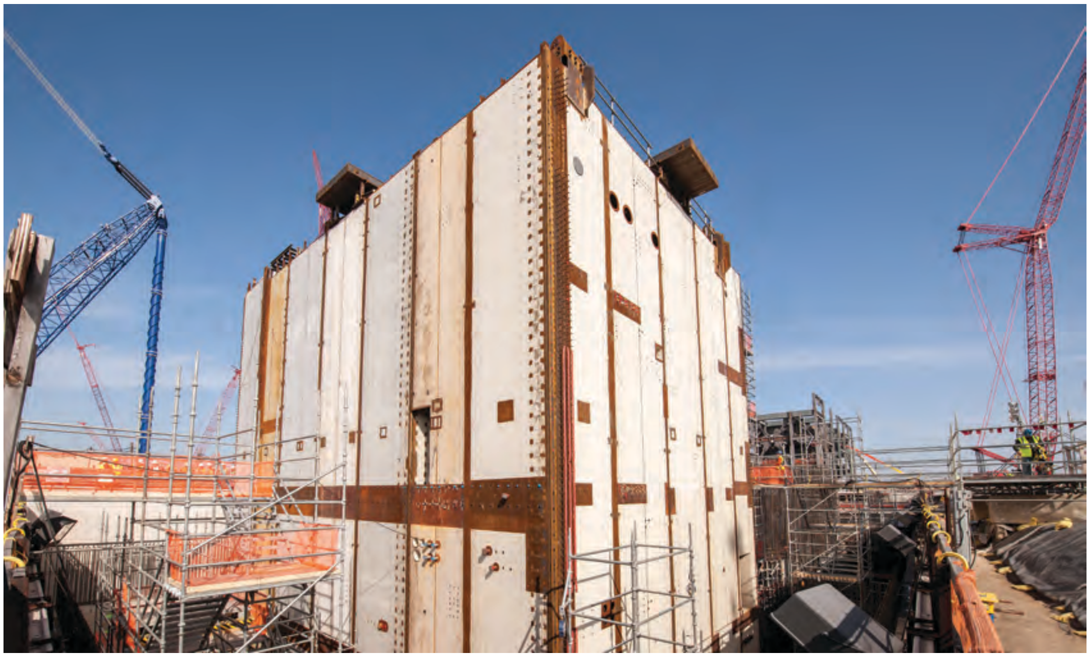

(g) Module erected at site

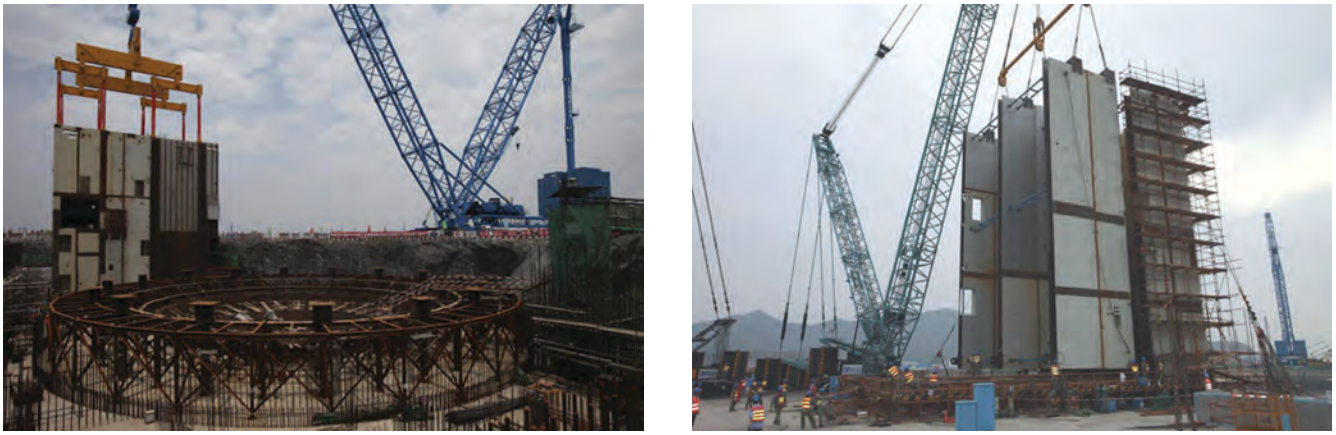

(h) Lifting and erection of SC modules (©2009 Sanmen Nuclear Power Company Ltd. All rights reserved)

Fig. 1-6. Fabrication, lifting and erection operations for AP1000 modules in China and the United States (continued).

prefabrication and specialized transportation, which may sometimes lead to the labor and material cost of these SC walls being higher than conventional RC construction. However, these limitations are addressed by choosing appropriate materials and utilizing the best practices in fabrication and construction.

1.4 ANSI/AISC N690 APPENDIX N9

Previously, the use of SC construction in the United States had been hindered by the absence of a U.S.-based design code for SC walls. However, in 2006 AISC formed a subcommittee on modular composite construction under the Committee on Specifications Task Committee 12 for nuclear structures. Over the next nine years, from 2006 to 2015, a specification for the design of SC walls in safety-related nuclear facilities was developed and finalized as an appendix (Appendix N9) to ANSI/AISC N690 (AISC, 2015). The new appendix was incorporated into ANSI/AISC N690 as Supplement No. 1. An outline of Appendix N9 and a brief discussion of how the provisions of the appendix may be used are provided in Bhardwaj et al. (2015b).

Appendix N9 is applicable to the design of SC walls and their connections and anchorages. The experimental database that forms the basis of the provisions is discussed in the commentary to Appendix N9. The appendix is limited to SC walls with two faceplates on exterior surfaces and no additional reinforcing bars. General requirements of the appendix specify the conditions necessary for applicability of the provisions. Detailing requirements of the appendix address SC-specific limit states of local buckling, interfacial shear failure, and section delamination. The appendix discusses the analysis procedures and presents the guidelines for analysis. The demand types and available strengths for individual demands are presented. The appendix also presents the interaction surfaces for combinations of demands. Connection design philosophy, detailing for regions around openings, design for impactive and impulsive loads, and quality assurance checks are other topics addressed by the supplement.

The Appendix is applicable to straight SC walls. If the SC walls in application have any curvature, the effects of curvature on detailing and design of the SC walls need to be evaluated. This is necessary as there is limited data available for curved SC walls at present (Yan et al., 2015; Yan et al., 2016). For the ratio of radius of curvature-to-thickness values greater than 20, the effects of curvature may be negligible, and the provisions of Appendix N9 would be applicable. However, for the ratio of radius of curvature-to-section thickness values less than 20, project-specific design and detailing requirements for SC walls is warranted.

Alternate design methods for SC walls not meeting the general provisions may be based on (1) project-specific large-scale test data, or (2) results of nonlinear inelastic analyses conducted using modeling approaches that are benchmarked against applicable test data and peer reviewed. Alternatively, subject to peer review, the wall design may also be performed in accordance with ACI 349-06 (ACI, 2006) provided that (1) the faceplate thickness and its composite action is minimized to primarily enable it to function as formwork; (2) conventional rebar is provided to develop adequate section strength for demands due to in-plane and out-of-plane forces and moments; and (3) the faceplates are evaluated for stresses and strains due to strain compatibility to ensure that they remain below the yield and local buckling threshold, similar to the design of liner plates in concrete containment structures according to ACI 359 (ACI, 2001).

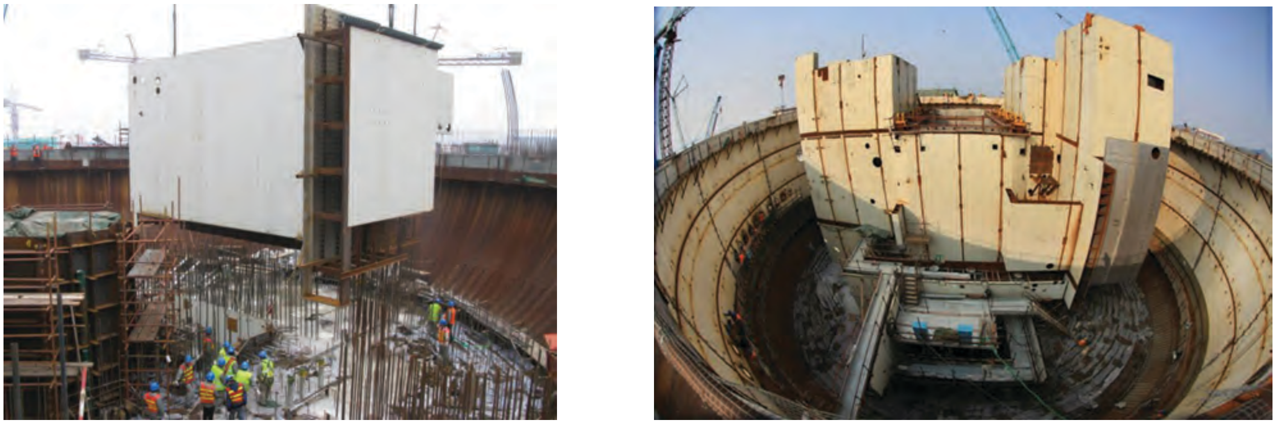

(i) Lifting and erection of SC modules (©WEC, LLC; ©Sanmen)

(j) Lifting and erection of SC modules (©WEC, LLC; ©Sanmen)

Fig. 1-6. Fabrication, lifting and erection operations for AP1000 modules in China and the United States (continued).

Chapter 2
Scope and Layout

This Guide is intended to facilitate the design of SC walls for safety-related nuclear facilities. The procedures outlined in this document are based on Supplement No. 1 to the AISC *Specification for Safety-Related Steel Structures for Nuclear* Facilities, ANSI/AISC N690 (AISC, 2015). Appendix N9, adopted into ANSI/AISC N690 as part of the Supplement, presents the requirements for the design of SC walls. Any reference to Appendix N9 in this Design Guide is referring to ANSI/AISC N690 Appendix N9. This Design Guide is to be used in conjunction with ANSI/AISC N690. The Design Guide:

- Addresses SC walls that meet the requirements of Appendix N9
- Provides supplementary recommendations for the design of modular SC structures using the provisions of Appendix N9
- Discusses the design of SC wall connections, including design philosophies and typical connection details
- Presents illustrations explaining the tolerance requirements for construction and fabrication of SC walls

This Design Guide provides primary procedural steps required for the design of SC structures. However, nuclear construction needs to satisfy other regulatory and environmental requirements, which may affect the design procedure. There may be project-specific scenarios that need to be considered in the design. The Design Guide may be used as a platform for the design of modular SC walls for nuclear construction.

This Design Guide discusses various aspects of the analysis and design of SC structures based on ANSI/AISC N690. The minimum requirements that an SC wall needs to meet in order for the provisions of Appendix N9 to be applicable are discussed. This Design Guide then discusses the detailing requirements for SC walls. These detailing requirements are provided to address specific SC limit states, such as faceplate local buckling. The requirements include faceplate slenderness requirements, and steel anchor and tie detailing. Guidelines for modeling and analysis of SC walls are presented. Additionally, the determination and basis of individual design strength equations will be presented. Interaction of demands is also discussed.

ANSI/AISC N690 provides procedural recommendations for the design of SC wall connections. This Design Guide addresses the design of connections in detail. Different connection philosophies, force transfer mechanisms, and types of connections are discussed with illustrations. The implementation of the provisions of ANSI/AISC N690 Appendix N9 is illustrated using a design example presented in Appendix A.

2.1 DESIGN EXAMPLE

This Design Guide provides a design example for an SC wall structure. An SC wall from a compartment of a typical safety-related nuclear facility is selected and all aspects of the design of that wall are discussed. The design example is presented in Appendix A. The example discusses the rationale for selecting the preliminary details of the structure. Discussion of the basis for the material selection is presented in the example. For brevity, the example does not present the details of the finite element analysis models, procedures, and results. Representative design demands are considered for design of the SC wall. The SC wall considered does not include any attachments or openings. The designed SC wall is not checked for impactive and impulsive loading in the example. It is considered that the fabrication and construction tolerances and quality assurance and control checks are performed during the erection of the SC wall.

The design of modular SC walls needs to consider constructability aspects, such as fabrication and erection issues. Based on transportation capabilities, the size of the prefabricated module is established. Specific analysis such as barge transportation analysis may need to be performed for submodules, based on the erection and fabrication sequencing, to consider the erection and fabrication loads, concrete casting pressure, and demands on ties and ribs prior to casting. Therefore, the designers need to be cognizant of the fabrication and erection procedures and sequence to ensure the design can be implemented without any issues. Appendix N9 provides fabrication and erection tolerances that need to be met for the provisions of Appendix A to be applicable. These tolerances are discussed in Section 13 of this Design Guide. While the design example presents the methodology for the design of modular SC walls, the designer needs to consider the constructability aspect of these walls during the analysis and detailing phases of the design.

Chapter 3
Minimum Requirements

The majority of SC wall tests have been performed on walls with two faceplates, where composite action is provided using either steel anchors or ties, or a combination of both. The provisions of Appendix N9 in ANSI/AISC N690 have been developed based on this experimental database and the associated mechanics-based behavioral models. As a result, Appendix N9 is limited to walls with two faceplates anchored to the concrete infill by means of steel anchors or ties, or a combination of both. The provisions are not applicable to SC walls reinforced with more than two steel plates, which may be used for the design of the primary shield structure supporting and shielding the reactor vessel. The design of such structures composed of extremely thick SC walls with three or more steel plates is discussed in Booth et al. (2013, 2015b).

Appendix N9 is limited to the design of SC walls with boundary elements or flanges, which are typically the purview of safety-related nuclear facilities consisting of labyrinthine SC walls connected to each other and to the concrete floor or basemat. The modular composite specification does not include provisions for the design of SC wall piers, with no flanges or large boundary columns, that are typically used in commercial building structures. The behavior and seismic design of SC wall piers is discussed in Kurt et al. (2016a), Epackachi et al. (2015), Bhardwaj et al. (2015a), and the AISC *Seismic Provisions for Structural Steel Buildings* (AISC, 2016b).

Table 3-1 summarizes some of the minimum requirements for SC walls based on Appendix N9. These minimum requirements were selected based on the range of parameters in the experimental database of SC walls, and some other criteria as described here. The minimum thickness, t_{sc}, for exterior walls is based on Table 1 of the Standard Review Plan (SRP), Section 3.5.3, Revision 3 (NRC, 2007). The maximum limit for t_{sc} is based on the experimental database of out-of-plane shear tests conducted on SC walls in Japan (Ozaki et al., 2001), South Korea (Hong et al., 2009), and the United States (Sener and Varma, 2014). The reinforcement ratio, ρ, is determined according to ANSI/AISC N690 Equation A-N9-1.

The limits for ρ, shown in Table 3-1, were established because a very low reinforcement ratio—less than 0.015—can lead to potential concerns regarding handling strength and stiffness of empty modules and higher residual stresses due to fabrication activities and concrete casting. The use of very high reinforcement ratios—greater than 0.050—can potentially result in higher concrete stresses and change the governing in-plane shear limit state from steel faceplate yielding to concrete compression strut failure, which can potentially reduce the strength and ductility of SC walls.

The limits for faceplate thickness, shown in Table 3-1, were established because a 0.25-in.-thick faceplate is needed for adequate stiffness and strength during concrete placement and rigging and handling operations. Additionally, faceplates thinner than 0.25 in. (6 mm) can have the material properties and imperfections associated with sheet metal, such as waviness, instead of structural plates (Bruhl and Varma, 2016). The maximum faceplate thickness of 1.5 in. (38 mm) corresponds to a reinforcement ratio of 0.050 for a 60-in. (1500 m)-thick SC wall. The minimum thickness for interior walls is based on the maximum reinforcement ratio of 0.050 and minimum faceplate thickness, t_p, equal to 0.25 in. (6 mm). The specified minimum values for interior as well as exterior walls are conservatively slightly larger than absolute minimum values.

A minimum yield stress of 50 ksi (350 MPa) is specified to prevent premature yielding of the steel faceplates due to residual stresses from concrete casting and thermally induced stresses from accident thermal scenarios, because such premature yielding could limit the strength and ductility of SC walls (Zhang, 2014). High-strength steels with a yield stress greater than 65 ksi (450 MPa) are typically less ductile and, hence, not desirable for demands beyond the design basis earthquake (Varma, 2000).

The use of concrete with a compressive strength less than 4 ksi (28 MPa) is rare in safety-related nuclear facilities, with the possible exception of the concrete basemat. The minimum concrete strength of 4 ksi (28 MPa) is also specified so that the minimum principal stress in concrete remains in the elastic range while faceplate yielding occurs under in-plane shear loading. The provisions of Appendix N9 are based on test results of specimens with a specified minimum concrete compressive strength of 8 ksi (55 MPa) or less. Figure 3-1 presents the range of concrete compressive strengths from the experimental database for out-of-plane shear tests conducted internationally and discussed in Sener and Varma (2014). In Figure 3-1, the ordinate presents the ratio of the experimental out-of-plane shear strength, V_{exp}, with respect to the nominal out-of-plane shear strength calculated using ACI 349-06 (ACI, 2006) code equations, $V_{n.ACI}$, as discussed in Sener and Varma (2014). The entire experimental database of SC walls consists of specimens with concrete compressive strengths in the range of 4 to 8 ksi (28 to 55 MPa).

Appendix N9 requires that for regions with holes, the effective rupture strength of the region needs to be greater than the yield strength, ensuring that the section undergoes a gross yielding failure and not a net section rupture.

Table 3-1. Minimum Requirements for SC walls

Parameter	Minimum Value	Maximum Value
Reinforcement ratio, ρ	0.015	0.050
Faceplate thickness, t_p	0.25 in. (6 mm)	1.50 in. (38 mm)
SC section thickness, t_{sc}—interior walls	12 in. (300 mm)	60 in. (1500 mm)
SC section thickness, t_{sc}—exterior walls	18 in. (450 mm)	60 in. (1500 mm)
Steel minimum yield stress, F_y	50 ksi (350 MPa)	65 ksi (450 MPa)
Concrete minimum compressive strength, f'_c	4 ksi (28 MPa)	8 ksi (55 MPa)

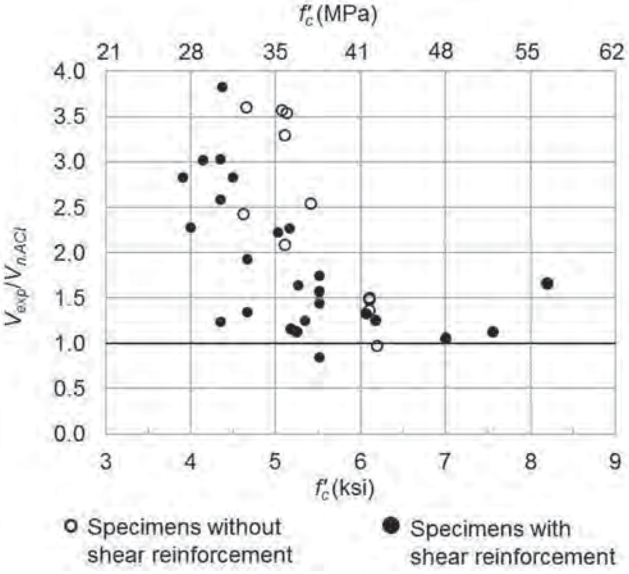

Fig. 3-1. Range of concrete compressive strength from experimental database (Sener and Varma, 2014).

The majority of the experimental investigations have been performed on SC walls with faceplates that have the same nominal thickness and yield strength. The lack of uniformity between the yield strength of the two faceplates exacerbates the potential for section delamination through the plain concrete. The requirements of Appendix N9, Section N9.1.5, consider delamination due to 50% nonuniformity between the faceplate yield strengths. However, Section N9.1.1 conservatively stipulates that the nominal yield strength and faceplate thickness be identical for both faceplates.

Appendix N9 permits that steel rib sections may be welded to the faceplates of SC walls to increase the stiffness and strength of the empty modules. This increased stiffness improves the behavior of the empty modules during transportation, handling and erection. The ribs also improve the resistance of the faceplates to hydrostatic pressure from concrete casting. After concrete hardening, the ribs prevent local buckling of the faceplates. Therefore, when used in SC walls, these steel ribs should be welded to the faceplates to fully develop the yield strength of their connected element. As shown in Figure 3-2, the embedment of the steel ribs into the concrete is limited to prevent the use of large depth steel ribs that can alter the mechanics of the SC wall behavior and to minimize the interference of ribs on the performance of the other steel anchors. However, the contribution of steel ribs is not considered for any design parameters, such as composite action or available strengths.

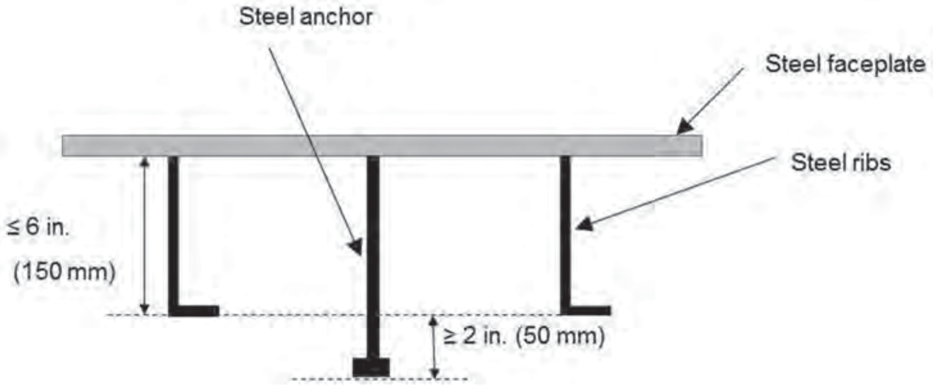

Fig. 3-2. Embedment depth of steel ribs.

Chapter 4
Faceplate Slenderness Requirement

Local buckling of steel faceplates is an important limit state to be considered in the design of SC walls. When subjected to compressive stresses, the steel faceplates of SC walls can undergo local buckling between the steel anchors. This local buckling behavior of steel faceplates has been investigated experimentally by Akiyama and Sekimoto (1991), Usami et al. (1995), Kanchi (1996), Choi and Han (2009), and Zhang (2014). These experimental studies have evaluated the effects of the plate slenderness ratio—defined as the steel anchor spacing, s, divided by the faceplate thickness, t_p, and the yield stress, F_y—on local buckling of faceplates. Zhang et al. (2014) have summarized these experimental studies, and conducted additional numerical analyses to confirm and expand the experimental database. Figure 4-1 shows the relationship between the normalized critical buckling strain, buckling strain/steel yield strain, $\varepsilon_{cr}/\varepsilon_y$, and the normalized faceplate slenderness ratio, $s/t_p \times F_y/E$. As shown, ε_{cr} is reasonably consistent with Euler's column buckling curve with partially fixed ($K = 0.7$) end conditions. Additionally, no data points are located in the shaded region, which implies that yielding in compression occurs before local buckling for a faceplate slenderness ratio, s/t_p, less than 1.0.

Based on this investigation, ANSI/AISC N690 limits the slenderness ratio—the width-to-thickness ratio of the faceplates—as given by ANSI/AISC N690 Equation A-N9-2. Because ties may also act as steel anchors, ANSI/AISC N690 Equation A-N9-2 considers the largest unsupported length between rows of steel anchors or ties, b. For steel faceplates with a specified minimum yield stress greater than or equal to 50 ksi (350 MPa), the specified slenderness limit of ANSI/AISC N690 Equation A-N9-2 implicitly addresses the influence of residual stresses or stresses due to concrete casting. The use of faceplates with a specified minimum yield stress less than 50 ksi (350 MPa) is not permitted because the slenderness limit of ANSI/AISC N690 Equation A-N9-2 cannot assure yielding in compression before local buckling due to the influence of residual stresses and concrete casting stresses (Zhang, 2014).

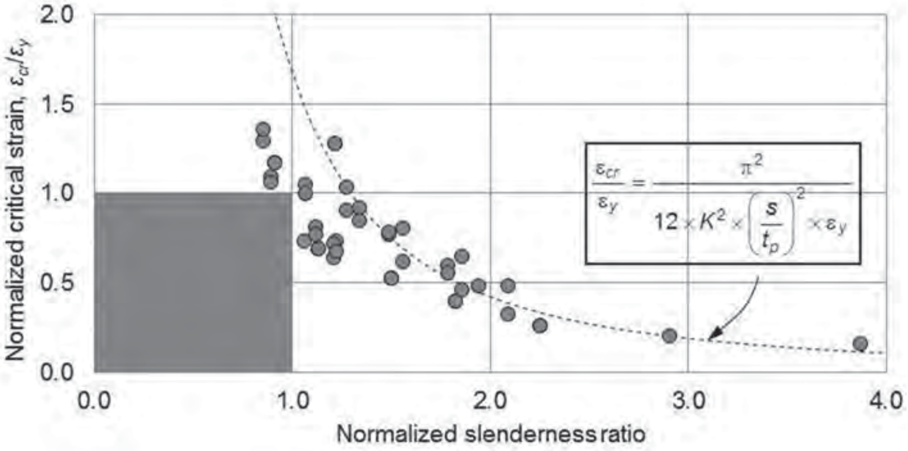

Fig. 4-1. Relationship between buckling strain and normalized slenderness ratio, K = 0.7 *(adapted from Zhang et al., 2014).*

Chapter 5
Steel Anchor Detailing

The steel faceplates are anchored to the concrete infill by steel anchors and ties. These anchors prevent local buckling of the steel faceplates as discussed in the previous section, and develop composite action between the faceplates and concrete infill by transferring interfacial shear forces and restraining slip between them. Developing composite action can be understood in terms of: (1) developing the strength of the composite section without premature failure of the anchors or (2) developing strain compatibility between the steel and concrete components.

Steel limit state design emphasizes developing the strength of the composite section. For example, consider the design of composite steel beams in ANSI/AISC N690 Chapter NI, Section I3, where full composite action is defined by the ability of the anchors to develop the strength of the composite section as governed by the yield strength of the steel or concrete components. This full composite action, in terms of strength, is accompanied with interfacial slip and lack of strain compatibility between the steel and concrete components. Enforcing full composite action in terms of strain compatibility between the steel and concrete components can be onerous in terms of the required number and spacing of steel anchors, while providing little to no additional strength over that achieved by developing full composite action in terms of strength (Selden et al., 2015). However, the corresponding lack of strain compatibility due to interfacial slip may lead to reduction in stiffness of the composite section, which is usually calculated assuming strain compatibility (plane sections remain plane).

Steel anchors used in SC construction may consist of steel headed studs, embedded steel shapes, ties (smooth or deformed), or a combination thereof, which can be attached to the faceplates by welding or bolting. The following subsections discuss (1) the classification of steel anchors as ductile or nonductile, (2) the required spacing to develop the yield strength of the steel faceplate, (3) the influence of interfacial slip on the stiffness, and (4) the required spacing of steel anchors to prevent interfacial shear failure from governing the behavior of SC walls.

5.1 CLASSIFICATION OF STEEL ANCHORS

Steel anchors that have a ductile shear force-slip behavior can redistribute the interfacial shear equally over several connectors. These connectors, such as steel headed stud anchors, are referred to as yielding type. Steel anchors that have a nonductile shear force-slip behavior cannot redistribute interfacial shear and are referred to as nonyielding type. As shown in Figure 5-1, an interfacial slip capability of at least 0.20 in. (5 mm) before reduction in shear strength to 90% of the available shear strength is required to qualify a yielding-type connector. Steel headed stud anchors are typically capable of sustaining at least 0.20 in. (5 mm) of interfacial slip in a ductile manner (Ollgaard et al., 1971). The available strength of steel headed stud anchors can be obtained from the AISC *Specification for Structural Steel Buildings*, hereafter referred to as the AISC *Specification* (AISC, 2010b). All other types of steel anchors need to be tested to determine their available shear strength and interfacial slip capability. An adequate number of tests must be performed to ascertain the available strength of nonyielding steel anchors. The safety factors applicable for nonyielding steel anchors can be obtained from the experimental studies by following the reliability analysis procedures used by Ravindra and Galambos (1978).

For cases where a combination of yielding and nonyielding steel anchors is used, the system is classified conservatively as nonyielding because the peak strengths of yielding and nonyielding steel anchors may not occur at similar slip displacement levels, and the post-peak behavior of yielding and nonyielding steel anchors may be significantly different, and as a result, the interfacial shear force cannot be distributed equally over several connectors. The system is classified as a nonyielding type, and the strength of yielding steel anchors has to be limited to the strength corresponding to the slip displacement at which the nonyielding steel anchors reach their ultimate strength. This is illustrated in Figure 5-2.

5.2 SPACING OF STEEL ANCHORS

The spacing of steel anchors is controlled by one of the following:

(a) The requirement to prevent the faceplate from buckling before yielding in compression.

(b) The requirement to achieve a desired development length.

(c) The requirement to prevent interfacial shear failure from occurring before out-of-plane shear failure.

While item (a), the faceplate slenderness requirement, was discussed in Section 4, the other two requirements are discussed in Sections 5.2.1 and 5.2.2.

5.2.1 Development Length

The steel anchors develop composite action between the steel faceplate and the concrete infill. The development length, L_d, is the distance over which the steel faceplate can develop its yield strength due to the shear strength and number of steel anchors. Thus, any target development length can be achieved by designing the size and spacing of steel anchors. The target development length has a direct influence on the degree of composite action, in terms of the strain compatibility achieved between the steel faceplate and concrete infill. This partial composite action—strain compatibility or interfacial slip—has a direct influence on the flexural stiffness, *EI*, of the composite section.

Zhang et al. (2014) investigated the relationship between the target development length and the degree of composite action (strain compatibility) between steel and concrete. They concluded that the target development length should not exceed three times the section (or wall) thickness, t_{sc}, and that 75 to 90% partial composite action (strain compatibility) can be achieved for target development lengths less than or equal to $3t_{sc}$. They also investigated the relationship between the partial composite action (strain compatibility) and flexural section stiffness, *EI*, of the composite section. They concluded that 75 to 90% partial composite action (strain compatibility) does not have a significant influence (less than 10%) on the cracked-transformed flexural stiffness, *EI*, of the composite section.

Based on Zhang et al. (2014), ANSI/AISC N690 Appendix N9 requires the development length to be less than or equal to $3t_{sc}$. For the range of geometric parameters used in nuclear construction—wall thickness t_{sc}, plate thickness t_p, and stud anchor diameter and spacing—this requirement ($L_d \le 3t_{sc}$) will result in faceplate development lengths that are comparable to ACI 349-06 (ACI, 2006) based development lengths calculated for No. 11, 14 or 18 rebar used typically in nuclear concrete construction.

Figure 5-3 shows the free-body diagram associated with the development length, L_d, of the steel faceplate. In the diagram, the width of the faceplate is equal to the transverse spacing of the stud anchors, s_T, and the faceplate develops the yield stress, F_y, over the development length. For designs with yielding stud anchors, the interfacial shear force is assumed to redistribute uniformly over the development length, and the value is governed by the available shear strength, Q_{cv}, of the yielding anchor. Zhang et al. (2014) developed Equation 5-1 using the free-body diagram shown in Figure 5-3 to relate the development length, L_d, to the available shear strength, Q_{cv}, and the spacing of yielding steel anchors:

$$Q_{cv}\frac{L_d}{s_L} \ge s_T t_p F_y \tag{5-1}$$

where

F_y = specified minimum yield stress, ksi (MPa)
L_d = development length for faceplate, in. (mm)
s_L = longitudinal spacing of steel anchors, in. (mm)
s_T = transverse spacing of steel anchors, in. (mm)
t_p = plate thickness, in. (mm)

Equation 5-2 was developed by the authors for nonyielding stud anchors. The interfacial shear force is assumed to distribute linearly over the development length, and the maximum value is governed by the available shear strength, Q_{cv}, of the nonyielding anchor. Both Equations 5-3 and 5-4 are based on the consideration that the total shear strength of the anchors over the development length should be greater than or equal to the yield strength of the faceplate:

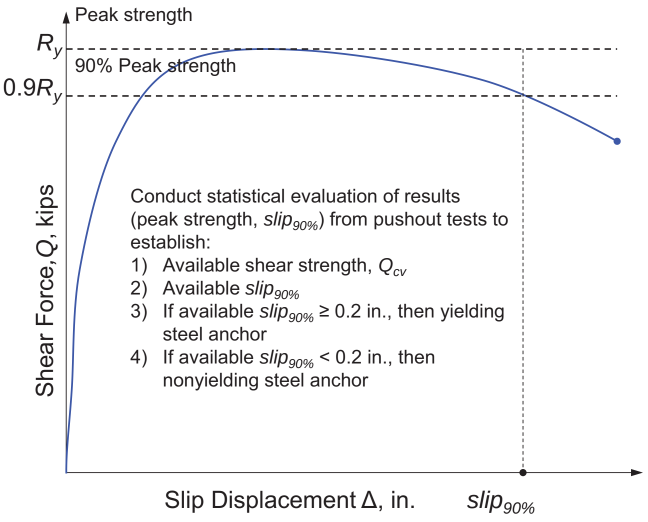

Conduct statistical evaluation of results (peak strength, $slip_{90\%}$) from pushout tests to establish:
1) Available shear strength, Q_{cv}
2) Available $slip_{90\%}$
3) If available $slip_{90\%} \ge 0.2$ in., then yielding steel anchor
4) If available $slip_{90\%} < 0.2$ in., then nonyielding steel anchor

Fig. 5-1. Typical steel anchor force-slip behavior from pushout tests (Bhardwaj et al., 2017).

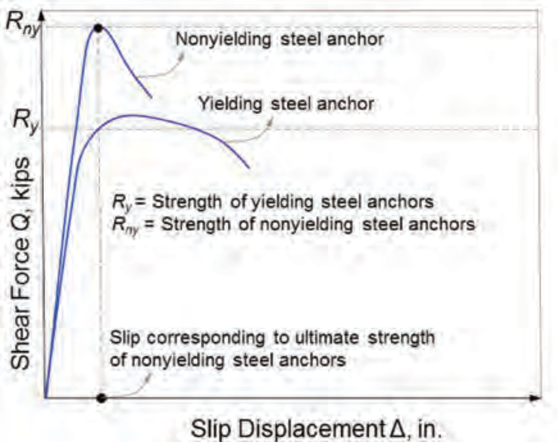

Fig. 5-2. Strength of yielding steel anchors that form part of a nonyielding steel anchor system (Bhardwaj et al., 2017).

$$\frac{1}{2} Q_{cv} \frac{L_d}{s_L} \geq s_T t_p F_y \tag{5-2}$$

The stud anchor spacing, s, is typically equal in the longitudinal, s_L, and transverse, s_T, directions, and Equation 5-1 and 5-2 can be simplified to Equation A-N9-3 of Appendix N9. The engineer selects or designs the development length, L_d, for the SC wall, and calculates the stud anchor spacing required to achieve it. The development length cannot exceed three times the wall thickness.

5.2.2 Interfacial Shear

When subjected to an out-of-plane shear force, V, there are three potential failure modes: (1) out-of-plane flexural yielding, (2) out-of-plane shear failure through the concrete infill and the ties, or (3) interfacial shear failure at the steel-concrete interface through the shear connectors. The out-of-plane flexural yielding limit state is discussed in detail by Sener et al. (2015b), and the out-of-plane shear failure mode is discussed in detail by Sener and Varma (2014). They have also provided available strength equations for SC walls. Appendix N9 includes equations for calculating the available flexural strength, $\phi_b M_n$ or M_n/Ω_b, based on Sener et al. (2015b), and the available out-of-plane shear strength, V_c, of SC walls based on Sener and Varma (2014). Therefore, this subsection focuses on the third failure mode—interfacial shear failure—which is somewhat similar to bond shear failure in reinforced concrete beams. The design philosophy is to prevent interfacial shear failure from occurring before out-of-plane shear failure; that is, interfacial shear failure should not be the governing failure mode of the three potential modes.

Figure 5-4(a) shows the free-body diagram of an SC wall subjected to out-of-plane shear force. The out-of-plane shear force, V, increases the out-of-plane bending moment, M, by Δ along the length of the shear span, L_v. As a result, the tensile force in the steel faceplate increases by Δ/jt_{sc} over the shear span length, where jt_{sc} is the arm length associated with the bending moment over the cross section and can be estimated conservatively as $0.9t_{sc}$ (Sener et al., 2015b). This increase in the tensile force is in equilibrium with the interfacial shear flow between the steel faceplate and concrete infill, which is resisted by the steel anchors as shown in Figure 5-4(b). The interfacial shear strength of the anchors must be greater than or equal to the shear flow demand to prevent failure.

Figure 5-4(c) shows the free-body diagram with yielding anchors resisting the interfacial shear flow. The interfacial shear strength is equal to the number of anchors—calculated as the shear span length divided by the longitudinal spacing, L_v/s_L—multiplied by the available shear strength, Q_{cv}, of the yielding anchor. As expressed by Equation 5-3, the interfacial shear strength should be greater than or equal to the demand shear flow. If the longitudinal and transverse spacing of anchors is equal, $s = s_L = s_T$, then Equation 5-3 can be simplified to Equation 5-4. In Equation 5-4, Δ/L_v is equal to the out-of-plane shear force, V, and is limited to the out-of-plane available shear strength, V_c, of the SC wall section. Thus, Equation 5-4 can be simplified to Appendix N9 Equation A-N9-4, which specifies the maximum spacing, s, of anchors to prevent interfacial shear failure from occurring before out-of-plane shear failure.

Similarly, Figure 5-4(d) shows the free-body diagram with nonyielding anchors resisting the interfacial shear flow. For this case, the interfacial shear strength is equal to one-half of the number of anchors, calculated as $L_v/2s_L$, multiplied by the available shear strength, Q_{cv}, of the nonyielding anchor, because the most stressed nonyielding anchor will fail before redistributing the shear flow over several anchors. Similar to the previous discussion, Equation A-N9-4 specifies the maximum spacing, s, of anchors to prevent interfacial shear failure from occurring before out-of-plane shear failure of the SC section. In Equation A-N9-4, the factor c_1 distinguishes between the design of yielding and nonyielding anchors.

$$Q_{cv} \frac{L_v}{s_L} \geq \frac{\Delta M_x}{0.9t_{sc}} s_T \tag{5-3}$$

$$s \leq \sqrt{\frac{Q_{cv}\,(0.9t_{sc})}{V_c}} \tag{5-4}$$

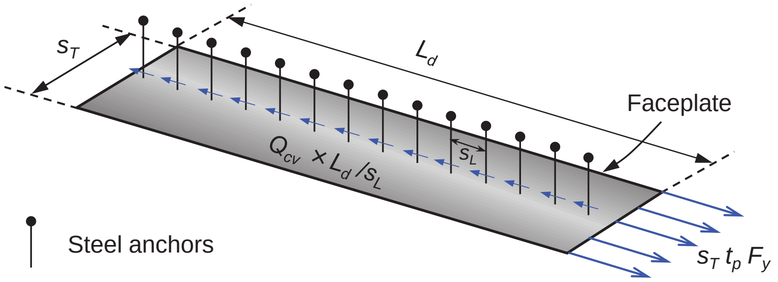

Fig. 5-3. Yielding steel anchor spacing requirement (Zhang et al., 2014).

where

L_v = length of shear span, in. (mm)

M_x = nominal flexural strength per unit width, kip-ft/in. (N-mm/m)

V_c = available out-of-plane shear strength per unit width in SC wall section, kip/ft (N/mm)

s = steel anchor spacing, in. (mm)

t_{sc} = SC section thickness, in. (mm)

The spacing of steel anchors needs to be the lesser of the spacing determined from Equations A-N9-3 and A-N9-4. Steel anchor spacing is typically governed by Equation A-N9-3, which includes the requirement for the development length to be no greater than $3t_{sc}$. However, for portions of the SC structure subjected to an extremely large out-of-plane moment gradient, Equation A-N9-4—the requirement for interfacial shear strength to be greater than the available out-of-plane shear strength—may control the steel anchor spacing.

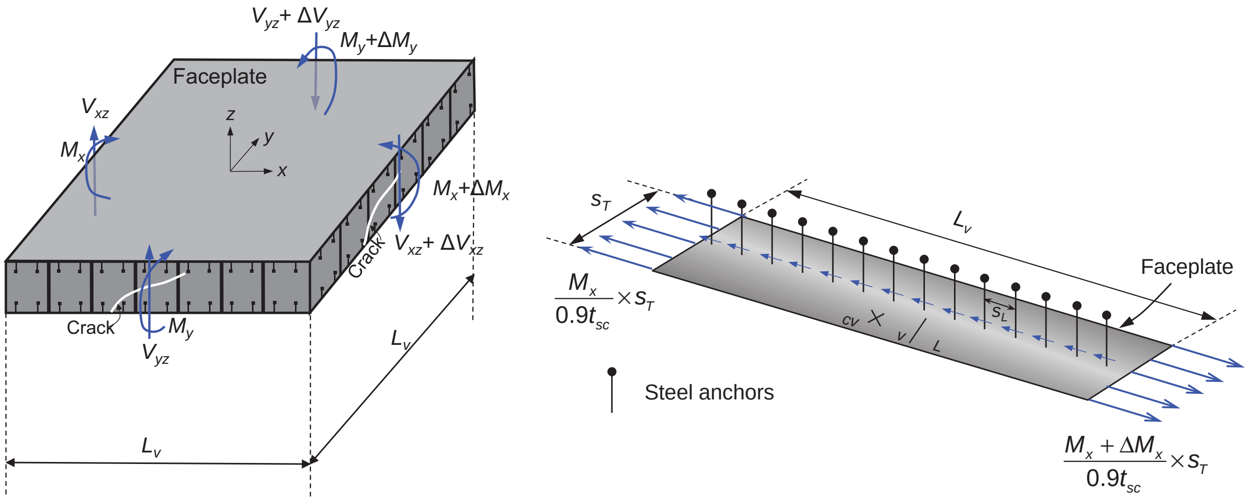

$V_{yz}+\Delta V_{yz}$
$M_y+\Delta M_y$
Faceplate
V_{xz}
M_x
z
y
x
$M_x+\Delta M_x$
Crack
$V_{xz}+\Delta V_{xz}$
Crack
M_y
V_{yz}
L_v
L_v
s_T
L_v
Faceplate
$\frac{M_x}{0.9t_{sc}} \times s_T$
s_L
cv × v / L
Steel anchors
$\frac{M_x+\Delta M_x}{0.9t_{sc}} \times s_T$

(a) Forces on SC wall section

(b) Forces on lower faceplate

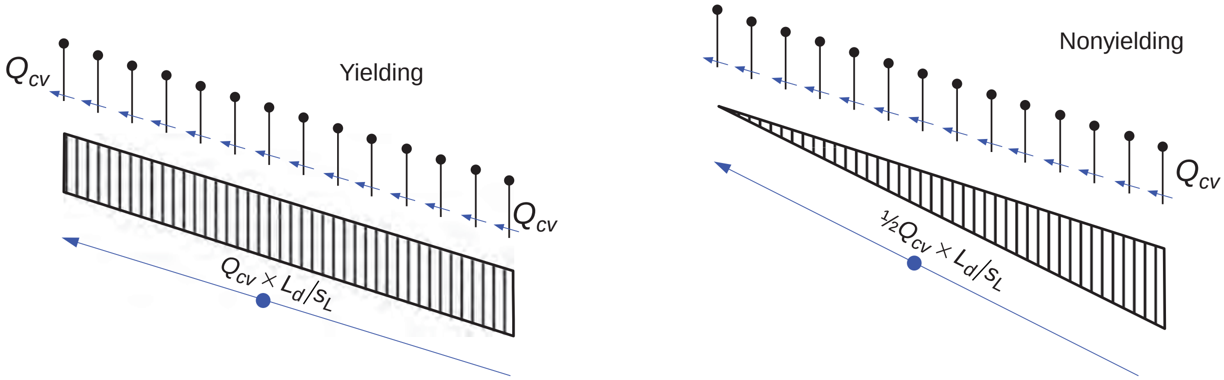

Q_{cv}
Yielding
Q_{cv}
$Q_{cv} \times L_d/s_L$
Nonyielding
Q_{cv}
$½Q_{cv} \times L_d/s_L$

(c) Shear resistance of yielding steel anchors

(d) Shear resistance of nonyielding steel anchors

Fig. 5-4. Steel anchor spacing requirement for preventing interfacial shear failure before out-of-plane shear failure (Bhardwaj et al., 2017).

Chapter 6
Tie Detailing

Ties are required by Appendix N9 to connect the steel faceplates of the SC wall through the concrete infill. A tie may be a single structural element, such as a tie rod, or an assembly of several structural elements, for example a tie with a gusset plate at one or both ends. They provide direct connectivity between the steel faceplates and, along with the stud anchors, enable the SC wall section to behave as an integral unit. SC walls for nuclear applications can be extremely thick, up to 60 in. as permitted by Appendix N9, with relatively thin (0.5- to 1.0-in.-thick) steel faceplates on the surfaces. If the steel faceplates are not tied together, there is a potential failure mode that consists of splitting or delamination of the wall section along a plane parallel to the faceplates through the concrete thickness. Such a failure mode has only been observed in the force transfer region of an axially loaded eccentric lap-splice connection (Seo et al., 2016), but not in member tests.

Ties serve multiple purposes in SC walls. They provide structural integrity in terms of resistance to delamination or splitting failure of the wall section through the concrete thickness. They provide out-of-plane shear reinforcement and contribute to the out-of-plane shear strength depending on their classification and spacing. Ties act in tandem with steel anchors to contribute to the interfacial shear strength of SC walls. Ties can also participate in the force transfer mechanisms associated with SC wall connections, if they are engaged appropriately. Additionally, the ties serve to maintain form—often supplemented by reinforcing ribs or additional formwork—before or during concrete casting.

6.1 CLASSIFICATION AND SPACING OF TIES

The design tensile strength of ties considers the limit states of gross yielding, net section rupture, and failure of tie-to-faceplate connections. If the limit state of gross yielding governs, the ties are considered as yielding; otherwise the ties are considered as nonyielding. Due to the differences between nominal and actual measured material properties, there may be cases where components that appear to be governed nominally by yielding may, in reality, be controlled by nonyielding limit states. Therefore, Appendix N9, Equation A-N9-5, specifies a minimum margin between the nominal strength calculated for yielding and nonyielding limit states. These requirements ensure that for ties to be classified as yielding, their nominal rupture strength, or the nominal strength of associated connections, should be at least 1.25 times the nominal yield strength. The nominal strength of the associated connection is calculated as the governing nominal strength of the welded or bolted connection of the tie to the faceplate. The classification of ties as yielding or nonyielding also governs their contribution to the out-of-plane shear strength.

The maximum spacing requirement for ties is influenced by the tie spacing requirement for compression members in ACI 349-06, Section 7.10.5.2 (ACI, 2006), which specifies that the tie spacing for reinforced concrete compression members is not to exceed 16 longitudinal bar diameters, 48 tie diameters, or the least dimension of the compression member. Due to the fundamental differences between reinforced concrete columns and SC walls, Appendix N9, Section N9.1.5, requires the ties to have a spacing no greater than the section thickness, t_{sc}.

6.1.1 Transfer Length

The transfer length, L_{TR}, is defined as the length required to develop strain compatibility between the steel and concrete portions of the composite section if only one of the portions is loaded at the end. The concept of transfer length is similar to load introduction length—the length over which steel anchors transfer longitudinal shear in composite sections—discussed in Section I6 of the AISC *Specification* (AISC, 2010b). Zhang et al. (2014) have analytically investigated transfer lengths for composite SC walls subjected to axial loading on the concrete only at the ends. As shown in Figure 6-1, strain compatibility (steel strain/concrete strain) or the percentage of composite action increases with distance from the concrete-only loaded ends. The transfer lengths are typically greater than or equal to $3t_{sc}$, for SC walls with reinforcement ratios of 0.015 to 0.050.

Zhang et al. (2014) show that SC walls designed with steel anchor spacing, s, to satisfy the faceplate slenderness requirement of Appendix N9, Equation A-N9-3, and to achieve development lengths, L_d, less than or equal to $3t_{sc}$, have transfer lengths, L_{TR}, greater than or equal to $3t_{sc}$. It is important to note that the development length, L_d, is associated with the shear strength of steel anchors and their ability to develop the yield strength of the faceplate. The transfer length, L_{TR}, is associated with the relative stiffness (force-slip behavior) of the steel anchors and their ability to develop strain compatibility between the faceplates and concrete infill. The transfer lengths are longer than the development lengths for typical SC wall designs.

The effects of having transfer lengths longer than the development lengths are inconsequential. The design capacities or available strengths of SC walls depend on developing the yield strength of the faceplates, not strain compatibility. The effective stiffness of the composite section depends on

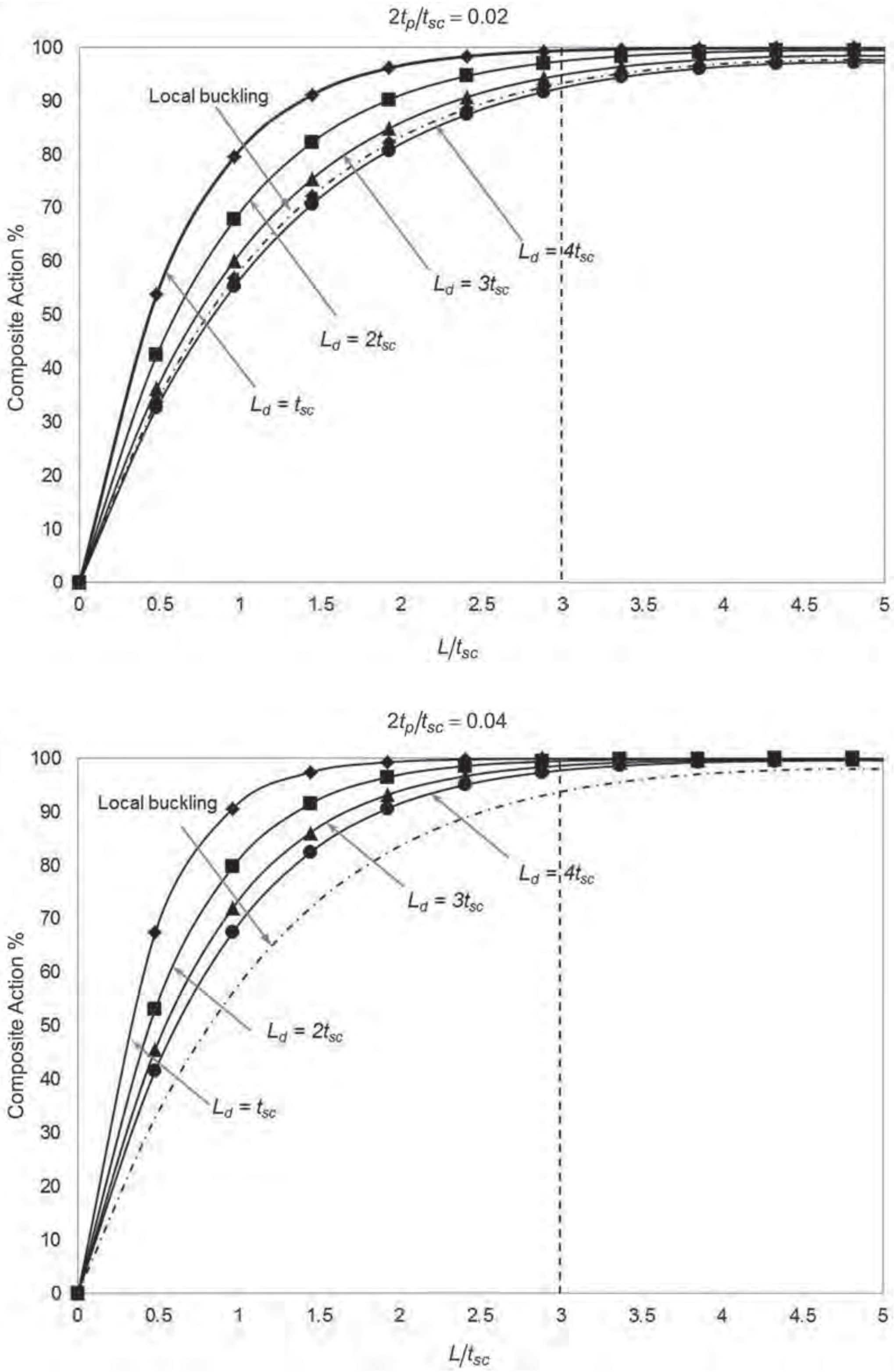

Fig. 6-1. Development of strain compatibility with distance from member end (from Zhang et al., 2014).

strain compatibility but is dominated by the effects of concrete cracking. The effects of having longer transfer lengths and 75 to 90% composite action on effective stiffness are marginal compared to the reduction due to concrete cracking (Zhang et al., 2014).

The transfer length used in the tie strength and spacing requirements discussed in the following sections is limited to $3t_{sc}$. Smaller values are improbable, and larger values will reduce the required tensile force, F_{req}, that the ties have to be designed for. Thus, using $L_{TR} = 3t_{sc}$ is conservative for the calculation of the required tensile strength.

6.2 REQUIRED TENSILE STRENGTH OF TIES

The required tensile strength for ties is based on a postulated failure mode of section delamination or splitting through the concrete thickness of the SC wall. As mentioned earlier, this failure mode has not been observed in any SC wall member or component tests. However, it is possible in the connection regions of SC walls where only one of the two components, faceplates or concrete infill, are directly loaded—for example, in eccentric lap splice anchorage of SC walls to the concrete basemat (Seo and Varma, 2017). This failure mode is improbable but catastrophic and can be prevented by appropriately designed ties. This section develops the required tensile strength of ties to prevent the occurrence of a postulated splitting or delamination failure mode in the connection and load transfer region of an SC wall.

There are two loading cases, where forces are applied to only one of the two components—faceplates or concrete infill—that can introduce an eccentric moment, M_o, in the SC walls. This eccentric moment is resisted by the ties. The required tensile strength of the ties to resist the eccentric moment can be determined as follows.

Case 1 is when the load is applied to concrete only, and the moment is resisted by the composite section. If the compressive forces are applied only to the concrete, they will transfer into the composite section over the transfer length, L_{TR}. Figures 6-2 and 6-3 illustrate the forces in the composite section. Over this transfer length, there will be an eccentric moment, M_o, that has to be resisted by the cross section without splitting. The resisting moment, M_R, is depicted in Figure 6-4.

Figure 6-2 considers a lateral section of the wall length along the transfer length, L_{TR}. The compressive force applied to the concrete on the left transfers to the composite section over the transfer length on the right. In Figure 6-3, K_s and K_c are the stiffnesses of steel and concrete, respectively. Figure 6-3 establishes that there is an eccentric moment, M_o, resulting from the significant thickness, t_{sc}, of the wall, and the fact that the force applied on the left-hand side and

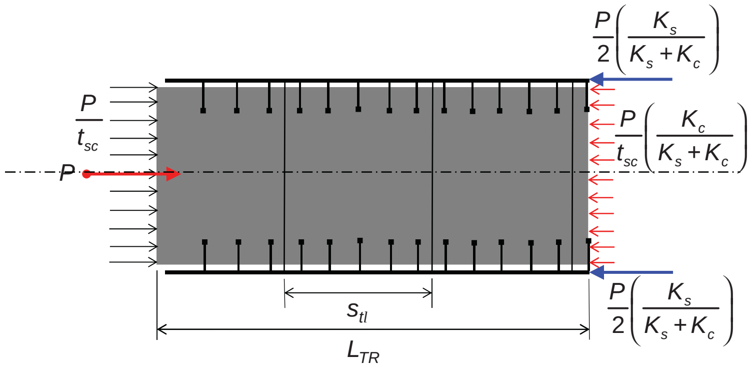
$\frac{P}{2}\left(\frac{K_s}{K_s+K_c}\right)$
$\frac{P}{t_{sc}}$
$\frac{P}{t_{sc}}\left(\frac{K_c}{K_s+K_c}\right)$
P
s_{tl}
L_{TR}
$\frac{P}{2}\left(\frac{K_s}{K_s+K_c}\right)$

Fig. 6-2. Load applied to concrete only, resisted by composite section.

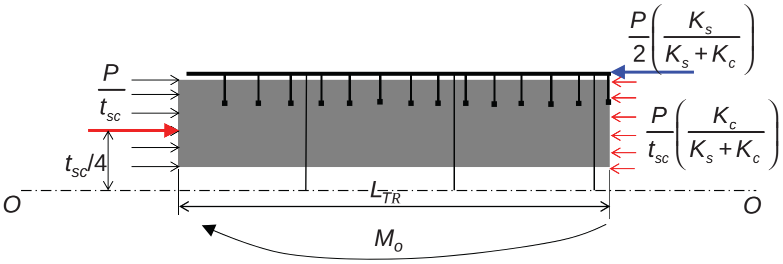
$\frac{P}{2}\left(\frac{K_s}{K_s+K_c}\right)$
$\frac{P}{t_{sc}}$
$\frac{P}{t_{sc}}\left(\frac{K_c}{K_s+K_c}\right)$
$t_{sc}/4$
O
L_{TR}
O
M_o

Fig. 6-3. Eccentric moment, M_o, *acting to split section.*

the resultant on the right-hand side are not collinear. The moment, M_o, is determined as shown in Equation 6-1:

$$M_o = \frac{P}{2}\left(\frac{K_s}{K_s + K_c}\right)\left(\frac{t_{sc}}{4}\right) = steel\ plate\ force\left(\frac{t_{sc}}{4}\right) \tag{6-1}$$

where

K_c = stiffness of concrete

K_s = stiffness of steel

P = applied force, kips (N)

t_{sc} = SC section thickness, in. (mm)

Figure 6-4 shows how the eccentric moment, M_o, is resisted by the ties with area, A_{tie}, acting along with the concrete in compression. As shown, the strain diagram is assumed to be linear, but the contribution of the concrete to resist tensile stresses is conservatively neglected. The size of the concrete compression block is also assumed to be very small to simplify calculations, and the contribution of the concrete compression block to the resisting moment, M_R, is also conservatively ignored. As shown by the plan view in Figure 6-4, a region of the wall with dimensions L_{TR} and s_{tt} with contributing ties is considered. The resisting moment, M_R, is calculated as shown in Equation 6-2 by including the contributions of all the ties in the wall region:

$$\begin{aligned} M_R &= \sum_{i=1}^{n-1}(2)(0.5A_{tie})\left(\frac{i}{n}\sigma_{req}^{n}\right)(i)(s_{tl}) + \\ &\quad (2)(0.25A_{tie})(\sigma_{req}^{n})(n)(s_{tl}) \\ &= \left[\frac{(n-1)(2n-1)}{6} + \frac{n}{2}\right]s_{tl}F_{req}^{n} \\ &= \left[\frac{1}{3}\left(\frac{L_{TR}}{s_{tl}}\right)^2 + \frac{1}{6}\right]s_{tl}F_{req}^{n} \end{aligned} \tag{6-2}$$

where

A_{tie} = area of ties, in.^{2} (mm^2)

F_{req}^{n} = tie force required to resist the overturning moment, kips (N)

$= A_{tie}\sigma_{req}^{n}$

L_{TR} = length of wall, in. (mm)

n = number of ties in the transfer length region

s_{tl} = width of wall, in. (mm)

σ_{req}^{n} = tie stress, ksi (MPa)

The required tie tensile strength for each individual tie, F_{req}, is estimated by setting M_R equal to M_o, and is given by Appendix N9, Equation A-N9-6. Based on the study by Zhang et al. (2014), a transfer length value of $3t_{sc}$ has been used in the formulation of Appendix N9, Equation A-N9-6.

The second case that can give rise to eccentric moments is when the tensile forces are applied only to the faceplates.

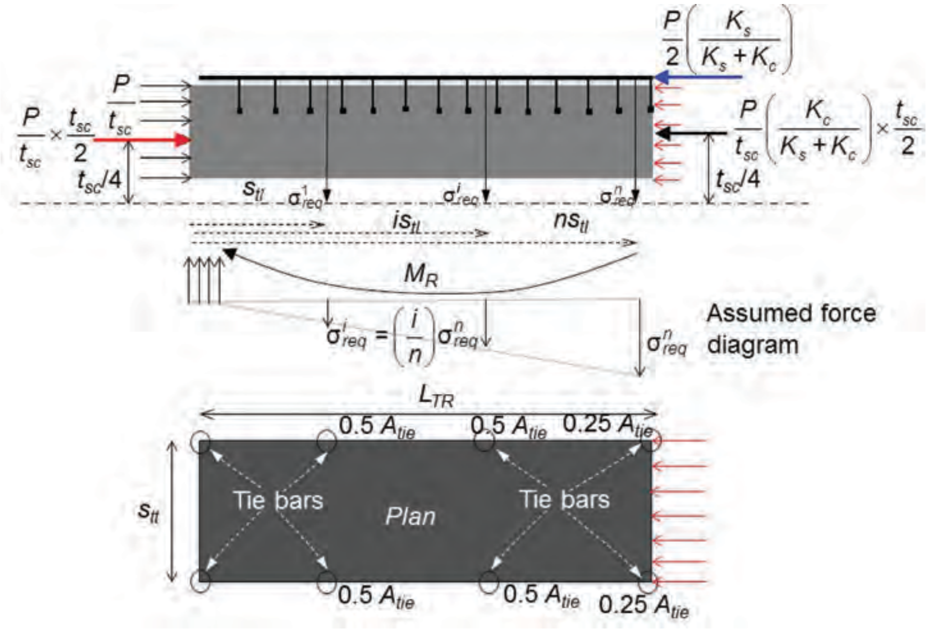
$\frac{P}{2}\left(\frac{K_s}{K_s+K_c}\right)$
$\frac{P}{t_{sc}}$
$\frac{P}{t_{sc}} \times \frac{t_{sc}}{2}$
$\frac{P}{t_{sc}}\left(\frac{K_c}{K_s+K_c}\right) \times \frac{t_{sc}}{2}$
$t_{sc}/4$
$t_{sc}/4$
s_{tl}
σ_{req}^{1}
σ_{req}^{i}
σ_{req}^{n}
is_{tl}
ns_{tl}
M_R
$\sigma_{req}^{i} = \left(\frac{i}{n}\right)\sigma_{req}^{n}$
σ_{req}^{n}
Assumed force diagram
L_{TR}
0.5 A_{tie}
0.5 A_{tie}
0.25 A_{tie}
s_{tt}
Tie bars
Plan
Tie bars
0.5 A_{tie}
0.5 A_{tie}
0.25 A_{tie}

Fig. 6-4. Resisting moment, M_R.

In this case, the forces will transfer to the composite section over the transfer length, L_{TR}, until concrete cracking occurs. Once beyond this transfer length, there will be an eccentric moment, M_o, that has to be resisted by the cross section without splitting. Additionally, there may be a case where there is an imbalance in the forces in the thick SC cross section due to different actual areas and yield strengths of the faceplates. For example, under in-plane shear loading, the composite section typically develops the yield strength of the section, which could imply slightly different yield forces in the faceplates due to differences in the actual areas or yield stresses (Appendix N9 requires the faceplates to have the same nominal thickness and yield stress). The required force, evaluated using Equation A-N9-6, is applicable for these cases as well.

The required force, F_{req}, is a hypothetical demand that has been posited to ensure the structural integrity of the SC wall by avoiding the splitting failure of the section. It should not be deducted from the available strength of the ties.

Chapter 7
Modeling Parameters for Analysis

SC wall structures are modeled using elastic finite elements. Other methods of analysis have been ruled out because the finite element method is the only practically feasible method for global analysis of continuum structures. These finite elements can be thick-shell finite elements—such as a thick shell with consideration of transverse shear stiffness/deformation, incompatible modes, or output of eight stress resultants—or solid finite elements. Rigid regions at joints may be modeled for consideration of out-of-plane shear results in connection regions. Finer meshes are used around section penetrations larger than half the wall thickness. When using shell elements to model the expanse of the SC walls, it is recommended to use meshes consisting of at least four to six elements along the short direction and six to eight elements along the long direction. These numbers are based on recommendations in ASCE 4-98 (ASCE, 1998) and will adequately capture local modes of vibration. Finite elements larger than $2t_{sc}$ are not recommended for the interior regions. Finite elements larger than t_{sc} are not recommended for connection regions or regions around section penetrations. These element size limits are recommended based on the design strength equations, which are calculated on a per unit width basis, that are deemed appropriate up to $2t_{sc} \times 2t_{sc}$; that is, the equations do not apply to the whole wall. The limit on the mesh size ensures that the analysis outputs are sufficiently accurate.

Seismic analyses of safety-related nuclear facilities are typically conducted using the multi-step approach in ASCE 4-98: the first step being dynamic soil structure interaction (SSI) analyses, and the second step being the subsequent equivalent static or dynamic analyses of the structure only, using response from the SSI analysis as input (Varma et al., 2014). The viscous damping ratios for a safe shutdown earthquake (SSE) seismic analysis can be assumed to not exceed 5%, and this is based on 1/10th scale tests of the entire containment internal structure (CIS) consisting of SC modules (Akiyama et al., 1989). However, for custom designs for an operating basis earthquake (OBE) where in-structure response spectra (ISRS) need to be generated, a damping ratio of 5% is unconservative and lower ratios may have to be used, for example, 2 to 3%. Additional dynamic analysis may be needed to determine the response of structures to impactive or impulsive loads. This is characteristic of the structural design of safety-related nuclear facilities and comparable to ACI 349-06, Appendix F (ACI, 2006), and also to ANSI/AISC N690, Section NB3.15.

Second-order analysis will generally be unnecessary for the labyrinthine structures where SC walls will be used. The thickness of SC walls in a nuclear application will generally exceed 2 ft (0.6 m). The typical wall height-to-thickness ratios will meet the requirements of ACI 318 and ACI 318M, Section 10.10.1(b) (ACI, 2008). In the rare situation that the ACI requirements are not satisfied, the structure will generally meet the limitations of AISC *Specification* Appendix 7, Section 7.3, allowing a first-order analysis to be performed with notional lateral loads in lieu of a second-order analysis. Second-order analysis by the direct analysis method is limited to steel frame structures with linear beam or column elements. It is not applicable to labyrinthine structures made up of SC or RC walls.

7.1 LOADS AND LOAD COMBINATIONS

Loads acting on the structure are determined based on ANSI/AISC N690 Chapter NB2. Load combinations consistent with those provided in Chapter NB2 are used to conduct analysis and calculate the design force demands. The load combinations imply linear superposition of the required strengths. Analysis is performed for operating thermal combinations, Condition A, and accident thermal combinations, Condition B. Because the analysis is elastic, the thermal demands are combined with demands due to mechanical loads using appropriate load combinations. The load combinations for operating thermal and seismic do not consider concrete cracking. However, concrete cracking is considered in accident thermal and seismic. The concrete is considered cracked for both mechanical and thermal loads, and thus the demands due to these loads are linearly superimposed.

7.2 GEOMETRIC AND MATERIAL PROPERTIES FOR ANALYSIS

An elastic finite element model of the composite SC section is developed using a single material. As mentioned earlier, this model is the basic model for dynamic SSI and subsequent analysis. The SSI analysis model is often coarsely meshed and will have soil and foundation modeled. The subsequent analysis model for structural design has finer mesh for more accurate stress calculations (ASCE, 1998). For this single material elastic model, the following steps are followed to determine the material properties:

(a) Poisson's ratio, thermal expansion coefficient, and thermal conductivity of the material are matched to those of the concrete, as these parameters will govern the thermally induced displacements of the structure.

(b) The model section thickness and material elastic modulus is calibrated so that the effective stiffnesses of the model match those of the physical SC wall section.

(c) The material density is calibrated to match the mass of the model with that of the physical section.

(d) The material specific heat is calibrated to match that of the concrete. This will allow transient heat transfer analysis to be accurately conducted using the elastic, single material, finite element model.

7.3 STIFFNESS VALUES FOR THE MODEL

The effective stiffness values used in the linear elastic model are determined for operating thermal and accident thermal conditions. Because there is uncertainty in the stiffness manifest during the thermal accident event, upper (operating thermal) and lower bound (accident thermal) stiffness values are both considered for the analysis. The stiffness values are determined by considering the expected pre-accident and post-accident cracking. The basis of these stiffness values is discussed in the following.

7.3.1 Effective Flexural Stiffness

The effective flexural stiffness for analysis of SC walls is determined according to ANSI/AISC N690, Equation A-N9-8. The equation is based on experimental studies by Booth et al. (2007) and Varma et al. (2009, 2011a). The studies indicate that the uncracked composite flexural stiffness is generally not manifest in SC walls. This is due to effects of locked-in shrinkage strains in the concrete core, partial composite action of the section, and reduced bond parameter due to discrete steel anchor locations.

The cracked transformed flexural stiffness of the SC wall for a wide range of parameters can be expressed using the stress, strain and force block in Figure 7-1, where n is the concrete-to-steel modular ratio, E_c/E_s; e_c is the top plate strain; c is the distance to the neutral axis; and strain compatibility between the extreme concrete fibers and the faceplates is assumed.

The depth of the neutral axis can be determined from equilibrium of the forces shown in Figure 7-1, which gives ANSI/AISC N690, Equation C-A-N9-1a. The corresponding flexural stiffness, $(EI)_{cr\text{-}tr}$, per unit width can then be calculated as given in ANSI/AISC N690, Equation C-A-N9-3a. However, Varma et al. (2011a) calibrated this equation to the simpler form given in ANSI/AISC N690, Equation A-N9-8. Studies from Booth et al. (2007) and Varma et al. (2009; 2011a) have further shown that operating thermal loading conditions produce linear thermal gradients, which develop gradually over time. As a result, there is little to no additional concrete cracking due to operating thermal loading and the cracked-transformed section flexural stiffness applies. However, accident thermal loading increases the faceplate temperature rapidly, while the concrete temperature lags behind. In addition, a nonlinear temperature gradient develops through the composite cross section because of the significantly lower thermal conductivity of concrete, and this gradient results in cracking of the concrete due to its low tensile stress, f_t'.

The flexural stiffness recommendation accounts for the potential cracking of the concrete due to the accident thermal gradient through the composite section. It considers temperature increases greater than 150°F (83°C) on the faceplates that result in full through-section concrete cracking—that is, the flexural stiffness will be equal to that of the steel, E_sI_s, alone. For faceplate surface temperature change from 0°F to 150°F (−18°C to 66°C), the cracked-transformed flexural stiffness, $E_sI_s + c_2E_cI_c$, is linearly reduced until it equals the steel section stiffness, E_sI_s, which is the minimum effective

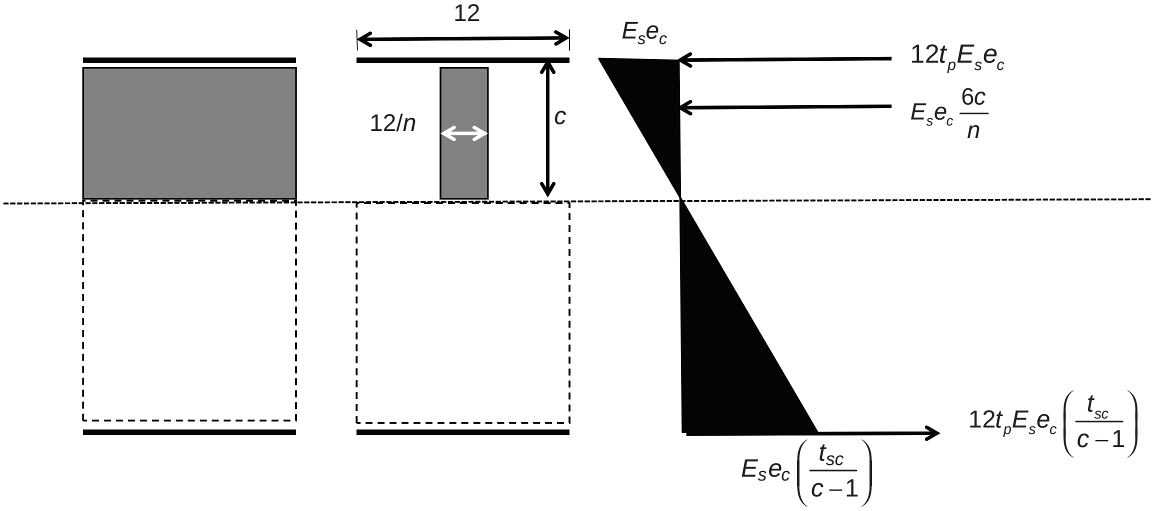
12
12/n
c
E_se_c
$12t_pE_se_c$
$E_se_c\frac{6c}{n}$
$12t_pE_se_c\left(\frac{t_{sc}}{c-1}\right)$
$E_se_c\left(\frac{t_{sc}}{c-1}\right)$

Fig. 7-1. Flexural stiffness of cracked-transformed section of SC walls.

flexural stiffness. The average of the maximum surface temperature increases, ΔT_{savg}, is calculated by taking the average of the maximum surface temperature increases on the two faceplates, ΔT_{s1}^{max} and ΔT_{s2}^{max}, due to accident thermal conditions.

7.3.2 Effective In-Plane Shear Stiffness

The in-plane shear behavior of SC walls without accident loading is governed by the plane-stress behavior of the faceplates and orthotropic cracked behavior of the concrete infill. Ozaki et al. (2004) and Varma et al. (2011e) have developed a trilinear shear force-shear strain model for SC walls with reinforcement ratios, ρ, from 0.015 to 0.050. According to this mechanics based model (MBM), composite uncracked behavior of the SC wall occurs when the in-plane shear force is less than or equal to the cracking threshold, S_{cr}. Figure 7-2 shows a plot of experimental versus calculated values of cracking strength by Varma et al. (2014). The cracking strength, S_{cr}, is calculated assuming the shrinkage strain, ε_{sh}, to be $0.063\sqrt{f_c'}/G_c$. The pre-cracking shear stiffness can be estimated as the composite shear stiffness, $GA_s + G_cA_c$. It is important to understand that the composite action between the faceplates and the concrete infill, facilitated through the steel anchors and ties, is discrete and not perfect.

After cracking, the tangent stiffness is governed by the cracked orthotropic behavior of concrete acting compositely with faceplates that are in a state of plane stress. However, under seismic loading, the cyclic behavior of SC walls is governed by secant stiffness, K_{xy}^{sec}, not tangent stiffness. The secant stiffness can be estimated as a function of the applied shear force, S_{rxy}. Figure 7-3 illustrates the variation of normalized secant stiffness with normalized in-plane shear-force for different values of the strength-adjusted reinforcement ratio, $\bar{\rho}$. The secant stiffness, K_{xy}^{sec}, is normalized with respect to the uncracked stiffness, K_{xy}^{uncr}, and the applied shear force, S_{rxy}, is normalized with respect to the nominal in-plane shear strength, V_{ni}. It is observed in Figure 7-3 that the secant stiffness drops exponentially after the occurrence of cracking, and reaches the cracked stiffness, K_{xy}^{cr}, asymptotically.

Considering this variation in the secant stiffness, Varma et al. (2011a) developed a simple model for estimating the secant stiffness of SC walls, as shown in Figure 7-4. The equations for in-plane shear stiffness of SC walls are based on this model. For in-plane shear force values, S_{rxy}, less than the cracking threshold, S_{cr}, the effective secant stiffness, K_{xy}^{sec}, is the uncracked stiffness of the section. For S_{rxy} values greater than twice the cracking threshold, the effective stiffness is the post-cracking shear stiffness. Between S_{cr} and $2S_{cr}$, S_{rxy} is determined by linear interpolation.

The use of stainless steel plates does not change the in-plane shear stiffness and strength of SC walls. The concrete infill is still the major contributor to the in-plane shear stiffness before and after cracking. The contribution of the stainless steel faceplates can be accounted for appropriately by using the corresponding value of shear modulus.

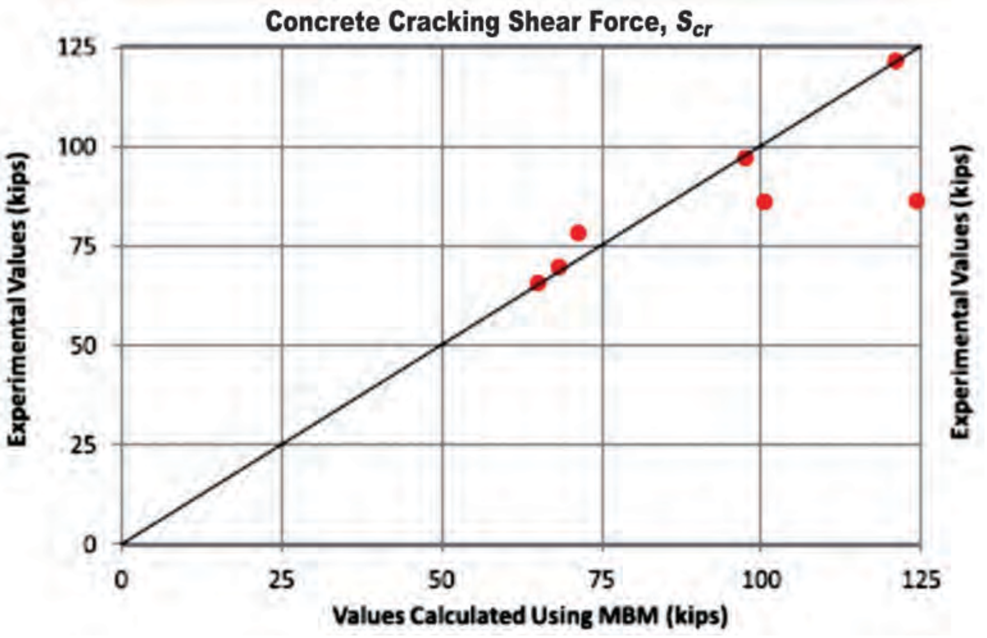

Fig. 7-2. Experimental versus calculated values of cracking strength (Varma et al., 2014).

Additionally, the in-plane shear strength from ANSI/AISC N690, Equation A-N9-19, will be slightly conservative for stainless steel plates due to its lower elastic modulus and early onset of strain hardening.

The in-plane shear stiffness of SC walls after accident thermal loading was evaluated experimentally by researchers in Japan (Ozaki et al., 2000). As discussed in Varma et al. (2011a), nonlinear (parabolic) thermal gradients develop through the concrete section due to the loading. This gradient induces concrete cracking in two orthogonal directions due to the expansion of faceplates and the low cracking threshold of the concrete. The accident thermal loading eliminates the uncracked shear force-strain behavior. Thus, the in-plane shear stiffness of SC walls after accident thermal loading can be estimated as the post-cracking shear stiffness of the composite section. These orthogonal cracks due to thermal loading do not reduce the in-plane shear strength of SC wall panels significantly.

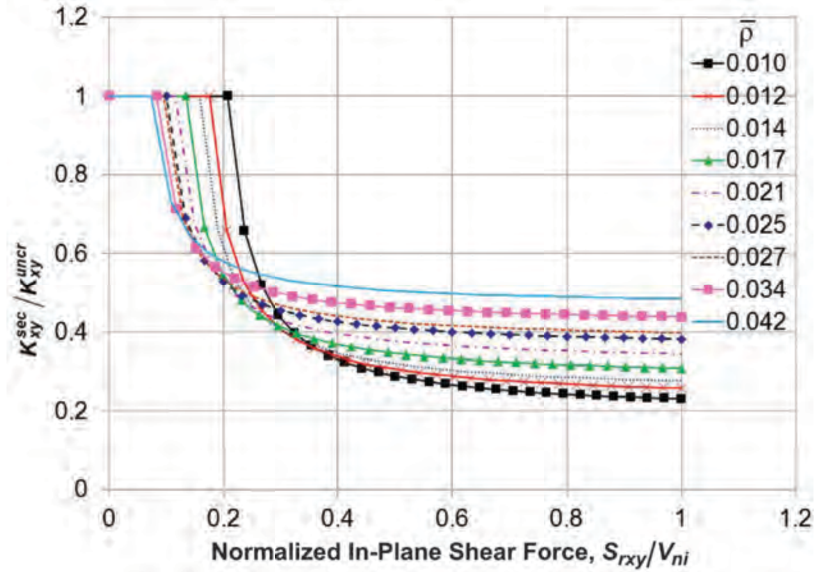

Fig. 7-3. Variation of secant stiffness of SC walls (Varma et al., 2011a).

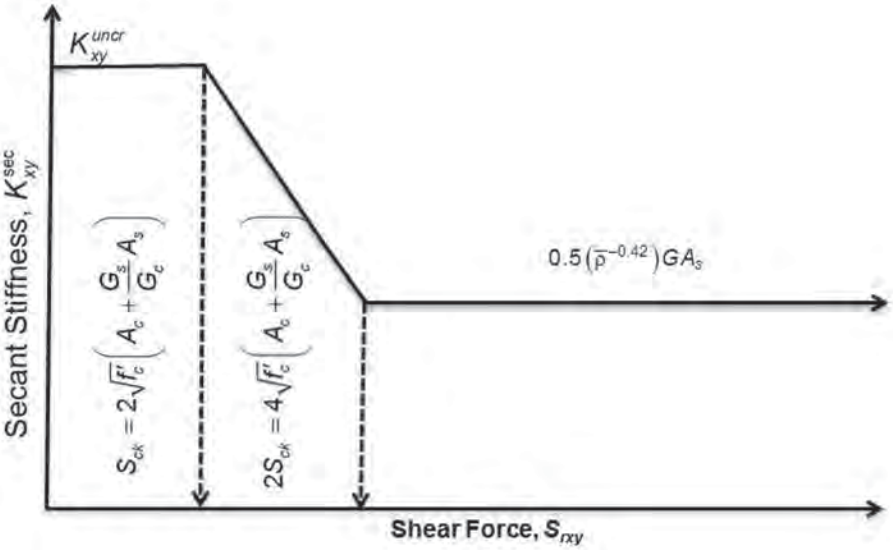

K_{xy}^{uncr}
Secant Stiffness, K_{xy}^{sec}
$S_{ck} = 2\sqrt{f'_c}\left(A_c + \frac{G_s}{G_c}A_s\right)$
$2S_{ck} = 4\sqrt{f'_c}\left(A_c + \frac{G_s}{G_c}A_s\right)$
$0.5\left(\bar{\rho}^{-0.42}\right)GA_s$
Shear Force, S_{rxy}

Fig. 7-4. A simple model for secant stiffness with no accidental thermal loading (Varma et al., 2011a).

7.4 MODELING THE OPENINGS

Any openings in the SC walls need to be modeled according to Section N9.1.7 of ANSI/AISC N690. The load redistribution around an opening creates stress concentrations, the severity of which depends on factors such as size of the opening, presence or absence of sharp reentrant corners, and type and magnitude of loading. Under severe loading, the faceplate may yield at or near the reentrant corners. However, the area over which yielding occurs and the magnitude of plastic strain remains below the fracture strain limit as long as (1) good detailing practices are used, and (2) the faceplate effective stress due to averaged demands over a small region around the opening is below the yield stress limit. This philosophy is the same as in ASME pressure vessel design (ASME, 2013).

In addition to the effect on demands, the presence of an opening affects the available strength of the SC panel section. This happens in two ways: (1) the region in the vicinity of the opening is not fully effective as an SC section due to the free edge of steel and concrete at the opening location, unless special detailing is provided to achieve a fully developed faceplate at the opening perimeter; see Section N9.1.7 of ANSI/AISC N690; and (2) the sharp reentrant corners of openings will lead to stress concentrations and large plastic strains in the faceplate. Good detailing practices such as avoiding sharp reentrant corners and development of the faceplate to help redistribute the demands to regions away from the edges and corners of the opening are required to avoid loss in panel section strength due to the opening.

The detailing requirements aim at reducing the stress concentration effects and, if desired, achieving a fully developed edge at the opening perimeter. Absent a fully developed edge at the opening perimeter, a fully effective SC panel section will be manifested some distance away from the free edge. The pertinent detailing requirement limits the distance from the free edge to the fully effective SC panel section.

Available literature provides data on the effect of small openings on the section strength. This presents the possibility that the effect of small openings can be accounted for by using simple prescriptive rules such that the analytical model need not include small openings. With this in mind, Appendix N9 classifies the openings as small or large based on whether their largest dimension is greater than or less than half the thickness of the wall. The limit of $t_{sc}/2$ is considered adequately small compared to the evaluation size, $2t_{sc}$, of panel section for calculating average design strength. The modeling, detailing and evaluation criteria to be followed for the SC wall region in the vicinity of small openings and large openings is discussed in the following section.

7.4.1 Design and Detailing Requirements Around Small Openings

To help ensure good connection performance, fully developed edges are required for small openings located within the connection region; however, this does not necessarily negate the need for connection qualification.

Design and Detailing for Free Edge at Opening Perimeter

Experiments conducted by Japanese researchers (Ozaki et al., 2004) indicate that the maximum decrease in SC panel section strength due to penetrations with an undeveloped edge is about 15 to 20%. Based on these test data, the effect of small openings is considered by conservatively taking a 25% reduction in the strength of the affected SC panel section(s). In case one panel section encompasses the opening (Opening A in Figure 7-5), the strength of just that panel

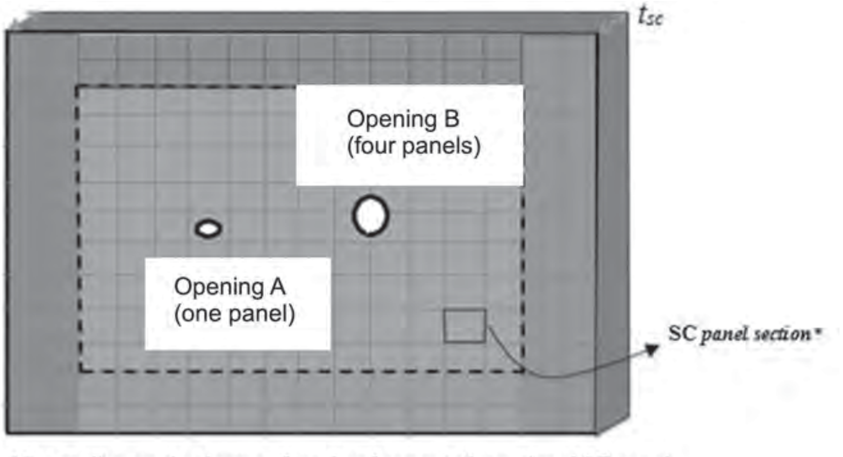

*Depending on the degree of mesh refinement, the notional SC panel section may/may not be the same as an element in the FE mesh.

Fig. 7-5. Reduction in strength due to presence of opening.

section is reduced. In case the opening lies in more than one panel section (Opening B in Figure 7-5), the strength of all panel sections that partially include the opening are reduced by 25%.

Openings with sharp reentrant corners can still be problematic for the faceplate. The available test data does not clearly address the effect of sharp reentrant corners. Because of these considerations, some provision for corner radii is warranted to avoid the potential for fracture at the sharp corners. The data point for this is derived from AISC Design Guide 2, *Steel and Composite Beams with Web Openings* (Darwin, 1990). Figure 7-6 illustrates the radius required to be provided at the reentrant corners. The coping radius, typically twice the thickness, has been limited to four times the thickness to try and further smooth the stress distribution. To help maintain structural integrity against any potential for splitting, a detailing requirement has been provided for locating the first tie within $t_{sc}/4$ from the edge of the opening.

Design and Detailing for Fully Developed Edge at Opening Perimeter

With a fully developed edge at the opening perimeter, the SC panel sections in the vicinity of the opening will be fully effective beginning at the opening edge. A fully developed edge is achieved by providing a welded steel sleeve across the opening. This sleeve has two flange plates welded at its ends to help transfer the faceplate stresses to the sleeve. Normal and tractive stresses at the edge of the faceplate are thus transferred to the sleeve, which in turn transfers them to the concrete infill because it is anchored into the concrete using steel anchors. The sleeve and flange plate thickness and yield stress are specified such that faceplate stresses can be adequately transferred to the concrete.

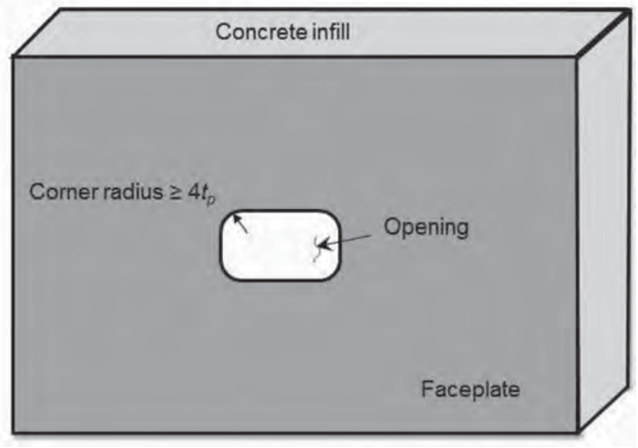

Fig. 7-6. Radius of reentrant corners (view of the SC panel section).

The detailing for the sleeve can be thought of as a cylinder spanning across the SC wall section with annular discs welded at its two edges. The flange plate is extended a minimum distance of one times the SC wall thickness to provide additional strength in the stress concentration region. As described in the following, the faceplate is welded to either just the flange plates, or both the flange plates and the sleeve depending on the thickness of the flange plate:

- In the case that the thickness of the flange plate is less than 1.25 times the faceplate thickness, then the faceplate acts as a doubler/reinforcing plate that helps deliver the concentrated stresses to the sleeve (see Figure 7-7).
- If the flange plate is thicker than 1.25 times the faceplate thickness, it is deemed capable of taking care of the stress concentration effects by itself. Hence, the faceplate need only be welded to the flange plate, which meets up with the sleeve (see Figure 7-8).

No reduction in SC panel section strength is considered because of exercising either of the detailing requirements. Furthermore, as in the case of an opening with a free edge, the stress concentration around openings is alleviated by avoiding sharp reentrant corners.

7.4.2 Design and Detailing Requirements Around Large Openings

Compared to the requirements for small openings, a more rigorous set of criteria is followed for large openings.

Design and Detailing for Free Edge at Opening Perimeter

When detailed as a free edge, the opening is required to be modeled as larger than the physical opening. The composite behavior of a wall section develops fully only after the development length is reached. The SC wall in the intervening region cannot attain its full strength and is, therefore, ignored in the analytical model. The faceplate development length, L_d, is typically no greater than $3t_{sc}$. Thus, considering a development length of just one times t_{sc}, the as-modeled opening dimension will be two times the section thickness more than the physical opening dimension, as seen in Figure 7-9. For example, under this free edge option, a 4-ft (1.2 m)-diameter circular opening in a 4-ft (1.2 m)-thick SC wall will have to be modeled as a 12-ft (3.6 m)-diameter opening, which may severely increase the resulting analysis-based demands for the surrounding SC panel sections This risks the possibility that they will be inadequate unless thicker faceplates are used locally.

Because the region of stress concentration and partial composite action has not been modeled, no reduction in strength needs to be considered for the as-modeled SC wall. As in the case of small openings, stress concentration effects are minimized by providing corner radii at reentrant corners.

To help maintain structural integrity against any potential for splitting, a detailing requirement has been provided for locating the first tie within $t_{sc}/4$ from the edge of the opening.

Design and Detailing for Fully Developed Edge at Opening Perimeter

The edge will be fully developed with the same detailing requirements as for small openings. However, the demands need to be obtained by modeling the physical opening.

7.4.3 Bank of Small Openings

The region affected by a concentrated bank of small openings needs to be considered as a large opening when the clear distance between adjacent small openings is equal to or smaller than:

(a) $2t_{sc}$ for openings designed and detailed for the free edge at the opening perimeter.

(b) t_{sc} for openings designed and detailed for the fully developed edge at the opening perimeter.

The physical dimensions of the large opening are equal to the distance between the outermost edges of the bank of small openings.

7.5 ANALYSIS INVOLVING ACCIDENT THERMAL LOADS

Analyses for load combinations involving accident thermal conditions (Condition B) needs to include heat transfer analyses. Heat transfer analyses is conducted using the geometric and material properties for the linear elastic material, to estimate the temperature histories and through-section

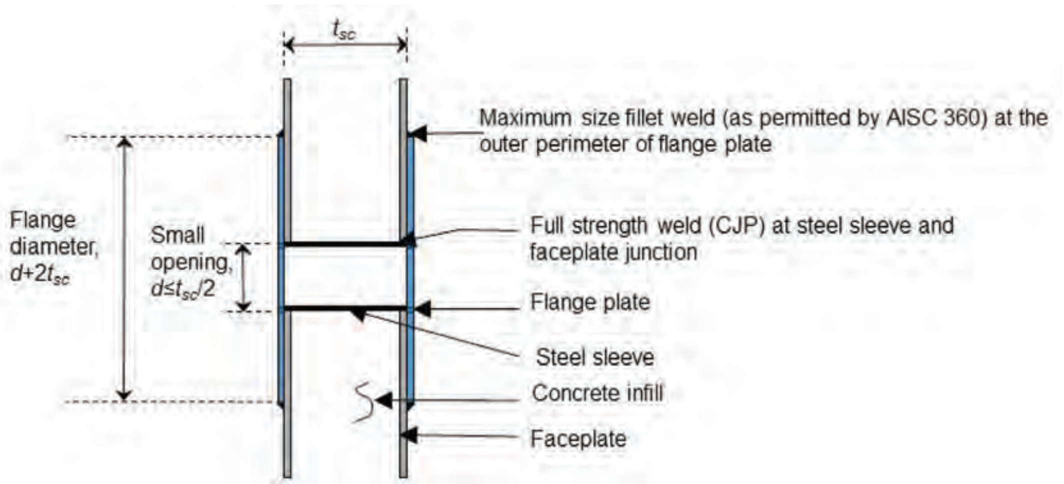
t_{sc}
Maximum size fillet weld (as permitted by AISC 360) at the outer perimeter of flange plate
Flange diameter, $d+2t_{sc}$
Small opening, $d \le t_{sc}/2$
Full strength weld (CJP) at steel sleeve and faceplate junction
Flange plate
Steel sleeve
Concrete infill
Faceplate

*Fig. 7-7. Small circular opening—detailing illustration for fully developed edge with flange plate thickness < 1.25*t_p.

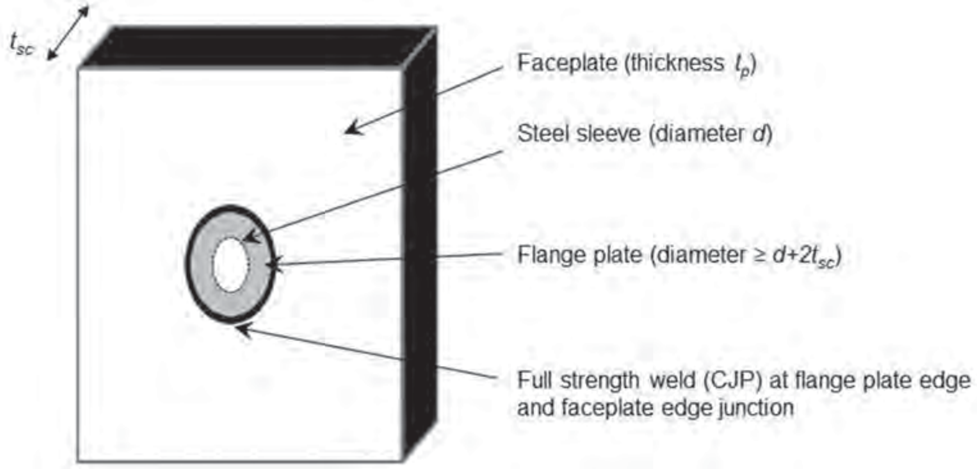
t_{sc}
Faceplate (thickness t_p)
Steel sleeve (diameter d)
Flange plate (diameter $\ge d+2t_{sc}$)
Full strength weld (CJP) at flange plate edge and faceplate edge junction

*Fig. 7-8. Small circular opening—detailing illustration for fully developed edge with flange plate thickness ≥ 1.25*t_p.

temperature profiles produced by the thermal accident conditions. The heat transfer analysis results are used to define thermal loading for the structural analyses.

Booth et al. (2007) and Varma et al. (2009) performed experimental and analytical studies to evaluate the effect of thermal loads—operating and accident—on the behavior of SC walls. It was concluded that operating thermal stiffness of the composite walls can be predicted using cracked transformed section properties. Upon applying accidental thermal loads, a nonlinear thermal gradient develops across the concrete cross section, causing the concrete to crack in tension, as can be seen in Figure 7-10.

Figure 7-10 compares the experimental temperatures and thermal gradients with those obtained from a fiber model. This fiber model was then used to predict the moment-curvature, M-ϕ, response of the SC walls for the design thermal loading. Figure 7-11 presents the M-ϕ responses predicted for the specimen. The figure shows that the thermal gradient shifts the diagram to the left with nonzero thermal curvature, ϕ_{th}, at zero moment and nonzero thermal moment, M_{th}, at zero curvature. Figure 7-12 also shows that the thermal moment can be related to the thermal curvature using the fully cracked section stiffness.

The stiffness of the SC wall subjected to ΔT_{savg} greater than or equal to 150°F (83°C) can be predicted using fully cracked, steel only section properties. Based on the discussed results, Varma et al. (2009) developed the equations given in ANSI/AISC N690 to predict the effects of combined thermal and mechanical loading in locations away from supports. These equations do not apply at supports that may be fully restrained from expansion. Temperature dependent properties for steel are not required for temperatures up to 400°F

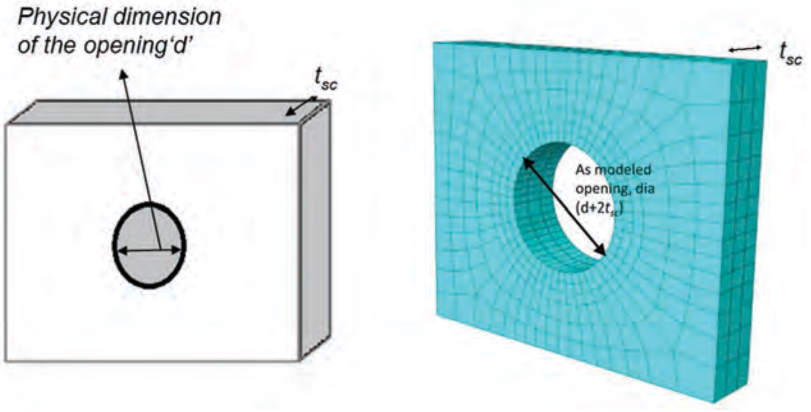

Fig. 7-9. Modeling of large openings with free edge at opening perimeter.

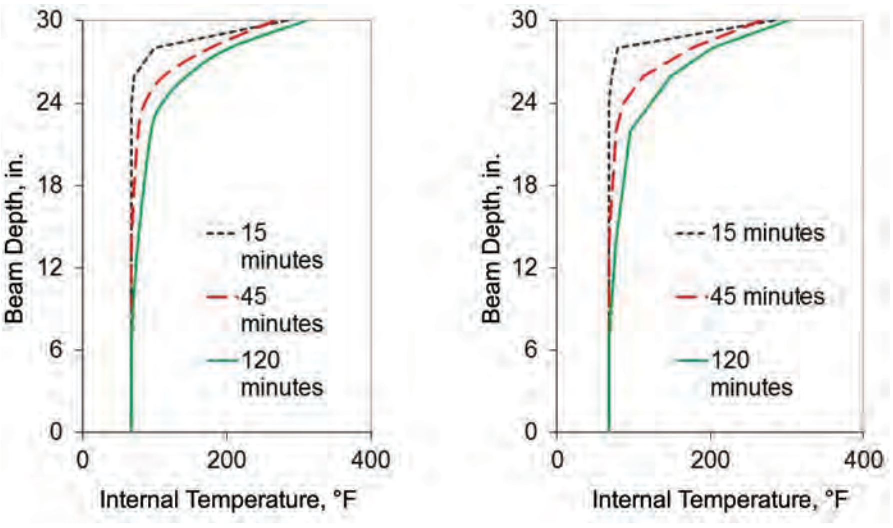

(a) Analytically determined

(b) Experimentally determined

Fig. 7-10. Comparison of analytically and experimentally determined thermal gradients (Varma et al., 2009).

(204°C). For temperatures greater than 400°F (204°C), temperature dependent properties from ANSI/AISC N690 Appendix N4 are recommended.

7.6 INTERIOR AND CONNECTION REGIONS

Labyrinthine SC walls of safety-related nuclear facilities are connected to each other and anchored to the concrete basemat. SC wall structures are connected to adjoining structures with the following connection types: SC wall-to-SC or -RC wall, SC wall-to-basemat, SC wall-to-SC or -RC slab, or splices between coplanar RC or SC walls. A connection may be defined as the assembly of steel connectors, including steel headed stud anchors, anchor rods, ties, reinforcing bars and dowels, post-tensioning bars, shear lugs, embedded steel shapes, welds and bolts, rebar mechanical couplers, and direct bearing in compression, and the surrounding concrete materials anchoring the rebar or providing bearing resistance that participate in the force transfer mechanisms for tension, compression, in-plane shear, out-of-plane shear, and out-of-plane flexure between two connected parts. It does not include any portions of the SC walls being connected. The connection region is specifically designed to undergo ductile yielding and energy dissipation during overloads. Force transfer from the composite SC wall to the supports or connected structures occurs within these connection regions. Additionally, the connection regions serve as transition regions wherein the faceplates and concrete infill of SC walls redistribute forces according to their relative stiffness and develop composite action.

According to ANSI/AISC N690 Section N9.2, SC walls are divided into interior regions and connection regions for design purposes. Connection regions consist of perimeter strips with a width not less than the section thickness, t_{sc}, and not more than twice the section thickness, $2t_{sc}$. Figure 7-13 illustrates the typical interior and connection regions for SC walls. The requirement for connection regions to be less

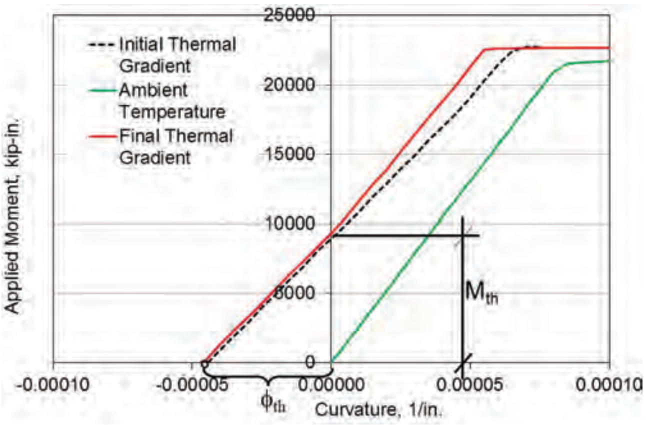

Fig. 7-11. Comparison of fiber model moment curvature to transformed cracked and fully cracked moment of inertia (Varma et al., 2009).

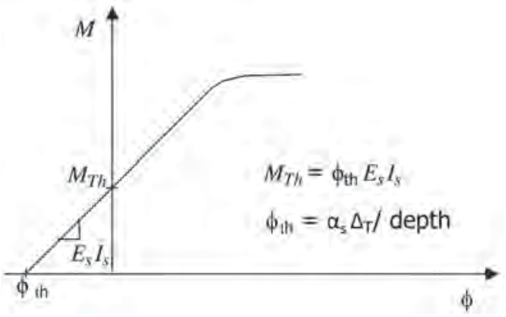

M
M_{Th}
$E_s I_s$
ϕ th
ϕ
$M_{Th} = \phi_{th} E_s I_s$
$\phi_{th} = \alpha_s \Delta_T$/ depth

Fig. 7-12. Relationship between moment and thermal gradient.

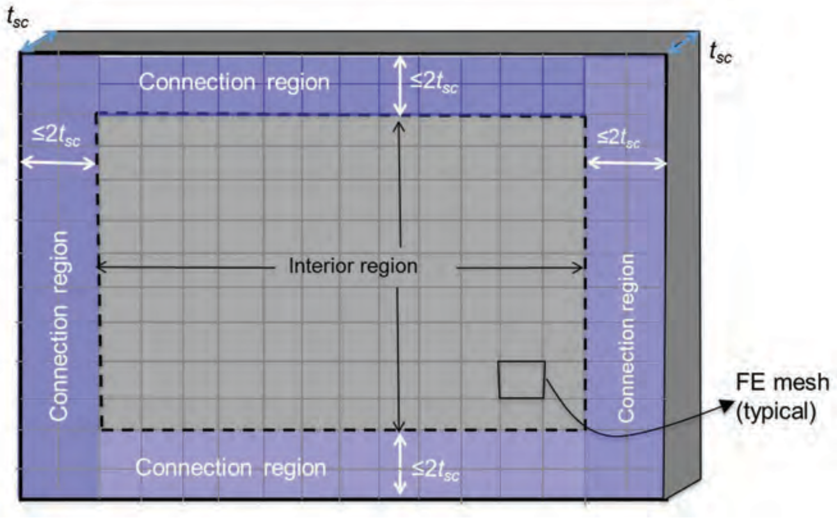

Fig. 7-13. The expanse of SC walls separated into connection regions and interior regions.

than or equal to twice the wall thickness ($\leq 2t_{sc}$) is based on typical development lengths of No. 11 to No. 18 reinforcing bars, which are used typically in nuclear construction. Specifying connection region lengths less than the wall thickness ($\leq t_{sc}$) can be impractical and lead to detrimental congestion of steel anchors and ties.

7.7 REQUIRED STRENGTH DETERMINATION

Averaging and design assessment for interior regions is done over $2t_{sc} \times 2t_{sc}$ panel sections because the resulting section demands account for a reasonable degree of yielding and force redistribution at stress concentrations—for example, first onset of significant inelastic deformation at SSE. While the development length, L_d, is typically three times the section thickness, $3t_{sc}$, a lower value for averaging has been used because $3t_{sc}$ is deemed to be large considering typical SC wall thicknesses, such as for a 4-ft (1.2 m)-thick SC wall. Keeping panel section dimensions at $3t_{sc}$ would result in 12-ft × 12-ft (3.6 m × 3.6 m) panel sections. This size may result in very few panel sections per wall leading to less accurate determination of demands for the SC walls. Averaging in connection regions and regions around openings has also been limited to t_{sc}, compared to the L_d value of $2t_{sc}$, for the same reasons. Additionally, $3t_{sc}$ is a notional value for the development length. In most cases, the faceplates of SC walls will be directly welded to steel base plates or other faceplates, which will develop them immediately at the weld location itself. Developing the faceplate yield strength over the panel sections would not be an issue in most cases. The sizing recommendations for panel sections are illustrated in Figure 7-14.

The required strengths for the panel sections of SC walls for each demand type is denoted as follows:

M_{rx} = required out-of-plane flexural strength per unit width in direction x, kip-in./ft (N-mm/m)

M_{ry} = required out-of-plane flexural strength per unit width in direction y, kip-in./ft (N-mm/m)

M_{rxy} = required twisting moment strength per unit width, kip-in./ft (N-mm/m)

S_{rx} = required membrane axial strength per unit width in direction x, kip/ft (N/m)

S_{ry} = required membrane axial strength per unit width in direction y, kip/ft (N/m)

S_{rxy} = required membrane in-plane shear strength per unit width, kip/ft (N/m)

V_{rx} = required out-of-plane shear strength per unit width along edge parallel to direction y, kip/ft (N/m)

V_{ry} = required out-of-plane shear strength per unit width along edge parallel to direction x, kip/ft (N/m)

x, y = local coordinate axes in the plane of the wall associated with the finite element model

These demand types are shown in Figures 5-4a (out-of-plane shears and moments) and 9-2 (in-plane forces and moments).

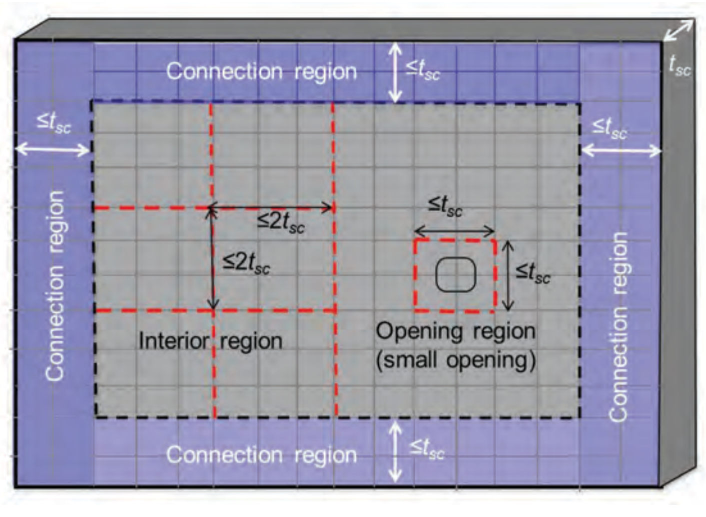

Fig. 7-14. Panel section sizing for averaging the design demands.

Chapter 8
Individual Design Available Strengths

The available strengths of the SC wall section for individual demand types are determined based on ANSI/AISC N690, Section N9.3. The concrete contribution to the tensile strength of the section is not considered. Neglecting concrete tensile strength is appropriate for SC sections because they experience a higher degree of cracking due to curing shrinkage than typically observed in reinforced concrete sections. This is due to locked-in tensile stresses in the SC concrete core that result from restraint of curing shrinkage by the faceplates, and also the discrete nature of the bond between the reinforcing steel and the concrete core. The steel ribs are provided primarily to increase faceplate stiffness and strength to handle rigging and construction loads, such as wet concrete pressure. Therefore, the contribution of the steel ribs to available strength is neglected.

8.1 UNIAXIAL TENSILE STRENGTH

The tensile strength of the SC wall panel section is determined according to AISC *Specification* Chapter D. The reduction in available tensile strength of the SC panel sections due to holes in faceplates is alleviated by avoiding tensile rupture in the faceplates.

8.2 COMPRESSIVE STRENGTH

The compressive strength of the SC wall panel sections is determined according to ANSI/AISC N690, Equation A-N9-15. This equation is based on AISC *Specification* Section I2.1b, with faceplates replacing the steel shape. The variables that need to be redefined are discussed in ANSI/AISC N690, Section N9.3.2. The SC wall panel sections are designed by calculating the available axial compressive strength on a per-foot basis. The calculation uses the clear length of the wall along the direction of loading and an effective SC stiffness per unit width for buckling evaluation, which is based on EI_{eff} of the filled composite columns in AISC *Specification* Chapter I. The equation for EI_{eff} for filled composite columns has been simplified conservatively to $E_sI_s+0.60E_cI_c$. The more accurate equation in AISC *Specification* Chapter I, which is a function of the reinforcement ratio, can also be used. Additionally, the effective length factor, K, has been conservatively taken as 1.0.

ANSI/AISC N690, Equation A-N9-15 gives the nominal compressive strength for SC wall panel sections with nonslender faceplates at operating temperatures. Varma et al. (2013) used benchmarked finite element models to

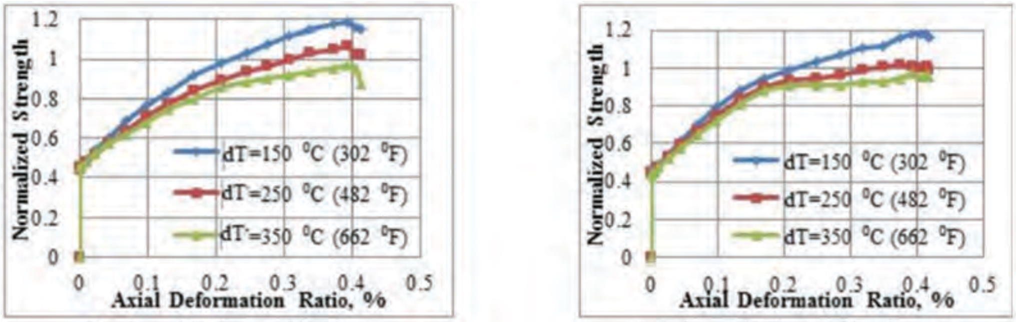

(a) s/t_p = 10, Time = 30 minutes (b) s/t_p = 20, Time = 30 minutes

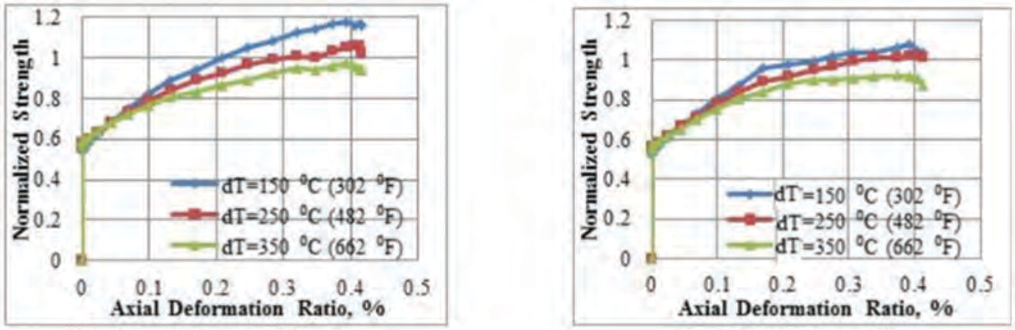

(c) s/t_p = 10, Time = 3 hours (d) s/t_p = 20, Time = 3 hours

Fig. 8-1. Load displacement curves: temperature magnitude as parameter (Varma et al., 2013).

analytically study the impact of elevated temperatures on the compressive strength of an SC wall.

Figure 8-1 shows the analysis results for different temperature magnitudes as well as faceplate slenderness ratios, s/t_p. The compressive strength of the analytical models has been normalized with respect to the design strength calculated using ANSI/AISC N690, Equation A-N9-15. The equation becomes slightly unconservative for temperatures above 482°F (250°C). The figure also indicates that the duration of heating does not affect the compressive strength of SC walls. Therefore, ANSI/AISC N690, Equation A-N9-15 is recommended for calculating the compressive strength of SC wall panel sections subjected to accident thermal loading causing surface temperatures up to 300°F (149°C).

8.3 OUT-OF-PLANE FLEXURAL STRENGTH

The flexural strength of the SC wall panels is determined for the limit state of faceplate yielding according to ANSI/AISC N690, Equation A-N9-18. The equation is based on the consideration that the majority of the concrete infill depth will be cracked in tension. The nominal flexural strength can also be calculated using the reinforced concrete principles mentioned in ACI 349-06, Section 10.2 (ACI, 2006). The design assumptions and limitations for determining available flexural strength of concrete members listed in the section can be applied to SC walls with slight modifications accounting for the differences from a RC design; in particular, having the faceplates on the exterior faces (Sener et al., 2015b).

SC design is inherently similar to that of doubly reinforced concrete beams. Therefore, the concrete will not fully crush ($\varepsilon = 0.003$) before the faceplate yields in compression ($\varepsilon = 0.002$). In this case, the neutral axis will be located at the inner surface of the faceplate. This limits the strain in the extreme fiber of the concrete in compression to the steel yield strain. Concrete stress variation can be assumed to be approximately linear up to the strain equal to the yield strain of typically used faceplates (about 2,000μ). Assuming a triangular stress variation in concrete below this strain level and transforming the compression faceplate to an equivalent concrete block, M_n can be calculated by summing moments about the centroid of the transformed block. Note that the stress in the transformed concrete block is assumed equal to the smaller of f_c' or F_y/n.

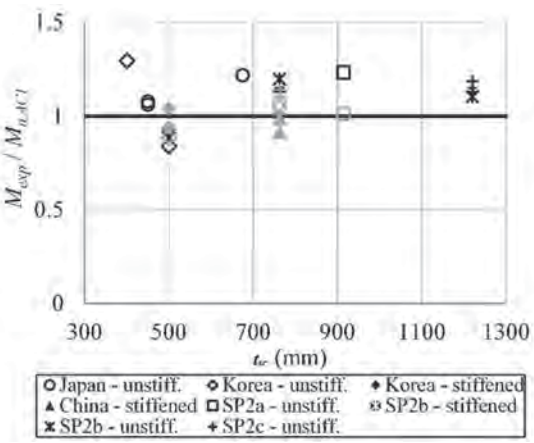

Fig. 8-2. Comparison of experimental flexural strength data with strength obtained using modified ANSI/AISC N690 Equation C-A-N9-11 (Sener et al., 2015b).

Sener et al. (2015b) compared the nominal flexural strength values, M_n, obtained using the ANSI/AISC N690 Appendix N9 Commentary methodology (Equation C-A-N9-11) with flexural strength data obtained from experimental studies by Japanese (Ozaki et al., 2001), South Korean (Hong et al., 2009) and United States (Varma et al., 2011c) researchers. Figure 8-2 plots the experimental out-of-plane strength data normalized with M_n obtained as discussed previously. As shown, the flexural strength equation conservatively estimates the majority of the specimen capacities. It is observed that there is no clear trend between the flexural strength and section depth.

8.4 IN-PLANE SHEAR STRENGTH

The in-plane shear strength of SC wall panel sections is determined according to ANSI/AISC N690, Equation A-N9-19. In-plane shear behavior of the SC walls is governed by the plane stress behavior of the faceplates and the orthotropic elastic behavior of concrete cracked in principal tension. Ozaki et al. (2004) and Varma et al. (2011e) developed the fundamental in-plane behavior, mechanics based model (MBM) for SC walls. The in-plane shear strength of SC walls can be estimated as the trilinear shear force-strain curve shown in Figure 8-3. The slope of the first part of the curve is the in-plane shear stiffness prior to concrete cracking, K_{xy}^{uncr}. The slope of the second part is the in-plane shear stiffness after the concrete cracking, K_{xy}^{cr}, but before the faceplate yields. The third part of the curve corresponds to the onset of faceplate Von Mises yielding. The expression for shear yield strength, V_{ni}, corresponding to the onset of yield was calibrated to the simplified ANSI/AISC N690, Equation A-N9-19. The calibration is for values of $\bar{\rho}$ between 0.01 and 0.04 for nuclear structures, where $\bar{\rho}$ is the strength-adjusted reinforcement ratio calculated according to ANSI/AISC N690, Equation A-N9-13. Thus, the in-plane shear behavior is a function of $\bar{\rho}$. Varma et al. (2014) compared the in-plane shear strength of the specimen predicted by the MBM with the experimental results. Figure 8-4 shows that the calculated and experimental values match closely, with the calculated MBM values being conservative.

Seo et al. (2016) verified the MBM using a large in-plane shear test experimental database. The experimental in-plane shear strength based on faceplate yielding was compared with design equations from ACI 349-06, the MBM, and ANSI/AISC N690. The comparisons are presented in Figure 8-5. The ACI 349-06, Section 11, equation predicts the in-plane shear strength slightly unconservatively; however, the predication improves for higher reinforcement ratios. The ANSI/AISC N690 in-plane strength equations predict the in-plane shear strength conservatively.

8.5 OUT-OF-PLANE SHEAR STRENGTH

The out-of-plane shear behavior of SC walls is similar to that of RC walls with some differences associated with crack spacing and width due to the more discrete nature of the bond—via steel anchors—in SC walls. Japanese (Ozaki et al., 2001), South Korean (Hong et al., 2009), and U.S. (Varma et al., 2011c) researchers have performed experiments to study the out-of-plane behavior of SC sections. Sener and Varma (2014) have compared the shear strengths obtained from this experimental database with the ACI 349-06 shear strength equations. The comparisons demonstrated that out-of-plane shear failure is a nonductile failure mode, and the concrete contribution to the out-of-plane shear strength reduces with increasing wall thickness due to size effects. Based on these observations, ANSI/AISC N690 requires the nominal out-of-plane shear strength to be established by conducting project-specific, large-scale, out-of-plane shear tests; by using applicable test results; or by using the provisions of ANSI/AISC N690, Section N9.3.5. This section addresses the nonductile out-of-plane shear failure by defining suitable values for the resistance factor (ϕ_{vo} = 0.75) and safety factor (Ω_{vo} = 2.00) based on the reliability analysis presented in Sener and Varma (2014). The nominal shear strength of the SC walls depends on the spacing of shear reinforcement and the classification of shear reinforcement: yielding or nonyielding.

If the shear reinforcement is spaced less than $t_{sc}/2$, the nominal out-of-plane shear strength will include out-of-plane shear contributions from concrete as well as from the steel, with the ties acting as shear reinforcement. ANSI/AISC N690

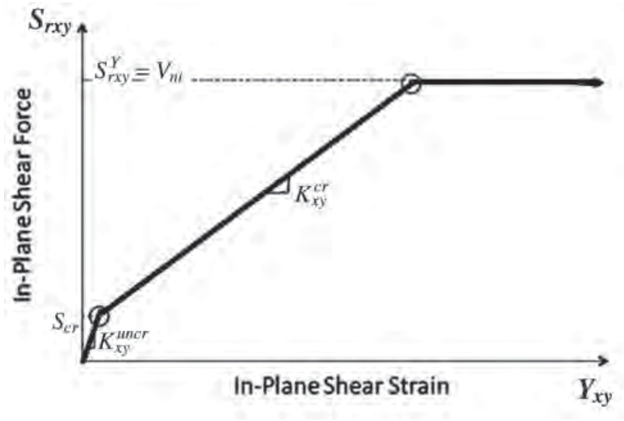

Fig. 8-3. In-plane shear strain curve (Varma et al., 2011e).

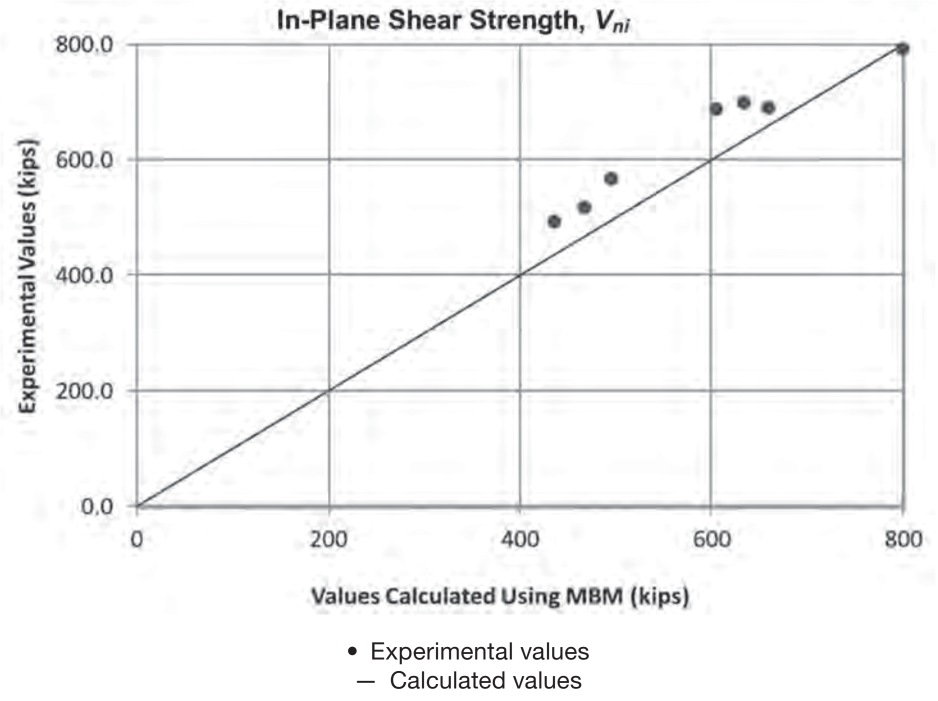

Fig. 8-4. Experimental versus calculated values of in-plane shear strength (Varma et al., 2014).

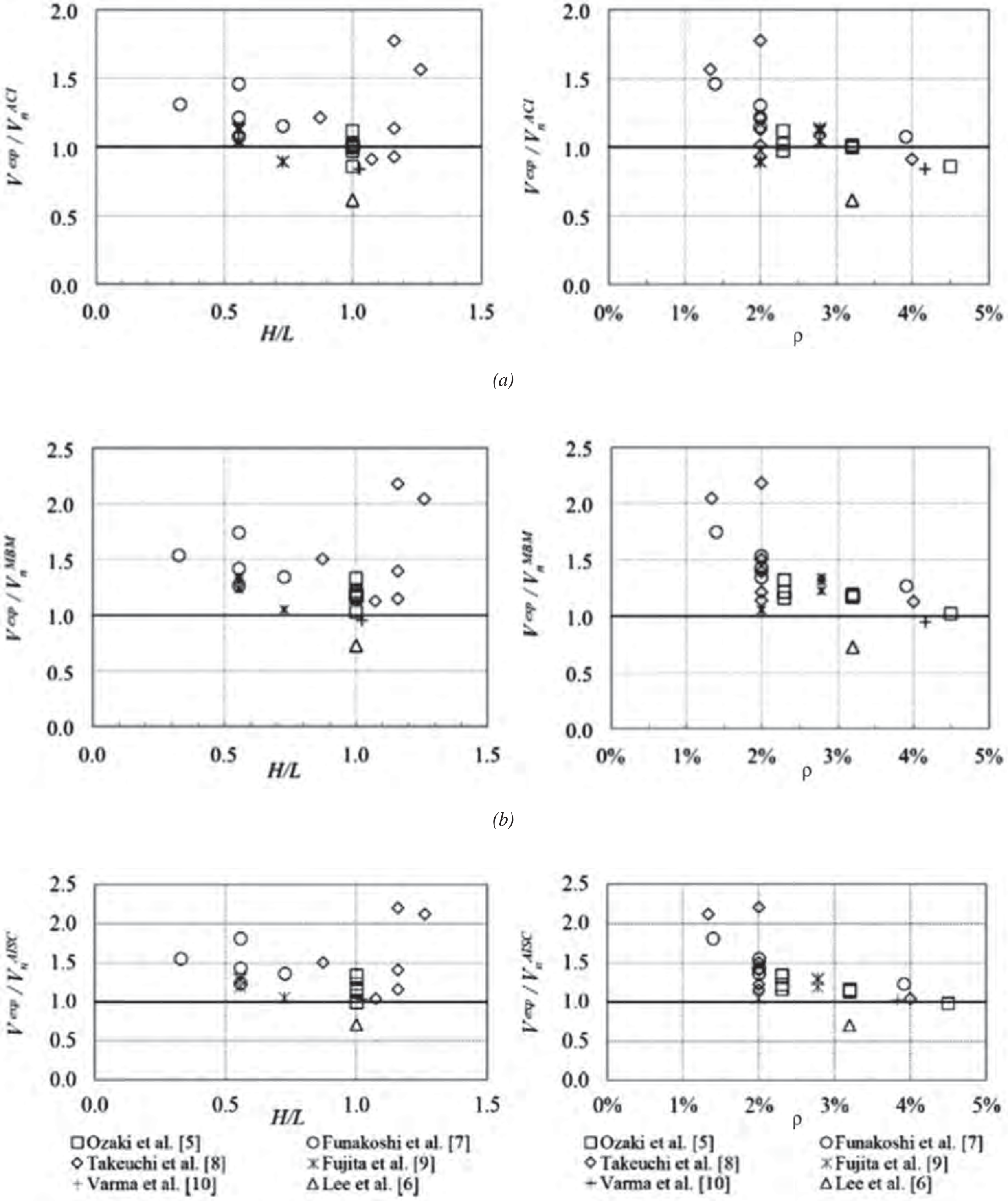

(a)

(b)

(c)

Fig. 8-5. In-plane shear strength of SC walls normalized with (a) ACI 349-06 equation, (b) MBM equation, and (c) ANSI/AISC N690 equation (Seo et al., 2016).

requires the out-of-plane shear strength for an SC wall with shear reinforcement spaced not greater than half the section thickness be determined by Equations A-N9-20 to A-N9-22. ANSI/AISC N690, Equation A-N9-21, addresses the size effect by limiting the out-of-plane shear contribution of the concrete in SC walls to $0.05\sqrt{f_c'}(\text{ksi})\left[1.5\sqrt{f_c'}(\text{psi})\right]$. The shear reinforcement contribution is based on the well-known mechanism of a shear or flexure-shear crack passing through several yielding-type shear reinforcement ties and engaging them in axial tension. The classification of the shear reinforcement, or ties, as yielding and the determination of the available axial tensile strength are important for this calculation. ANSI/AISC N690, Equation A-N9-22, limits the maximum possible contribution of shear reinforcement to out-of-plane shear strength to $0.25\sqrt{f_c'}A_c(\text{ksi})\left[8\sqrt{f_c'}A_c(\text{psi})\right]$, where A_c is the area of concrete per unit width. This upper limit is based on ACI 349-06.

For nonyielding tie shear reinforcement, spaced no greater than $t_{sc}/2$, it is possible that the concrete shear or flexure-shear crack will activate all the individual shear reinforcements that it will pass through. However, it is unclear whether these individual shear reinforcements will be able to develop their individual design strengths before one of them—the one with the largest axial force—fails in a nonductile manner. Therefore, the shear reinforcement contribution given in ANSI/AISC N690, Equation A-N9-22, has been reduced to one-half.

If the spacing of the yielding shear reinforcement is greater than one-half of the section thickness, the maximum out-of-plane shear strength is limited to the greater of the concrete shear strength contribution, or the shear reinforcement contribution alone. This is based on the ability of the SC section to develop an internal truss mechanism for equilibrium. The strength of this truss mechanism is limited to that of the tie shear reinforcement. The concrete and steel contributions cannot be added for shear reinforcement spacing greater than $t_{sc}/2$ because the shear or flexural-shear crack may not pass through more than one tie.

ANSI/AISC N690 Appendix N9 requires that the out-of-plane shear strength for an SC wall with shear reinforcement spaced greater than half the section thickness needs to be the greater of V_{conc} (ANSI/AISC N690, Equation A-N9-21) and V_s (ANSI/AISC N690, Equation A-N9-22). The behavior of nonyielding and yielding shear reinforcement with spacing greater than half the wall thickness will be the same.

Chapter 9
Interaction of Design Available Strengths

The interaction of design demands needs to be checked for all load combinations. ANSI/AISC N690, Section N9.3.6 defines the limiting interaction of demands for SC walls.

9.1 INTERACTION OF OUT-OF-PLANE SHEAR FORCES

The out-of-plane shear demands in both the x, or V_{rx}, and y, or V_{ry}, directions rely on using the same ties for the steel contribution, V_s. Both V_{rx} and V_{ry} subject the steel shear reinforcement to axial tensile demand after the concrete cracks and the concrete shear strength contribution, V_{conc}, in respective directions is exceeded. Additionally, shear reinforcement and steel anchors are subject to interfacial shear demands in both the x and y directions, where x and y are the local coordinate axes in the plane of the wall, as shown in Figure 5-4(a). An equation was developed to check the interaction of out-of-plane shear and interfacial shear demands on an SC wall.

If the required out-of-plane shear strength per unit width for both the x and y axes, V_{rx} and V_{ry}, is greater than the available out-of-plane shear strength provided by the concrete per unit width of the SC panel section, $V_{c\ conc}$, and the out-of-plane shear reinforcement is spaced no greater than half the section thickness, the interaction of out-of-plane shear forces is limited by ANSI/AISC N690, Equation A-N9-23. The interaction equation is based on the shear-tension interaction equation in ACI 349-06, Appendix D, Commentary RD.7 (ACI, 2006), which is applicable to connectors with ductile and nonductile limit states. In the first part of the interaction equation, the numerators are the tensile force demands in the ties, which are calculated as the portions of the out-of-plane shear demands greater than the corresponding concrete contribution, V_{conc}. The denominators are the available strength contributions of the ties, V_s. The second term in the interaction equation accounts for the shear demand in the ties and steel anchors due to the participation in resisting interfacial shear demands, which are the result of out-of-plane shear demands as discussed previously. The numerator is the vector sum of the out-of-plane shear demands, V_{rx} and V_{ry}, obtained by mathematical manipulation of ANSI/AISC N690, Equation A-N9-4. The denominator is the weighted average of the shear strength contributions of ties and steel anchors, Q_{cv}^{avg}, and can be calculated according to Equation 9-1.

$$Q_{cv}^{avg} = \frac{n_{et} Q_{cv}^{tie} + n_{es} Q_{cv}}{n_{et} + n_{es}} \tag{9-1}$$

where

Q_{cv}^{tie} = available interfacial shear strength of tie, kip (N)

n_{es} = effective number of shear connectors contributing to a unit cell

n_{et} = effective number of ties contributing to a unit cell (the unit cell is the quadrilateral region defined by a grid of four adjacent ties)

The unit cell is illustrated in Figure 9-1 for an SC wall of thickness 36 in. (900 mm), with ties spaced at 36 in. (900 mm) and steel anchors spaced at 9 in. (225 mm). As shown in the figure, the ties at the corners participate in four adjoining unit cells, and the steel anchors at the boundaries participate in two adjacent unit cells. The steel anchors within the boundaries of the unit cells contribute fully. The contribution of shear anchors needs to be modified in case the anchors are nonyielding. For the example shown in Figure 9-1, the effective number of ties contributing to the unit cell, n_{et}, is equal to 1, and the effective number of steel anchors, n_{es}, is equal to 15 $\left[(1)(9) + (0.5)(12) = 15\right]$.

When the spacing of the shear reinforcement is greater than half the section thickness, the nominal out-of-plane shear strength is governed by the greater of the steel or concrete contributions, as discussed previously. When the steel contribution is greater than the concrete contribution, ANSI/AISC N690, Equation A-N9-23, will not contain a concrete contribution.

When one of the out-of-plane shear demands, V_{cx} or V_{cy}, is less than the concrete contribution, there will be no interaction of out-of-plane shear demands. For shear reinforcement spaced at greater than half of the section thickness, and if the concrete contribution is more than the shear reinforcement contribution, the concrete infill will be subject to two-way punching shear—or one-way shear, depending on the wall configuration—which will be resisted by the perimeter of the unit cell for the SC panel section.

9.2 IN-PLANE FORCES AND OUT-OF-PLANE MOMENTS

The design adequacy of SC panel sections subjected to the three in-plane required membrane strengths (S_{rx}, S_{ry}, S_{rxy}) and three out-of-plane required flexural or twisting strengths (M_{rx}, M_{ry}, M_{rxy}) needs to be evaluated. ANSI/AISC N690 requires this evaluation for each notional half of the SC section that consists of one faceplate and half the concrete thickness. ANSI/AISC N690 limits the interaction for each notional half by Equations A-N9-24 to A-N9-26. The equations utilize the maximum and minimum required principal in-plane strengths for the notional half of the SC panel section, $S_{r,max}$ and $S_{r,min}$, calculated using Equations A-N9-27 to A-N9-30. Alternately, for each notional half, the interaction can be limited directly with the required in-plane membrane strengths per unit width (S'_{rx}, S'_{ry} and S'_{rxy}), using Equations A-N9-31 to A-N9-33. The values of S'_{rx}, S'_{ry} and S'_{rxy} are calculated using Equations A-N9-28 to A-N9-30.

The combined in-plane forces (S_{rx}, S_{ry}, S_{rxy}) and out-of-plane moments (M_{rx}, M_{ry}, M_{rxy}) are shown in Figure 9-2(a). The interaction equations were developed based on the conservative simplified design approach developed by Varma et al. (2014), which consists of (1) dividing the SC panel section into two notional halves, (2) calculating the required in-plane strengths (S'_{rx}, S'_{ry} and S'_{rxy}) for each notional half, and (3) calculating the required in-plane principal strengths ($S_{r,max}$ and $S_{r,min}$) for each notional half.

Each notional half consists of one faceplate and half the concrete infill thickness as shown in Figure 9-2(b). The required in-plane strengths (S'_{rx}, S'_{ry} and S'_{rxy}) for each notional half are calculated by representing the out-of-plane moments as force couples with effective arm lengths: 0.90 times the wall thickness for tension dominated situations with significant concrete cracking and 0.67 times the wall thickness for compression dominated situations with limited concrete cracking. The required in-plane principal strengths ($S_{r,max}$ and $S_{r,min}$) can be calculated for each notional half using the required in-plane strengths (S'_{rx}, S'_{ry} and S'_{rxy}) and appropriate equations.

Varma et al. (2014) developed a conservative simplified interaction surface in principal force space for checking the design adequacy of the notional halves of the SC wall panel section. As shown in Figure 9-3, the interaction surface has four regions in principal force space:

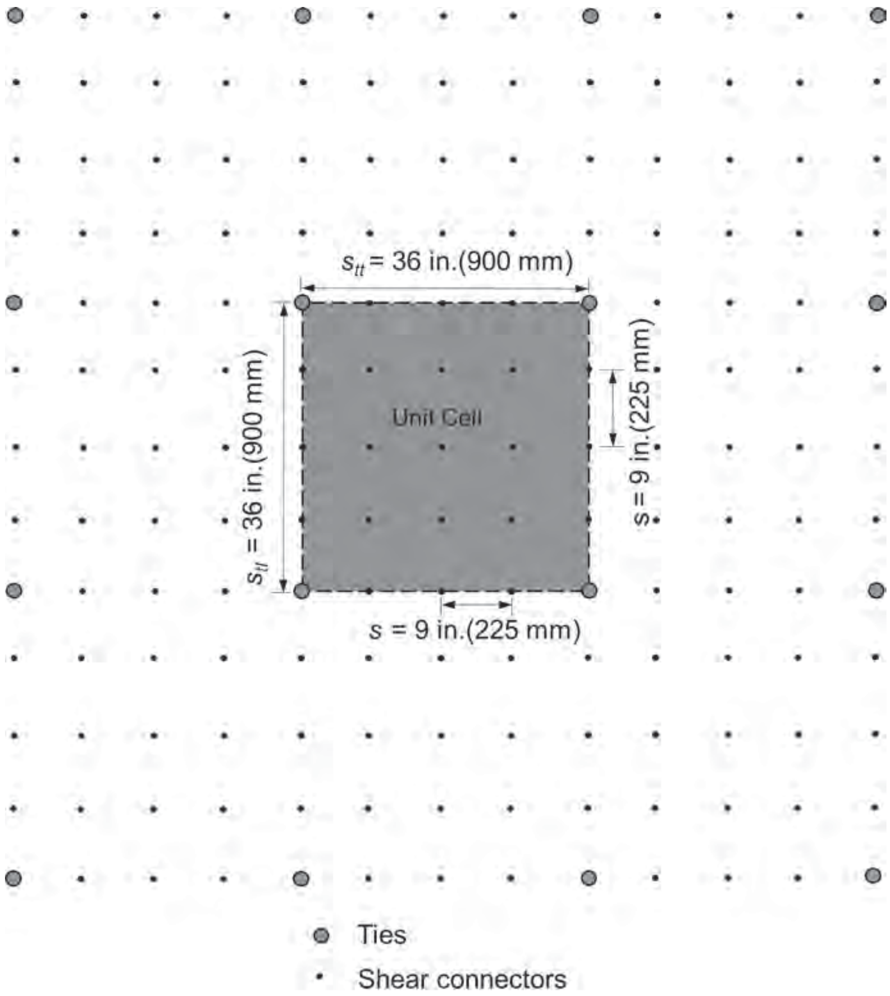

Fig. 9-1. Unit cell for calculating Q_{cv}^{avg} *(Bhardwaj et al., 2017).*

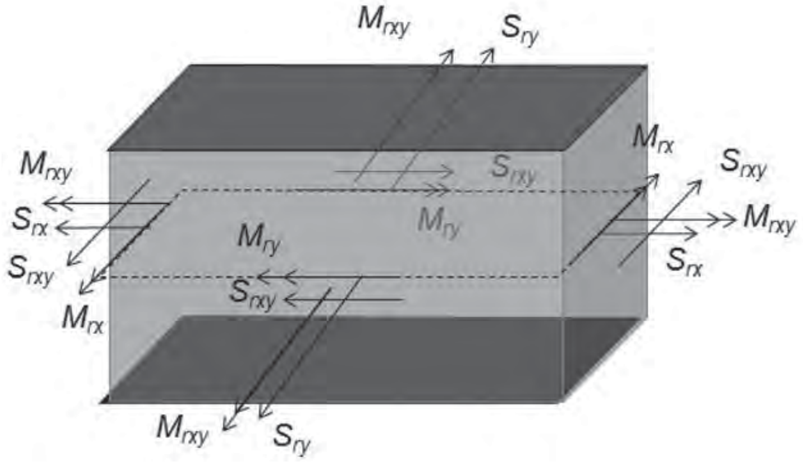
M_{rxy}
S_{ry}
M_{rxy}
S_{rx}
S_{rxy}
M_{rx}
S_{rxy}
M_{ry}
M_{ry}
S_{rxy}
M_{rx}
S_{rxy}
M_{rxy}
S_{rx}
M_{rxy}
S_{ry}

(a) Forces on panel section

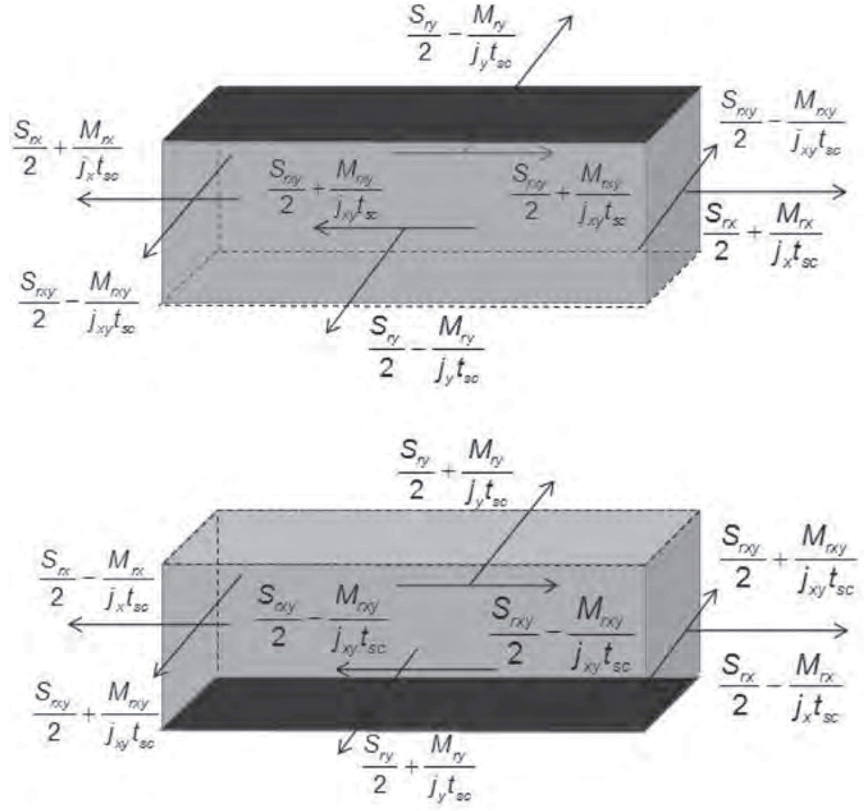
$\frac{S_{ry}}{2} - \frac{M_{ry}}{j_y t_{sc}}$
$\frac{S_{rx}}{2} + \frac{M_{rx}}{j_x t_{sc}}$
$\frac{S_{rxy}}{2} - \frac{M_{rxy}}{j_{xy} t_{sc}}$
$\frac{S_{rxy}}{2} + \frac{M_{rxy}}{j_{xy} t_{sc}}$
$\frac{S_{rxy}}{2} + \frac{M_{rxy}}{j_{xy} t_{sc}}$
$\frac{S_{rx}}{2} + \frac{M_{rx}}{j_x t_{sc}}$
$\frac{S_{rxy}}{2} - \frac{M_{rxy}}{j_{xy} t_{sc}}$
$\frac{S_{ry}}{2} - \frac{M_{ry}}{j_y t_{sc}}$
$\frac{S_{ry}}{2} + \frac{M_{ry}}{j_y t_{sc}}$
$\frac{S_{rx}}{2} - \frac{M_{rx}}{j_x t_{sc}}$
$\frac{S_{rxy}}{2} + \frac{M_{rxy}}{j_{xy} t_{sc}}$
$\frac{S_{rxy}}{2} - \frac{M_{rxy}}{j_{xy} t_{sc}}$
$\frac{S_{rxy}}{2} - \frac{M_{rxy}}{j_{xy} t_{sc}}$
$\frac{S_{rx}}{2} - \frac{M_{rx}}{j_x t_{sc}}$
$\frac{S_{rxy}}{2} + \frac{M_{rxy}}{j_{xy} t_{sc}}$
$\frac{S_{ry}}{2} + \frac{M_{ry}}{j_y t_{sc}}$

(b) Forces on notional halves

Fig. 9-2. Combined forces acting on panel section and notional halves (Varma et al., 2014).

(1) region I = biaxial tension
(2) region II = axial tension + in-plane shear
(3) region III = axial compression + in-plane shear
(4) region IV = biaxial compression

The interaction surface and these four regions are defined by anchor points located at 50% of the total section strengths in uniaxial tension, biaxial tension, pure in-plane shear, uniaxial compression, and biaxial compression. The 50% reduction reflects that the interaction surface was for each notional half of the SC panel section. The interaction equations for each of these four regions are also provided in Varma et al. (2014).

For further simplification, regions I and II were combined into one region described by a straight line connecting the anchor points of pure shear and biaxial tension in the principal force space. This conservatively eliminated the uniaxial tension as an independent anchor point and reduced the number of regions and equations needed for the interaction surface.

As shown in Figure 9-4, the uniaxial tensile strength is conservatively adjusted to be collinear with the straight line joining the anchor points of pure in-plane shear and biaxial tension in principal force space. This is always slightly conservative because of several reasons: The pure in-plane shear strength is always less than or equal to $A_sF_y/2$; the biaxial tension point is anchored at $A_sF_y/2$; and the resistance factors are less than or equal to one, whereas the corresponding safety factors are greater than one. Therefore, the resulting unaxial tension anchor point will be slightly less than $A_sF_y/2$.

The resistance and safety factors for available demands for the notional halves are less conservative than those for the corresponding individual demands on the panel sections because the maximum individual required tensile and shear demands will rarely occur in the same panel section.

Varma et al. (2014) confirmed the conservatism of the design approach by developing an MBM that accounts for the complex behavior of the composite SC panel section subjected to combined in-plane forces and moments, and also by developing a detailed nonlinear inelastic finite element model of SC panel sections subjected to combined in-plane forces and moments. Figure 9-5 confirms the conservatism of the design approach by comparing the bending moment and in-plane shear (M_{rx}, S_{rxy}) interaction predicted for an SC panel section by all three methods: design approach, MBM, and finite element model. As shown, the design approach is very conservative.

The alternate interaction equations of ANSI/AISC N690 were obtained by recasting the interaction equations, which are in terms of the principal force $S_{r,max}$ and $S_{r,min}$, directly into terms of S'_{rx}, S'_{ry} and S'_{rxy}. The alternate interaction equations mathematically represent the same interaction surface

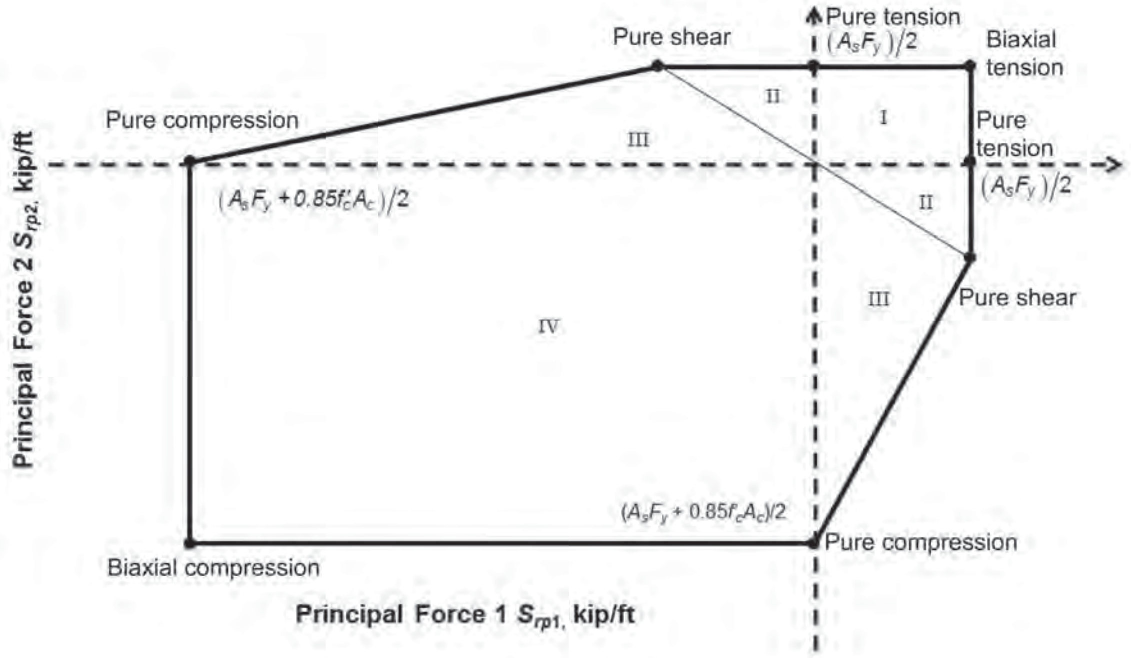

Fig. 9-3. Interaction surface for in-plane forces in principal force space (Varma et al., 2014).

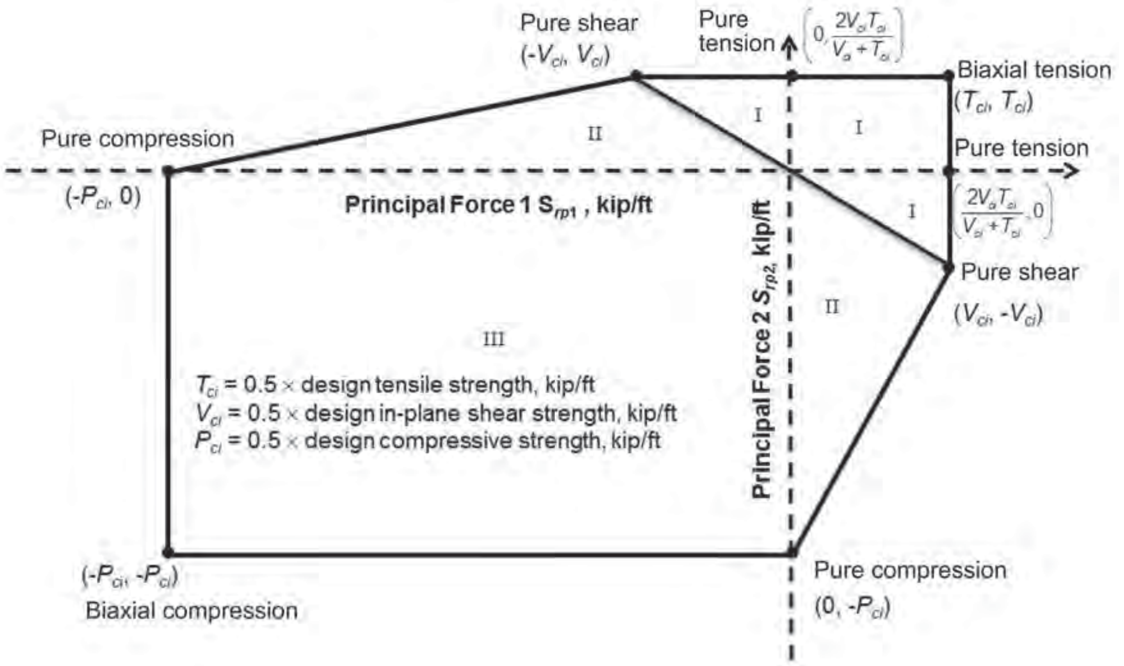
Pure shear
$(-V_{ci}, V_{ci})$
Pure tension
$\left(0, \frac{2V_{ci}T_{ci}}{V_{ci}+T_{ci}}\right)$
Biaxial tension
(T_{ci}, T_{ci})
Pure compression
$(-P_{ci}, 0)$
I
I
I
II
Pure tension
$\left(\frac{2V_{ci}T_{ci}}{V_{ci}+T_{ci}}, 0\right)$
Principal Force 1 S_{rp1} , kip/ft
Principal Force 2 S_{rp2}, kip/ft
Pure shear
$(V_{ci}, -V_{ci})$
II
III
T_{ci} = 0.5 × design tensile strength, kip/ft
V_{ci} = 0.5 × design in-plane shear strength, kip/ft
P_{ci} = 0.5 × design compressive strength, kip/ft
$(-P_{ci}, -P_{ci})$
Biaxial compression
Pure compression
$(0, -P_{ci})$

Fig. 9-4. Simplified interaction surface plotted in principal force space.

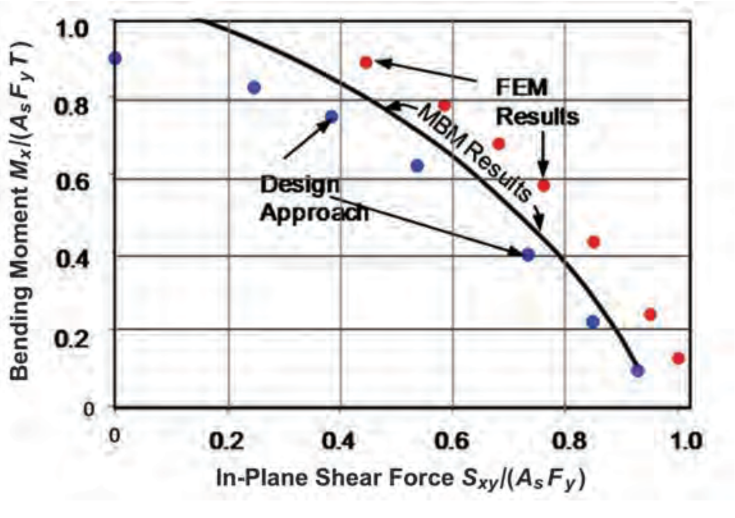

Fig. 9-5. Moment-shear interaction for SC wall (Varma et al., 2014).

as the original interaction equations in terms of the principal forces. This was confirmed by plotting the interaction surface using both forms of the interaction equations.

Figure 9-6 shows the interaction surface defined by the interaction equations in terms of the principal forces and some data points that were obtained using the alternate forms of the interaction equations, which confirms their equivalency. Figure 9-6 was developed using 0.5-in. (13 mm)-thick faceplates made from 50-ksi (350 MPa) steel filled with 29 in. (725 mm) of 6-ksi (40 MPa) concrete to develop a 30-in. (750 mm)-thick SC wall panel section. The anchor points in Figure 9-6 are without phi factors.

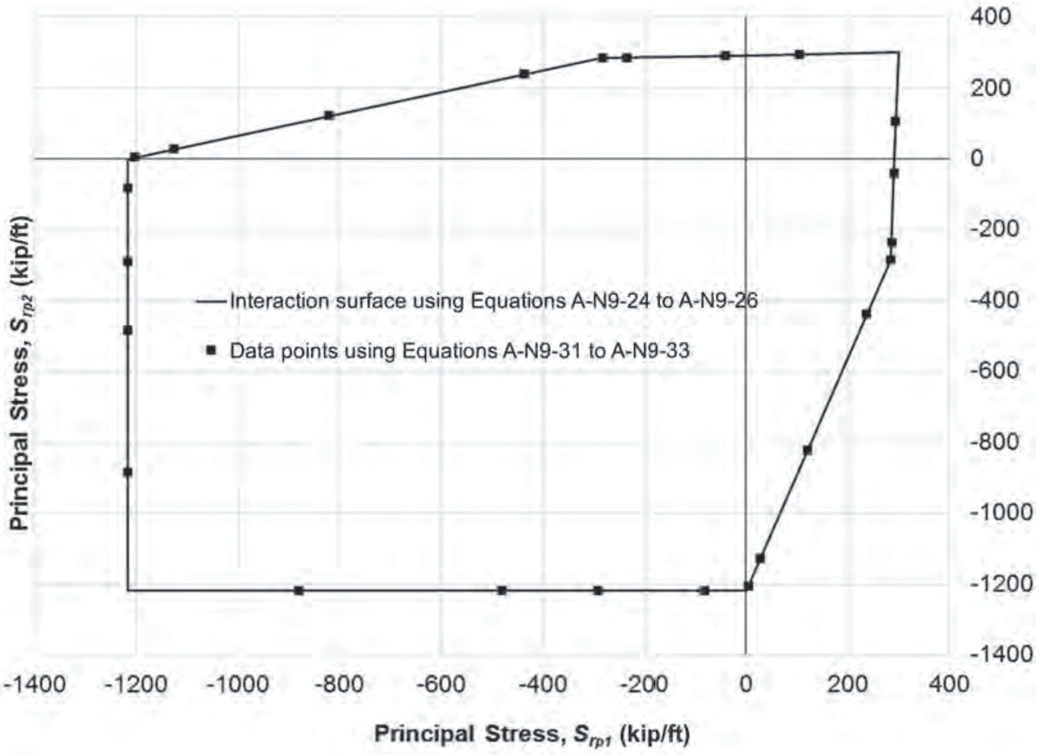

Fig. 9-6. Interaction surface and data points using alternate forms of interaction equations.

Chapter 10
Demand Capacity Ratios and Interaction Surfaces

For each loading combination, the SC wall design needs to be checked for both individual force demands and combined force demands. The demand capacity ratios (DCRs) for all elements of the SC walls need to be calculated for each load combination. For combined force demands, the principal force pairs are plotted on the interaction surface—the boundary region based on the limiting values of the combination of demands. The DCR can then be calculated by measuring the distance to the failure surface, considering the loading to be proportionally incremental. The interaction can also be checked by satisfying the interaction equations, Equations A-N9-23 and A-N9-24 to A-N9-26, provided in ANSI/AISC N690.

Chapter 11
Design of SC Wall Connection

SC wall connection regions are defined in Section 7.6. The concept of connection regions for SC walls is similar to that of load transfer regions for composite columns specified by AISC *Specification* Section I6 (AISC, 2010b). The connection regions of SC walls are designed and detailed according to ANSI/AISC N690, Section N9.4. Bolting and welding are used as connection elements in steel structures; column anchorages involve base plates, anchor rods and shear lugs. Well-established rules and methods exist for sizing these connections. Embedded rebar, shear-friction rebar, and joint ties are used as connection elements across RC-to-RC joints—often construction joints—and again, established rules exist for designing RC connections. These rules for steel and RC structures are applicable to specific configurations, details or elements of SC wall connections; for example, the faceplates for SC wall-to-wall connections can be designed and detailed according to guidelines for steel-to-steel connections. Some general guidelines for various types of connections follow.

For steel-to-steel connections, bolts and welds can be easily sized and installed to provide adequate strength; that is, to match the required strengths or the capacity of the connecting elements. Assuring adequate ductility, especially in seismic applications, sometimes requires further consideration and testing to ensure that the connecting elements are able to accommodate large inelastic deformations in the connected members [e.g., post-Northridge research of moment frame connections and development of the AISC standard, *Prequalified Connections for Special and Intermediate Steel Moment Frames for Seismic Applications* (AISC, 2010a)]. For bracing connections or extended plate connections, simple empirical methods exist, such as the uniform force method, that are adequate for design instead of having to perform design using complex finite element analyses.

For anchorage of linear steel components, linear steel members, such as columns, can be anchored into concrete using anchor rods and lugs. This is a case of connection between linear steel members and RC elements, such as piers and basemats. Anchor rods are typically used to resist pullout forces and bending moments, while lugs are used to resist shear forces. Design rules are based on tests that exist for sizing anchor rods—ACI 349-06, Appendix D (ACI, 2006)—and lugs—AISC Design Guide 2 (Darwin, 1990). Demands on connecting elements due to simultaneous forces and moments acting on the anchored member can be easily determined for adequate sizing.

For connections to RC elements, linear or continuum RC elements, such as beams/columns and walls/floors, are often connected with other RC elements, usually across construction joints. Typical connecting elements are dowels. Dowels act as splices for transfer of tension and bending moments, and they act as shear-friction reinforcement for transfer of shear forces. Closely spaced ties are used to achieve high strain capacity and high shear strength within the beam-column joints. Substantial test data and prescriptive design rules exist to adequately size RC connections.

Generally, no prescriptive rules exist for designing connections between linear composite members and RC elements, such as filled composite column anchorage. However, various types of connection elements can be used to connect composite members and RC members, including post-tensioned bars or strands, steel headed stud anchors, dowels, lugs, and anchor rods. Possible interaction due to simultaneously acting forces and moments needs to be considered when sizing the connecting elements. The behavior of connecting elements under cyclic loads such as seismic loading needs to be considered.

SC connections are more complicated than connections involving linear composite members because multiple types of demands exist on plate/shell type SC elements. Unlike RC walls, SC walls have very large required in-plane shear strength; use of shear friction reinforcement alone may not be sufficient to match the required strength. Various types of connecting elements may be used to resist various demands; however, often the same type of connecting element may resist different types of demands simultaneously. Unlike RC member connections, it is not easy to embed rebar in SC walls because it is in the form of continuous faceplates.

Behavior beyond SSE performance needs to be considered, especially if the connection involves a brittle failure mode or if the design needs to satisfy a review level earthquake—a representation of an earthquake ground motion in the form of a response spectrum, applied at a certain depth or location, used as the basis for the analyses performed in a seismic margin assessment. It is possible that the connection will need to be designed to be weaker than the connected elements, particularly for in-plane shear. Adequate inelastic deformation capacity will need to be specified. Interaction due to various types of demands will need to be accounted for, preferably on a small element basis in the range of two times the SC wall thickness, rather than considering the entire SC wall as one unit. The local and global ductility requirements need to be addressed. Local ductility in the connection regions can be achieved by following the minimum requirements and detailing provisions of ANSI/AISC N690. Global ductility can be achieved by choosing the appropriate connection design philosophy.

11.1 CONNECTION DEMAND TYPES

Connection demands can be obtained from finite element (FE) analyses conducted in accordance with ANSI/AISC N690, Section N9.2. Elastic finite element (EFE) analyses are conducted for static loading conditions, and for Condition A (operating thermal + seismic loading) and Condition B (accident thermal + seismic loading), using appropriate stiffness values accounting for the effects of concrete cracking where applicable (discussed in Sections 7.1 and 7.5). A summary of the applicable loading combinations typically considered is provided in the design example in Appendix A in Table A-1. The results from the FE analyses can be used to determine the design demands per unit length of the connection, depending on the connection design philosophy, which are membrane axial force, N_u, membrane in-plane shear force, V_u^{in}, out-of-plane shear force, V_u^{out}, and out-of-plane bending moment, M_u. These are illustrated in Figure 11-1. Based on the connection design philosophy, each connection design demand may need to be differentiated into demands due to seismic loading (Condition A or B), and demands due to nonseismic loading, such as static loads and thermal loads.

11.2 FORCE TRANSFER MECHANISM

For each of the required strengths, N_r, V_u^{in}, V_u^{out} or M_r, a clearly identifiable force transfer mechanism needs to be identified. Each force transfer mechanism involves connectors of the same type in the connection region. If more than one force transfer mechanism is possible for resisting a particular demand type, the one with the largest connection design strength is the governing force transfer mechanism. Commonly used connectors include steel headed stud anchors, anchor rods, ties, reinforcing bars and dowels, post-tensioning bars, shear lugs, embedded steel shapes, welds and bolts, rebar mechanical couplers, and direct bearing in compression. Direct bond transfer between the steel plate and the concrete is not considered as a valid connector or force transfer mechanism.

11.3 CONNECTION DESIGN PHILOSOPHY AND REQUIRED STRENGTH

Capacity design is a fundamental aspect of the seismic design philosophy for structures (ASCE, 2013). It can be achieved by (1) designing the connections to be stronger than the expected strength of the weaker of the two connected parts, which is considered a full-strength connection, or (2) detailing the connected parts to have adequate ductility to undergo inelastic deformations and dissipate energy for beyond design basis events, which is considered an overstrength connection. ANSI/AISC N690, Section N9.4.2, permits design of SC wall connection regions using either of the philosophies. However, full-strength connections are the preferred option. The connection designed according to one of these philosophies—full-strength or overstrength connection—is further evaluated for the combined force demands for the load combinations, as shown in Figure 11-1. This design approach ensures that the connections are typically stronger than the weaker of the connected parts, and the structure will have ductile failure modes occurring in the SC walls, not in the associated connections, governing the overall response if the SC wall becomes overloaded. Figure 11-2 presents the procedure for determining the required strength of a connection. The two connection design philosophies are discussed in the following paragraphs.

11.3.1 Full-Strength Connection Design

The full-strength connection design philosophy develops the expected strength of the weaker of the two connected parts. The connection ensures ductile behavior with yielding and inelasticity occurring away from the connection in one of the connected SC walls or RC slabs. This ductile design approach is consistent with the concrete anchorage design provisions given in Section D.3.6.1 of ACI 349-06.

A full-strength connection is designed to transfer 1.25 times the individual nominal strengths—axial tension, in-plane shear, out-of-plane shear, or bending moment—of the weaker of the two connected parts. A load increase factor

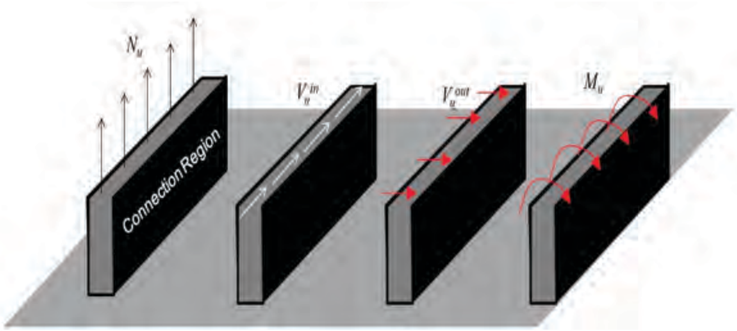

Fig. 11-1. Connection design demands per unit length.

(LIF) of 1.25 is selected to be consistent with ACI 349-06 requirements, which is the prevalent code for design of safety-related nuclear concrete facilities. The regulatory agency also considers the precedence established by ACI 349-06 to be the relevant rubric for evaluating and accepting SC structures currently being built in the United States, which are primarily replacements for RC structures. This factor takes into consideration the strain hardening and overstrength that will be expected in SC walls. Clearly identifiable force transfer mechanisms are used to transfer each of the individual strengths. These force transfer mechanisms involve connectors that are well established in practice; for example, steel welding, welded rebar couplers, and direct shear. The available strength of the connectors is determined using applicable design codes as mentioned in ANSI/AISC N690, Section N9.4.3.

Additionally, the full-strength connection is checked for the design force and moment demands calculated from the EFE analyses of the connected elements for design basis load combinations. These design force and moment demands are assumed to occur concurrently, which is conservative. The connection adequacy is assessed by first calculating the concurrent superimposed demands on the connectors that are involved in the force transfer mechanisms for the design force and moment demands, and then checking the connector strength while accounting for interaction effects in accordance with load combinations according to Section 7.1. For certain connection types such as basemat anchorage connections, ACI 349-06 or ASME *Boiler & Pressure Vessel Code* Section III, Division 2 (ASME, 2013) may also be applicable.

In summary, the full-strength connection is designed to have predominantly elastic behavior and adequate strength for design basis loads and load combinations. It is further designed to be stronger than the expected strengths of the weaker of the connected parts. Therefore, for beyond design basis loads and load combinations, inelastic deformations and energy dissipation will occur in the weaker of the connected parts. The connected parts are detailed accordingly to have good ductility and to prevent nonductile failure modes, such as out-of-plane shear and SC specific failure modes. Full-strength connection design can provide acceptable performance for accident thermal loading events, as inelastic behavior and ductility at elevated temperatures is expected from the connected SC wall and not the connections. SC walls are expected to have good behavior and ductility for accident thermal events. The connection can be verified analytically and experimentally. Because the failure is expected

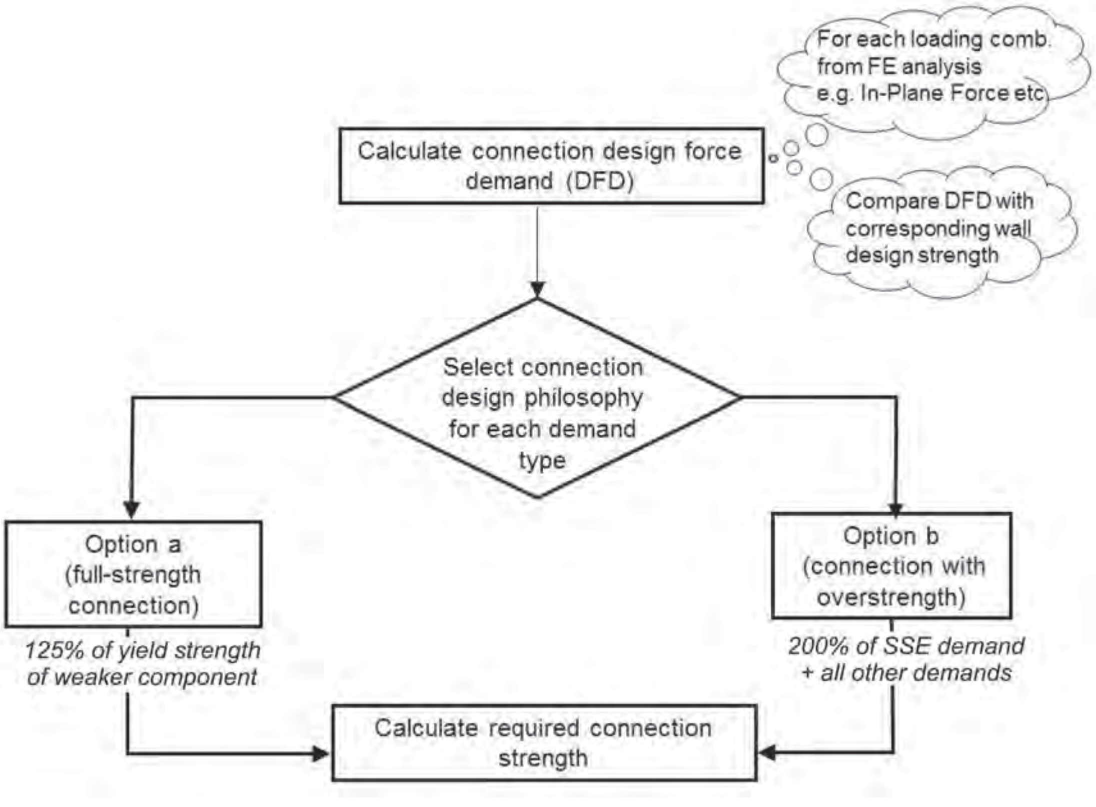
For each loading comb. from FE analysis e.g. In-Plane Force etc
Calculate connection design force demand (DFD)
Compare DFD with corresponding wall design strength
Select connection design philosophy for each demand type
Option a (full-strength connection)
Option b (connection with overstrength)
125% of yield strength of weaker component
200% of SSE demand + all other demands
Calculate required connection strength

Fig. 11-2. Calculation of connection required strength.

to occur in the connected SC walls or RC walls, only one or two scaled tests may be needed to confirm and demonstrate the ductile inelastic behavior. In some cases, analytical verification by means of benchmarked models may be sufficient.

11.3.2 Overstrength Connection Design

In some limited situations, it is not feasible to provide a full-strength connection. For example, a full-strength connection design may not be feasible if the associated SC wall or RC slab is significantly overdesigned with respect to the EFE calculated force and moment demands due to radiation shielding requirements. In such cases, the connection is designed to provide direct overstrength in the connection design with respect to the calculated force and moment demands. The overstrength connection design philosophy, adopted here, requires the connection to be designed for 200% of the seismic demands plus 100% of the nonseismic demands calculated from EFE analyses of the SC wall structure for loads and load combinations. The goal of this connection design philosophy is to provide high confidence of low probability of failure (HCLPF) for 1.67 times the SSE, which is accomplished conservatively by increasing the SSE force and moment demands by a factor of 2.0. This LIF factor of 2.0 achieves the seismic margin of 1.67 while accounting for the slight difference in the failure probability levels required by HCLPF and those provided inherently by ACI 349-06 or similar code equations for component or connector strength.

Overstrength connections are expected to fail before the connected SC walls. Therefore, these connections have to be checked for the simultaneous actions of amplified design demands calculated from FE analysis of loading combinations. This can be complicated as the simultaneous demands will subject the connectors to a combination of stresses. The connections will have to be evaluated for accident thermal loading scenarios and thermal gradients producing concrete cracking. Additionally, experimental verification of overstrength connections will be challenging as the failure will be nonductile. The connection behavior needs to be verified for various demand combinations and thermal loading.

It is important to note that the overstrength connection design philosophy should be used only in limited situations where a full-strength connection cannot be provided. Furthermore, the overstrength connection design philosophy should preferably be used only for the particular force transfer mechanisms in the connection that cannot be designed to achieve the full strength of the connected wall. Additionally, all connectors utilized in overstrength connection force transfer mechanisms need to be designed to exhibit ductile failure modes involving steel yielding.

11.3.3 Connection Evaluation for Combined Forces

The connections designed using either of the connection design philosophies need to be checked for the combination of the individual force demands discussed in Section 11.1—N_u, V_u^{in}, V_u^{out} and M_u. The force transfer mechanisms discussed in Section 11.2 are used with these individual force demands to determine the required strengths for the contributing connectors. The total required strength, R_u, for the connectors is calculated as the superposition of the required strengths from all the individual demands.

The total required strength is compared with the connector available strengths, ϕR_n, calculated as described in Section 11.4, while accounting for the effects of superposition of force demands as applicable. For example, rebar anchors may be subjected to superposition of tension and shear forces, the interaction of which is considered explicitly.

Note that some connections may be governed by more than one code. For example, the SC wall-to-basemat anchorage connection is governed by ANSI/AISC N690 and liner design requirements of the ASME *Boiler & Pressure Vessel Code* Section III, Division 2, which is applicable when the SC wall is a part of the nuclear containment structure. These connections need to meet the requirements of all applicable codes.

11.4 CONNECTION AVAILABLE STRENGTH

The connection design strengths—ϕN_n, ϕV_n^{in}, ϕV_n^{out} and ϕM_n—for each of the corresponding connection required strengths—N_r, V_r^{in}, V_r^{out}, V_r^{out} and M_r—are calculated using the applicable force transfer mechanism identified and the design strength of its contributing connectors. The available strength of the connectors is determined according to Section N9.4.3 of ANSI/AISC N690. The available strength of the connection is determined as shown in Figure 11-3.

11.4.1 Connector Available Strength

For a force transfer mechanism, the available strength of the contributing connectors is determined based on the following:

(a) For steel headed stud anchors, the available strength is determined in accordance with AISC *Specification* Section I8.3 (AISC, 2010).

(b) For welds and bolts, the available strength is determined in accordance with AISC *Specification* Chapter J.

(c) For compression transfer via direct bearing on concrete, the available strength is determined in accordance with AISC *Specification* Section I6.3a.

(d) For the shear-friction load transfer mechanism, the available strength is determined in accordance with ACI 349-06, Section 11.7.

(e) For embedded shear lugs and shapes, the available strength is determined in accordance with ACI 349-06, Appendix D.

(f) For anchor rods, the available strength is determined from ACI 349, Appendix D.

11.5 SC WALL-TO-BASEMAT ANCHORAGE CONNECTION

The SC wall-to-basemat connections can be detailed differently depending on project-specific design considerations and site conditions. The connections may be designed as full-strength or overstrength connections. Three typical configurations of the SC wall-to-basemat connections are discussed here. Each connection configuration is discussed along with possible force transfer mechanisms. The adequacy of the connection, considering the connection is designed as a full-strength connection, is checked for individual demand types corresponding to 1.25 times the available strength of the SC wall. The connection is additionally checked for a combination of demands, obtained from finite element analysis, in the wall for different load combinations.

11.5.1 Single Base Plate Connection

The single base plate SC wall-to-basemat connection consists of a base plate welded to the faceplates of the SC wall. The base plate is connected to the concrete infill of SC wall by means of steel anchors and to the basemat by means of welded coupled bars. The connection layout is presented in Figure 11-4(a). Typical connection detailing is presented in Figure 11-4(b). The design of a full-strength single base plate SC wall-to-basemat connection is presented in Step 12 of the design example in Appendix A.

The force transfer mechanism for individual demand types is discussed in the following. The section discusses only one force transfer mechanism for each demand type. However, more than one force transfer mechanism may be possible for some demand types, in which case the one with the largest connector design strength will be the governing mechanism.

Tensile Force Demand

The available tensile strength of the SC wall is governed by the resistance of the faceplates. The SC wall-to-base plate weld needs to be designed for 1.25 times the available tensile strength of the SC wall. The force transfer mechanism is illustrated in Figure 11-5. As shown, the SC faceplate-to-base plate weld needs to resist the tensile demand of the SC wall. The mechanism conservatively considers that there is no force transfer through the steel anchors at the SC concrete infill base plate interface. The force in the base plate will be transferred to the concrete basemat by means of anchor rods welded to base plate and embedded in the basemat concrete. The base plate will also be designed for any bending stresses based on the configuration of anchor rods.

Compression Demand

The compression strength of the SC wall-to-basemat connection is governed by the faceplate and concrete compressive

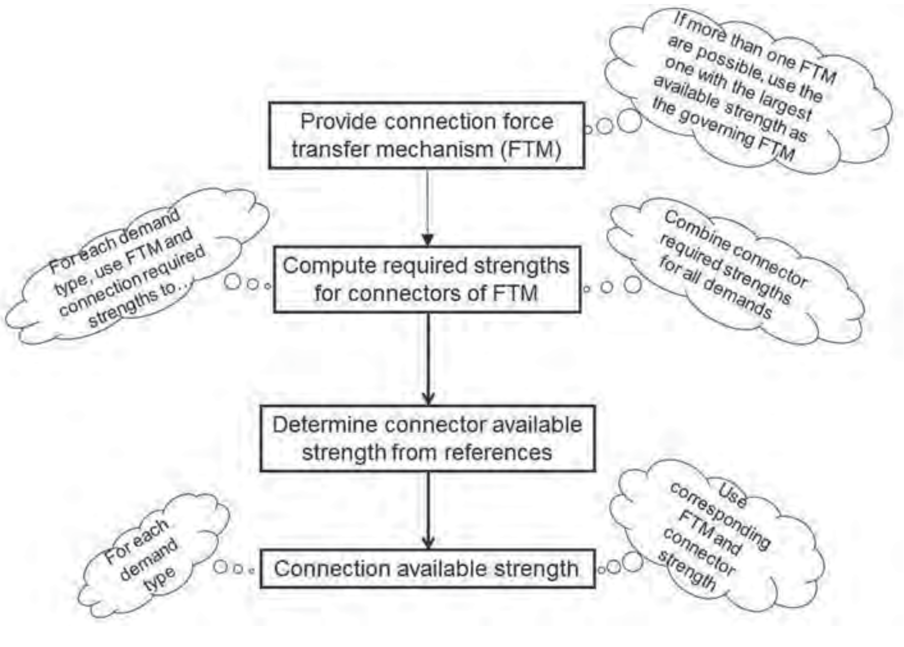
Provide connection force transfer mechanism (FTM)
If more than one FTM are possible, use the one with the largest available strength as the governing FTM
For each demand type, use FTM and connection required strengths to...
Compute required strengths for connectors of FTM
Combine connector required strengths for all demands
Determine connector available strength from references
For each demand type
Connection available strength
Use corresponding FTM and connector strength

Fig. 11-3. Calculation of connection available strength.

strengths. The base plate needs to resist the bearing forces transferred from the SC wall. Further, the bearing force will transfer from the base plate to the basemat. The force transfer mechanism is illustrated in Figure 11-6. The limit states of bearing for the concrete and yielding for the base plate need to be checked for this force transfer mechanism (Fisher and Kloiber, 2006). Any cantilever bending in the base plate due to the reaction from basemat also needs to be considered.

In-Plane Shear Demand

The in-plane shear strength of the SC wall-to-basemat connection is governed by the available shear strength of the steel anchors and the friction force between the base plate and the basemat concrete. The in-plane shear demand in the SC wall is transferred to the base plate by means of steel anchors. The fraction of the in-plane shear demand carried by the faceplates is transferred to the base plate through the faceplate-to-base plate connection, typically a welded connection. The demand is then transferred to the basemat by means of shear friction force between the base plate and the basemat. The force transfer mechanism is illustrated in Figure 11-7. Other force transfer mechanisms may also be considered for transfer of force from the base plate to the basemat; for example, shear lugs or concrete bearing on rebar couplers.

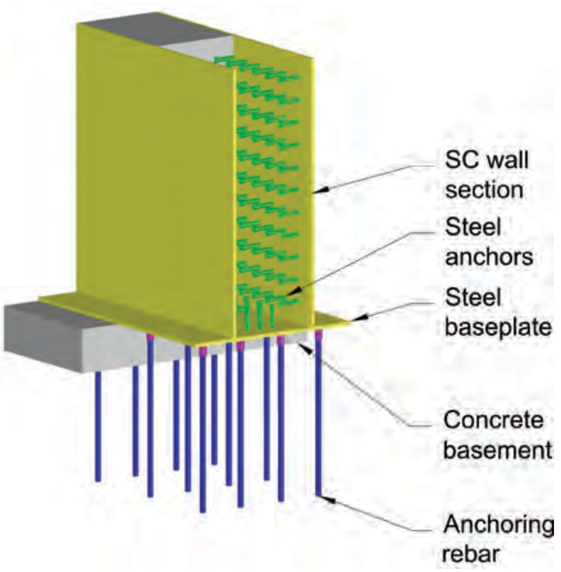
SC wall section
Steel anchors
Steel baseplate
Concrete basement
Anchoring rebar

(a) Connection layout

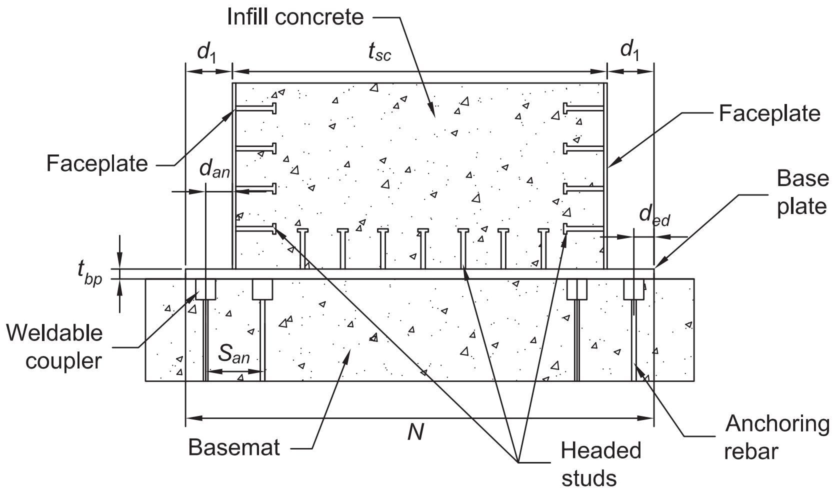
Infill concrete
d_1
t_{sc}
d_1
Faceplate
Faceplate
d_{an}
Base plate
d_{ed}
t_{bp}
Weldable coupler
S_{an}
Basemat
N
Headed studs
Anchoring rebar

(b) Cross-section view of connection

Fig. 11-4. Single base plate SC wall-to-basemat connection.

Out-of-Plane Shear Demand

The out-of-plane shear strength of the SC wall-to-basemat connection is governed by the available shear strength of the steel anchors and the friction force between the base plate and the basemat concrete. For a full-strength connection, this demand may be associated with developing the out-of-plane plastic available flexural strength of the section. The force transfer mechanism for out-of-plane shear force demands is presented in Figure 11-8. The force transfer mechanism is the same as for in-plane shear demands. Alternatively, the force transfer can be considered to be achieved through a diagonal compression strut anchored at the bottom corner of the faceplate/base plate interface. Because this strut-tie mechanism involving the tie-bars and infill concrete does not involve standard connectors, the existence of this mechanism may need to be confirmed by experiments or relevant literature.

Out-of-Plane Flexural Demand

The force transfer mechanism for out-of-plane flexure is illustrated in Figure 11-9. As shown in the figure, the out-of-plane flexural demand can be considered as an equivalent force couple acting on the faceplates. The resulting tension and compression forces in the faceplates are transferred to the basemat by means of the force transfer mechanisms for tension and compression demands discussed earlier.

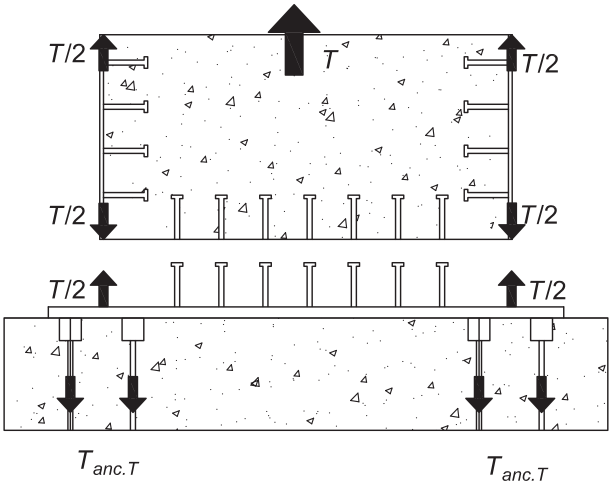

Fig. 11-5. Force transfer mechanism for tensile demand.

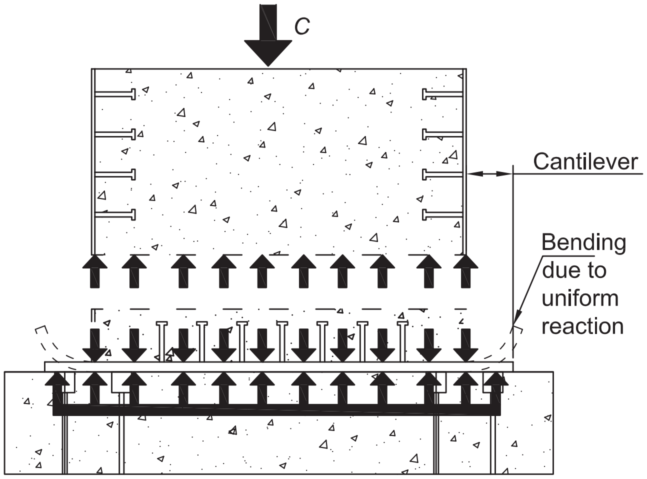

Fig. 11-6. Force transfer mechanism for compression demand.

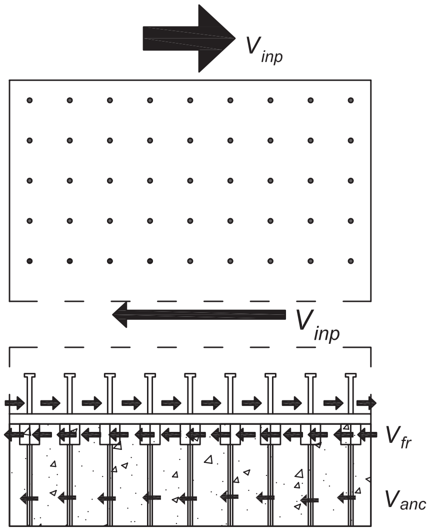

Fig. 11-7. Force transfer mechanism for in-plane shear demand.

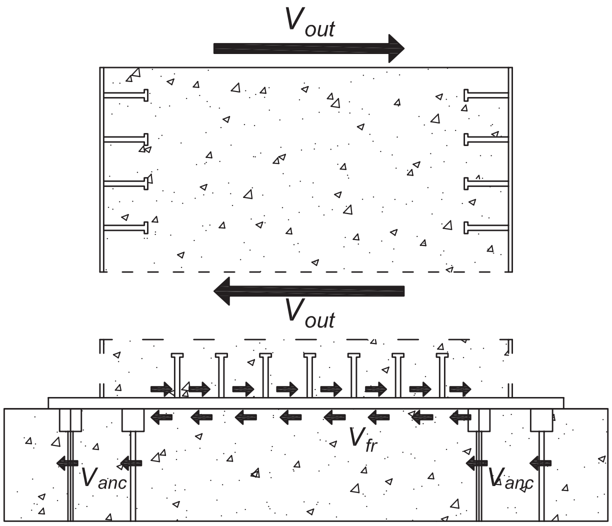

Fig. 11-8. Force transfer mechanism for out-of-plane shear demand.

11.5.2 Split Base Plate Connection

The split base plate SC wall-to-basemat connection is a variant of the single base plate connection, wherein two separate base plates are provided instead of a single base plate. Typical layout of the connection is presented in Figure 11-10. Because there is not enough interface between the base plates and the SC concrete infill, no steel anchors are provided. The split base plate connection is economical considering the typical thickness of SC wall (3–5 ft). The force transfer mechanisms for tension and out-of-plane flexural demands are the same as in single base plate connections. For the compression demand, the compression force in the SC wall concrete infill is transferred in bearing directly to the basemat concrete. The force transfer mechanisms for in-plane and out-of-plane shear demands is shear friction at the interface of the SC concrete infill and the basemat concrete. Other force transfer mechanisms such as shear transferred through the base plate and anchoring rebar may be considered.

11.5.3 Rebar SC Wall-to-Basemat Connection

The rebar SC wall-to-basemat connection employs reinforcement bars to transfer SC wall demands to the basemat. The connection is similar to those for RC wall-to-basemat connections. The details of the connection can be varied depending on if the connection is full-strength or overstrength and constructability concerns. An overstrength connection may be accomplished by leaving reinforcing bars projecting from the concrete basemat. The empty SC module is assembled around the reinforcing bars, and the concrete is then cast. The SC infill concrete can also be cast monolithically with the basemat. The faceplates can either be embedded into the basemat or be terminated at the surface of the basemat. The connection detail with faceplates embedded is presented in Figure 11-11. However, this detail is difficult to construct as the faceplates may interfere with basemat reinforcement. Additionally, embedding faceplates may result in the faceplates participating in some force transfer mechanisms. This may increase the embedment depth required for these faceplates, thus increasing the difficulty in construction. The second option of ending the faceplates at the surface base plates is easier to construct. However, in this case, the bottom portion of the SC wall behaves as an RC wall. This type of connection may be employed for overstrength design because achieving the full-strength of the SC wall through a connection that essentially behaves as an RC wall-to-basemat conncection may result in very heavy reinforcement. The high amount of reinforcement may adversely affect the constructability of the connection.

Tensile Demand

The tensile demand in the SC wall is transferred to the basemat by means of direct tension in the reinforcement bars. The tensile demand in the SC wall is primarily carried by the faceplates. This force demand is transferred to the concrete infill in the SC-to-RC transition region through faceplate steel headed stud anchors. The force is then transferred to the reinforcing bars through bond. The force transfer mechanism is shown in Figure 11-12. The amount of reinforcement is determined based on the tensile demand. Sufficient

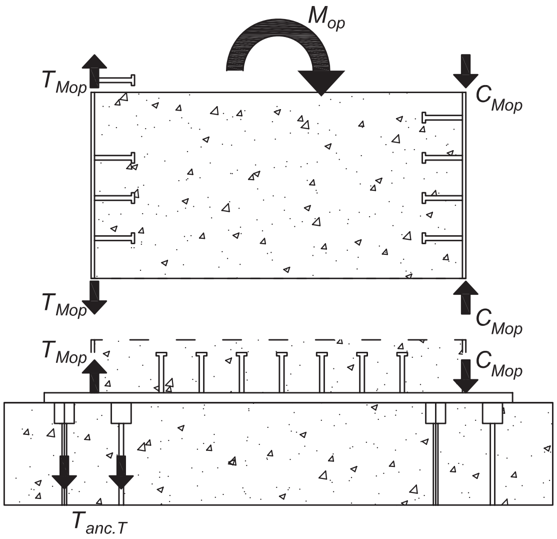

Fig. 11-9. Force transfer mechanism for out-of-plane moment demand.

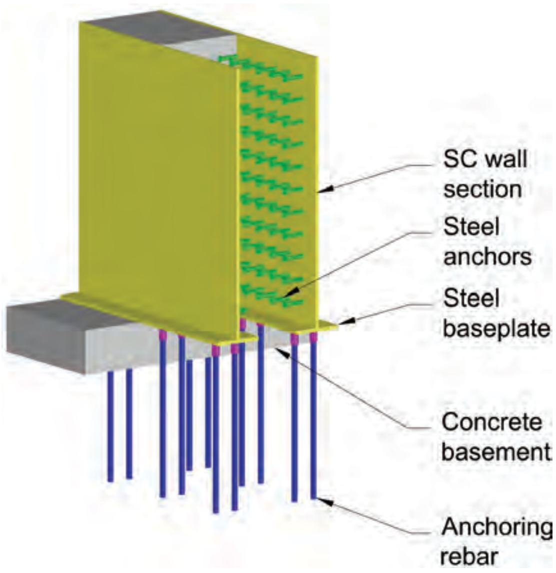

Fig. 11-10. Typical connection layout for split base plate SC wall-to-basemat connection.

embedment length of reinforcement bars (lap splice length per ACI 349) is provided to develop the tensile strength of the bars.

Compression Demand

The compression demand in the SC wall is transferred to the basemat in bearing. The limit state of bearing for concrete needs to be checked for this force transfer mechanism (Fisher and Kloiber, 2006).

In-Plane Shear Demand

The in-plane shear demand of the SC wall is transferred to the basemat through shear friction between infill concrete and the basemat concrete. The shear forces in the faceplates are transferred to the concrete infill through the faceplate steel headed stud anchors. The force transfer mechanism is shown in Figure 11-13. Direct shear in the rebar—shear force transferred from the SC wall directly to the basemat rebar—also needs to be checked in order to avoid failure of the connection.

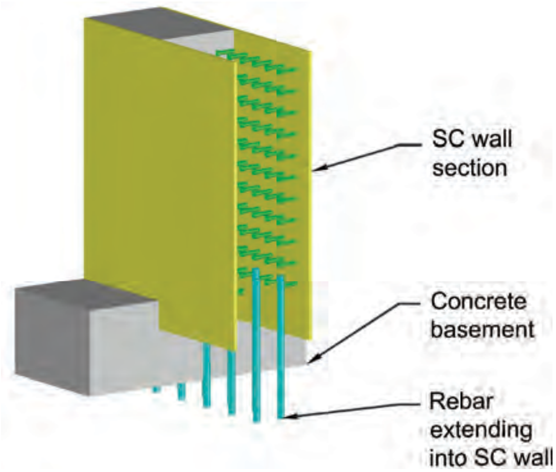

Fig. 11-11. Typical connection layout for rebar SC wall-to-basemat connection.

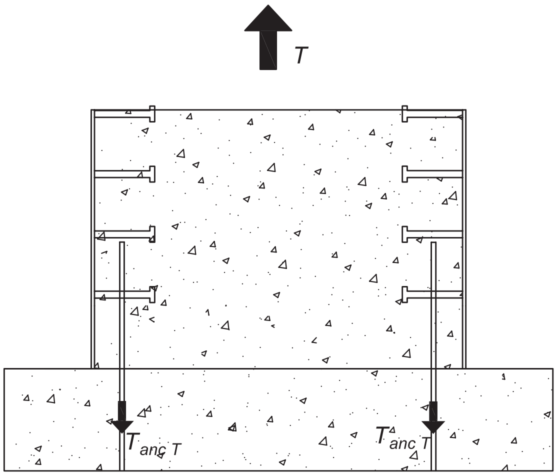

Fig. 11-12. Force transfer mechanism for tensile demand.

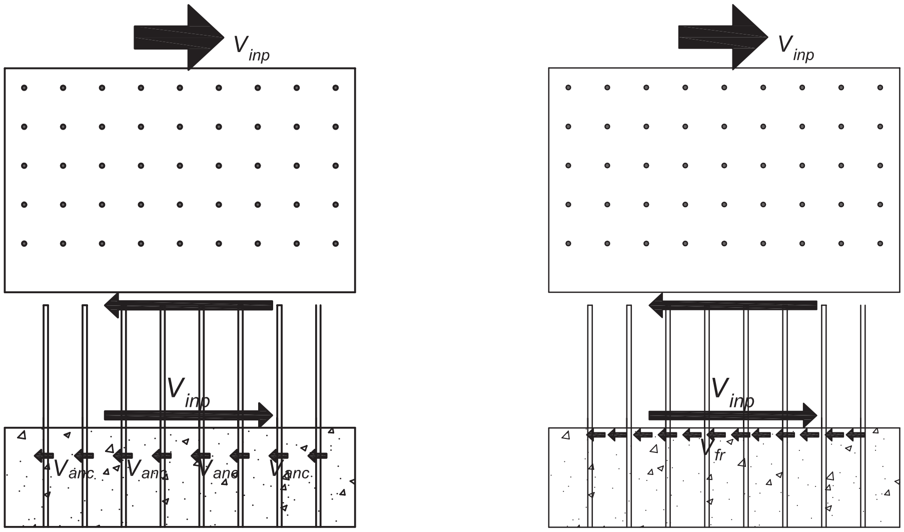

(a) Load transfer using rebar direct shear

(b) Load transfer using shear friction

Fig. 11-13. Force transfer mechanism for in-plane shear demand.

Out-of-Plane Shear Demand

The force transfer mechanism for out-of-plane shear is the same as for the in-plane shear demand.

Out-of-Plane Flexural Demand

The out-of-plane available flexural strength of the connection may be idealized as a plastic compression mechanism in the basemat concrete—concrete in compression reaches its capacity—and tension forces in the reinforcement bars on the opposite side. The force transfer mechanism is shown in Figure 11-14. Adequate resistance and development length of the rebar need to be provided to transfer the force demands from the SC walls to the concrete basemat.

11.6 SC WALL-TO-WALL JOINT CONNECTION

The internal forces generated in SC walls by the load combinations are either anchored to the basemat or transferred to connected walls through joints. The SC wall-to-basemat connection has been discussed previously. Figure 11-15 presents the plan view of a typical SC wall-to-wall joint connection. The connection can be designed as a full-strength or overstrength connection.

The typical SC wall-to-wall T-joint connection consists of a discontinuous SC wall that is connected to an orthogonal continuous SC wall. The force demands need to be transferred from the discontinuous SC wall to the continuous SC wall through the joint region. For a full-strength connection, the individual demand types can be transferred by considering the following force transfer mechanisms.

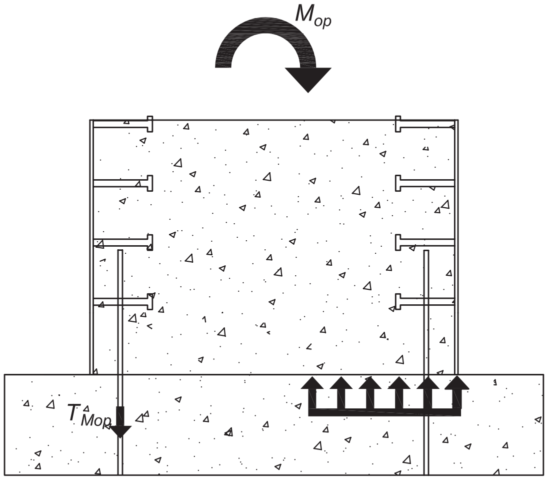

Fig. 11-14. Force transfer mechanism for out-of-plane flexural demand.

Axial Tensile Demand

Full-strength connection design corresponds to the development of a plastic mechanism accompanied by the formation of plastic hinges in the continuous SC wall at locations outside the joint region as shown in Figure 11-16. This plastic mechanism will provide ductility and energy dissipation for beyond design basis events and will limit the maximum axial tension for which the joint needs to be designed. If M_p^{exp-c} is the expected plastic flexural strength of the continuous SC wall, the maximum axial tension, N_r, that can be transferred through the joint will be equal to four times M_p^{exp-c} divided by the length, L, of the continuous SC wall, as shown in Figure 11-16. The length, L, is the clear span of the wall between the supports. This maximum axial tension, N_r, is the connection required strength in axial tension. The joint region will need to be designed for the forces and joint shears, V_{js}, associated with connection required strength, N_r, in axial tension. The force transfer mechanism due to axial tensile strengths is shown in Figure 11-17. The various connector elements need to be designed for the demands corresponding to the force transfer mechanism.

In-Plane Shear Demand

Full-strength connection design requires the transfer of expected in-plane shear strength, $V_n^{i\text{-}exp\text{-}dc}$, which is the design in-plane shear demand, of the discontinuous SC wall to the continuous SC wall. The various connector elements in the joint region need to be designed for the forces and joint shear demands associated with the mechanism shown in Figure 11-18.

Out-of-Plane Shear Demand

Full-strength connection design requires the transfer of the expected out-of-plane shear strength, $V_n^{o\text{-}exp\text{-}dc}$, which is the design out-of-plane shear demand, for the connection of the discontinuous SC wall as shown in Figure 11-19. The various connector elements in the joint region need to be designed for the forces and joint shear, V_{js}, demands associated with the mechanism shown in Figure 11-20.

Out-of-Plane Flexural Demand

Full-strength connection design requires the transfer of the expected out-of-plane flexural strength, M_p^{exp-dc}, which is the design out-of-plane flexure demand, of the discontinuous SC wall. The mechanism corresponds to the development of a plastic hinge in the discontinuous SC wall as shown in Figure 11-21. This plastic hinge will provide ductility and energy dissipation for beyond design basis events. The various connector types in the joint region need to be designed for the forces and joint shear demands associated with the transfer mechanism shown in Figure 11-22.

Joint Shear Demand

The joint region for SC wall-to-wall connection is designed to be stronger than the connected walls. The region is shown in Figure 11-15. The design consists of steel diaphragm plates, steel anchors, and tie bars. The steel diaphragm plates confine the concrete and the region can be treated as a filled composite columns. The joint region is designed for the forces and joint shears, V_{js}, associated with the transfer of each demand type. The joint shears produced by the force transfer mechanisms are presented in Figure 11-17 (due to tensile demand), Figure 11-20 (due to out-of-plane shear demand), and Figure 11-22 (due to out-of-plane flexural demand). Seo et al. (2013) and Seo (2014) conducted experimental studies that observed the joint behavior for SC wall-to-wall connections. The studies found that significant joint shear is induced by the out-of-plane shear and flexural demands. Seo et al. observed that the joint shear strength can be conservatively predicted by ACI 349-06, Section 21.5.3, considering the value of γ as 12 for an SC wall-to wall joint.

11.7 RC SLAB-TO-SC WALL JOINT CONNECTION

Figure 11-23 presents a typical RC slab-to-SC wall connection detail. One conceptual design of the connection is presented in Figure 11-24. The connection can be designed as a full-strength or overstrength connection. The connection consists of a discontinuous RC slab that is connected to an orthogonal continuous SC wall at both sides. The force demands need to be transferred from the discontinuous RC slab to the continuous SC wall through the joint region. For a full-strength connection, the individual demand types can be transferred by considering the following force transfer mechanisms.

Axial Tensile Demand

Axial tension is transferred from the RC slab to the SC wall through a load path consisting of rebar, rib plates and/or ties, which are in direct tension. The tensile demand type is shown in Figure 11-25. The load transfer connectors need to be developed adequately to transfer the factored demand.

In-Plane Shear Demand

Steel anchors welded to the outside of the SC wall embedded in the RC slab and the anchors located on the inside of the SC wall provide the direct load path for the in-plane shear demands. Figure 11-26 shows the in-plane shear demand type for the connection. Shear friction resulting from engaging slab rebar at the SC faceplate provides an additional, independent, full-strength force transfer mechanism.

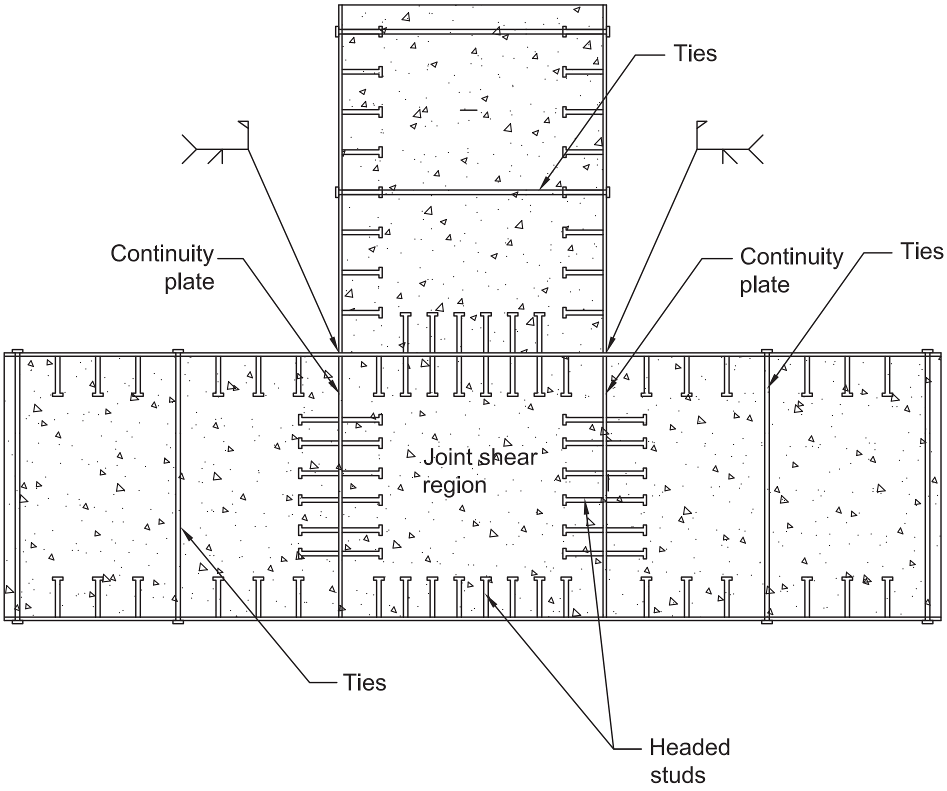

Fig. 11-15. Typical SC wall-to-wall joint connection.

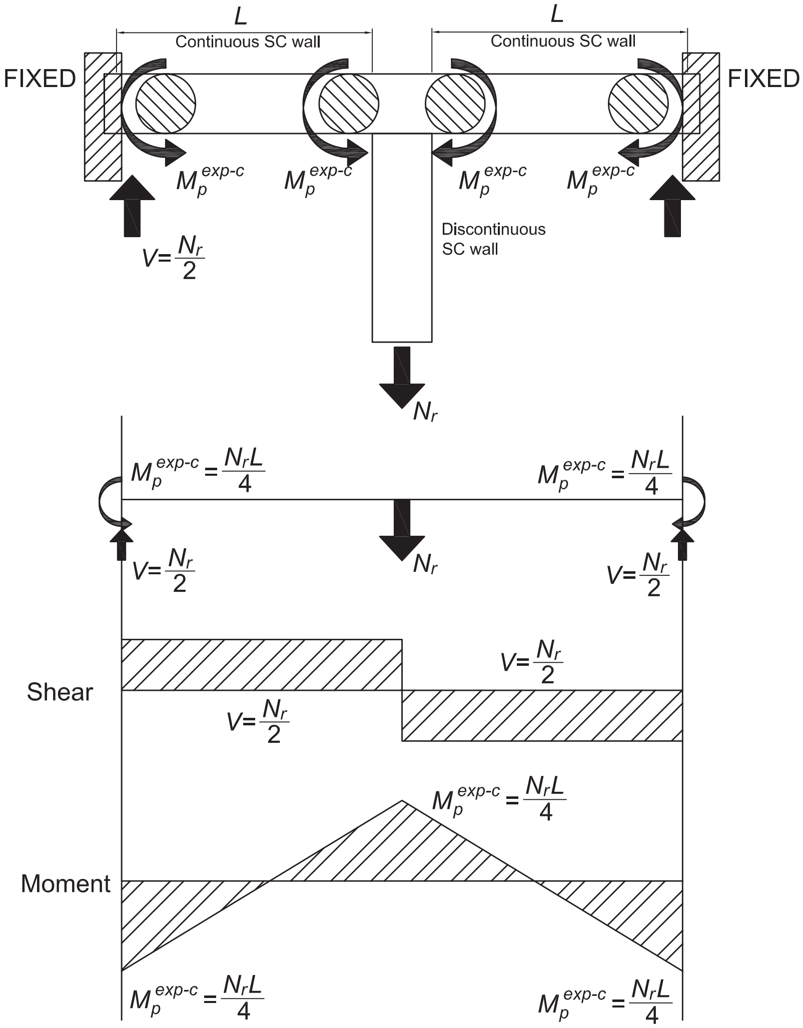
L
Continuous SC wall
L
Continuous SC wall
FIXED
FIXED
$M_p^{exp\text{-}c}$
$M_p^{exp\text{-}c}$
$M_p^{exp\text{-}c}$
$M_p^{exp\text{-}c}$
$V=\frac{N_r}{2}$
Discontinuous
SC wall
N_r
$M_p^{exp\text{-}c}=\frac{N_rL}{4}$
$M_p^{exp\text{-}c}=\frac{N_rL}{4}$
N_r
$V=\frac{N_r}{2}$
$V=\frac{N_r}{2}$
Shear
$V=\frac{N_r}{2}$
$V=\frac{N_r}{2}$
$M_p^{exp\text{-}c}=\frac{N_rL}{4}$
Moment
$M_p^{exp\text{-}c}=\frac{N_rL}{4}$
$M_p^{exp\text{-}c}=\frac{N_rL}{4}$

Fig. 11-16. Failure mechanism due to tensile demand in the discontinuous SC wall (Seo, 2014).

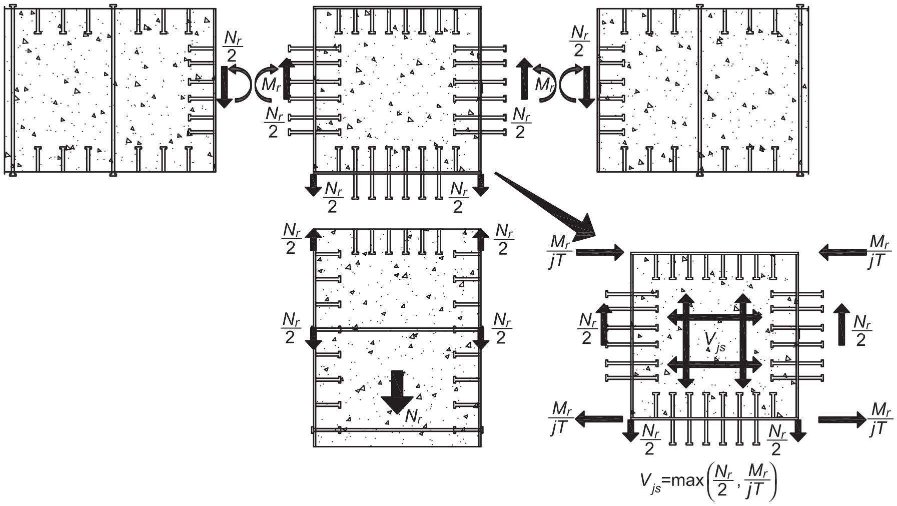
$\frac{N_r}{2}$
M_r
$\frac{N_r}{2}$
$\frac{N_r}{2}$
M_r
$\frac{N_r}{2}$
$\frac{N_r}{2}$
$\frac{N_r}{2}$
$\frac{N_r}{2}$
$\frac{N_r}{2}$
$\frac{N_r}{2}$
$\frac{N_r}{2}$
N_r
$\frac{M_r}{jT}$
$\frac{M_r}{jT}$
$\frac{N_r}{2}$
V_{js}
$\frac{N_r}{2}$
$\frac{M_r}{jT}$
$\frac{M_r}{jT}$
$\frac{N_r}{2}$
$\frac{N_r}{2}$
$V_{js}=\max\left(\frac{N_r}{2},\frac{M_r}{jT}\right)$

Fig. 11-17. Force transfer mechanism due to tensile strength (Seo, 2014).

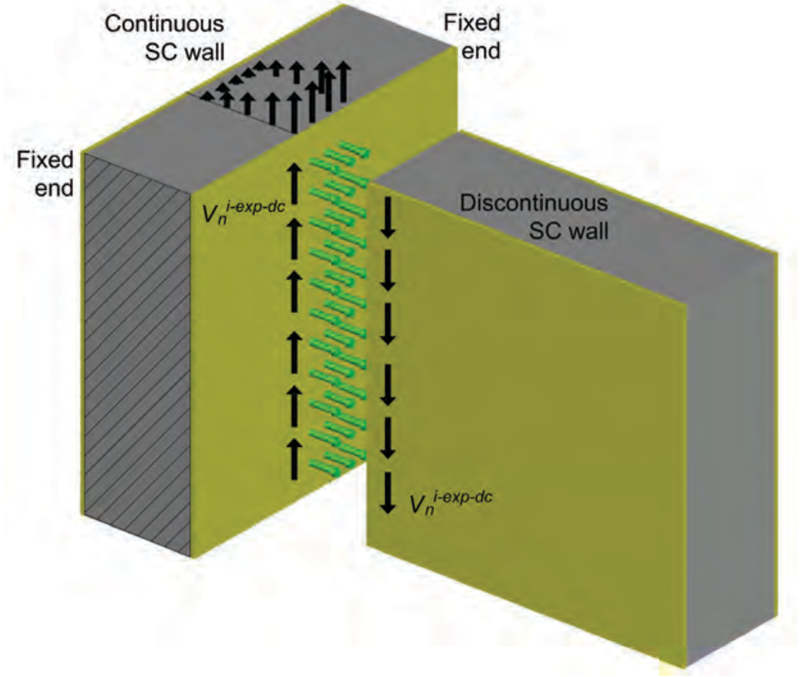
Continuous SC wall
Fixed end
Fixed end
$V_n^{i\text{-}exp\text{-}dc}$
Discontinuous SC wall
$V_n^{i\text{-}exp\text{-}dc}$

Fig. 11-18. Load transfer mechanism for in-plane shear demand.

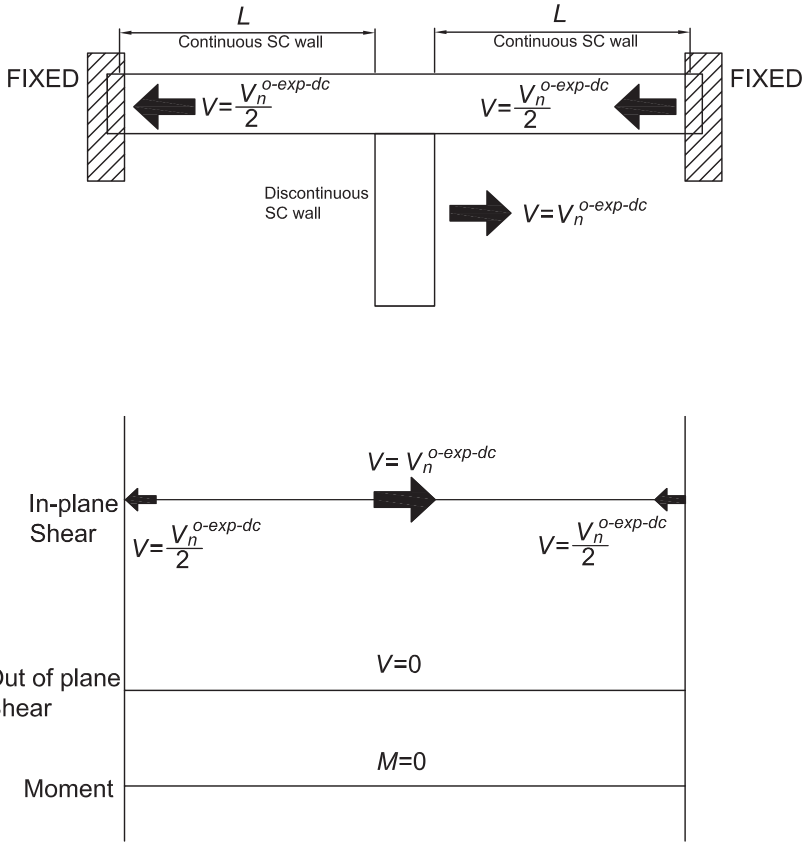
L
Continuous SC wall
L
Continuous SC wall
FIXED
FIXED
$V=\frac{V_n^{o\text{-}exp\text{-}dc}}{2}$
$V=\frac{V_n^{o\text{-}exp\text{-}dc}}{2}$
Discontinuous SC wall
$V=V_n^{o\text{-}exp\text{-}dc}$
$V=V_n^{o\text{-}exp\text{-}dc}$
In-plane Shear
$V=\frac{V_n^{o\text{-}exp\text{-}dc}}{2}$
$V=\frac{V_n^{o\text{-}exp\text{-}dc}}{2}$
$V=0$
Out of plane Shear
$M=0$
Moment

Fig. 11-19. Moments and shears due to design out-of-plane shear demand (Seo, 2014).

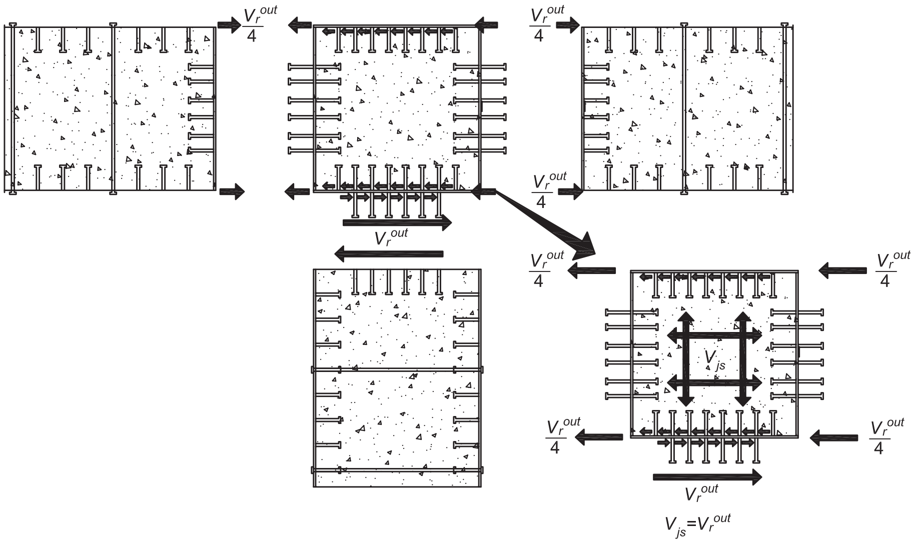

$\frac{V_r^{out}}{4}$
V_r^{out}
V_{js}
$V_{js}=V_r^{out}$

Fig. 11-20. Force transfer mechanism for out-of-plane shear demand (Seo, 2014).

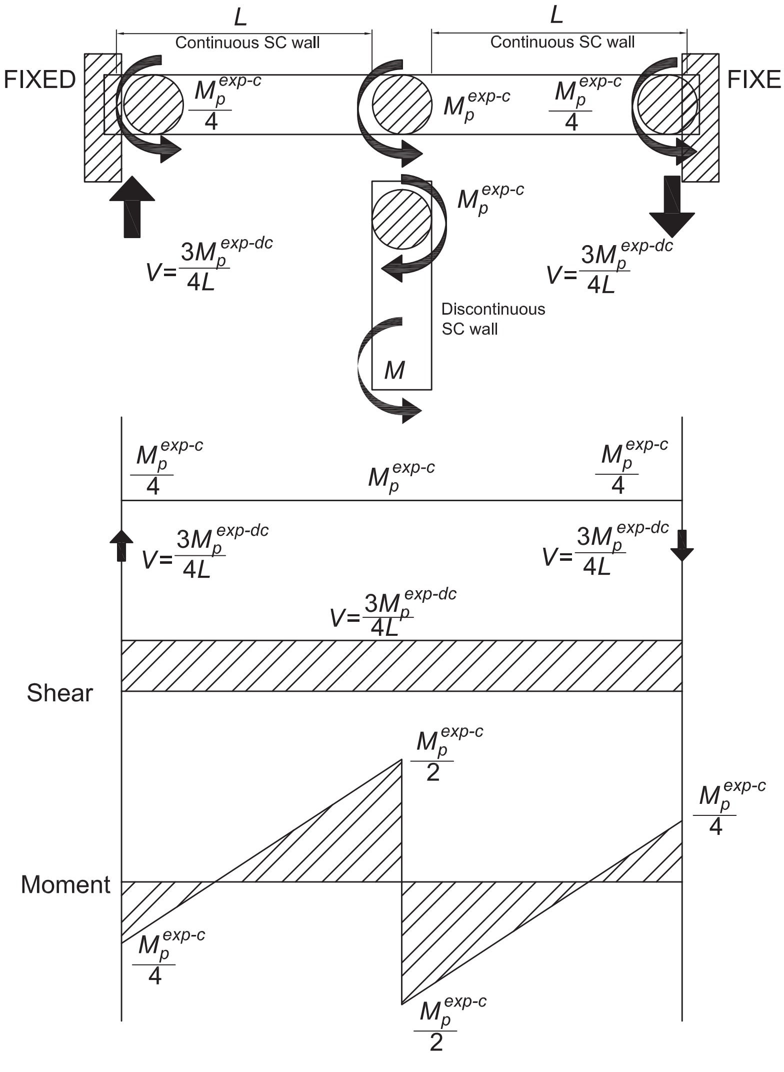

L
Continuous SC wall
L
Continuous SC wall
FIXED
FIXED
$\frac{M_p^{exp\text{-}c}}{4}$
$M_p^{exp\text{-}c}$
$\frac{M_p^{exp\text{-}c}}{4}$
$M_p^{exp\text{-}c}$
$V=\frac{3M_p^{exp\text{-}dc}}{4L}$
$V=\frac{3M_p^{exp\text{-}dc}}{4L}$
Discontinuous SC wall
M
$\frac{M_p^{exp\text{-}c}}{4}$
$M_p^{exp\text{-}c}$
$\frac{M_p^{exp\text{-}c}}{4}$
$V=\frac{3M_p^{exp\text{-}dc}}{4L}$
$V=\frac{3M_p^{exp\text{-}dc}}{4L}$
$V=\frac{3M_p^{exp\text{-}dc}}{4L}$
Shear
$\frac{M_p^{exp\text{-}c}}{2}$
$\frac{M_p^{exp\text{-}c}}{4}$
Moment
$\frac{M_p^{exp\text{-}c}}{4}$
$\frac{M_p^{exp\text{-}c}}{2}$

Fig. 11-21. Failure mechanism due to out-of-plane flexural demand on discontinuous SC wall (Seo, 2014).

Out-of-Plane Shear Demand

Figure 11-27 shows the out-of-plane shear demand for the connection. Steel anchors welded to the outside of the SC wall embedded in the RC slab and the anchors located on the inside of the SC wall provide the direct load path for the out-of-plane shear demands. Shear friction resulting from engaging the slab rebar at the SC faceplate provides an additional, independent, full-strength force transfer mechanism.

Out-of-Plane Flexural Demand

Figure 11-28 shows the out-of-plane flexural demand for the connection. The tensile demand resulting from the out-of-plane moment is transferred from the slab to the SC wall through direct tension in rebar, rib plates and/or ties. The resulting compression force is mainly transferred through concrete in bearing.

The out-of-plane flexural demand will lead to a joint shear demand for the connection, as shown in Figure 11-28. The demand is resisted by the concrete joint shear capacity determined by ACI 349-06, Section 21.5.3.

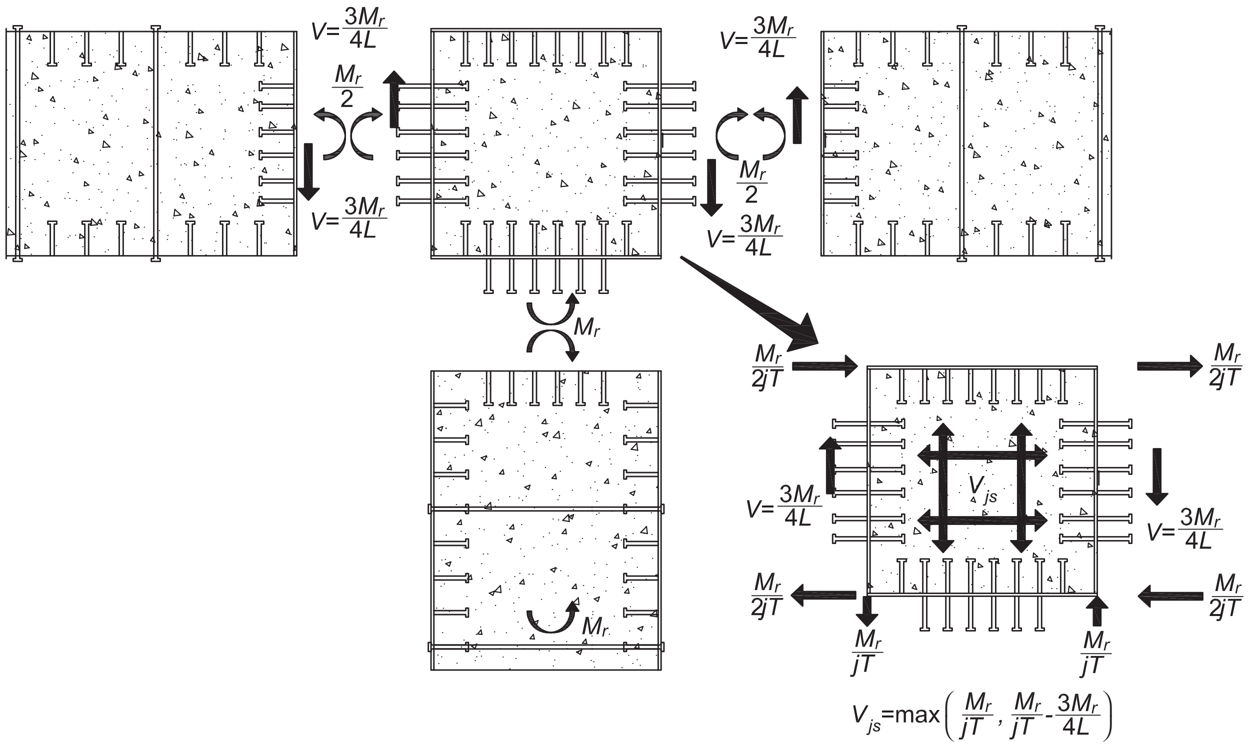

$V=\frac{3M_r}{4L}$
$\frac{M_r}{2}$
$V=\frac{3M_r}{4L}$
$V=\frac{3M_r}{4L}$
$\frac{M_r}{2}$
$V=\frac{3M_r}{4L}$
M_r
$\frac{M_r}{2jT}$
$\frac{M_r}{2jT}$
V_{js}
$V=\frac{3M_r}{4L}$
$V=\frac{3M_r}{4L}$
$\frac{M_r}{2jT}$
$\frac{M_r}{2jT}$
M_r
$\frac{M_r}{jT}$
$\frac{M_r}{jT}$
$V_{js}=\max\left(\frac{M_r}{jT}, \frac{M_r}{jT}-\frac{3M_r}{4L}\right)$

Fig. 11-22. Force transfer mechanism for out-of-plane flexural demand (Seo, 2014).

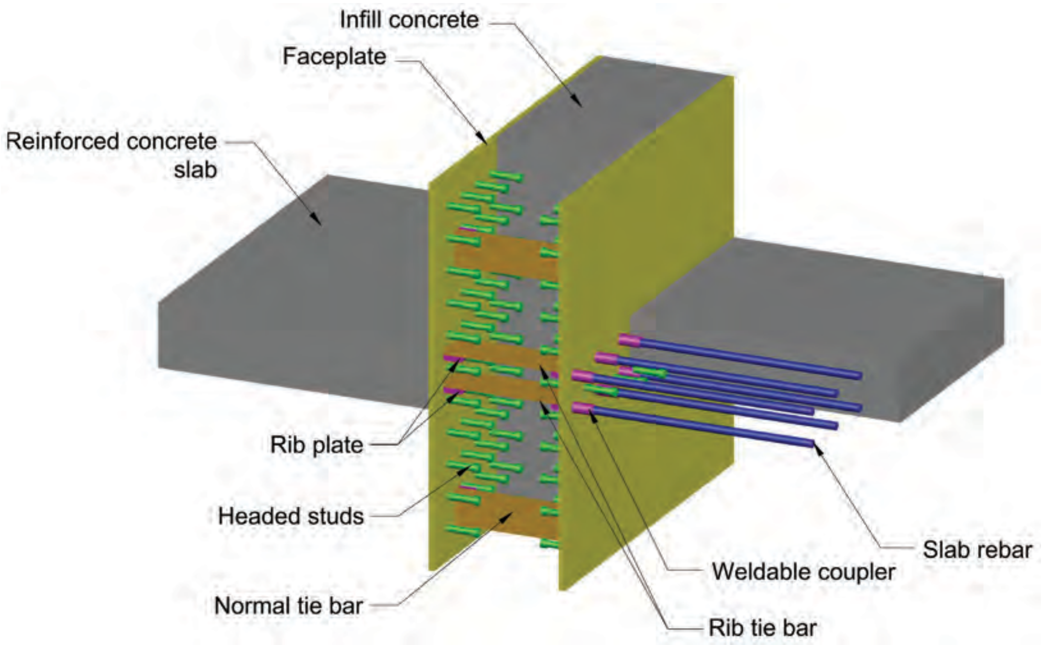
Infill concrete
Faceplate
Reinforced concrete slab
Rib plate
Headed studs
Normal tie bar
Slab rebar
Weldable coupler
Rib tie bar

Fig. 11-23. Typical RC slab-to-SC wall joint connection.

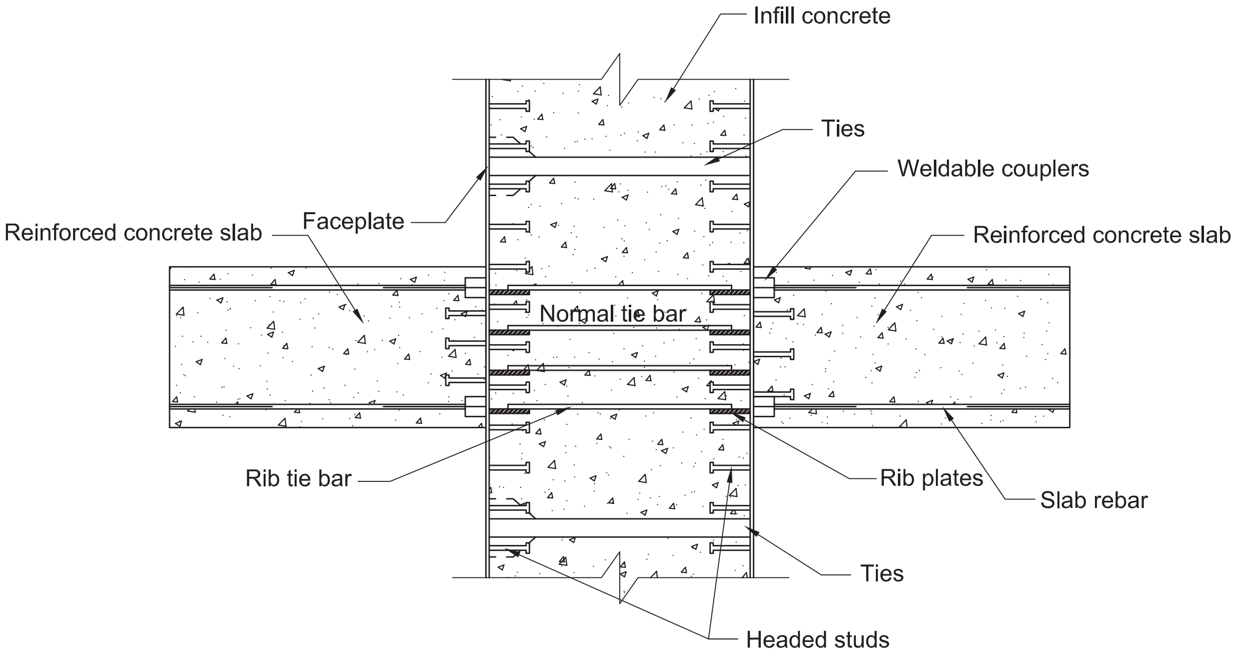
Infill concrete
Ties
Weldable couplers
Faceplate
Reinforced concrete slab
Reinforced concrete slab
Normal tie bar
Rib tie bar
Rib plates
Slab rebar
Ties
Headed studs

Fig. 11-24. Conceptual details of SC wall-to-RC slab connection.

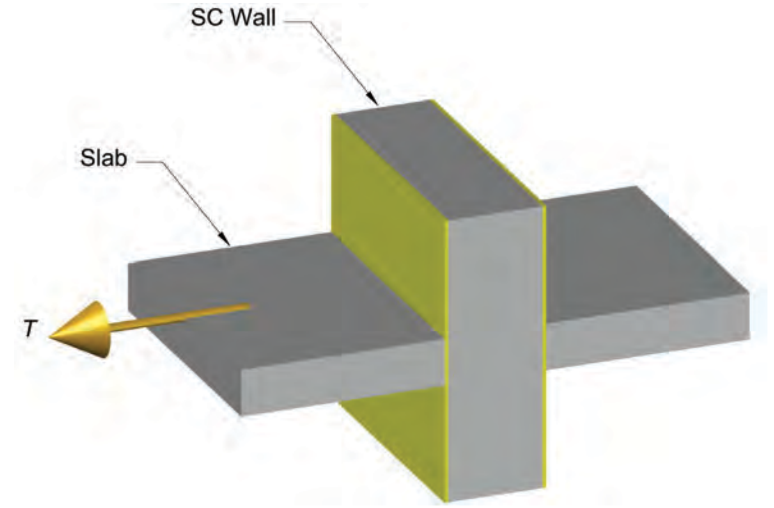
SC Wall
Slab
T

Fig. 11-25. Axial tension strength demand for RC slab-to-SC wall joint.

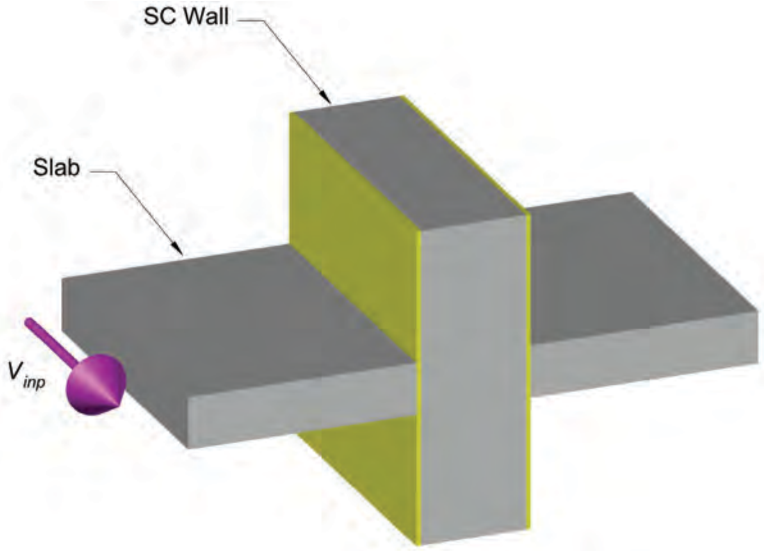
SC Wall
Slab
V_{inp}

Fig. 11-26. In-plane shear strength demand for RC slab-to-SC wall joint.

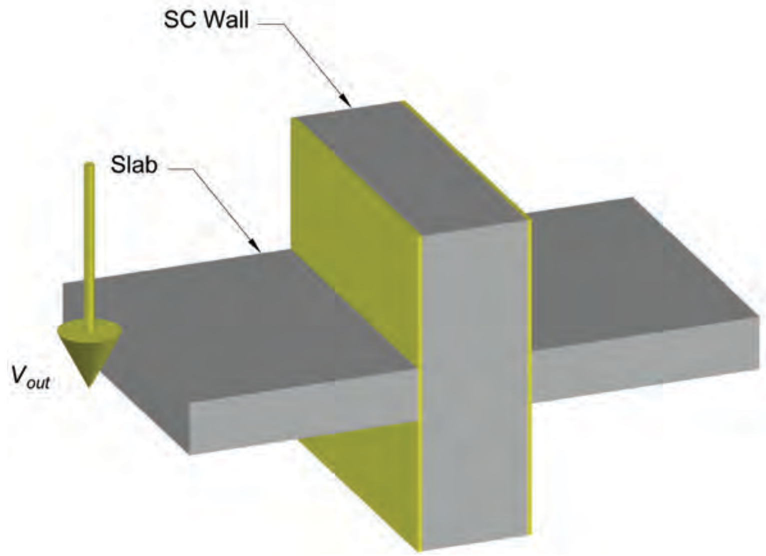
SC Wall
Slab
V_{out}

Fig. 11-27. Out-of-plane shear strength demand for RC slab-to-SC wall joint.

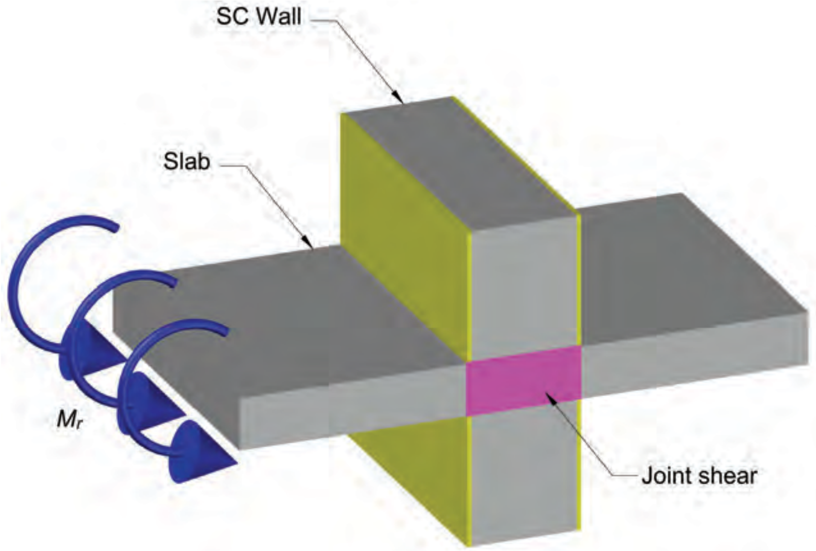
SC Wall
Slab
M_r
Joint shear

Fig. 11-28. Out-of-plane flexural demand and joint shear demand for RC slab-to-SC wall joint.

Chapter 12
Impactive and Impulsive Loads

The design of SC walls for safety-related nuclear facilities may need to be checked for impactive loads, such as tornado-borne missiles, whipping pipes, aircraft missiles, or other internal and external missiles, and for impulsive loads, such as jet impingement loads, blast pressure, compartment pressurization, or jet shield reactions. The effects for impactive and impulsive loads are considered in extreme environmental and abnormal load combinations concurrent with other loads. These effects are permitted to be determined using inelastic analysis with limits on the ductility ratio demand, μ_{dd}, defined as the ratio of maximum displacement from analysis to the effective yield displacement in ANSI/AISC N690, Equation A-N9-7, as given in Table 12-1. Yield displacement is established using the cross-sectional effective flexural stiffness for analysis, EI_{eff}, according to ANSI/AISC N690, Equation A-N9-8.

The ductility of the member at failure is more dependent on the failure mode than on the type of loading. This is observed in the values of ductility ratios in Table 12-1. A ductility ratio greater than 1.0 is permitted for brittle failure modes because even brittle structures have been observed to display some inelastic deformation capabilities.

The available strength of SC walls for impulsive and impactive loads may be governed by flexural yielding or out-of-plane shear failure. ANSI/AISC N690 Appendix N9 classifies SC walls as flexure-controlled if the available strength for the limit state of flexural yielding is less than the available strength for the limit state of out-of-plane shear failure by at least 25%. Otherwise, SC walls are classified as shear-controlled. This requirement is based on the fact that the increase in strength under rapid strain exhibited by steel is better established than that for the shear strength of concrete. Careful consideration should be given to special cases where the flexural behavior goes significantly past yield into the strain-hardening range. In such cases, the margin for available strength in shear over the available strength in flexure should be higher.

ANSI/AISC N690 Appendix N9 permits dynamic increase factors (DIFs) based on the strain rates involved to be applied to static material strengths of steel and concrete for purposes of determining section strength. However, the DIF values are limited by ANSI/AISC N690, Table N9.1.1. The DIF is limited to 1.0 for all materials where the dynamic load factor associated with the impactive or impulsive loading is less than 1.2 (NRC, 2001). Plastic hinge rotation capacity need not be considered if the deformation limit is kept under 10 for flexure controlled sections (Varma et al., 2011c). For the axial ductility ratio, the effective yield displacement is calculated using the cross-sectional effective axial stiffness. This axial stiffness is calculated using the material elastic modulus and the model section thickness calibrated in accordance with ANSI/AISC N690, Section N9.2.3.

At the rates of strain that are characteristic of certain impactive and impulsive loads, both the concrete and the structural steel exhibit elevated yield strengths, while the strain at the onset of strain hardening and the tensile strength increase slightly. The modulus of elasticity remains nearly constant. The DIF values given in ANSI/AISC N690 represent the ratio of dynamic to static yield strengths or ultimate strengths, and are direct functions of the strain rates involved. The values have been taken from NEI 07-13 (NRC, 2011).

Response of SC walls subjected to impulsive loads can be determined by one of the following methods:

a. The dynamic effects of impulsive loads are considered based on approximation of the wall panel as a single degree of freedom (SDOF) elastic, perfectly plastic system, where the resistance function and limiting ductility are defined as in ANSI/AISC N690, Section N9.1.6b. System response is determined by either a nonlinear time history analysis or, for well-defined impulse functions, rectangular and triangular pulses, selected from established response charts such as those in Biggs (1964).

b. The dynamic effects of impulsive loads are considered based on the approximation of the wall panel as a SDOF system with bilinear stiffness. System response is determined by a nonlinear time history analysis. Either the ductility is limited as defined in ANSI/AISC N690, Section N9.1.6b, or the plate principal strain may be limited to 0.05.

c. The dynamic effects of impulsive loads are considered by performing a nonlinear FE analysis. The plate principal strain is limited to 0.05.

In cases of impulsive and impactive loads that are expected to deform the structure beyond its elastic limits, the usefulness of load combinations given in ANSI/AISC N690, Section NB, is rather limited. These combinations do not provide any means of accounting for the additional work done by the static loads, which may be present as the structure deforms beyond its effective yield point.

If the energy balance method is used, only the energy available to resist the impactive and impulsive loads should be used. Alternatively, if an elastoplastic analysis is performed, the effective ductility ratio, μ', to be used in the analysis for impactive and impulsive loading is given by Equation 12-1:

Table 12-1. Ductility Ratio Demand

Description of Element	Ductility Ratio Demand, μ_{dd}
Flexure controlled SC walls	$\mu_{dd} \leq 10$
Shear controlled SC walls (yielding shear reinforcement spaced at section thickness divided by two or smaller)	$\mu_{dd} \leq 1.6$
Shear controlled SC walls (other configurations of yielding or nonyielding shear reinforcement)	$\mu_{dd} \leq 1.3$
For axial compressive loads	$\mu_{dd} \leq 1.3$

$$\mu' = \frac{\mu_{dd} D_y - D_s}{D_y - D_s} \tag{12-1}$$

where

D_s = displacement due to static loads, in. (mm)

D_y = displacement at yield, in. (mm)

μ_{dd} = ductility factor

The effective ductility ratio is to be used in conjunction with the effective available resistance, which is equal to the available resistance less the force due to static loads. Instead of a more rigorous analysis, seismic forces can be conservatively treated as equivalent static loads in the analysis for determining the adequacy of the structure for impactive and impulsive loading.

Design of SC walls for impactive loads needs to satisfy the criteria for both local effects and overall structural response. Local impact effects include perforation of the SC wall. For a structural system to act as a missile barrier, the member needs to be sufficiently thick to prevent perforation. Bruhl et al. (2015a) have presented a three-step approach to design an individual SC wall for a specific missile. The evaluation procedure is explained in Figure 12-1. The front surface faceplate is conservatively neglected in this analysis. Thus, impact of a projectile on the concrete dislodges a conical concrete plug, which in turn impacts the rear faceplate.

Step 1. The design method involves first selecting a concrete wall thickness, t_c. An existing wall thickness can be used to verify the protection afforded by a given wall. For new designs, the concrete thickness can be obtained from governing design requirements or 70% of the thickness for an RC wall determined using DOE-STD-3014 (DOE, 2006) or NEI 07-13 (NRC, 2011).

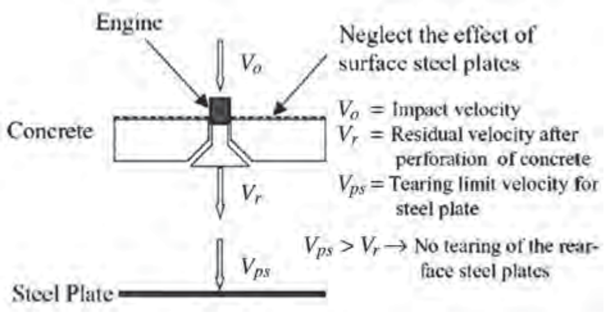
Engine
V_o
Neglect the effect of surface steel plates
Concrete
V_o = Impact velocity
V_r = Residual velocity after perforation of concrete
V_{ps} = Tearing limit velocity for steel plate
V_r
$V_{ps} > V_r \rightarrow$ No tearing of the rear-face steel plates
V_{ps}
Steel Plate

Fig. 12-1. Evaluation procedure for tearing of SC panels against impact (Mizuno et al., 2005).

Step 2. Next, the residual velocity of the missile after passing through the concrete is estimated using the formula in NEI 07-13, which is valid for rigid non-deformable missiles with initial velocity less than the perforation velocity. The ejected concrete plug is assumed to travel at the same residual velocity as the missile as the two, together, impact the rear faceplate.

Step 3. The required faceplate thickness, t_p, can then be calculated using the formula presented by Børvik et al. (2009). The corresponding equations for this method are found in Bruhl et al. (2015a).

Using the three-step method, graphs can be generated for various missile types or specific wall configurations. Using the procedure outlined in Bruhl et al. (2015a), Figure 12-2 has been generated for a flat-nosed, 6-in.-diameter, rigid missile impacting walls of any thickness. Similarly, Figure 12-3 has been generated for the minimum practical SC wall—an interior wall of 12-in.-section thickness, t_{sc}, with 0.25-in.-thick faceplates impacted by missiles of various diameters.

For SC walls with 0.015 and 0.050 reinforcement ratios, respectively, Figures 12-2(a) and (b) provide the required concrete wall thickness for an initial missile velocity for a variety of missile weights. Figure 12-3 is used to determine the capacity of a 12-in.-thick SC wall (minimum permissible section thickness) for different missile types. If the specified missile to design against—diameter, weight and initial velocity—falls below the applicable line, the wall will prevent perforation. An increase of 25% in the faceplate thickness over the value calculated by empirical methods is necessitated by the scatter in the experimental data. This scatter, which is essentially independent of empirical equations, is accounted for by a 25% increase in faceplate thickness based on the ASCE *Structural Analysis and Design of Nuclear Plant Facilities Manual* (ASCE, 1980).

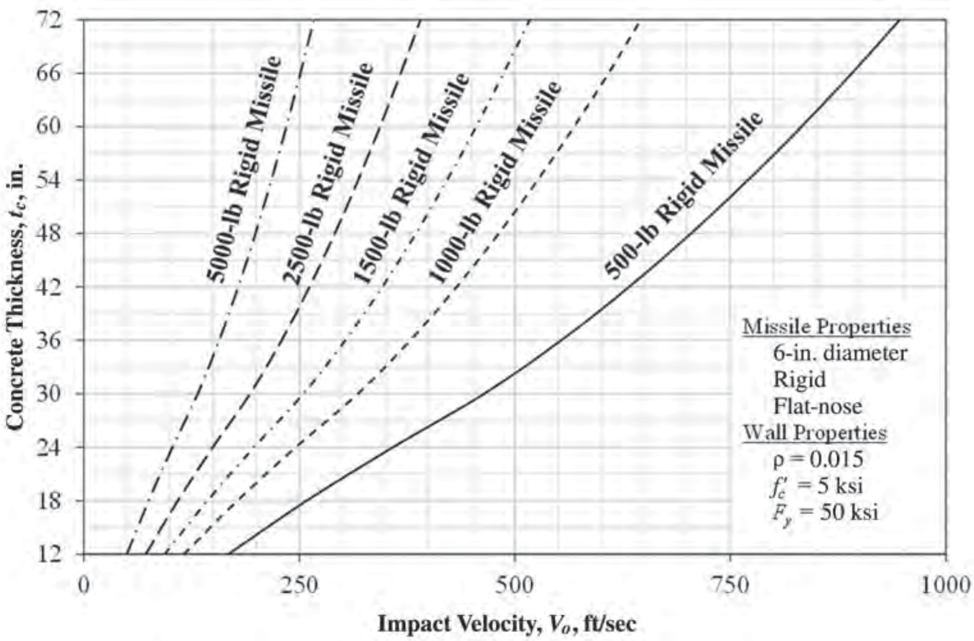

(a) 6-in.-diameter, flat-nose, rigid missile, 0.015 reinforcement ratio

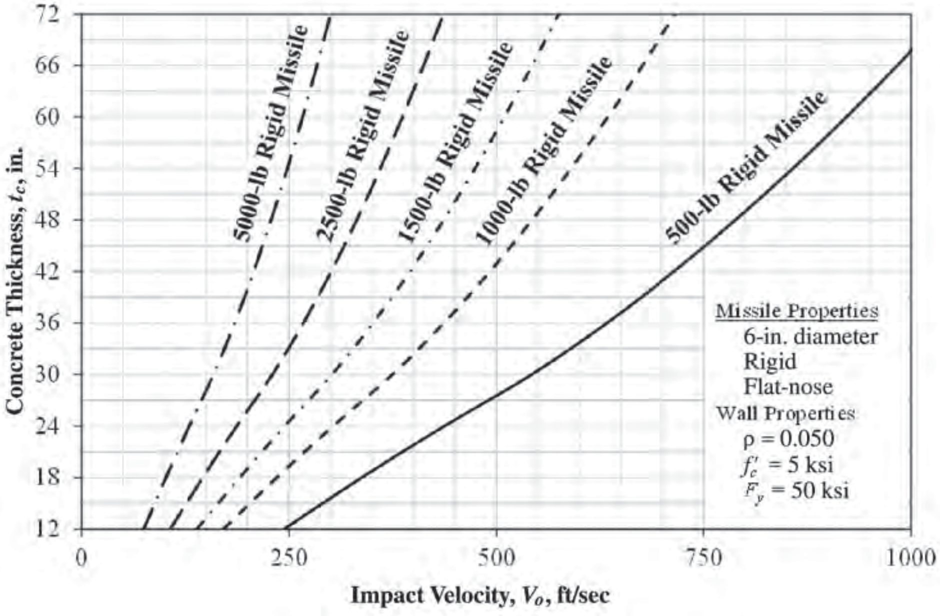

(b) 6-in.-diameter, flat-nose, rigid missile, 0.050 reinforcement ratio

Fig. 12-2. Required SC wall thickness to prevent perforation.

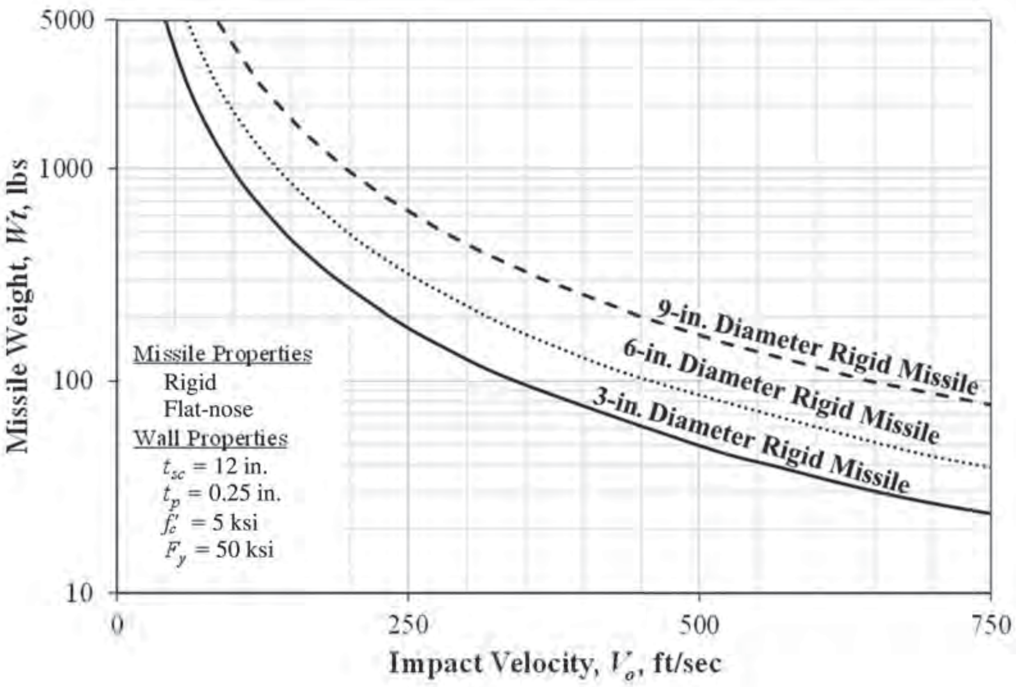

Fig. 12-3. Non-deformable (rigid) missile resistance of minimum SC wall.

Chapter 13
Fabrication, Erection and Construction Requirements

13.1 DIMENSIONAL TOLERANCES FOR FABRICATION

The dimensional tolerances discussed in ANSI/AISC N690, Chapter NM, need to be satisfied during the fabrication, erection and construction of SC panels, sub-modules and modules. Modular SC construction consists of different phases. Dimensional tolerances are applicable to:

(a) SC wall panels and sub-modules fabricated in the shop and inspected before release.

(b) Adjacent SC walls panels, sub-modules, and modules just before connecting them.

(c) Erected SC wall modules before concrete casting.

(d) Constructed SC structures after concrete casting.

SC wall panels are typically fabricated in the shop and then shipped to the field. The overall dimensions of the fabricated SC wall panels are limited by the applicable shipping restrictions. SC wall panels that are shipped by road are limited to 8 to 12 ft (2.5 to 3.7 m) in width and 40 to 50 ft (12 to 15 m) in maximum length, as shown in Figure 13-1. Additionally, SC wall sub-modules that may consist of corner, joint or splicing modules may also be fabricated in the shop and then shipped to the field. They are subjected to the same size restrictions as the wall panels. There may be additional height restrictions based on the mode of transportation.

SC wall panels and sub-modules are connected at the site by welding or bolting to make larger modules, as shown in Figure 13-2. The size and shape of a module is driven by rigging, handling, and field erection/connection considerations. These modules are erected and connected to other modules by welding or bolting to make SC structures, as shown in Figure 13-3. The tolerances ensure that the faceplates of empty SC modules are sufficiently aligned and plumb prior to concrete placement. Concrete is then poured into assembled and erected SC modules and structures.

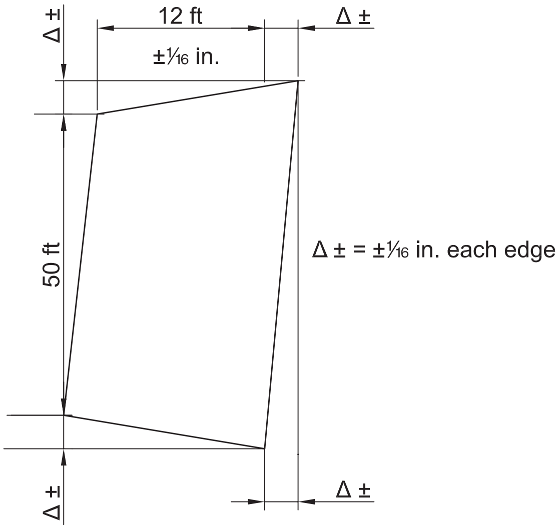

Fig. 13-1. Phase I: Fabrication of individual panels with applicable tolerances.

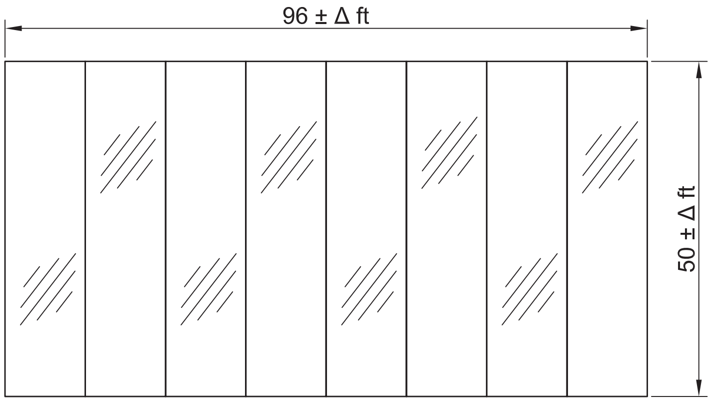

Fig. 13-2. Phase II: Combinations of panels to form a sub-module.

If the tolerances mentioned in ANSI/AISC N690, Chapter NM, are met, no additional considerations in analysis need to be made. Deviations in excess of specified tolerances are not acceptable, and need to be given due consideration by performing reconciliatory analysis or by fixing the modules to meet the tolerances. The dimensional tolerances for SC wall panels and sub-modules fabricated in the shop have to be inspected before release for shipping to the site. The dimensional tolerances are primarily for the fabricated panel thickness, t_{sc}, where the tolerance at tie locations is equal to $t_{sc}/200$ rounded up to the nearest 1⁄16 in.(2 mm), and the tolerance between tie locations is equal to $t_{sc}/100$ rounded up to the nearest 1⁄16 in. (2 mm).

Due to restricted access within the expanse of the fabricated panels, inspection is required only along the free edges. Because the fit-up tolerances ensure that panels or sub-modules can be combined together, measuring these tolerances at the free edges is considered sufficient. Additionally, it is understood that the maximum deviation of SC wall panels from permissible fit-up tolerances will be at the free edges. Shipping restrictions limit the maximum width to 10 ft (3 m). Project-specific inspection plans can be developed by the fabricators as needed. The dimensional tolerance on tie locations is based on the tolerance for steel headed stud anchor locations in AWS D1.1/D1.1M (AWS, 2010) or AWS D1.6/D1.6M (AWS, 2007), as applicable. This dimensional tolerance also constrains the tolerances for tie spacing and the tie angle with respect to the attached faceplates.

The fabricated panels and sub-modules are shipped to the site and then connected by welding or bolting to make larger modules. The dimensional tolerances for faceplates of adjoining panels, sub-modules or modules that are connected by welding are governed by the applicable weld tolerances from the AWS code (AWS D1.1/D1.1M for carbon steel and AWS D1.6/D1.6M for stainless steel). For welds that are qualified using project-specific qualification criteria in AWS, the dimensional tolerances should be based on that specified in the qualified weld procedure for the project. No additional squareness or skewed alignment tolerances are needed except those specified for the faceplates of adjoining panels, sub-modules or modules.

The dimensional tolerances for the erected SC modules before concrete placement are based on those for steel structures in the AISC *Code of Standard Practice* (AISC, 2016a). The dimensional tolerances for the constructed SC modules and structures after concrete placement are based on those for concrete construction in ACI 349-06 (ACI, 2006) and ACI 117 (ACI, 2010). The faceplate waviness needs to be checked following concrete placement to limit excessive faceplate displacement due to concrete placement. ANSI/AISC N690 Equation NM2.1 provides the waviness requirement. Figure 13-4 illustrates how faceplate waviness is measured. The faceplate waviness discussed refers to the total out-of-straightness of the faceplates and is not the net difference between waviness before and after concrete hardening. Corrective measures or reconciliatory analysis need to be performed in case the faceplate waviness requirement is not met.

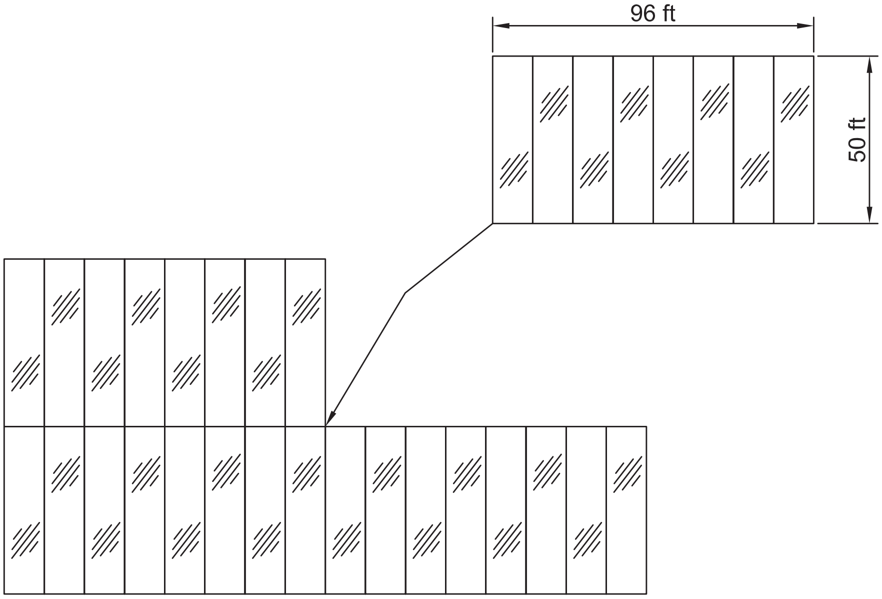

Fig. 13-3. Phase III: Erection of a module at the site prior to concreting.

Benchmarked finite element models (Zhang et al., 2014) were used to study the effect of faceplate waviness on the compressive strength of SC walls with nonslender and slender faceplates. Finite element models of nonslender SC walls with faceplate waviness up to $0.65t_p$ were analyzed. The faceplates developed more than 95% of their yield strength, $0.95A_sF_y$, at the axial compressive strength. Figure 13-5 was developed using the results of the finite element analyses. It illustrates the compression force, F_{steel}, carried by the faceplates normalized with respect to its yield strength, A_sF_y, versus the average strain over the length. For nonslender faceplates, $s/t_p = 24$, the reduction in the normalized compressive strength of the faceplates is less than 5% for an increase in imperfection from $0.1t_p$ to $0.6t_p$. However, for slender faceplates, $s/t_p = 36$, that are not permitted by ANSI/AISC N690 Appendix N9, this reduction in the normalized compressive strength is more substantial, and the post-peak behavior is degrading. Bhardwaj and Varma (2016) observed that SC walls meeting the faceplate waviness requirement and the detailing requirements of Appendix N9 that shear reinforcement is spaced at $t_{sc}/2$, do not experience significant loss in available compressive strength due to initial imperfections and concrete casting pressure when considering a typical pour height of 10 ft. However, the effects of imperfections need to be considered when the concrete pour height is larger or the ties are spaced at the section thickness.

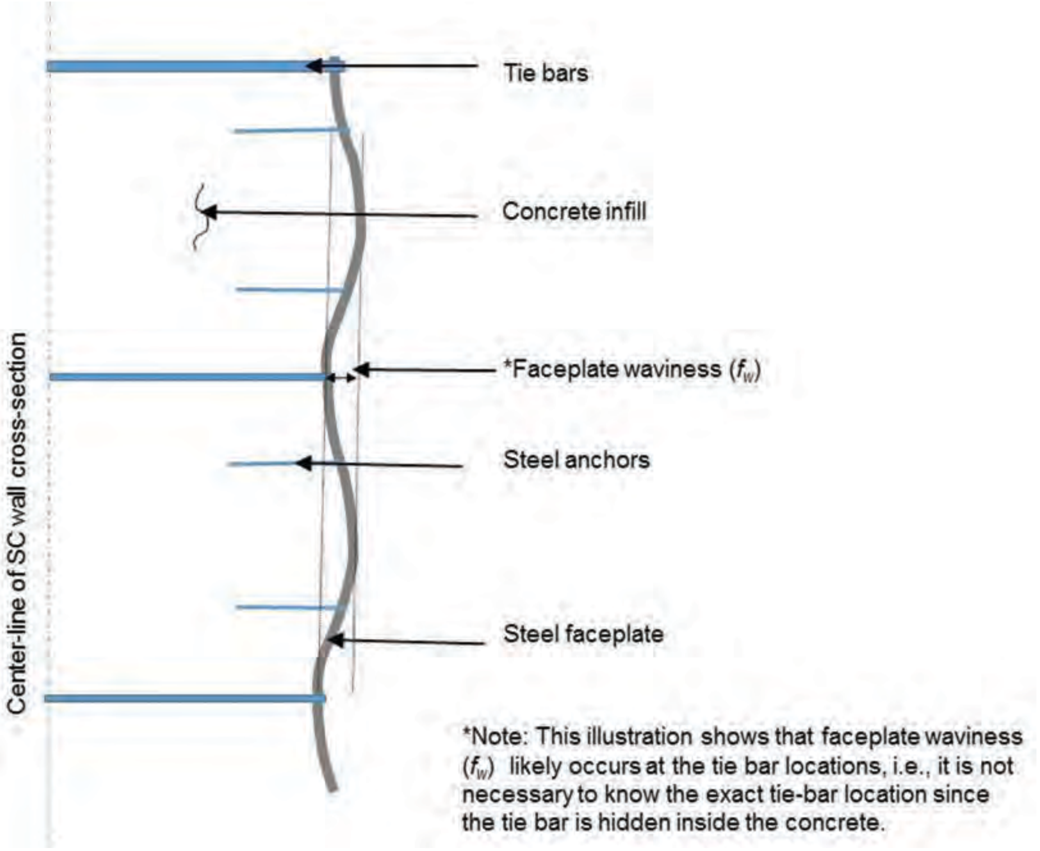
Tie bars
Concrete infill
*Faceplate waviness (f_w)
Steel anchors
Steel faceplate
Center-line of SC wall cross-section

*Note: This illustration shows that faceplate waviness (f_w) likely occurs at the tie bar locations, i.e., it is not necessary to know the exact tie-bar location since the tie bar is hidden inside the concrete.

Fig. 13-4. Faceplate waviness—the faceplate waviness and the variation in tie dimensions have been exaggerated for illustration purposes.

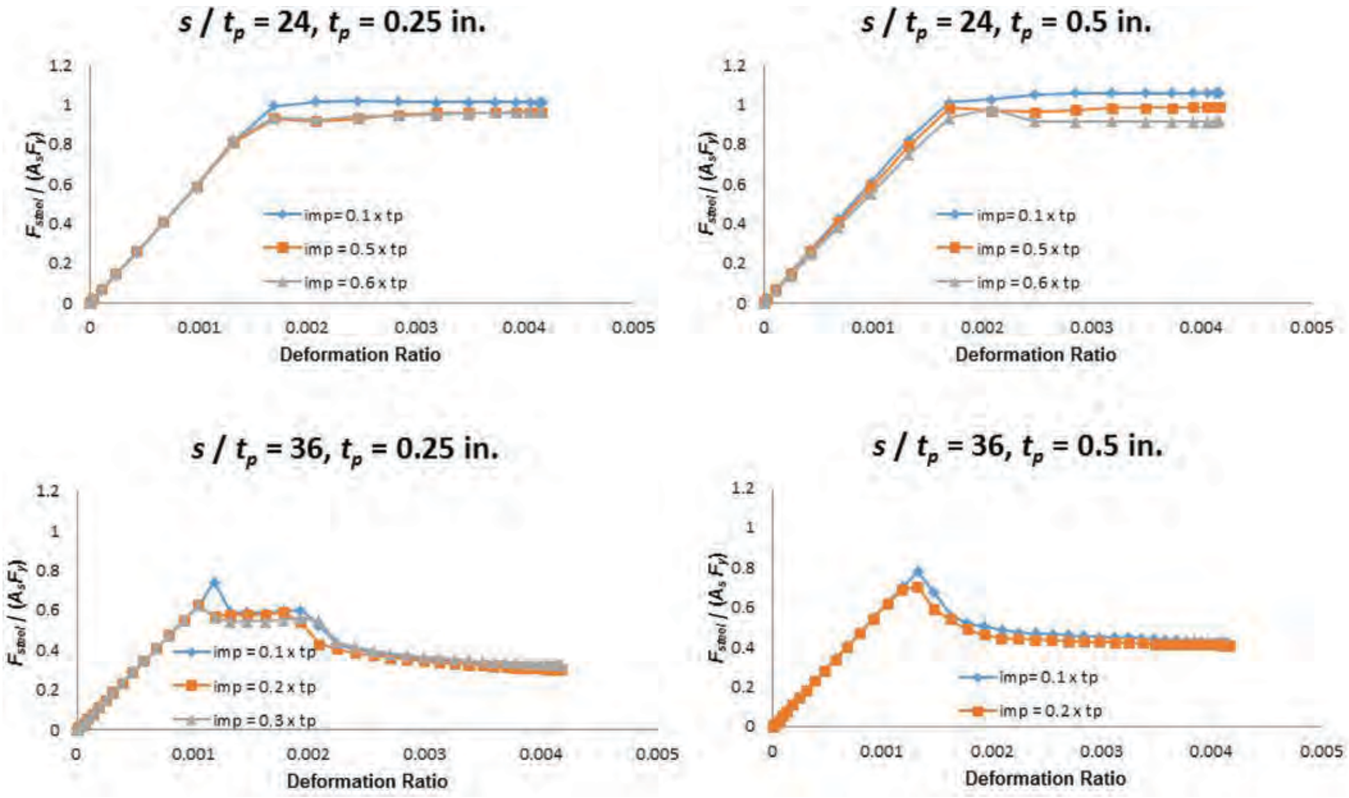
$s / t_p = 24$, $t_p = 0.25$ in.

$s / t_p = 24$, $t_p = 0.5$ in.

$s / t_p = 36$, $t_p = 0.25$ in.

$s / t_p = 36$, $t_p = 0.5$ in.

Fig. 13-5. Normalized force carried by faceplates versus average strain.

Chapter 14
Quality Assurance and Quality Control Requirements

The construction of SC walls needs to meet the quality assurance (QA) and quality control (QC) requirements provided in ANSI/AISC N690, Chapter NN. This section requires inspections to be performed for faceplates and installation of ties and steel anchors before concrete placement. After the concrete placement, the steel faceplates need to be inspected for waviness. The acceptance or rejection of the elements needs to be documented.

Appendix A: Design Example

Given:

Verify the design of a sample SC wall using the provisions of ANSI/AISC N690 Appendix N9 (AISC, 2015). For the purpose of this calculation, realistic SC wall details are considered. Use ASTM A572 Grade 50 steel for the faceplates and the ties. Assume that the ties act as the shear reinforcement for this SC wall and that the ties are connected to the SC walls by complete-joint-penetration (CJP) groove welds. Use normal weight concrete with $w_c = 145$ lb/ft^3 and a compressive strength of $f_c' = 5$ ksi.

The procedure followed in this calculation is consistent with that outlined in ANSI/AISC N690 Appendix N9, Figure C-A-N9.1.1. Unless mentioned otherwise, the sections mentioned in the calculation correspond to ANSI/AISC N690. The symbols and units used are consistent with ANSI/AISC N690.

The calculation can be organized into the following steps:

Step 0. Preliminary details of SC walls

Step 1. Minimum Appendix N9 applicability requirements

Step 2. Faceplate slenderness requirement

Step 3. Shear connector detailing

Step 4. Tie detailing

Step 5. Stiffness and other parameters for modeling SC walls

Step 6. Analysis results and required strength summary

Step 7. Individual design available strengths

Step 8. Interaction of design available strengths

Step 9. Demand capacity ratios and interaction surfaces

Step 10. Demands for anchorage design

Step 11. Impactive and impulsive loading

Step 12. Design of SC wall connections

Step 13. Combination of demands

Step 14. Connection detailing

Step 15. Design optimization

Note: The calculation does not consider any penetrations in the SC wall. The calculation uses U.S. customary units. Calculations can also be performed using SI units, with corresponding equations and parameter values provided in ANSI/AISC N690 Appendix N9. Because the demands are calculated for LRFD load combinations, the demand capacity ratio checks have been performed using LRFD. ASD calculations can be performed if the demands are obtained for ASD load combinations.

Solution

From AISC *Manual* Table 2-4, the material properties are as follows:

Faceplates:	Ties:
ASTM A572 Grade 50	ASTM A572 Grade 50
$F_y = 50$ ksi	$F_{y.tie} = 50$ ksi
$F_u = 65$ ksi	$F_{u.tie} = 65$ ksi

Steel properties are as follows:

$E_s = 29{,}000$ ksi
$G = 11{,}200$ ksi

From AISC *Specification* Appendix 4:

α_s = thermal expansion coefficient of steel
$= 7.8 \times 10^{-6}/°\text{F}$ for temperature > 150°F

From the AISC *Steel Construction Manual* Table 17-12 for rolled steel:

γ_s = density of steel
$= 490 \text{ lb/ft}^3$

From Appendix N9, Section N9.2.2, concrete properties are as follows:

$$E_c = (w_c)^{1.5}\sqrt{f'_c}$$
$$= (145 \text{ lb/ft}^3)^{1.5}\sqrt{5 \text{ ksi}}$$
$$= 3{,}900 \text{ ksi}$$

$$G_c = 772\sqrt{f'_c}$$
$$= 772\sqrt{5 \text{ ksi}}$$
$$= 1{,}730 \text{ ksi}$$

From Hong and Varma (2009):

c_c = specific heat

$$= 255.4\frac{\text{Btu}}{\text{lb} \times \Delta°\text{F}}$$

$\upsilon_c = 0.17$

From CEN (2009):

k_c = thermal conductivity (Eurocode Eq. 4)

$$= 0.013\frac{\text{Btu}}{\text{ft} \times \text{sec} \times \Delta°\text{F}}$$

From ACI (2008):

α_c = thermal expansion coefficient
$= 5.6 \times 10^{-6}/°\text{F}$ for temperature = 392°F

Step 0. Preliminary Details of SC Walls

The SC wall details assumed to begin with are based on typical plant layout details provided to the structural engineers at the beginning of the process. Plant layout engineers and designers often select the wall thickness and other parameters based on shielding requirements and past practice. During the plant layout design phase, structural engineers recommend standard steel ratios and section details to be simple and consistent. During the detailed design stage, the structural engineer's job is to check, design and finalize the SC wall details.

The critical section of the wall is selected from a portion of the refueling cavity, in the elevation range between the operating floor slabs at top-of-concrete elevations 40 ft and 66 ft. For this calculation, the following parameters are used:

h_{wall} = unsupported height of SC wall
= 66.0 ft − 40.0 ft
= 26.0 ft

t_{sc} = SC section thickness
= 56.0 in.

t_p = faceplate thickness
= 0.500 in.

s = shear connector spacing
= 6.00 in.

s_{tt} = shear reinforcement transverse spacing
= 24.0 in.

s_{tl} = shear reinforcement longitudinal spacing
= s_{tt}
= 24.0 in.

Steel headed stud anchors with a diameter, d_s, of ¾ in. are used as shear connectors and flat bars, 0.5 in. × 6 in., are used as tie bars.

$A_{tie} = t_s l_s$
= (0.500 in.)(6.00 in.)
= 3.00 in.^{2}

$F_{u.sc}$ = 65 ksi

d_s = 0.750 in.

l_s = 6.00 in.

Thermal conditions are as follows:

Ambient temperature
T_{amb} = 70°F

Operating temperature
T_{op} = 120°F

All calculations are performed for a unit width of the wall, l = 12.0 in./ft

Step 1. Minimum Appendix N9 Applicability Requirements

For the provisions of ANSI/AISC N690 Appendix N9 to be applicable, the SC wall needs to satisfy the general provisions of Section N9.1.1. This step of the calculation verifies that the SC wall being considered meets these requirements. The requirements are checked in the same order they appear in Section N9.1.1. If a provision is not satisfactorily met, the wall parameters will be updated to satisfy these requirements.

(a) SC section thickness, t_{sc}
Requirement: 18 in. $\le t_{sc} \le$ 60 in. for exterior SC walls

t_{sc} = 56.0

Therefore, the SC section thickness considered is permitted.

(b) Faceplate thickness, t_p
Requirement: 0.25 in. $\le t_p \le$ 1.5 in.

t_p = 0.500 in.

Therefore, the SC faceplate thickness considered is permitted.

(c) Reinforcement ratio, ρ
Requirement: $0.015 \le \rho \le 0.050$

$$\begin{aligned}\rho &= \frac{2t_p}{t_{sc}} &&\text{(N690 Eq. A-N9-1)}\\ &= \frac{2(0.500\text{ in.})}{56.0\text{ in.}}\\ &= 0.018\end{aligned}$$

Therefore, the reinforcement ratio considered is permitted.

(d) Specified minimum yield stress of faceplates, F_y

Requirement: $50\text{ ksi} \le F_y \le 65\text{ ksi}$

$F_y = 50\text{ ksi}$

Therefore, the specified minimum yield stress of faceplates considered is permitted.

(e) Specified minimum concrete compressive strength, f'_c

Requirement:

$4\text{ ksi} \le f'_c \le 8\text{ ksi}$; lightweight concrete is not permitted

$f'_c = 5\text{ ksi}$; normal weight concrete is used

Therefore, the specified minimum concrete compressive strength considered is permitted. Also, lightweight concrete is not used.

(f) Check that the faceplate is nonslender

This requirement will be checked in Step 2 of the calculation. In case the requirement is not met, the shear connector or shear reinforcement spacing will be adjusted.

(g) Ensure composite action between faceplates and concrete using shear connectors

The development of composite action will be verified in Step 3. In case the requirement is not met, the shear connector spacing will be adjusted.

(h) Ensure tie requirements are met

The tie requirements are checked in Step 4. If required, the tie spacing and area will be updated to satisfy the requirements.

(i) Ensure ductile failure of faceplates with holes

Because the SC wall considered does not have any holes, this requirement does not need to be checked.

(j) Nominal faceplate thickness, t_p, and yield stress, F_y, is required to be the same for both faceplates

Both faceplates have the same nominal thickness and yield stress; therefore, this requirement is satisfied.

(k) Steel rib embedment and welds

Steel ribs are not used in this example, and therefore the embedment and weld requirements for ribs are not discussed here.

(l) Splices between faceplates

The region of SC wall considered does not have any splices. Therefore, the splice connection strength requirements are not checked.

Step 2. Faceplate Slenderness Requirement

The faceplates are required to be nonslender according to ANSI/AISC N690, Section N9.1.3.

$$\frac{b}{t_p} \le 1.0\sqrt{\frac{E_s}{F_y}} \qquad \text{(N690 Eq. A-N9-2)}$$

$b = \min(s, s_{tt}, s_{tl})$

$s = 6.00$ in.

$s_{tt} = 24.0$ in.

$s_{tl} = 24.0$ in.

$b = 6.00$ in.

The value of b is calculated for the arrangement of shear connectors and ties shown in Figure A-1. For different arrangements, b may have to be calculated differently. The tie bars and steel headed stud anchors contributing to the unit cell shown are used to calculate the Q_{cv}^{avg} value in Step 8a of this example.

$$\frac{b}{t_p} = \frac{6.00}{0.500}$$

$$= 12.0$$

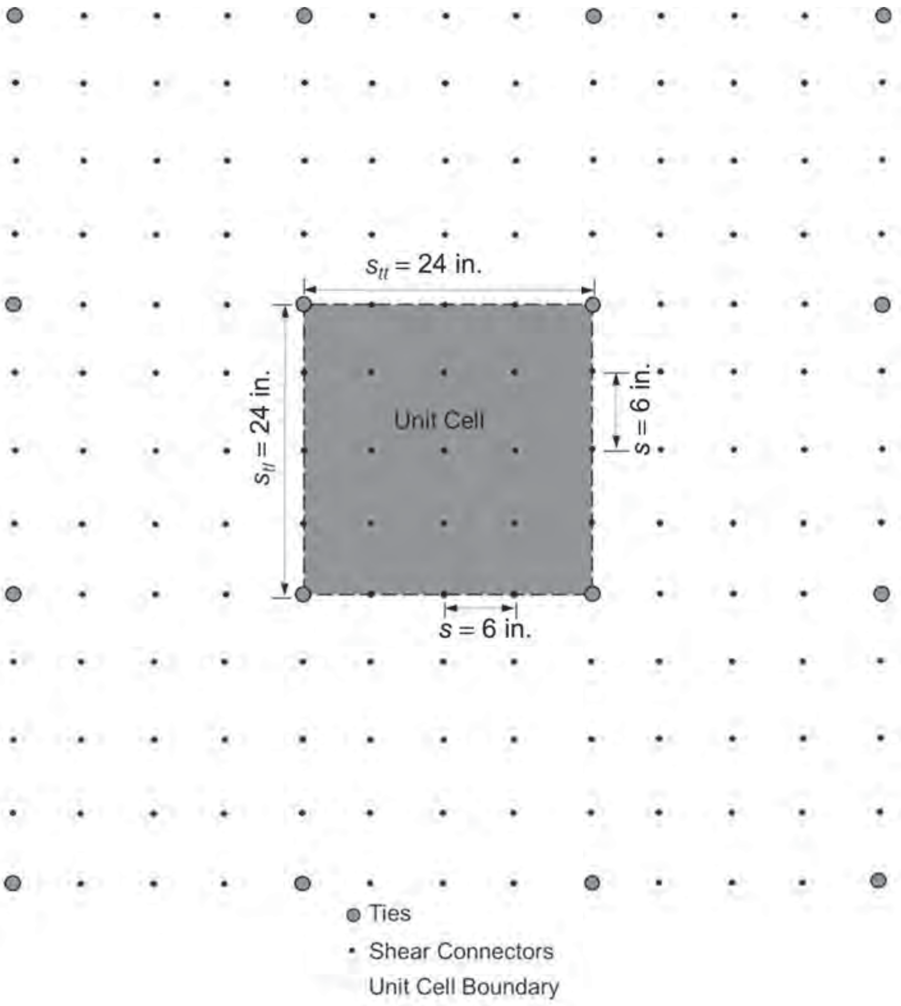
s_{tt} = 24 in.
s_{tl} = 24 in.
Unit Cell
s = 6 in.
s = 6 in.
Ties
Shear Connectors
Unit Cell Boundary

Fig. A-1. Arrangement of shear connectors and ties.

$$1.0\sqrt{\frac{E_s}{F_y}} = 1.0\sqrt{\frac{29{,}000 \text{ ksi}}{50 \text{ ksi}}}$$

$$= 24.0$$

$$\frac{b}{t_p} = 12.0 < 24.0$$

Therefore, the faceplate slenderness requirement is satisfied.

Step 3. Shear Connector Detailing

The detailing of shear connectors needs to be checked to meet the requirements of ANSI/AISC N690, Section N9.1.4. These requirements ensure the composite action of SC walls.

(a) Classification of steel anchors

According to Section N9.1.4a, steel headed stud anchors are yielding shear connectors. In case any other type of steel anchors are used, the classification and available strength, Q_{cv}, need to be established through testing.

(b) Spacing of steel anchors

According to Section N9.1.4b, the spacing of steel anchors need not exceed the following:

(1) Spacing, s, required to develop the yield strength of the faceplates over the development length, L_d

$$s \le c_1\sqrt{\frac{Q_{cv}L_d}{T_p}} \qquad \text{(N6901 Eq. A-N9-3)}$$

where

L_d = development length, in.

$\le 3t_{sc}$

$= 3(56.0 \text{ in.})$

$= 168 \text{ in.}$

Q_{cv} = available shear strength of steel anchor, kips

$= \phi_v Q_{nv}$

$= \phi_v F_{u.sc} A_{sa}$ (from *Spec*. Eq. I8-3)

and where

$$A_{sa} = \frac{\pi}{4}d_s^2$$

$$= \frac{\pi}{4}(0.750 \text{ in.})^2$$

$$= 0.442 \text{ in.}^2$$

$\phi_v = 0.65$

and then

$Q_{cv} = 0.65(65 \text{ ksi})(0.442 \text{ in.}^2)$

$= 1.87 \text{ kips}$

T_p = faceplate tensile strength per unit width, kip/in.

$= F_y t_p$

$= (50 \text{ ksi})(0.500 \text{ in.})$

$= 25.0 \text{ kip/in.}$

c_1 = factor used to determine spacing of steel anchors

= 1.0 for yielding steel anchors

$$c_1\sqrt{\frac{Q_{cv}L_d}{T_p}} = 1.0\sqrt{\frac{(18.7\text{ kips})(168\text{ in.})}{25.0\text{ kip/in.}}} \qquad \text{(from N690 Eq. A-N9-3)}$$

$$= 11.2$$

$s = 6.00$ in. < 11.2 in.

Therefore, the spacing requirement based on the development length is satisfied.

(2) Spacing required to prevent interfacial shear failure before out-of-plane shear failure

$$s \le c_1\sqrt{\frac{Q_{cv}l}{V_c/0.9t_{sc}}} \qquad \text{(N690 Eq. A-N9-4)}$$

The value of available out-of-plane shear strength of the SC wall is needed to check this requirement. Because this requirement will typically not govern, it will not be checked at this point. It will be checked after available strengths have been calculated in Step 7.

(3) Requirements of AISC *Specification* Sections I8.1 and I8.3e

(i) Diameter of the stud:

$d_s \le 2.5t_p$

0.750 in. ≤ 2.5(0.500 in.)

0.750 in. < 1.25 in. **o.k.**

(ii) Spacing requirements according to Section I8.3e:

$s \ge 4d_s$

6.00 in. ≥ 4(0.750 in.)

6.00 in. > 3.00 in. **o.k.**

$s \le 32d_s$

6.00 in. ≤ 32(0.750 in.)

6.00 in. < 24.0 in. **o.k.**

Therefore, the steel headed stud anchor requirements of the AISC *Specification* are satisfied.

Step 4. Tie Detailing

Ties provide structural integrity to the SC wall. Tie bar requirements of ANSI/AISC N690, Section N9.1.5, need to be satisfied.

(a) Tie bar spacing

ANSI/AISC N690 requires the tie bar spacing to be less than or equal to the section thickness, t_{sc}.

$s_{tt} \le t_{sc}$

$s_{tl} \le t_{sc}$

$s_{tt} = 24.0$ in. < $t_{sc} = 56.0$ in.

$s_{tl} = 24.0$ in. < $t_{sc} = 56.0$ in.

Therefore, the spacing requirement is satisfied.

(b) Classification of ties

Ties are to be classified as yielding or nonyielding shear reinforcement based on the provisions of ANSI/AISC Section N9.1.5a.

Ties are classified as yielding shear reinforcement when:

$$F_{ny} \leq 0.8F_{nr} \qquad \text{(N690 Eq. A-N9-5)}$$

where

F_{nr} = nominal rupture strength of the tie, kips
$= F_{u.tie}A_{tie}$
$= (65 \text{ ksi})(3.00 \text{ in.}^2)$
$= 195$ kips

F_{ny} = nominal yield strength of the tie, kips
$= F_{y.tie}A_{tie}$
$= (50 \text{ ksi})(3.00 \text{ in.}^2)$
$= 150$ kips

$F_{ny} \leq 0.8F_{nr}$

$150 \text{ kips} \leq 0.8(195 \text{ kips})$

$150 \text{ kips} < 156 \text{ kips}$

Because the tie bars are connected to faceplates using complete-joint-penetration groove welds, the nominal strength of the connection will be equal to or greater than the member strength.

Therefore, the reinforcement is classified as yielding shear reinforcement.

(c) Required tensile strength of ties

The required tensile strength for individual ties, F_{req}, is:

$$F_{req} = \left(\frac{t_p F_y t_{sc}}{4}\right)\left(\frac{s_{tt}}{s_{tl}}\right)\left[\frac{6}{18\left(\frac{t_{sc}}{s_{tl}}\right)^2 + 1}\right] \qquad \text{(N690 Eq. A-N9-6)}$$

$$= \left[\frac{(0.500 \text{ in.})(50 \text{ ksi})(56.0 \text{ in.})}{4}\right]\left(\frac{24.0 \text{ in.}}{24.0 \text{ in.}}\right)\left[\frac{6}{18\left(\frac{56.0 \text{ in.}}{24.0 \text{ in.}}\right)^2 + 1}\right]$$

$$= 21.2 \text{ kips}$$

The available tensile strength of a tie should be greater than the required strength.

From AISC *Specification* Section J4.1(a), the available yield strength of the ties is:

$\phi_{t.y} = 0.90$

$\phi_{t.y}F_{ny} = 0.90(150 \text{ kips})$
$= 135$ kips

From AISC *Specification* Section J4.1(b), the available rupture strength of the tie is:

$\phi_{t.r} = 0.75$

$\phi_{t.r}F_{nr} = 0.75(195 \text{ kips})$
$= 146$ kips

$\min(\phi_{t.y}F_{ny}, \phi_{t.r}F_{nr}) = 135 \text{ kips} \geq F_{req} = 21.2 \text{ kips}$

Therefore, the ties meet the tensile strength requirements. The ties also contribute to the out-of-plane shear strength of SC walls. The contribution of ties will be considered when available strengths are calculated in Step 7.

Step 5. Stiffness and Other Parameters for Modeling SC Walls

A three-dimensional elastic finite element model of the structure comprised of SC walls is analyzed in commercial finite element software. The walls are modeled according to ANSI/AISC N690, Sections N9.2.1 and N9.2.3.

(a) General Provisions—Section N9.2.1

(1) A three-dimensional SC wall is analyzed using elastic, thick-shell finite elements.

(2) Second-order effects

As discussed in ANSI/AISC N690, Section N9.1.2b, if provisions of ACI 318, Section 6.2.5, are met, second-order effects need not be considered. Because the SC walls are braced at floor levels, ACI 318, Equation 6.2.5b is considered:

$$\frac{kl_u}{r} \leq 34 - 12\left(M_1/M_2\right) \leq 40 \qquad \text{(ACI 318 Eq. 6.2.5b)}$$

where

k = effective length factor

l_u = unsupported length of compression member, in.

r = radius of gyration, in.

Based on the recommendations in ACI 318, Section 10.10.1:

$$k = 1.0$$

$$\begin{aligned} r &= 0.3t_{sc} \\ &= 0.3(56.0 \text{ in.}) \\ &= 16.8 \text{ in.} \end{aligned}$$

Also, conservatively consider single curvature and $M_1/M_2 = 1.0$.

Solving Equation 10-7 for l_u, the largest unsupported height permitted is:

$$\begin{aligned} l_u &= \frac{\left[34 - (12)\left(M_1/M_2\right)\right]r}{k} \\ &= \frac{\left[34 - (12)(1.0)\right](16.8 \text{ in.})}{1.0\left(12 \text{ in./ft}\right)} \\ &= 30.8 \text{ ft} \end{aligned}$$

$$\begin{aligned} h_{wall} &= \text{actual wall height} \\ &= 26 \text{ ft} \end{aligned}$$

$$h_{wall} \leq l_u$$

Because the actual wall height is less than the largest unsupported height permitted, second-order effects do not need to be considered.

(3) Analysis for accident thermal loads has been conducted as required by ANSI/AISC N690, Section N9.2.4. The loads from accident thermal conditions are linearly superimposed on other loads (condition B load combinations). This is explained in more detail in Step 6, where analysis results are presented.

(4) For safe shutdown earthquake seismic analysis, a viscous damping ratio of 5% is assumed.

(b) Stiffness for analysis

The stiffness for analysis is calculated according to ANSI/AISC N690, Section N9.2.2. Different stiffness values are needed for operating thermal (Condition A) and accident thermal (Condition B).

(1) Effective flexural stiffness for analysis, EI_{eff}

The effective flexural stiffness is determined for the operating thermal condition and for the accident thermal condition using ANSI/AISC N690, Equation A-N9-8:

$$EI_{eff} = (E_s I_s + c_2 E_c I_c)\left(1 - \frac{\Delta T_{savg}}{150}\right) \geq E_s I_s \qquad \text{(N690 Eq. A-N9-8)}$$

where

I_c = moment of inertia of concrete infill per unit width, in.^{4}/ft

$= \dfrac{lt_c^3}{12}$

and where

t_c = thickness of concrete infill, in.

$= t_{sc} - 2t_p$

= 56.0 in. − 2(0.500 in.)

= 55.0 in.

$$I_c = \frac{(12 \text{ in./ft})(55.0 \text{ in.})^3}{12}$$

$= 166{,}000 \text{ in.}^4\text{/ft}$

I_s = moment of inertia of faceplates per unit width, in.^{4}/ft

$$= \frac{lt_p(t_{sc} - t_p)^2}{2}$$

$$= \frac{(12 \text{ in./ft})(0.500 \text{ in.})(56.0 \text{ in.} - 0.500 \text{ in.})^2}{2}$$

$= 9{,}240 \text{ in.}^4\text{/ft}$

c_2 = calibration constant for determining effective flexural stiffness

$= 0.48\rho' + 0.10$

and where

ρ' = stiffness adjusted modular ration

$= \rho n$

n = modular ratio of steel to concrete

$$= \frac{E_s}{E_c}$$

$$= \frac{29{,}000 \text{ ksi}}{3{,}900 \text{ ksi}}$$

= 7.44

$\rho' = 0.018(7.44)$

= 0.134

$c_2 = 0.48(0.134) + 0.10$

= 0.164

(i) Operating thermal condition (Condition A)

Using ANSI/AISC N690, Equation A-N9-8, shown previously with $\Delta T_{savg} = 0$ based on the User Note in Section N9.2.2(a):

$$EI_{eff} = (E_sI_s + c_2E_3I_c)\left(1 - \frac{\Delta T_{savg}}{150}\right) \geq E_sI_s \qquad \text{(N690 Eq. A-N9-8)}$$

$$= \left[(29{,}000 \text{ ksi})(9{,}240 \text{ in.}^4\text{/ft}) + 0.164(3{,}900 \text{ ksi})(166{,}000 \text{ in.}^4\text{/ft})\right]\left(1 - \frac{0}{150}\right)$$

$$= 3.74 \times 10^8 \text{ kip-in.}^2\text{/ft}$$

$$E_sI_s = (29{,}000 \text{ ksi})(9{,}240 \text{ in.}^4\text{/ft})$$

$$= 2.68 \times 10^8 \text{ kip-in.}^2\text{/ft}$$

$$EI_{eff.op} = \max\left[(E_sI_s + c_2E_cI_c)\left(1 - \frac{\Delta T_{savg}}{150}\right), E_sI_s\right]$$

$$= 3.74 \times 10^8 \text{ kip-in.}^2\text{/ft}$$

(ii) Accident thermal condition (Condition B)

Accident thermal loading is obtained from heat transfer analysis, as discussed in ANSI/AISC N690, Section N9.2.4. It is explained in detail in Section 7.5. Heat transfer analysis results are not presented in this example.

$\Delta T_{savg} = 190\Delta°\text{F}$ (from heat transfer analysis)

$$EI_{eff} = (E_sI_s + c_2E_cI_c)\left(1 - \frac{\Delta T_{savg}}{150}\right) \geq E_sI_s \qquad \text{(N690 Eq. A-N9-8)}$$

$$= \left[(29{,}000 \text{ ksi})(9{,}240 \text{ in.}^4\text{/ft}) + 0.164(3{,}900 \text{ ksi})(166{,}000 \text{ in.}^4\text{/ft})\right]\left(1 - \frac{190}{150}\right)$$

$$= -9.99 \times 10^7 \text{ kip-in.}^2\text{/ft}$$

$$E_sI_s = (29{,}000 \text{ ksi})(9{,}240 \text{ in.}^4\text{/ft})$$

$$= 2.68 \times 10^8 \text{ kip-in.}^2\text{/ft}$$

$$EI_{eff.acc} = \max\left[(E_sI_s + c_2E_cI_c)\left(1 - \frac{\Delta T_{savg}}{150}\right), E_sI_s\right]$$

$$= 2.68 \times 10^8 \text{ kip-in.}^2\text{/ft}$$

(2) Effective in-plane shear stiffness per unit width, GA_{eff}

According to ANSI/AISC N690, Section N9.2.2(b), to use the provisions of this Appendix, the value of the average in-plane shear demand for the wall, S_{rxy}, relative to the concrete cracking threshold, S_{cr}, needs to be known. However, this is not possible before the analysis is done.

To proceed with the analysis, it is assumed that the average in-plane shear demand is 1.5 times the concrete cracking threshold for Condition A analysis. This assumption will be verified after the demands are obtained from the analysis in Step 6.

$$GA_{eff} = GA_{uncr} - \left(\frac{GA_{uncr} - GA_{cr}}{S_{cr}}\right)(S_{rxy.as} - S_{cr}) \qquad \text{(from N690 Eq. A-N9-11)}$$

where

$$GA_{cr} = 0.5(\bar{\rho})^{-0.42} GA_s \qquad \text{(N690 Eq. A-N9-12)}$$

and where

$$A_s = 2lt_p$$

$$= 2(12 \text{ in./ft})(0.500 \text{ in.})$$

$$= 12.0 \text{ in.}^2\text{/ft}$$

$$\bar{\rho} = \frac{A_s F_y}{31.6 A_c \sqrt{f'_c}} \qquad \text{(N690 Eq. A-N9-13)}$$

and where

A_c = area of concrete infill per unit width, in.^{2}/ft
= lt_c
= (12.0 in./ft)(55.0 in.)
= 660 in.^{2}/ft

$$\bar{\rho} = \frac{(12.0\text{ in.}^2\text{/ft})(50\text{ ksi})}{31.6(660\text{ in.}^2\text{/ft})\sqrt{5\text{ ksi}}}$$

$= 0.0129$

Therefore:

GA_{cr} = 0.5(0.0129)$^{-0.42}$(11,200 ksi)(12 in.^{2}/ft)
= 418,000 kip/ft

$GA_{eff} = GA_{uncr}$ (N690 Eq. A-N9-9)
$= GA_s + G_cA_c$
= (11,200 ksi)(12.0 in.^{2}/ft) + (1,730 ksi)(660 in.^{2}/ft)
= 1.28 × 10^6 kip/ft

S_{cr} = concrete cracking threshold, kip/ft

$$= \frac{0.063\sqrt{f'_c}}{G_c} GA_{uncr} \qquad \text{(N690 Eq. A-N9-10)}$$

$$= \frac{0.063\sqrt{5\text{ ksi}}}{1{,}730\text{ ksi}}(1.28\times10^6\text{ kip/ft})$$

= 104 kip/ft

Because S_{rxy} is assumed to be 1.5S_{cr}:

$S_{rxy.as} = 1.5S_{cr}$
= 1.5(104 kip/ft)
= 156 kip/ft

$$GA_{eff} = (1.28\times10^6\text{ kip/ft}) - \left[\frac{(1.28\times10^6\text{ kip/ft}) - (4.18\times10^5\text{ kip/ft})}{104\text{ kip/ft}}\right](156\text{ kip/ft} - 104\text{ kip/ft})$$

$$= 849{,}000\text{ kip/ft}$$

(3) For accident thermal load conditions (Condition B in Step 6), GA_{eff} is taken as GA_{cr}.

(4) The SC wall connection-to-basemat is considered rigid for out-of-plane moment demands and is modeled as a rigid connection.

(c) Geometric and material properties for elastic finite element analysis

The geometric and material properties used for elastic finite element analysis are consistent with ANSI/AISC N690, Section N9.2.3.

(1) For the following properties, concrete values are used for the finite elements:

Poisson's ratio

$\upsilon_m = \upsilon_c$
= 0.17

Thermal expansion coefficient

$$\begin{aligned}\alpha_m &= \alpha_c \\ &= 5.6\times10^{-6}/°\text{F}\end{aligned}$$

Thermal conductivity

$$\begin{aligned}k_m &= k_c \\ &= 0.01\ \frac{\text{Btu}}{\text{ft}\times\text{sec}\times\Delta°\text{F}}\end{aligned}$$

(2) Model elastic modulus, E_m, and model thickness, t_m

These parameters for the finite element model are obtained by calibrating the effective flexural and shear stiffnesses. The flexural and shear stiffnesses of the model are equated with the corresponding effective stiffnesses determined in Step 5(b):

$$E_m\frac{lt_m^3}{12} = EI_{eff}$$

$$\frac{E_m}{2(1+\upsilon_m)}lt_m = GA_{eff}$$

These equations are solved to obtain t_m and E_m as follows:

(i) For operating thermal conditions (Condition A)

$$t_{m.op} = \sqrt{\left(\frac{EI_{eff.op}}{GA_{eff}}\right)\left[\frac{12}{2(1+\upsilon_m)}\right]} \tag{A-1}$$

$$\begin{aligned}&= \sqrt{\left(\frac{3.74\times10^8\ \text{kip-in.}^2/\text{ft}}{849{,}000\ \text{kip/ft}}\right)\left[\frac{12}{2(1+0.17)}\right]} \\ &= 47.5\text{ in.}\end{aligned}$$

$$E_{m.op} = \frac{GA_{eff}\,2(1+\upsilon_m)}{t_{m.op}l} \tag{A-2}$$

$$\begin{aligned}&= \frac{(849{,}000\text{ kip/ft})(2)(1+0.17)}{(47.5\text{ in.})(12\text{ in./ft})} \\ &= 3{,}490\text{ ksi}\end{aligned}$$

(ii) For accident thermal conditions (Condition B)

$$t_{m.acc} = \sqrt{\left(\frac{EI_{eff.acc}}{GA_{eff}}\right)\left[\frac{12}{2(1+\upsilon_m)}\right]} \tag{A-3}$$

$$\begin{aligned}&= \sqrt{\left(\frac{2.68\times10^8\ \text{kip-in.}^2/\text{ft}}{849{,}000\ \text{kip/ft}}\right)\left[\frac{12}{2(1+0.17)}\right]} \\ &= 40.2\text{ in.}\end{aligned}$$

$$E_{m.acc} = \frac{GA_{eff}\,2(1+\upsilon_m)}{t_{m.acc}l} \tag{A-4}$$

$$= \frac{(849{,}000 \text{ kip/ft})(2)(1+0.17)}{(40.2 \text{ in.})(12 \text{ in./ft})}$$

$$= 4{,}120 \text{ ksi}$$

(3) Material density, γ_m

(i) For operating thermal conditions (Condition A)

$$\gamma_{m.op} = \frac{\gamma_s(2t_p)+w_c t_c}{t_{m.op}} \tag{A-5}$$

$$= \frac{(490 \text{ lb/ft}^3)(2)(0.500 \text{ in.})+(145 \text{ lb/ft}^3)(55.0 \text{ in.})}{47.5 \text{ in.}}$$

$$= 178 \text{ lb/ft}^3$$

(ii) For accident thermal conditions (Condition B)

$$\gamma_{m.acc} = \frac{\gamma_s(2t_p)+w_c t_c}{t_{m.acc}} \tag{A-6}$$

$$= \frac{(490 \text{ lb/ft}^3)(2)(0.500 \text{ in.})+(145 \text{ lb/ft}^3)(55.0 \text{ in.})}{40.2 \text{ in.}}$$

$$= 186 \text{ lb/ft}^3$$

(4) Specific heat, c_m

Specific heat is the same for both operating and accident thermal conditions.

$$c_m = \frac{c_c w_c t_c}{\gamma_{m.op} t_{m.op}} \tag{A-7}$$

$$= \frac{\left(255.4 \;\dfrac{\text{Btu}}{\text{lb}\times\Delta°\text{F}}\right)(145 \text{ lb/ft}^3)(55.0 \text{ in.})}{(178 \text{ lb/ft}^3)(47.5 \text{ in.})}$$

$$= 241 \;\frac{\text{Btu}}{\text{lb}\times\Delta°\text{F}}$$

(d) Analysis involving accident thermal conditions (Condition B)

Heat transfer analysis is performed for accident loading. The results of this analysis serve as input for the structural analysis. The analysis is conducted using the geometric and material properties defined. Temperature histories and through-thickness temperature profiles obtained from heat transfer analysis are used in the structural analysis. This design example does not discuss the heat transfer analysis results. Because the thermal loads are applied as a uniform temperature increase through the wall, a thermal gradient out-of-plane moment needs to be added to the out-of-plane demands. The magnitude of moment considered is determined in the following.

The maximum temperature difference between faceplates due to accident thermal conditions, obtained from the accident data, is:

$$\Delta T_{sg} = 28.5 \;\Delta°\text{F}$$

Table A-1. Load Combinations for Analysis

S. No.	Load Combination	ANSI/AISC N690 Equation
1	$1.4(D + R_o + F) + T_o + C$	NB2-1
2	$1.2(D + R_o + F) + 1.6(L + H) + 0.5(L_r \text{ or } R \text{ or } S) + 1.2T_o + 1.4C$	NB2-2
3	$1.2(D + R_o + F) + 0.8(L + H) + 1.6(L_r \text{ or } R \text{ or } S) + 1.2T_o + 1.4C$	NB2-3
4	$1.2(D + R_o + F) + W + 0.8L + 1.6H + 0.5(L_r \text{ or } R \text{ or } S) + T_o + C$	NB2-4
5	$1.2(D + R_o + F) + W + 0.8L + 1.6H + 0.5(L_r \text{ or } R \text{ or } S) + T_o + C$	NB2-4
6	$1.2(D + R_o + F) + 1.6E_o + 0.8L + 1.6H + 0.2(L_r \text{ or } R \text{ or } S) + T_o + C$	NB2-5
7	$1.2(D + R_o + F) + 1.6E_o + 0.8L + 1.6H + 0.2(L_r \text{ or } R \text{ or } S) + T_o + C$	NB2-5
8	$D + 0.8L + C + T_o + R_o + E_s + F + H$	NB2-6
9	$D + 0.8L + C + T_o + R_o - E_s + F + H$	NB2-6
10	$D + 0.8L + T_o + R_o + W_t + F + H$	NB2-7
11	$D + 0.8L + T_o + R_o - W_t + F + H$	NB2-7
12	$D + 0.8L + C + 1.2P_a + R_a + T_a + F + H$	NB2-8
13	$D + 0.8L + P_a + R_a + T_a + Y_r + Y_j + Y_m + 0.7Es + F + H$	NB2-9
14	$D + 0.8L + P_a + R_a + T_a + Y_r + Y_j + Y_m - 0.7Es + F + H$	NB2-9

$$M_{r\text{-}th} = EI_{eff.acc}\left(\frac{\alpha_s \Delta T_{sg}}{t_{sc}}\right) \qquad \text{(from N690 Eq. A-N9-14)}$$

$$= (2.68\times10^{8} \text{ kip-in.}^2\text{/ft})\left[\frac{(7.8\times10^{-6}/\text{°F})(28.5\,\text{°F})}{56.0 \text{ in.}}\right]$$

$$= 1{,}060 \text{ kip-in./ft}$$

Note: This limit is not applicable to connection regions. The out-of-plane thermal moment will be determined from finite element analysis.

Step 6. Analysis Results and Required Strength Summary

The expanse of the wall considered is 44 ft × 26 ft. Thick shell finite elements are used. The material properties discussed in Step 5 are used. The element size is 2 ft × 2 ft. The wall is modelled using 120 elements. Load combinations for analysis are based on ANSI/AISC N690, Chapter NB. Table A-1 presents the load combinations considered.

As discussed earlier, two sets of analyses are performed. Load combinations 1 through 11 use analysis results based on condition A (operating thermal). Load combinations 12 through 14 use analysis results for condition B (accident thermal). The finite element analysis data for each element and load combination is combined and studied. The database consists of element number, load combination and associated demands for each element. The demands are measured per unit width.

For this design example, the whole data set is not presented. Data for only the elements with the highest individual demands is presented in Table A-2. The highest magnitude required strength of each individual demand has been boldfaced. The out-of-plane moment due to accident thermal gradient calculated from ANSI/AISC N690, Equation A-N9-14, has been added to the moment demands obtained from finite element analysis. The nomenclature for required strengths is based on ANSI/AISC N690, Section N9.2.5. Consistent with the design practice, the required strengths for each element are compared with the available strengths. In case the demand is greater than the available strength, the required strengths are permitted to be averaged as discussed in ANSI/AISC N690, Section N9.2.5.

Table A-2. Peak Demands for Elements

Element No.	Load Comb.	S_{rx} (kip/ft)	S_{ry} (kip/ft)	S_{rxy} (kip/ft)	M_{rx} (kip-in./ft)	M_{ry} (kip-in./ft)	M_{rxy} (kip-in./ft)	V_{rx} (kip/ft)	V_{ry} (kip/ft)
Condition A									
54664	9	–105	–237	–88.4	–1400	–2320	–364	–14	–58.4
54664	8	59.7	146	**261**	1680	2520	528	16.2	50.3
54692	8	262	26.6	37.0	1160	1810	165	28.7	33.2
54664	8*	93.5	160	258	1900	3070	559	13.8	54.1
Condition B									
54692	13	193	–75.1	–67.6	4300	6350	223	61.5	**123**
54664	12	–369	**342**	215	2350	**7000**	540	16.7	107
39007	13	–237	159	60.0	**7640**	3600	–58.1	–5.18	–30.2
39001	14	–350	–137	–307	–2660	–2110	**–1250**	**–48.2**	–31.2
54664	14	**–444**	–57.9	–143	–3990	–3250	–500	-4.67	–40.1

*Includes reaction and pressure loads.

For the design of the SC wall section, demand capacity ratios for each element are checked for all the load combinations. This is done for individual as well as combined demands.

The average in-plane shear demand, S_{rxy}, for a particular operating thermal (Condition A) load combination is determined by averaging the in-plane shear demands of all the elements for that load combination. It is observed that the maximum average in-plane shear demands occur for load combinations 8 and 9. Figure A-2 presents the ratio of in-plane shear demand and concrete cracking threshold for each element for load combination 9. The average ratio for all elements is around 1.5. The average demand is close to the assumption of $1.5S_{cr}$ for determining the in-plane shear stiffness that was used in Step 5(b), and therefore the assumption is valid. However, there may be cases where the average in-plane shear demand is not in the range of the value assumed to ascertain shear stiffness. In that case, the process of calculating shear stiffness and the analysis will need to be repeated.

Step 7. Individual Design Available Strengths

The available strengths of the SC wall section for individual demand types are determined based on ANSI/AISC N690, Section N9.3.

(a) Uniaxial tensile strength

The available uniaxial tensile strength is determined according to the provisions of AISC *Specification* Chapter D. Because no holes are present in the expanse of the SC wall being designed, the rupture strength need not be greater than the yield strength. Here the contribution of the concrete is ignored.

The available tensile strength is determined as the lesser of the tensile yielding strength or the tensile rupture strength.

For tensile yielding:

$$\phi P_{n.ten} = \phi_{t.y} F_y A_g \qquad \text{(from } \textit{Spec.} \text{ Eq. D2-1)}$$

where

$$A_g = (2t_p)(l)$$
$$= 2(0.500 \text{ in.})(12 \text{ in./ft})$$
$$= 12.0 \text{ in.}^2\text{/ft}$$

$$\phi_{t.y} = 0.90$$

And thus:

$$
\begin{aligned}
P_{n.ten} &= F_y A_g \\
&= (50\text{ ksi})(12\text{ in.}^2/\text{ft}) \\
&= 600\text{ kip/ft} \\
\phi P_{n.ten} &= (0.90)(600\text{ kip/ft}) \\
&= 540\text{ kip/ft} \qquad \textbf{governs}
\end{aligned}
$$

For tensile rupture:

$$\phi P_{n.ten} = \phi_{t.r} F_u A_g \qquad \text{(from } \textit{Spec}\text{. Eq. D2-2)}$$

where

$\phi_{t.r} = 0.75$

And thus:

$$
\begin{aligned}
P_{n.ten} &= F_u A_g \\
&= (65\text{ ksi})(12\text{ in.}^2/\text{ft}) \\
&= 780\text{ kip/ft} \\
\phi P_{n.ten} &= (0.75)(780\text{ kip/ft}) \\
&= 585\text{ kip/ft}
\end{aligned}
$$

The available tensile strength of the SC wall is

$\phi P_{n.ten} = 540$ kip/ft

(b) Compressive strength

The available compressive strength of the SC wall section is determined using AISC *Specification* Section I2.1b, with the faceplates taking the place of the steel shape.

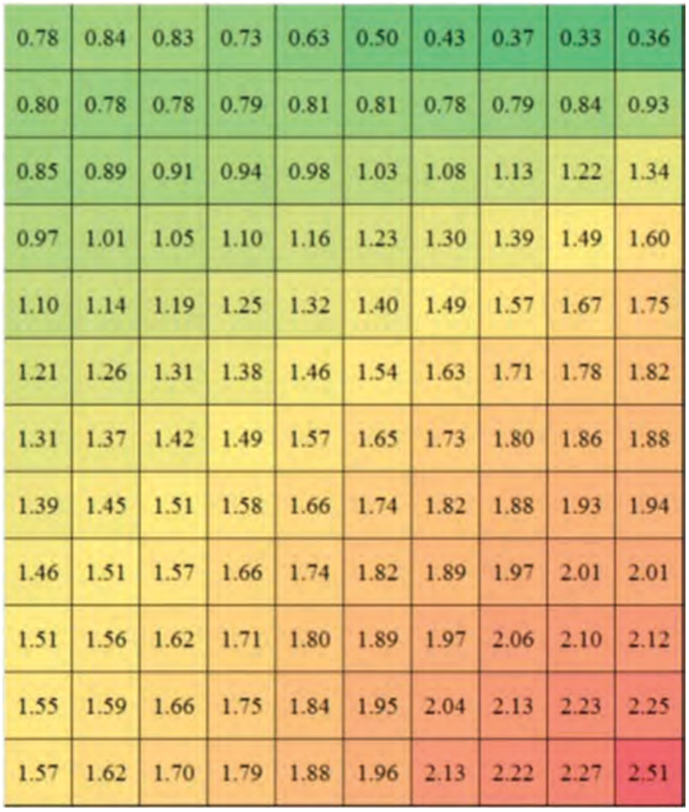

0.78	0.84	0.83	0.73	0.63	0.50	0.43	0.37	0.33	0.36
0.80	0.78	0.78	0.79	0.81	0.81	0.78	0.79	0.84	0.93
0.85	0.89	0.91	0.94	0.98	1.03	1.08	1.13	1.22	1.34
0.97	1.01	1.05	1.10	1.16	1.23	1.30	1.39	1.49	1.60
1.10	1.14	1.19	1.25	1.32	1.40	1.49	1.57	1.67	1.75
1.21	1.26	1.31	1.38	1.46	1.54	1.63	1.71	1.78	1.82
1.31	1.37	1.42	1.49	1.57	1.65	1.73	1.80	1.86	1.88
1.39	1.45	1.51	1.58	1.66	1.74	1.82	1.88	1.93	1.94
1.46	1.51	1.57	1.66	1.74	1.82	1.89	1.97	2.01	2.01
1.51	1.56	1.62	1.71	1.80	1.89	1.97	2.06	2.10	2.12
1.55	1.59	1.66	1.75	1.84	1.95	2.04	2.13	2.23	2.25
1.57	1.62	1.70	1.79	1.88	1.96	2.13	2.22	2.27	2.51

Fig. A-2. S_{rxy}/S_{cr} *ratio for load combination 9.*

The ratio of the nominal compressive strength of zero length, P_{no}, to the elastic critical buckling load, P_e, must first be determined in order to ascertain which equation for the nominal compressive strength, P_n, will control.

$$P_e = \frac{\pi^2 EI_{eff.buck}}{L^2} \qquad \text{(from N690 Eq. A-N9-16)}$$

$$P_{no} = F_y A_{sn} + 0.85 f'_c A_c \qquad \text{(N690 Eq. A-N9-15)}$$

where

A_{sn} = net area of faceplates per unit width, in.^{2}/ft
$= A_s$
$= 12.0$ in.^{2}/ft

$EI_{eff.buck} = E_s I_s + 0.60 E_c I_c$ (from N690 Eq. A-N9-17)
= (29,000 ksi)(9,240 in.^{4}/ft) + 0.60(3,900 ksi)(166,000 in.^{4}/ft)
= 6.56×10^8 kip-in.^{2}/ft

$L = h_{wall}$
= (26.0 ft)(12 in./ft)
= 312 in.

P_e and P_{no} can then be calculated:

$$\begin{aligned} P_e &= \frac{\pi^2 EI_{eff.buck}}{L^2} && \text{(from } \textit{Spec.} \text{ Eq. I2-5)} \\ &= \frac{\pi^2 (6.56 \times 10^8 \text{ kip-in.}^2\text{/ft})}{(312 \text{ in.})^2} \\ &= 66{,}500 \text{ kip/ft} \end{aligned}$$

$$\begin{aligned} P_{no} &= F_y A_s + 0.85 f'_c A_c && \text{(from } \textit{Spec.} \text{ Eq. I2-4)} \\ &= (50 \text{ ksi})(12.0 \text{ in.}^2\text{/ft}) + 0.85(5 \text{ ksi})(660 \text{ in.}^2\text{/ft}) \\ &= 3{,}410 \text{ kip/ft} \end{aligned}$$

$$\begin{aligned} \frac{P_{no}}{P_e} &= \frac{3{,}410 \text{ kip/ft}}{66{,}500 \text{ kip/ft}} \\ &= 0.0513 \end{aligned}$$

Because $\dfrac{P_{no}}{P_e} < 2.25$:

$$\begin{aligned} P_{n.com} &= P_{no}\left(0.658^{\frac{P_{no}}{P_e}}\right) && \text{(from } \textit{Spec.} \text{ Eq. I2-2)} \\ &= (3{,}410 \text{ kip/ft})(0.658^{0.0513}) \\ &= 3{,}340 \text{ kip/ft} \end{aligned}$$

From AISC *Specification* Section I2.1b:

$$\phi c = 0.75$$

$$\begin{aligned} \phi P_{n.com} &= \phi_c P_{n.com} \\ &= (0.75)(3{,}340 \text{ kip/ft}) \\ &= 2{,}510 \text{ kip/ft} \end{aligned}$$

(c) Out-of-plane flexural strength

The nominal flexural strength per unit width of the SC wall is determined for the limit state of yielding using AISC N690, Section N9.3.3:

$$M_n = F_y A_s^F (0.9 t_{sc}) \qquad \text{(N690 Eq. A-N9-18)}$$

$\phi_b = 0.90$

where

A_s^F = gross cross-sectional area of faceplate in tension due to flexure per unit width, in.^{2}/ft

$= \dfrac{A_s}{2}$

$= \dfrac{12.0 \text{ in.}^2\text{/ft}}{2}$

$= 6.00 \text{ in.}^2\text{/ft}$

$M_n = F_y A_s^F (0.9 t_{sc})$
$= (50 \text{ ksi})(6.00 \text{ in.}^2\text{/ft})(0.9)(56.0 \text{ in.})$
$= 15{,}100$ kip-in./ft

$\phi M_n = \phi_b M_n$
$= (0.90)(15{,}100$ kip-in./ft$)$
$= 13{,}600$ kip-in./ft

(d) In-plane shear strength

The design in-plane shear strength of the SC wall per unit width, $\phi_{vi} V_{ni}$, is determined for the limit state of yielding of the faceplates using ANSI/AISC N690, Section N9.3.4:

$$V_{ni} = \kappa F_y A_s \qquad \text{(N690 Eq. A-N9-19)}$$

$\phi_{vi} = 0.90$

where

$\kappa = 1.11 - 5.16\overline{\rho} \le 1.0$
$= 1.11 - 5.16(0.013)$
$= 1.04 > 1.0 \rightarrow$ therefore $\kappa = 1.0$

$V_{ni} = \kappa F_y A_s$
$= (1.0)(50 \text{ ksi})(12.0 \text{ in.}^2\text{/ft})$
$= 600$ kip/ft

$\phi V_{ni} = \phi_{vi} V_{ni}$
$= 0.90(600$ kip/ft$)$
$= 540$ kip/ft

(e) Out-of-plane shear strength

ANSI/AISC N690 Appendix N9 recommends that out-of-plane shear strength be established by conducting project specific large-scale out-of-plane shear tests, using applicable test results, or using the provisions of the Appendix. Because no such tests have been done for this example, the provisions of the Appendix are used to determine the out-of-plane shear strength.

The shear reinforcement has been classified as yielding shear reinforcement in Step 4 of this calculation. Comparing the spacing of shear reinforcement with the section thickness:

$s_{tt} \le \dfrac{t_{sc}}{2}$

$s_{tt} = 24.0 \text{ in.}$

$\dfrac{t_{sc}}{2} = \dfrac{56.0 \text{ in.}}{2} = 28.0 \text{ in.}$

$24.0 \text{ in.} < 28.0 \text{ in.}$

Therefore, ANSI/AISC N690, Section N9.3.5(a), will be used to determine the out-of-plane shear strength of the wall.

$$V_{no} = V_{conc} + V_s \qquad \text{(N690 Eq. A-N9-20)}$$

where

$V_{conc} = 0.05(f_c')^{0.5} t_c l$ (N690 Eq. A-N9-21)

$= 0.05(5 \text{ ksi})^{0.5}(55.0 \text{ in.})(12 \text{ in./ft})$

$= 73.8 \text{ kip/ft}$

$V_s = \zeta p_s F_t \dfrac{l}{s_{tt}} \le 0.25(f_c')^{0.5} t_c l$ (N690 Eq. A-N9-22)

$F_t = \min(F_{ny}, F_{nr})$

$= 150 \text{ kips}$

$p_s = \dfrac{t_c}{s_{tl}}$

$= \dfrac{55.0 \text{ in.}}{24.0 \text{ in.}}$

$= 2.29$

$\xi = 1.0$ for yielding shear reinforcement

$V_s = (1.0)(2.29)(150 \text{ kips})\left(\dfrac{12 \text{ in./ft}}{24.0 \text{ in.}}\right)$

$= 172 \text{ kip/ft}$

$0.25(f_c')^{0.5} t_c l = 0.25(5 \text{ ksi})^{0.5}(55.0 \text{ in.})(12 \text{ in./ft})$

$= 369 \text{ kip/ft}$

$172 \text{ kip/ft} < 369 \text{ kip/ft} \rightarrow V_s = 172 \text{ kip/ft}$

$V_{no} = V_{conc} + V_s$

$= 73.8 \text{ kip/ft} + 172 \text{ kip/ft}$

$= 246 \text{ kip/ft}$

$\phi_{vo} = 0.75$

$V_c = \phi_{vo} V_{no}$

$= 0.75(246 \text{ kip/ft})$

$= 185 \text{ kip/ft}$

The spacing requirement for shear connectors can now be checked using ANSI/AISC N690, Equation A-N9-4:

$$s = 6 \text{ in.} \le c_1 \sqrt{\frac{Q_{cv} l}{V_c / 0.9 t_{sc}}} \qquad \text{(N690 Eq. A-N9-4)}$$

$$\le 1.0 \sqrt{\frac{(18.7 \text{ kips})(12 \text{ in./ft})}{(185 \text{ kip/ft})/(0.9)(56.0 \text{ in.})}}$$

$< 7.82 \text{ in.}$ **o.k.**

Therefore, the shear connector spacing requirement of ANSI/AISC N690, Equation A-N9-4, is met.

Step 8. Interaction of Design Available Strengths

The interaction of required demands needs to be limited according to the provisions of ANSI/AISC N690, Section N9.3.6. The interaction for each element needs to be checked for all the load combinations.

This example illustrates the process by checking the interaction for one element for a particular load combination. Because element 54692 has high demands for accident thermal load combinations, the interaction of forces acting on this element for load combination 13 is checked.

The individual demands as shown in Table A-2 are as follows:

$S_{rx} = 193$ kip/ft
$S_{ry} = -75.1$ kip/ft
$S_{rxy} = -67.6$ kip/ft
$M_{rx} = 4{,}300$ kip-in./ft
$M_{ry} = 6{,}350$ kip-in./ft
$M_{rxy} = 223$ kip-in./ft
$V_{rx} = 61.5$ kip/ft
$V_{ry} = 123$ kip/ft

(a) Interaction of out-of-plane shear forces

To determine the applicable interaction equation, $V_{c.conc}$ must be calculated:

$$\begin{aligned} V_{c.conc} &= \phi_{vo} V_{conc} \\ &= 0.75(73.8 \text{ kip/ft}) \\ &= 55.4 \text{ kip/ft} \end{aligned}$$

Because $V_{rx} > V_{c.conc}$ and $V_{ry} > V_{c.conc}$, and $s_{tt} \le \dfrac{t_{sc}}{2}$, case (a) of Appendix Section N9.3.6a is applicable:

$$DCR_{ops} = \left[\left(\frac{V_r - V_{c.conc}}{V_c - V_{c.conc}} \right)_x + \left(\frac{V_r - V_{c.conc}}{V_c - V_{c.conc}} \right)_y \right]^{5/3} + \left[\frac{\sqrt{V_{rx}{}^2 + V_{ry}{}^2} \Big/ (0.9 t_{sc})}{\psi \left(l Q_{cv}^{avg} \big/ s^2 \right)} \right]^{5/3} \le 1.0 \qquad \text{(N690 Eq. A-N9-23)}$$

where

$$Q_{cv}^{avg} = \frac{n_{et} Q_{cv}^{tie} + n_{es} Q_{cv}}{n_{et} + n_{es}} \qquad \text{(N690 Eq. C-A-N9-14)}$$

Q_{cv}^{tie} = available interfacial shear strength of tie bars, kips

The contribution of tie bars to the interfacial shear strength, Q_{cv}^{tie}, is considered to be zero in this design example.

However, when considered, the interfacial available shear strength of tie bars needs to be determined according to ANSI/AISC N690, Section N9.1.4a.

Based on Figure A-1 and the commentary to Section N9.3.6a of ANSI/AISC N690:

$n_{et} = 1.00$
$n_{es} = 15.0$

and

$$\begin{aligned} Q_{cv}^{avg} &= \frac{(1.00)(0.00 \text{ kips}) + (15.0)(18.7 \text{ kips})}{1.00 + 15.0} \\ &= 17.5 \text{ kips} \end{aligned}$$

$\psi = 1.0$ for panel sections with yielding shear reinforcement and yielding shear connectors

$$DCR_{ops} = \left[\left(\frac{61.5\text{ kip/ft} - 55.4\text{ kip/ft}}{185\text{ kip/ft} - 55.4\text{ kip/ft}}\right) + \left(\frac{123\text{ kip/ft} - 55.4\text{ kip/ft}}{185\text{ kip/ft} - 55.4\text{ kip/ft}}\right)\right]^{5/3}$$

$$+ \left\{\frac{\sqrt{(61.5\text{ kip/ft})^2 + (123\text{ kip/ft})^2}\Big/0.9(56.0\text{ in.})}{1.0\left[(12\text{ in./ft})(17.5\text{ kips})\big/(6.00\text{ in.})^2\right]}\right\}^{5/3}$$

$$= 0.672 < 1.0$$

Therefore, the interaction satisfies the requirements of ANSI/AISC N690, Equation A-N9-23.

(b) In-plane membrane forces and out-of-plane moments

The design adequacy of panel sections subjected to three in-plane required membrane strengths (S_{rx}, S_{ry}, S_{rxy}) and three out-of-plane required flexural or twisting strengths (M_{rx}, M_{ry}, M_{rxy}) is evaluated for each notional half of the SC section, which consists of one faceplate and half the concrete thickness, according to the provisions of ANSI/AISC N690, Section N9.3.6b.

For each notional half, the interaction is checked using the equations in principal force space using ANSI/AISC N690, Equations A-N9-24 to A-N9-26. (Alternatively, the interaction can also be checked using Equations A-N9-31 to A-N9-33. The two sets of equations represent the same interaction surface.)

For $S_{r,max} + S_{r,min} \geq 0$

$$DCR = \alpha\left(\frac{S_{r,max} + S_{r,min}}{2V_{ci}}\right) + \left(\frac{S_{r,max} - S_{r,min}}{2V_{ci}}\right) \leq 1.0 \qquad \text{(N690 Eq. A-N9-24)}$$

For $S_{r,max} > 0$ and $S_{r,max} + S_{r,min} < 0$

$$DCR = \frac{S_{r,max}}{V_{ci}} - \beta\left(\frac{S_{r,max} + S_{r,min}}{V_{ci}}\right) \leq 1.0 \qquad \text{(N690 Eq. A-N9-25)}$$

For $S_{r,max} \leq 0$ and $S_{r,min} \leq 0$

$$DCR = -\beta\left(\frac{S_{r,min}}{V_{ci}}\right) \leq 1.0 \qquad \text{(N690 Eq. A-N9-26)}$$

where

$$S_{r,max}, S_{r,min} = \frac{S'_{rx} + S'_{ry}}{2} \pm \sqrt{\left(\frac{S'_{rx} - S'_{ry}}{2}\right)^2 + (S'_{rxy})^2} \qquad \text{(N690 Eq. A-N9-27)}$$

Interaction in principal plane:

j_x = 0.9 if $S_{rx} > -0.6\,P_{no}$, otherwise it is 0.67

j_y = 0.9 if $S_{ry} > -0.6\,P_{no}$, otherwise it is 0.67

j_{xy} = 0.67

S_{rx} = 193 kip/ft > $-0.6P_{no}$ = –2,040 kip/ft, therefore $j_x = 0.9$.

S_{ry} = –75.1 kip/ft > $-0.6P_{no}$ = –2,040 kip/ft, therefore $j_y = 0.9$.

For notional half 1 (top)	**For notional half 2 (bottom)**
$S'_{rx.1} = \frac{S_{rx}}{2} + \frac{M_{rx}}{j_x t_{sc}}$ (from N690 Eq. A-N9-28) $= \frac{193\text{ kip/ft}}{2} + \frac{4{,}300\text{ kip-in./ft}}{0.9(56.0\text{ in.})}$ $= 182\text{ kip/ft}$	$S'_{rx.2} = \frac{S_{rx}}{2} - \frac{M_{rx}}{j_x t_{sc}}$ (from N690 Eq. A-N9-28) $= \frac{193\text{ kip/ft}}{2} - \frac{4{,}300\text{ kip-in./ft}}{0.9(56.0\text{ in.})}$ $= 11.2\text{ kip/ft}$

For notional half 1 (top)	**For notional half 2 (bottom)**
$S'_{ry.1} = \dfrac{S_{ry}}{2} + \dfrac{M_{ry}}{j_y t_{sc}}$ (from N690 Eq. A-N9-29) $= \dfrac{-75.1 \text{ kip/ft}}{2} + \dfrac{-6{,}350 \text{ kip-in./ft}}{0.9(56.0 \text{ in.})}$ $= -164 \text{ kip/ft}$	$S'_{ry.2} = \dfrac{S_{ry}}{2} - \dfrac{M_{ry}}{j_y t_{sc}}$ (from N690 Eq. A-N9-29) $= \dfrac{-75.1 \text{ kip/ft}}{2} - \dfrac{-6{,}350 \text{ kip-in./ft}}{0.9(56.0 \text{ in.})}$ $= 88.4 \text{ kip/ft}$
$S'_{rxy.1} = \dfrac{S_{rxy}}{2} - \dfrac{M_{rxy}}{j_{xy} t_{sc}}$ (from N690 Eq. A-N9-30) $= \dfrac{-67.6 \text{ kip/ft}}{2} - \dfrac{223 \text{ kip-in./ft}}{0.67(56.0 \text{ in.})}$ $= -39.7 \text{ kip/ft}$	$S'_{rxy.2} = \dfrac{S_{rxy}}{2} + \dfrac{M_{rxy}}{j_{xy} t_{sc}}$ (from N690 Eq. A-N9-30) $= \dfrac{-67.6 \text{ kip/ft}}{2} + \dfrac{223 \text{ kip-in./ft}}{0.67(56.0 \text{ in.})}$ $= -27.9 \text{ kip/ft}$
$S_{r,max.1} = \dfrac{S'_{rx.1} + S'_{ry.1}}{2} + \sqrt{\left(\dfrac{S'_{rx.1} - S'_{ry.1}}{2}\right)^2 + \left(S'_{rxy.1}\right)^2}$ (from N690 Eq. A-N9-27) $= \dfrac{182 \text{ kip/ft} - 164 \text{ kip/ft}}{2}$ $+ \sqrt{\left(\dfrac{182 \text{ kip/ft} + 164 \text{ kip/ft}}{2}\right)^2 + (-39.7 \text{ kip/ft})^2}$ $= 187 \text{ kip/ft}$	$S_{r,max.2} = \dfrac{S'_{rx.2} + S'_{ry.2}}{2} + \sqrt{\left(\dfrac{S'_{rx.2} - S'_{ry.2}}{2}\right)^2 + \left(S'_{rxy.2}\right)^2}$ (from N690 Eq. A-N9-27) $= \dfrac{11.2 \text{ kip/ft} + 88.4 \text{ kip/ft}}{2}$ $+ \sqrt{\left(\dfrac{11.2 \text{ kip/ft} - 88.4 \text{ kip/ft}}{2}\right)^2 + (-27.9 \text{ kip/ft})^2}$ $= 97.4 \text{ kip/ft}$
$S_{r,min.1} = \dfrac{S'_{rx.1} + S'_{ry.1}}{2} - \sqrt{\left(\dfrac{S'_{rx.1} - S'_{ry.1}}{2}\right)^2 + \left(S'_{rxy.1}\right)^2}$ (from N690 Eq. A-N9-27) $= \dfrac{182 \text{ kip/ft} - 164 \text{ kip/ft}}{2}$ $- \sqrt{\left(\dfrac{182 \text{ kip/ft} + 164 \text{ kip/ft}}{2}\right)^2 + (-39.7 \text{ kip/ft})^2}$ $= -169 \text{ kip/ft}$	$S_{r,min.2} = \dfrac{S'_{rx.2} + S'_{ry.2}}{2} - \sqrt{\left(\dfrac{S'_{rx.2} - S'_{ry.2}}{2}\right)^2 + \left(S'_{rxy.2}\right)^2}$ (from N690 Eq. A-N9-27) $= \dfrac{11.2 \text{ kip/ft} + 88.4 \text{ kip/ft}}{2}$ $- \sqrt{\left(\dfrac{11.2 \text{ kip/ft} - 88.4 \text{ kip/ft}}{2}\right)^2 + (-27.9 \text{ kip/ft})^2}$ $= 2.17 \text{ kip/ft}$
$S_{r,max.1} + S_{r,min.1} = 187 \text{ kip/ft} - 169 \text{ kip/ft}$ $= 18.0 \text{ kip/ft}$	$S_{r,max.2} + S_{r,min.2} = 97.4 \text{ kip/ft} + 2.17 \text{ kip/ft}$ $= 99.6 \text{ kip/ft}$

Checking the interaction for the top notional half:

Because $S_{r,max.1} + S_{r,min.1} > 0$, the interaction is limited by ANSI/AISC N690, Equation A-N9-24:

$$DCR = \alpha\left(\frac{S_{r,max} + S_{r,min}}{2V_{ci}}\right) + \left(\frac{S_{r,max} - S_{r,min}}{2V_{ci}}\right) \leq 1.0 \qquad \text{(N690 Eq. A-N9-24)}$$

where

$\alpha = \dfrac{V_{ci}}{T_{ci}}$

$V_{ci} = \phi_{vs}\left(\dfrac{V_{ni}}{2}\right)$

$\phi_{vs} = 95$

$$V_{ci} = 0.95\left(\frac{600 \text{ kip/ft}}{2}\right)$$
$$= 285 \text{ kip/ft}$$
$$T_{ci} = \phi_{ti}\left(\frac{P_n}{2}\right)$$
$$\phi_{ti} = 1.00$$
$$T_{ci} = 1.00\left(\frac{600 \text{ kip/ft}}{2}\right)$$
$$= 300 \text{ kip/ft}$$

And thus, from ANSI/AISC Section N9.3.6b:

$$\alpha = \frac{V_{ci}}{T_{ci}}$$
$$= \frac{285 \text{ kip/ft}}{300 \text{ kip/ft}}$$
$$= 0.950$$

The interaction for the top notional half is:

$$DCR_{NH1} = 0.950\left[\frac{187 \text{ kip/ft} + 169 \text{ kip/ft}}{2(285 \text{ kip/ft})}\right] + \left[\frac{187 \text{ kip/ft} - 169 \text{ kip/ft}}{2(285 \text{ kip/ft})}\right]$$
$$= 0.625 < 1.0$$

The interaction for the top notional half is within the permissible limits.

For the bottom notional half:

Because $S_{r,max.2} + S_{r,min.2} > 0$, the interaction is limited by ANSI/AISC N690, Equation A-N9-24:

$$DCR_{NH2} = \alpha\left(\frac{S_{r,max.2} + S_{r,min.2}}{2V_{ci}}\right) + \left(\frac{S_{r,max.2} - S_{r,min.2}}{2V_{ci}}\right) \qquad \text{(from N690 Eq. A-N9-24)}$$
$$= 0.950\left[\frac{97.4 \text{ kip/ft} + 2.17 \text{ kip/ft}}{2(285 \text{ kip/ft})}\right] + \left[\frac{97.4 \text{ kip/ft} - 2.17 \text{ kip/ft}}{2(285 \text{ kip/ft})}\right]$$
$$= 0.333 < 1.0$$

The interaction for the bottom notional half is within the permissible limits.

Step 9. Demand Capacity Ratios and Interaction Surfaces

For checking the design of the SC wall section, the demand capacity ratios (DCRs) for all individual demands acting on every element for each load combination need to be checked. The DCRs are calculated by taking the ratio of required strengths calculated in Step 6 to available strength determined in Step 7.

This example presents the DCRs for all the elements for just one load combination, load combination 12. Figures A-3 to A-8 show the plots for DCRs for individual demand types for all the elements of the SC wall section. The DCR for each element is mentioned at the element location in these figures.

(a) Uniaxial tensile forces

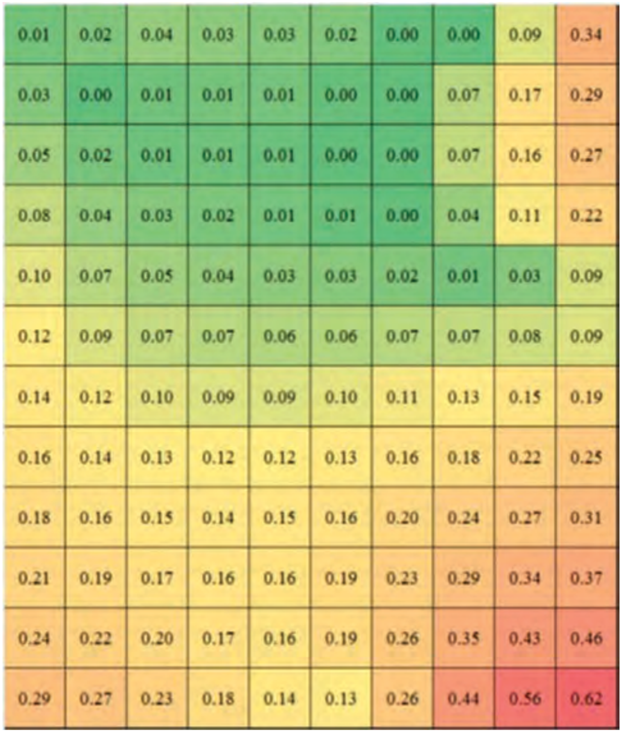

0.01	0.02	0.04	0.03	0.03	0.02	0.00	0.00	0.09	0.34
0.03	0.00	0.01	0.01	0.01	0.00	0.00	0.07	0.17	0.29
0.05	0.02	0.01	0.01	0.01	0.00	0.00	0.07	0.16	0.27
0.08	0.04	0.03	0.02	0.01	0.01	0.00	0.04	0.11	0.22
0.10	0.07	0.05	0.04	0.03	0.03	0.02	0.01	0.03	0.09
0.12	0.09	0.07	0.07	0.06	0.06	0.07	0.07	0.08	0.09
0.14	0.12	0.10	0.09	0.09	0.10	0.11	0.13	0.15	0.19
0.16	0.14	0.13	0.12	0.12	0.13	0.16	0.18	0.22	0.25
0.18	0.16	0.15	0.14	0.15	0.16	0.20	0.24	0.27	0.31
0.21	0.19	0.17	0.16	0.16	0.19	0.23	0.29	0.34	0.37
0.24	0.22	0.20	0.17	0.16	0.19	0.26	0.35	0.43	0.46
0.29	0.27	0.23	0.18	0.14	0.13	0.26	0.44	0.56	0.62

Fig. A-3. DCR for uniaxial tensile forces for load combination 12.

(b) Compressive forces

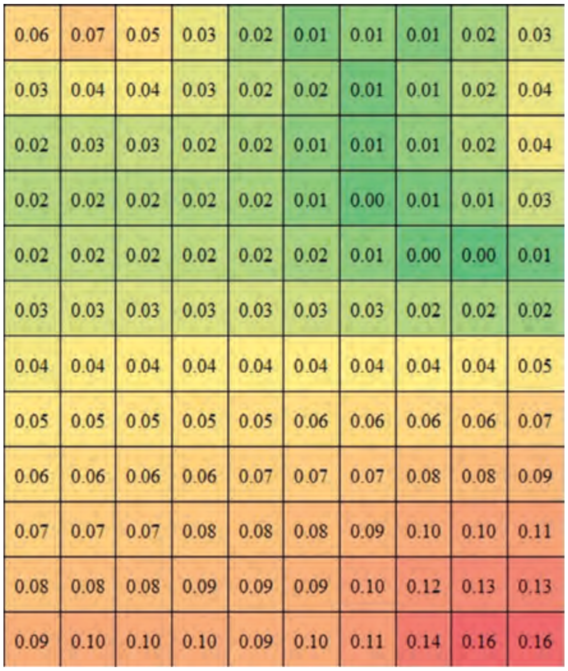

0.06	0.07	0.05	0.03	0.02	0.01	0.01	0.01	0.02	0.03
0.03	0.04	0.04	0.03	0.02	0.02	0.01	0.01	0.02	0.04
0.02	0.03	0.03	0.02	0.02	0.01	0.01	0.01	0.02	0.04
0.02	0.02	0.02	0.02	0.02	0.01	0.00	0.01	0.01	0.03
0.02	0.02	0.02	0.02	0.02	0.02	0.01	0.00	0.00	0.01
0.03	0.03	0.03	0.03	0.03	0.03	0.03	0.02	0.02	0.02
0.04	0.04	0.04	0.04	0.04	0.04	0.04	0.04	0.04	0.05
0.05	0.05	0.05	0.05	0.05	0.06	0.06	0.06	0.06	0.07
0.06	0.06	0.06	0.06	0.07	0.07	0.07	0.08	0.08	0.09
0.07	0.07	0.07	0.08	0.08	0.08	0.09	0.10	0.10	0.11
0.08	0.08	0.08	0.09	0.09	0.09	0.10	0.12	0.13	0.13
0.09	0.10	0.10	0.10	0.09	0.10	0.11	0.14	0.16	0.16

Fig. A-4. DCR for compressive forces for load combination 12.

(c) In-plane shear forces

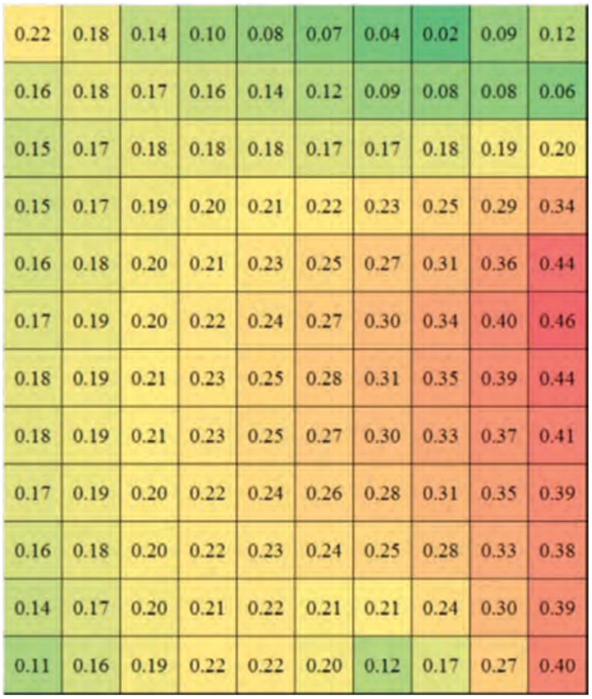

0.22	0.18	0.14	0.10	0.08	0.07	0.04	0.02	0.09	0.12
0.16	0.18	0.17	0.16	0.14	0.12	0.09	0.08	0.08	0.06
0.15	0.17	0.18	0.18	0.18	0.17	0.17	0.18	0.19	0.20
0.15	0.17	0.19	0.20	0.21	0.22	0.23	0.25	0.29	0.34
0.16	0.18	0.20	0.21	0.23	0.25	0.27	0.31	0.36	0.44
0.17	0.19	0.20	0.22	0.24	0.27	0.30	0.34	0.40	0.46
0.18	0.19	0.21	0.23	0.25	0.28	0.31	0.35	0.39	0.44
0.18	0.19	0.21	0.23	0.25	0.27	0.30	0.33	0.37	0.41
0.17	0.19	0.20	0.22	0.24	0.26	0.28	0.31	0.35	0.39
0.16	0.18	0.20	0.22	0.23	0.24	0.25	0.28	0.33	0.38
0.14	0.17	0.20	0.21	0.22	0.21	0.21	0.24	0.30	0.39
0.11	0.16	0.19	0.22	0.22	0.20	0.12	0.17	0.27	0.40

Fig. A-5. DCR for in-plane shear forces for load combination 12.

(d) Out-of-plane flexural forces

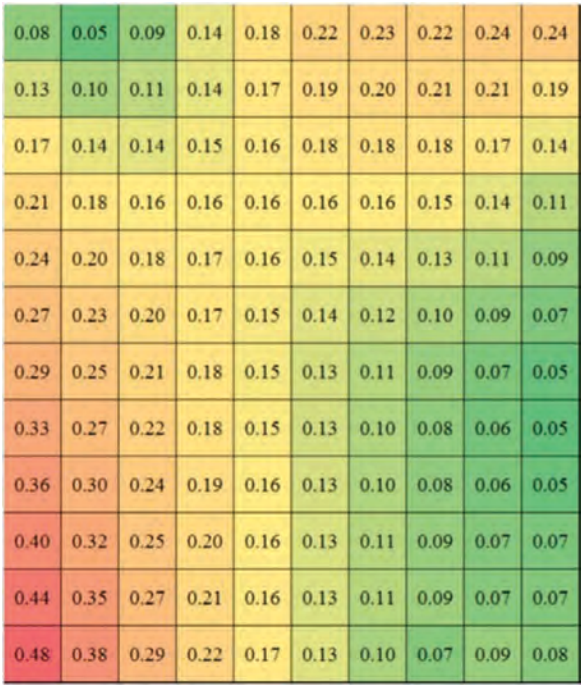

0.08	0.05	0.09	0.14	0.18	0.22	0.23	0.22	0.24	0.24
0.13	0.10	0.11	0.14	0.17	0.19	0.20	0.21	0.21	0.19
0.17	0.14	0.14	0.15	0.16	0.18	0.18	0.18	0.17	0.14
0.21	0.18	0.16	0.16	0.16	0.16	0.16	0.15	0.14	0.11
0.24	0.20	0.18	0.17	0.16	0.15	0.14	0.13	0.11	0.09
0.27	0.23	0.20	0.17	0.15	0.14	0.12	0.10	0.09	0.07
0.29	0.25	0.21	0.18	0.15	0.13	0.11	0.09	0.07	0.05
0.33	0.27	0.22	0.18	0.15	0.13	0.10	0.08	0.06	0.05
0.36	0.30	0.24	0.19	0.16	0.13	0.10	0.08	0.06	0.05
0.40	0.32	0.25	0.20	0.16	0.13	0.11	0.09	0.07	0.07
0.44	0.35	0.27	0.21	0.16	0.13	0.11	0.09	0.07	0.07
0.48	0.38	0.29	0.22	0.17	0.13	0.10	0.07	0.09	0.08

Fig. A-6. DCR for out-of-plane flexural forces for load combination 12.

(e) Out-of-plane shear forces

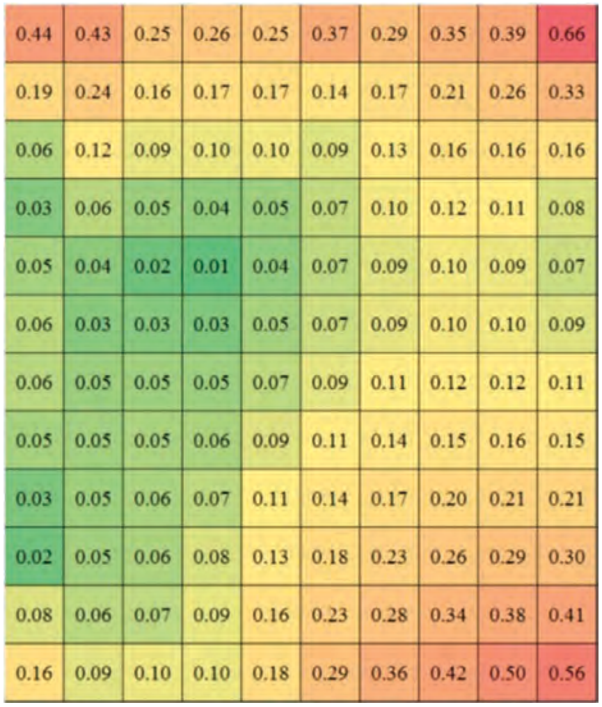

0.44	0.43	0.25	0.26	0.25	0.37	0.29	0.35	0.39	0.66
0.19	0.24	0.16	0.17	0.17	0.14	0.17	0.21	0.26	0.33
0.06	0.12	0.09	0.10	0.10	0.09	0.13	0.16	0.16	0.16
0.03	0.06	0.05	0.04	0.05	0.07	0.10	0.12	0.11	0.08
0.05	0.04	0.02	0.01	0.04	0.07	0.09	0.10	0.09	0.07
0.06	0.03	0.03	0.03	0.05	0.07	0.09	0.10	0.10	0.09
0.06	0.05	0.05	0.05	0.07	0.09	0.11	0.12	0.12	0.11
0.05	0.05	0.05	0.06	0.09	0.11	0.14	0.15	0.16	0.15
0.03	0.05	0.06	0.07	0.11	0.14	0.17	0.20	0.21	0.21
0.02	0.05	0.06	0.08	0.13	0.18	0.23	0.26	0.29	0.30
0.08	0.06	0.07	0.09	0.16	0.23	0.28	0.34	0.38	0.41
0.16	0.09	0.10	0.10	0.18	0.29	0.36	0.42	0.50	0.56

Fig. A-7. DCR for out-of-plane shear forces for load combination 12.

(f) Combined out-of-plane shear demands

According to ANSI/AISC N690, Section N9.3.6a, the forces in only one element meet the criteria for interaction for out-of-plane shear forces to be considered. The DCR for that element has been calculated and plotted in Figure A-8.

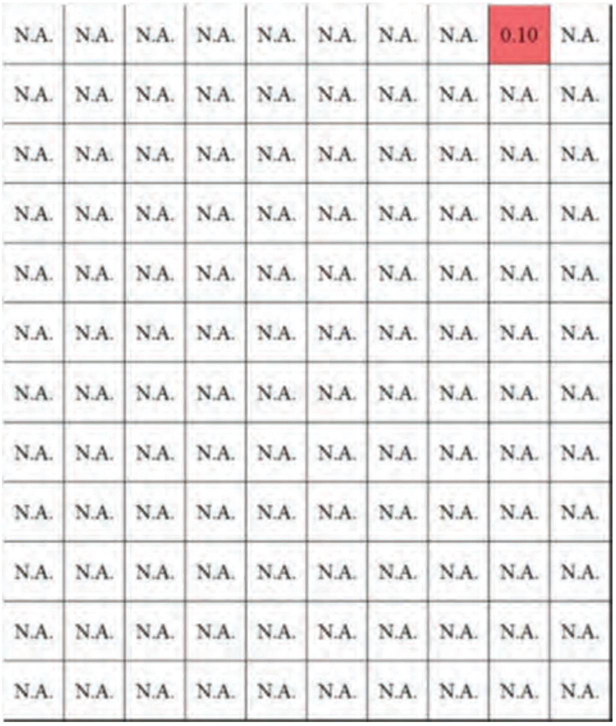

N.A.	N.A.	N.A.	N.A.	N.A.	N.A.	N.A.	N.A.	0.10	N.A.
N.A.	N.A.	N.A.	N.A.	N.A.	N.A.	N.A.	N.A.	N.A.	N.A.
N.A.	N.A.	N.A.	N.A.	N.A.	N.A.	N.A.	N.A.	N.A.	N.A.
N.A.	N.A.	N.A.	N.A.	N.A.	N.A.	N.A.	N.A.	N.A.	N.A.
N.A.	N.A.	N.A.	N.A.	N.A.	N.A.	N.A.	N.A.	N.A.	N.A.
N.A.	N.A.	N.A.	N.A.	N.A.	N.A.	N.A.	N.A.	N.A.	N.A.
N.A.	N.A.	N.A.	N.A.	N.A.	N.A.	N.A.	N.A.	N.A.	N.A.
N.A.	N.A.	N.A.	N.A.	N.A.	N.A.	N.A.	N.A.	N.A.	N.A.
N.A.	N.A.	N.A.	N.A.	N.A.	N.A.	N.A.	N.A.	N.A.	N.A.
N.A.	N.A.	N.A.	N.A.	N.A.	N.A.	N.A.	N.A.	N.A.	N.A.
N.A.	N.A.	N.A.	N.A.	N.A.	N.A.	N.A.	N.A.	N.A.	N.A.
N.A.	N.A.	N.A.	N.A.	N.A.	N.A.	N.A.	N.A.	N.A.	N.A.

Fig. A-8. Interaction of out-of-plane shear forces for load combination 12.

(g) Interaction of in-plane forces and out-of-plane moments

The principal stresses on each notional half for each element are plotted on the interaction surface defined by the provisions of ANSI/AISC N690, Section N9.3.6b. Because the interaction is checked for only one load combination, the data points for the required strengths for each notional half of the elements lie in the same region, as shown in Figure A-9. When checked for all load combinations, the data plots would have a wider spread. As seen in Figure A-9, one data point lies outside the interaction surface, and data points for the top notional half lie closer to the interaction surface. There are a few data points close to the interaction surface.

Therefore, the wall needs to be redesigned. One possible alternative is to use Grade 65 faceplates, which have a yield stress of 65 ksi. The design of the SC wall needs to be rechecked with updated section parameters. Another option is to average the demands (with ductile failure limit states) in the regions where the demand exceeds the available strength. In accordance with ANSI/AISC N690, the demands can be averaged over a span of $2t_{sc} \times 2t_{sc}$ for interior regions and $t_{sc} \times t_{sc}$ for connection regions. The averaging would normally be required over localized regions of stress concentrations. If averaging is required over a large portion of the designed wall—DCR exceed 1.0 over many elements—the wall should be redesigned. The redesign is not discussed in this design example.

Note: All the mentioned DCRs need to be determined for all the load combinations and elements, and the design needs to be updated if required.

Step 10. Demands for Anchorage Design

The design of SC wall-to-anchorage connection is presented in Step 12. The required strengths for the connection are provided in this section. ANSI/AISC N690, Section N9.4, discusses the provisions for SC wall connections. Section N9.4.1 discusses the permissible connectors and force transfer mechanisms.

ANSI/AISC N690 , Section N9.4.2, provides two design philosophies for determining the required strength of the connection.

The full-strength connection, ANSI/AISC N690, Section N9.4.2 option (a), stipulates that the required strength of the connection will be 1.25 times the smaller of the nominal strengths of the connected parts. Therefore, the individual required strengths for connection design are:

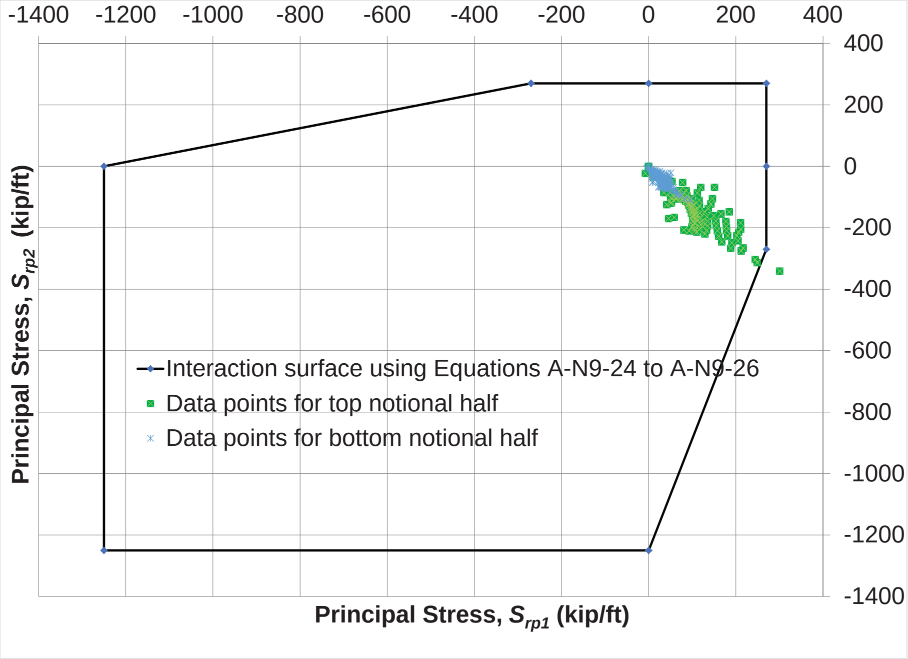

Fig. A-9. Plot of principal stresses in the element notional half on the interaction surface in the principal plane.

Required uniaxial tensile strength

From Step 7(a), $P_{n.ten} = 600$ kip/ft; therefore, the required tensile strength is:

$$\begin{aligned} S_{r.t.con} &= 1.25P_{n.ten} \\ &= 1.25(600 \text{ kip/ft}) \\ &= 750 \text{ kip/ft} \end{aligned}$$

The required uniaxial compressive strength is:

$$\begin{aligned} S_{r.c.con} &= 1.25(P_{n.ten} + 0.85f_c' t_c) \\ &= 1.25\left[600 \text{ kip/ft} + 0.85(5 \text{ ksi})(55.0)(12 \text{ in./ft})\right] \\ &= 4{,}260 \text{ kip/ft} \end{aligned}$$

Required in-plane shear strength

From Step 7(d), $V_{ni} = 600$ kip/ft; therefore, the required in-plane shear strength is:

$$\begin{aligned} S_{r.vi.con} &= 1.25V_{ni} \\ &= 1.25(600 \text{ kip/ft}) \\ &= 750 \text{ kip/ft} \end{aligned}$$

Required out-of-plane flexural strength

From Step 7(c), $M_n = 15{,}100$ kip-in./ft; therefore, the required out-of-plane flexural strength is:

$$\begin{aligned} S_{r.flex.con} &= 1.25M_n \\ &= 1.25(15{,}100 \text{ kip-in./ft}) \\ &= 18{,}900 \text{ kip-in./ft} \end{aligned}$$

Required out-of-plane shear strength

From Step 7(e), $V_{no} = 246$ kip/ft; therefore, the required out-of-plane shear strength is:

$$\begin{aligned} S_{r.vo.con} &= 1.25V_{no} \\ &= 1.25(246 \text{ kip/ft}) \\ &= 308 \text{ kip/ft} \end{aligned}$$

ANSI/AISC N690, Section N9.4.2 option (b), requires that the required connection strength be determined as 200% of the required strength due to seismic loads plus 100% of the required strength due to nonseismic loads, including thermal loads.

ANSI/AISC N690, Section N9.4.2, recommends option (a). However, if option (b) must be used, the seismic demands need to be separately evaluated. Twice the demands due to seismic loads need to be added to the demands due to other load cases to obtain the required strength for the anchorage connection. The connection would then need to be designed for all the individual demand types acting together.

Step 11. Impactive and Impulsive Loading

The design of the SC wall also needs to be checked for impactive and impulsive loads according to ANSI/AISC N690, Section N9.1.6. The procedure is not discussed in this example. This is an interior wall and will not be subject to the impact of tornado-borne missiles. However, for illustration purposes, the wall is treated as an external SC wall, and Figure A-10 is provided to present the local response of this SC wall to flat-nosed non-deformable missiles. When the walls are checked for impactive and impulsive loads, both the local and global effects of these loads need to considered.

Figure A-10 is based on Bruhl et al. (2015a), and the procedure is discussed in the commentary to ANSI/AISC N690, Section N9.1.6. The figure presents the response of a typical SC wall to flat-nosed missiles. Flat-nosed missiles are appropriate for use for typical tornado-borne missiles such as a pipe, rod or utility pole. The missiles with mass and velocity to the left of the curves will not perforate the SC wall, while the others will. Although the faceplate thickness is 0.5 in., the figure is based on 0.4-in.-thick faceplates. This is because ANSI/AISC N690 requires that the faceplate thickness provided be 1.25 times the thickness required to prevent perforation.

Step 12. Design of SC Wall Connections

The SC wall connections may be the following types:

- (a) Connection between the SC wall and the basemat
- (b) Connection between SC walls (or SC walls and RC walls) in the same alignment (continuity)
- (c) Connection between intersecting (orthogonal) SC walls (or SC walls and RC walls or slabs)

This example presents the wall-to-basemat connection for the SC wall designed.

The types of SC wall-to-basemat connections possible are discussed in Section 11.5. This design example presents the design of an SC wall-to-basemat connection that involves the use of a single base plate. The connection is designed as a full-strength connection. The connection should be designed for the demand types shown in Figure A-11. These demand types are:

- (a) Tensile strength [Figure A-11(a)]
- (b) Compression strength [Figure A-11(b)]
- (c) In-plane shear strength [Figure A-11(c)]
- (d) Out-of-plane shear strength [Figure A-11(d)]
- (e) Out-of-plane flexural strength [Figure A-11(e)]

General geometry of the connection is shown in Figure A-12.

(a) Tensile Strength

The available tensile strength of the SC wall is governed by the resistance of the faceplates. The SC wall-to-base plate weld needs to be designed for 1.25 times the available tensile strength of the SC wall. The force transfer mechanism considered is discussed in Section 11.5.1 and shown in Figure A-13.

The following parameters are considered for the design of the connection. Some of these parameters need to be iterated based on the design.

B_{bp} = unit width of base plate
= 12.0 in.

F_{EXX} = 70 ksi

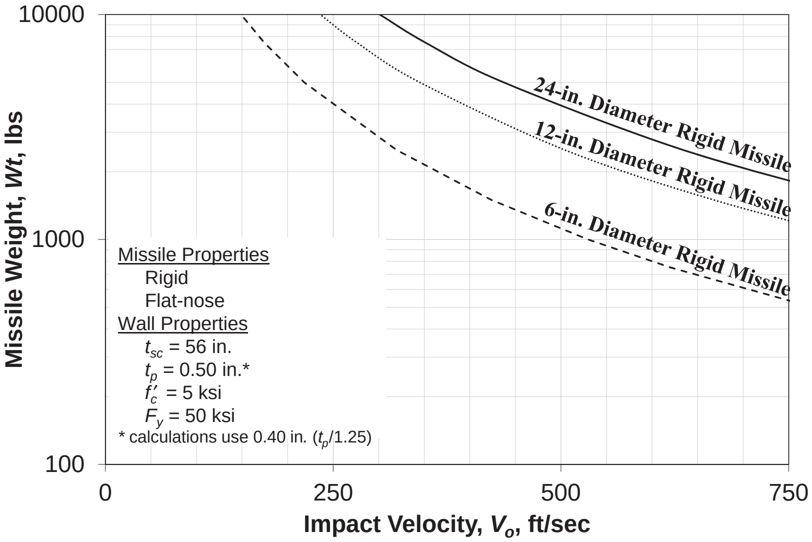

Fig. A-10. Response of SC wall to flat-nosed rigid missiles.

$F_{y.an}$ = specified minimum anchor yield strength
= 60 ksi for ASTM A615 rebar

$F_{u.an}$ = specified minimum tensile strength of anchors
= 88 ksi for ASTM A615 rebar

S_{an} = transverse spacing of rebar anchors
= 8.50 in.

$T_{SC.con}$ = connection design tensile force
= $S_{r.t.con}$
= 750 kip/ft

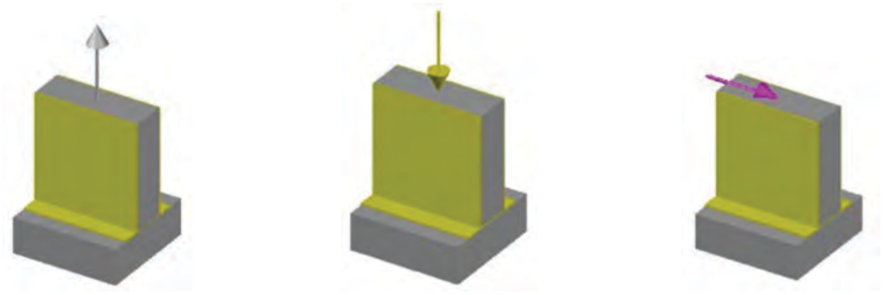

(a) Tensile demand (b) Compression demand (c) In-plane shear demand

(d) Out-of-plane shear demand (e) Out-of-plane flexural demand

Fig. A-11. Individual demand types for SC wall-to-basemat connections.

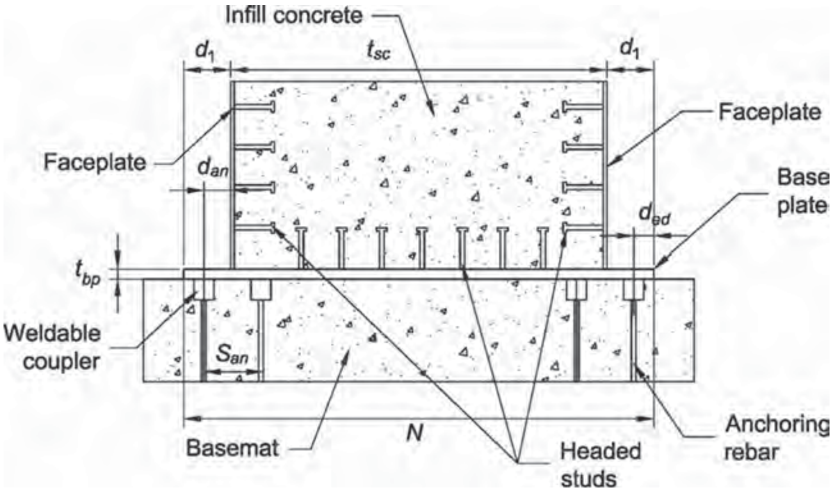
Infill concrete
d_1
t_{sc}
d_1
Faceplate
Faceplate
d_{an}
Base plate
d_{ed}
t_{bp}
Weldable coupler
S_{an}
Basemat
N
Headed studs
Anchoring rebar

Fig. A-12. Geometry for SC wall-to-basemat connection—elevation.

d_{an} = distance from anchor to the faceplate
$= 4.00$ in.

d_{anc} = anchor diameter
$= 2.26$ in. for #18 rebar

d_{ed} = distance from the anchor to edge of the base plate
$= 7.00$ in.

t_{we} = fillet weld thickness
$= 1.13$ in.

ϕ_w = resistance factor for welds
$= 0.75$

(1) Weld tensile strength

$A_{e.w}$ = weld area resisting tensile force
$= B_{bp}t_{we}$
$= (12.0 \text{ in.})(1.13 \text{ in.})$
$= 13.6 \text{ in.}^2$

d_1 = distance from faceplate to edge of the base plate
$= d_{ed} + d_{an}$
$= 7.00 \text{ in.} + 4.00 \text{ in.}$
$= 11.0$ in.

N_{bp} = base plate length
$= t_{sc} + 2d_1$
$= 56.0 \text{ in.} + 2(11.0 \text{ in.})$
$= 78.0$ in.

The available strength of the weld is then:

$$\phi R_{n.w} = 2\phi_w(0.6F_{EXX})A_{e.w}$$
$$= 2(0.75)(0.6)(70 \text{ ksi})(13.6 \text{ in.}^2)$$
$= 857$ kips on both faceplates

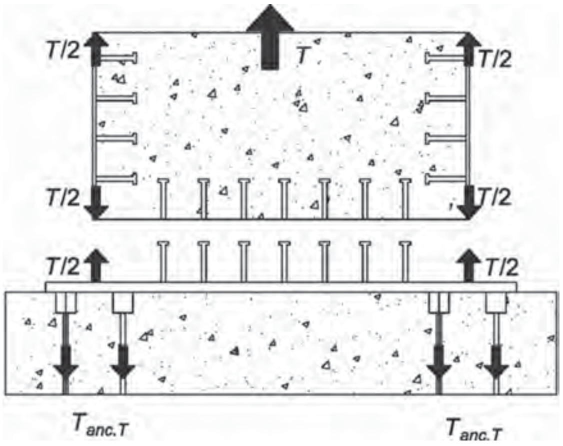

Fig. A-13. Force transfer mechanism for tensile demands.

And the demand capacity ratio is:

$$\begin{aligned} DCR &= \frac{T_{SC.con}}{\phi R_{n.w}} \\ &= \frac{750 \text{ kip/ft}}{857 \text{ kips}} \\ &= 0.875 < 1.0 \end{aligned}$$

Therefore, the weld is adequate. The base metal check for the welds has not been performed because the faceplate yield strength will be less than the tensile demand for the full-strength connection design.

(2) Base plate flexural check

The base plate may bend due to the tensile force acting in the faceplate, as shown in Figure A-14. A minimum base plate thickness is required to address this. The design is on a per-unit width basis. It is assumed that the width of the base plate is significantly greater than the length, and therefore, the base plate will undergo one-way bending.

Bending moment in the base plate due to tension:

$$\begin{aligned} M_{t.bp} &= \frac{T_{SC.con} S_{an}}{8} \\ &= \frac{(750 \text{ kip/ft})(8.50 \text{ in.})}{8} \\ &= 797 \text{ kip-in./ft} \end{aligned}$$

Then according to AISC Design Guide 1, Equation 3.4.7a (Fisher and Kloiber, 2006), the required thickness of the base plate due to the bending moment is:

$$\begin{aligned} t_{req.m} &= 2.11\sqrt{\frac{M_{t.bp}}{F_y}} \\ &= 2.11\sqrt{\frac{(797 \text{ kip-in./ft})/(12 \text{ in./ft})}{50 \text{ ksi}}} \\ &= 2.43 \text{ in.} \end{aligned}$$

A thickness of 3 in. is provided for the base plate. The flexural resistance of the base plate is computed as follows:

$$\phi M_{bp} = \frac{t_{bp}^2 F_y}{4.45}$$

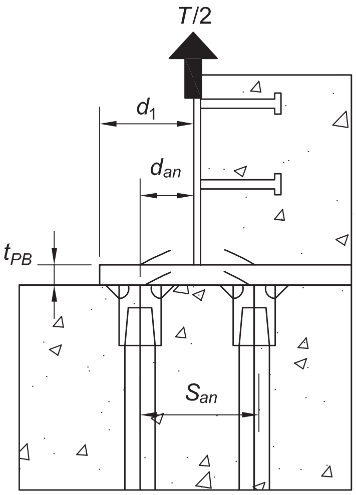

Fig. A-14. Bending on the base plate due to tension.

where

t_{bp} = thickness of base plate
= 3.00 in.

$$\phi M_{bp} = \frac{(3.00\text{ in.})^2(50\text{ ksi})}{(4.45)/(12\text{ in./ft})}$$
$$= 1{,}220\text{ kip-in./ft}$$

The demand capacity ratio is then:

$$DCR = \frac{M_{t.bp}}{\phi M_{bp}}$$
$$= \frac{797\text{ kip-in./ft}}{1{,}220\text{ kip-in./ft}}$$
$$= 0.667 < 1.0$$

Therefore, the base plate thickness is adequate. Because the base plate is thick, it is not checked for prying action.

(3) Anchor tensile strength check

The design tensile demand is resisted by the anchor bars.

From AISC *Specification* Section B3.3, the resistance factor for tension is:

$$\phi_{ten} = 0.90$$

Gross area of each anchor:

$$A_{an} = \frac{\pi d_{anc}^2}{4}$$
$$= \frac{\pi(2.26\text{ in.})^2}{4}$$
$$= 4.01\text{ in.}^2$$

Design tensile strength of each anchor:

$$\phi R_{n.an} = \phi_{ten} A_{an} F_{y.an}$$
$$= 0.90(4.01\text{ in.}^2)(60\text{ ksi})$$
$$= 217\text{ kips}$$

Number of anchors needed per faceplate per ft:

$$N_{anc} = \frac{T_{SC.con}}{2\phi R_{n.an}}$$
$$= \frac{750\text{ kip/ft}}{2(217\text{ kips})}$$
$$= 1.73\text{ anchors/ft}$$

Two #18 anchors are required per faceplate per foot. However, the direct shear demand in the anchors, which is checked later, requires four anchors per faceplate per foot. Anchors spaced at 6 in. in the longitudinal direction and 8.5 in. in the transverse direction are provided on each faceplate.

Demand capacity ratio:

$$DCR = \frac{T_{SC.con}}{8\phi R_{n.an}}$$
$$= \frac{750\text{ kip/ft}}{8(217\text{ kips})}$$
$$= 0.432 < 1.0$$

The weld of the coupler to the base plate also needs to be designed.The number of couplers below the base plate per foot:

$$N_c = 8$$

(4) Weldable coupler weld check

The geometric properties of a Lenton weldable coupler for a #18 rebar are shown in Figure A-15.

$$D_{rc} = 3.13 \text{ in.}$$
$$\mathrm{B}_{rc} = 4.50 \text{ in.}$$
$$G_{rc} = 1.75 \text{ in.}$$

$$\begin{aligned} t_{wanc} &= \text{effective throat of weld} \\ &= 1.20 \text{ in.} \end{aligned}$$

$$\begin{aligned} t_{wanc.f} &= \text{throat of fillet weld} \\ &= 0.750 \text{ in.} \end{aligned}$$

The total length of the coupler welds (based on AWS D1.1, Figure 2.16) is:

$$\begin{aligned} L_{anc} &= 2\pi\left[\frac{G_{rc}}{2} + \frac{t_{wanc}}{(4)\cos 45°}\right] \\ &= 2\pi\left[\frac{1.75 \text{ in.}}{2} + \frac{1.20 \text{ in.}}{(4)\cos 45°}\right] \\ &= 8.16 \text{ in.} \end{aligned}$$

And the tensile force per rebar is:

$$\begin{aligned} T_{anc.T} &= \frac{T_{SC.con} B_{bp}}{N_c} \\ &= \frac{(750 \text{ kip/ft}/12 \text{ in./ft})(12.0 \text{ in.})}{8.00} \\ &= 93.8 \text{ kips} \end{aligned}$$

The design strength of the coupler weld is:

$$\phi R_{n.w.anc} = \phi_w (0.6 F_{EXX}) A_{e.w.anc}$$

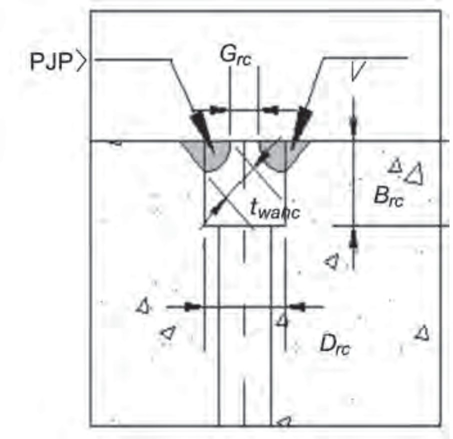

Fig. A-15. Geometry of weldable coupler.

where

$$A_{e.w.anc} = t_{wanc}L_{anc}$$
$$= (1.20\text{ in.})(8.16\text{ in.})$$
$$= 9.79\text{ in.}^2$$

Therefore:

$$\phi R_{n.w.anc} = 0.75(0.6)(70\text{ ksi})(9.79\text{ in.}^2)$$
$$= 308\text{ kips}$$

According to ACI 349-06, Section 21.5.1.1 (ACI, 2006), to ensure ductility:

$$T_{anc.f} = 1.25R_{n.an}$$
$$= 1.25(241\text{ kips})$$
$$= 301\text{ kips}$$

$$T_{anc} = \max(T_{anc.T}, T_{anc.f})$$
$$= 301\text{ kips}$$

Demand capacity ratio:

$$DCR = \frac{T_{anc}}{\phi R_{n.w.anc}}$$
$$= \frac{301\text{ kips}}{308\text{ kips}}$$
$$= 0.977 < 1.0$$

Although the margin is small, because this is a full-strength connection design, the anchor weld design is adequate.

(b) In-Plane Shear Strength

The in-plane shear strength of the SC wall-to-basemat connection is governed by the available shear strength of the anchors and the friction force between the base plate and the basemat concrete; see Figure A-16.

(1) Required number of anchors

The number of stud anchors required to transfer the shear force in the concrete to the base plate is determined as follows:

$$V_{inp} = S_{r.is.con}$$
$$= 750\text{ kip/ft}$$

$$d_s = 0.750\text{ in.}$$

$$A_{sa} = 0.442\text{ in.}^2$$

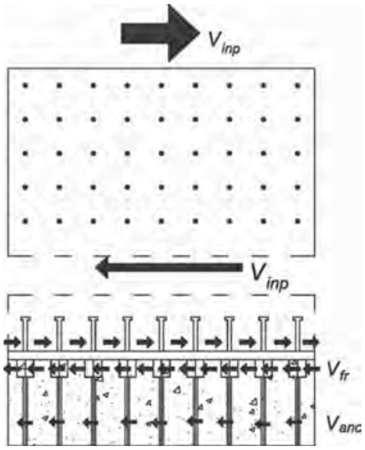

Fig. A-16. Force transfer mechanism for in-plane shear.

Required number of anchors per ft:

$$N_{SC.c} = \frac{V_{inp}}{\phi_v Q_{nv}}$$
$$= \frac{750 \text{ kip/ft}}{(0.65)(28.7 \text{ kips})}$$
$$= 40.2 \text{ anchors/ft}$$

Forty-two steel headed stud anchors are provided per foot on the face plate. The studs are spaced at 3 in. in the longitudinal direction and at 4 in. in the transverse direction.

(2) Friction under the base plate check

The force transfer mechanism under the base plate is considered to be direct shear friction. The force may also be transferred by shear lugs, concrete bearing on rebar couplers, or other mechanisms. The shear friction contribution based on ACI 349-06 is calculated as follows:

Alternate shear strength reduction factor (ACI 349-06, Section RC.3): $\phi_S = 0.85$

Shear coefficient of friction (ACI 349-06, Section 11.7.4.3, base plate concrete): $\mu_f = 0.70$

Area of anchor:

$$A_{an} = 4.01 \text{ in.}^2$$

Total area of anchors:

$$A_{an.tot} = 8A_{an}$$
$$= 8(4.01 \text{ in.}^2)$$
$$= 32.1 \text{ in.}^2$$

Shear friction available strength:

$$\phi V_{n.sf} = \phi_S \mu_f A_{an.Tot} F_{y.an} \qquad \text{(from ACI 349-06 Eq. 11-25)}$$
$$= 0.85(0.70)(32.1 \text{ in.}^2)(60 \text{ ksi})$$
$$= 1{,}150 \text{ kips}$$

Demand capacity ratio:

$$DCR = \frac{V_{inp} B_{bp}}{\phi V_{n.sf}}$$
$$= \frac{(750 \text{ kip/ft}/12.0 \text{ in./ft})(12.0 \text{ in.})}{1{,}150 \text{ kips}}$$
$$= 0.652 < 1.0 \qquad \textbf{o.k.}$$

Required width of base plate based on the upper limit of shear friction according to ACI 349, Section 11.7.5:

$$N_{bp.req} = \frac{V_{inp}}{\min(0.2 f_c', 800 \text{ psi})}$$
$$= \frac{(750 \text{ kip/ft}/12 \text{ in./ft})(1{,}000 \text{ lb/kip})}{800 \text{ psi}}$$
$$= 78.1 \text{ in.}$$

Extension needed on the base plate:

$$N_{bp.ex} = \frac{N_{bp.req} - N_{bp}}{2}$$
$$= \frac{78.1 \text{ in.} - 78.0 \text{ in.}}{2}$$
$$= 0.0500 \text{ in.}$$

The base plate does not need to be extended to transfer the total in-plane shear of the wall.

(3) Direct shear in the anchors check

Direct shear in the anchors is checked as follows.

Number of couplers below the base plate:

$N_c = 8$

Area of the anchor:

$A_{an} = 4.01 \text{ in.}^2$

Total area of the anchors:

$$\begin{aligned} A_{an.tot} &= 8A_{an} \\ &= 8(4.01 \text{ in.}^2) \\ &= 32.1 \text{ in.}^2 \end{aligned}$$

The alternate shear strength resistance factor from AISC *Specification* Section G1 is:

$\phi_{S.r} = 0.90$

Direct shear available strength of the anchors:

$$\begin{aligned} \phi V_n &= \phi_{S.r}(0.6F_{y.an})A_{an.tot} \\ &= 0.90(0.6)(60 \text{ ksi})(32.1 \text{ in.}^2) \\ &= 1{,}040 \text{ kips} \end{aligned}$$

Demand capacity ratio:

$$\begin{aligned} DCR &= \frac{V_{inp}B_{bp}}{\phi V_n} \\ &= \frac{(750 \text{ kip/ft}/12 \text{ in./ft})(12.0 \text{ in.})}{1{,}040 \text{ kips}} \\ &= 0.721 < 1.0 \end{aligned}$$

Therefore, the anchors are adequate in direct shear.

(c) Out-of-Plane Shear Strength

The out-of-plane shear strength of the SC wall-to-basemat connection is governed by the available shear strength of the bolts and the friction force between the base plate and the basemat concrete. The force transfer mechanism for out-of-plane shear force demands is presented in Figure A-17.

The out-of-plane shear force demand in the SC wall will be transferred to the base plate by means of steel headed stud anchors welded to the base plate. The force from the base plate will be transferred to the basemat by means of shear friction in the concrete. This force transfer mechanism is the same as for in-plane demands. Because the in-plane shear strength of

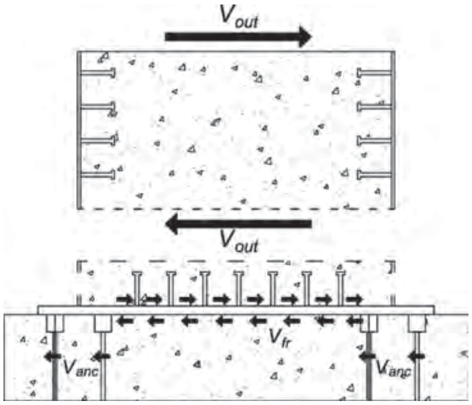

Fig. A-17. Force transfer mechanism for out-of-plane shear.

the wall is more than the out-of-plane shear strength, the connection designed for in-plane demands will be adequate for out-of-plane demands. The combination of demands on the connectors, based on the force transfer mechanism considered, is discussed in Step 13.

(d) Out-of-Plane Flexural Strength

The SC wall-to-base plate connection is designed for out-of-plane flexural demands as follows.

The flexural demand can be resolved into a force couple acting on the faceplates as shown in Figure A-18. The design of the wall-to-basemat connection can be checked for these tensile and compressive demands as discussed earlier, as follows:

$$\begin{aligned}M_{op} &= S_{r.flex.con}\\ &= 18{,}900 \text{ kip-in./ft}\end{aligned}$$

$$\begin{aligned}T_{Mop} &= \frac{M_{op}}{t_{sc} - t_p}\\ &= \frac{18{,}900 \text{ kip-in./ft}}{56.0 \text{ in.} - 0.500 \text{ in.}}\\ &= 341 \text{ kip/ft}\end{aligned}$$

$$\begin{aligned}\frac{T_{SC.con}}{2} &= \frac{750 \text{ kip/ft}}{2}\\ &= 375 \text{ kip/ft}\end{aligned}$$

Because the tensile demand due to the out-of-plane moment, T_{Mop}, is less than the uniaxial tensile demand of the SC wall, $T_{SC.con}/2$, no additional checks are required. The compression demand will be transferred to the base plate, and then to the basemat in bearing.

(e) Compression Strength

The available compression strength of the SC wall is governed by the faceplate and concrete compressive strengths. However, the SC wall thickness is governed by shielding requirements instead of calculated demands. This is evidenced by the DCRs for compression demands in the SC wall, shown in Figure A-4. The maximum DCR for compression demand is 0.160, which is representative of nuclear construction. Designing the connection for the full expected compression capacity of the SC wall is impractical and unnecessary, although permitted by ANSI/AISC N690, Section N9.4. Designing as an

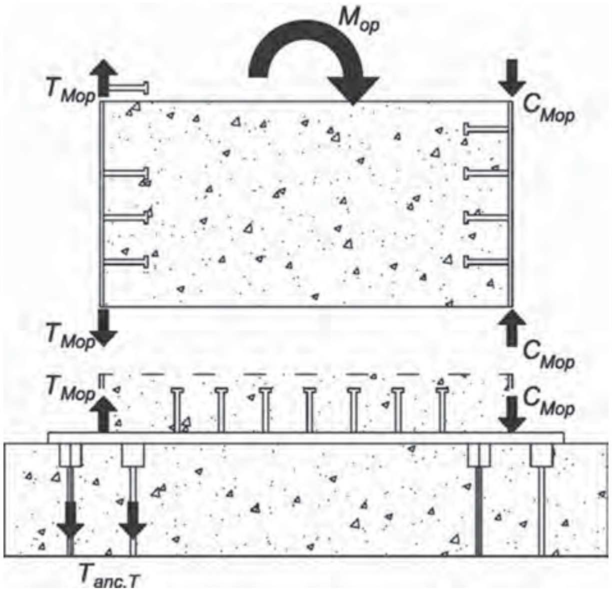

Fig. A-18. Force couple acting on the SC wall corresponding to out-of-plane flexural demand.

overstrength connection for the compression demand only is also permitted by ANSI/AISC N690 and is the preferred option of the two options discussed here. The following options are available to design the connection for compression demands.

For full-strength connection design, according to Section 11.3.1, the connection, including the base plate area and thickness, can be designed for the expected compression strength of the SC wall. The minimum base plate area required for compression bearing, and the minimum base plate thickness required for cantilever bending due to the compression reaction on the base plate can be checked using AISC Design Guide 1 (Fisher and Kloiber, 2006). In accordance with AISC Design Guide 1, a uniform pressure reaction can be considered on the base plate, as shown in Figure A-19. This is conservative because the base plate reaction will be concentrated under the SC wall. Alternatively, the base plate reaction can be considered to be uniform under the SC wall and reduced linearly to zero at the edge of the base plate. The cantilever length of the base plate (currently at 11 in.) will govern the base plate thickness required for the limit state of yielding associated with bending (shown in Figure A-19) due to the uniform reaction. This cantilever length can be optimized by changing the steel anchor distance from the faceplate and base plate edge.

For overstrength design in compression, the connection can be designed conservatively for 200% of the calculated total compression demand (instead of 200% of seismic demand + 100% of nonseismic demands) as follows.

Because the connection is designed as overstrength for compression demand, the connection design compressive force is two times the peak compression demand in the SC wall. The compression demand can be back calculated from the peak DCR of 0.160.

Using the available compressive strength calculated in Step 6, the connection design compressive force is:

$$\begin{aligned} P_u &= 2DCR(\phi P_{n.com}) \\ &= 2(0.16)(2{,}510 \text{ kip/ft}) \\ &= 804 \text{ kip/ft} \end{aligned}$$

(1) Minimum base plate area check

The base plate is designed according to AISC Design Guide 1. Due to the configuration of the connection, the supporting surface, A_2, is considerably wider than the base plate area, A_1. Therefore, the amplifier factor $\sqrt{(A_1/A_2)}$ is taken as 2.

Resistance factor for direct bearing according to AISC *Specification* Section I6.3a:

$$\phi_B = 0.65$$

Area of the base plate provided:

$$\begin{aligned} A_{BP.sum} &= (t_{sc} + 2d_1)(12.0 \text{ in.}) \\ &= [56.0 \text{ in.} + 2(11.0 \text{ in.})](12.0 \text{ in.}) \\ &= 936 \text{ in.}^2 \end{aligned}$$

Area of the base plate required:

$$\begin{aligned} A_{BP.req} &= \frac{P_u B_{bp}}{\phi_B (1.7 f_c')} && \text{(from } \textit{Spec.} \text{ Eq. I6-3)} \\ &= \frac{(804 \text{ kip/ft}/12 \text{ in./ft})(12.0 \text{ in.})}{(0.65)(1.7)(5 \text{ ksi})} \\ &= 146 \text{ in.}^2 \end{aligned}$$

Demand capacity ratio:

$$\begin{aligned} DCR &= \frac{A_{BP.req}}{A_{BP.sum}} \\ &= \frac{146 \text{ in.}^2}{936 \text{ in.}^2} \\ &= 0.155 < 1.0 \end{aligned}$$

Therefore, the base plate area is adequate for bearing on the concrete.

(2) Minimum base plate thickness check (see Figure A-19)

According to AISC Design Guide 1, Section 3.1.3, the value for the critical base plate cantilever dimension, l_{can}, needs to be adjusted due to the type of connecting element. This connection can be considered similar to an HSS column, which means that the yielding lines are located at 0.95 times the dimension of the SC wall.

Idealized cantilever length in the direction of N:

$$\begin{aligned} m_y &= \frac{N_{bp} - 0.95(t_{sc})}{2} \\ &= \frac{78.0\text{ in.} - 0.95(56.0\text{ in.})}{2} \\ &= 12.4\text{ in.} \end{aligned}$$

Idealized cantilever length in the direction of B:

$$n_y = 0\text{ in.}$$

$$\begin{aligned} l_{can} &= \max(m_y, n_y) \\ &= 12.4\text{ in.} \end{aligned}$$

Required minimum base plate thickness due to compressive force:

$$\begin{aligned} t_{bp} &= l_{can}\sqrt{\frac{2P_u}{\phi_b F_y N_{bp}}} \\ &= (12.4\text{ in.})\sqrt{\frac{2(804\text{ kip/ft}/12\text{ in./ft})}{0.90(50\text{ ksi})(78.0\text{ in.})}} \\ &= 2.42\text{ in.} \end{aligned}$$

The 3-in. base plate thickness provided is greater than the thickness required due to compressive force.

Step 13. Combination of Demands

The full-strength SC wall-to-basemat connection is evaluated for the combined demands obtained from the finite element analysis for various load combinations. This evaluation needs to be performed for both full-strength and overstrength connections. For a full-strength connection, these demands need not be separated into seismic and nonseismic demands. The connection is designed as overstrength for compression demand, however 200% of both seismic and nonseismic demands are conservatively being considered. All the elements need to be checked for demands obtained from all load combinations. The finite elements at the connection will have a stress concentration and there may be areas of potential stress concentration. The demands may need to be averaged as discussed in Section 7.7. For this design example, no averaging has been done, and the demands for element 54664

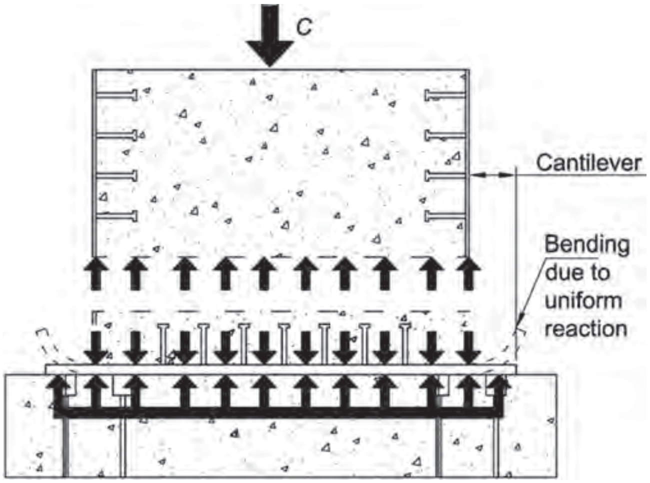

Fig. A-19. Force transfer mechanism and bending in the base plate due to compression.

for load combination 12 (Case B) presented in the following are considered. The demands are back-calculated by multiplying the DCR calculated in Step 9 for the demand type with the available strength. The element is located at the connection between the SC wall and the basemat. This check needs to be performed for all elements at the connection for all loading combinations.

Tensile demand:

$$\begin{aligned} T_{req} &= 0.62\phi P_{n.ten} \\ &= 0.62(540 \text{ kip/ft}) \\ &= 335 \text{ kip/ft} \end{aligned}$$

In-plane shear demand:

$$\begin{aligned} V_{req.is} &= 0.4\phi V_{ni} \\ &= 0.4(540 \text{ kip/ft}) \\ &= 216 \text{ kip/ft} \end{aligned}$$

The compression demand is 200% of the peak demand from of the finite element analysis:

$$\begin{aligned} P_{req} &= 2(0.16)\phi \mathrm{P}_{n.com} \\ &= 2(0.16)(2{,}510 \text{ kip/ft}) \\ &= 804 \text{ kip/ft} \end{aligned}$$

Out-of-plane shear demand:

$$\begin{aligned} \mathrm{V}_{req.os} &= 0.56\phi_{vo} V_{no} \\ &= 0.56(185 \text{ kip/ft}) \\ &= 104 \text{ kip/ft} \end{aligned}$$

Out-of-plane flexural demand:

$$\begin{aligned} M_{req.o} &= 0.48\phi_b M_n \\ &= 0.48(13{,}600 \text{ kip-in./ft}) \\ &= 6{,}530 \text{ kip-in./ft} \end{aligned}$$

Individual connector types need to be checked for the forces they transfer based on the force transfer mechanisms. The combination of demands for connector types needs to satisfy the interaction equation presented in the following. Only the applicable demand types for the connectors have been used to satisfy the equation in the calculations that follow.

$$\frac{T_{req}}{\phi R_T} + \frac{P_{req}}{\phi R_C} + \frac{V_{req}}{\phi R_V} + \frac{M_{req}}{\phi R_M} \le 1.0$$

(a) Faceplate Welds

The weld of the faceplate to the base plate transfers direct tension in the faceplate and the resultant tension from the force couple due to out-of-plane moment action. Because the demands are taken from finite element analysis, the tensile demand may already include the out-of-plane flexural demand. However, this check conservatively considers both the demands separately. Available resistance of the weld was obtained in Step 12.

Demand from direct tension:

$$\begin{aligned} T_{req.w.T} &= \frac{T_{req}}{2} \\ &= \frac{335 \text{ kip/ft}}{2} \\ &= 168 \text{ kip/ft} \end{aligned}$$

Demand from out-of-plane moment:

$$
\begin{aligned}
T_{req.w.M} &= \frac{M_{req.o}}{t_{sc}} \\
&= \frac{6{,}530 \text{ kip-in./ft}}{56.0 \text{ in.}} \\
&= 117 \text{ kip/ft}
\end{aligned}
$$

$$
\begin{aligned}
DCR_w &= \frac{T_{req.w.T} + T_{req.w.M}}{\left(\phi R_{n.w}/2\right)/B_{bp}} \\
&= \frac{\left(168 \text{ kip/ft} + 117 \text{ kip/ft}\right)/12 \text{ in./ft}}{\left(857 \text{ kips}/2\right)/12.0 \text{ in.}} \\
&= 0.667
\end{aligned}
$$

Therefore, the faceplate welds are adequate for the combination of demands. If the in-plane shear force transfer mechanism considers the faceplate-to-baseplate fillet welds, then the interaction DCR_w needs to include that contribution as well.

(b) Steel Headed Stud Anchors

The stud anchors are located at the top of the base plate. The anchors transfer the out-of-plane and in-plane shear forces to the base plate. Available strength of the steel headed studs was obtained in Step 12.

In-plane shear:

$$
\begin{aligned}
V_{req.an.is} &= \frac{V_{req.is}}{\#\text{ studs}} \\
&= \frac{216 \text{ kip/ft}}{42 \text{ studs}} \\
&= 5.14 \text{ kip/ft}
\end{aligned}
$$

Out-of-plane shear:

$$
\begin{aligned}
V_{req.an.os} &= \frac{V_{req.os}}{\#\text{ studs}} \\
&= \frac{104 \text{ kip/ft}}{42 \text{ studs}} \\
&= 2.48 \text{ kip/ft}
\end{aligned}
$$

Resultant shear:

$$
\begin{aligned}
V_{req.an} &= \sqrt{V_{req.an.is}^2 + V_{req.an.os}^2} \\
&= \sqrt{\left(5.14 \text{ kip/ft}\right)^2 + \left(2.48 \text{ kip/ft}\right)^2} \\
&= 5.71 \text{ kip/ft}
\end{aligned}
$$

$$
\begin{aligned}
DCR_{an} &= \frac{V_{req.an}}{\left(\phi_v Q_{nv}\right)/B_{bp}} \\
&= \frac{\left(5.71 \text{ kip/ft}/12 \text{ in./ft}\right)}{\left(18.7 \text{ kips}/12.0 \text{ in.}\right)} \\
&= 0.305 < 1.0
\end{aligned}
$$

Therefore, the steel headed stud anchors are adequate for the combination of demands.

(c) Coupled Bars

The coupled bars are located at the bottom of the base plate. These bars are subject to shear demand due to in-plane shear and out-of-plane shear, tensile demands from direct tension and from the force couple due to out-of-plane moment. The available strength of the coupled bars was obtained in Step 12.

In-plane shear:

$$\begin{aligned}V_{req.cb.is} &= \frac{V_{req.is}}{N_c}\\ &= \frac{216\text{ kip/ft}}{8}\\ &= 27.0\text{ kip/ft}\end{aligned}$$

Out-of-plane shear:

$$\begin{aligned}V_{req.cb.os} &= \frac{V_{req.os}}{N_c}\\ &= \frac{104\text{ kip/ft}}{8}\\ &= 13.0\text{ kip/ft}\end{aligned}$$

Resultant shear:

$$\begin{aligned}V_{req.cb} &= \sqrt{V_{req.cb.is}^2 + V_{req.cb.os}^2}\\ &= \sqrt{(27.0\text{ kip/ft})^2 + (13.0\text{ kip/ft})^2}\\ &= 30.0\text{ kip/ft}\end{aligned}$$

Direct tension:

$$\begin{aligned}T_{req.cb.T} &= \frac{T_{req}}{N_c}\\ &= \frac{335\text{ kip/ft}}{8}\\ &= 41.9\text{ kip/ft}\end{aligned}$$

Tension from out-of-plane flexure:

$$\begin{aligned}T_{req.cb.M} &= \frac{M_{req.o}}{t_{sc}\left(\dfrac{N_c}{2}\right)}\\ &= \frac{6{,}530\text{ kip-in./ft}}{(56.0\text{ in.})\left(\dfrac{8}{2}\right)}\\ &= 29.2\text{ kip/ft}\end{aligned}$$

The interaction will be considered based on ACI 349, Section D.7:

Design shear strength of the bars	$\phi V_n = 1{,}040$ kips
Design tensile strength of the bars	$\phi R_{n.an} = 217$ kips

Because the tensile demand is greater than 0.2 times the available tensile strength, the interaction needs to be considered.

$$\begin{aligned}DCR_{cb} &= \frac{T_{req.cb.T} + T_{req.cb.M}}{\phi R_{n.an}} + \frac{V_{req.cb}}{\phi V_n}\\ &= \frac{41.9\text{ kip/ft} + 29.2\text{ kip/ft}}{217\text{ kips}} + \frac{30.0\text{ kip/ft}}{1{,}040\text{ kips}}\\ &= 0.356\end{aligned}$$

Because the interaction ratio is less than 1.2, the coupled bars are adequate for the interaction of demands.

(d) Base Plate

The base plate is subject to moments due to direct tension as well as tension from out-of-plane moment. The cantilever moment due to the bearing reaction resulting in compression forces is also considered. The available strength of the base plate was obtained in Step 12.

Direct tension:

$$
\begin{aligned}
T_{req.bp.T} &= \frac{T_{req}}{2} \\
&= \frac{335\text{ kip/ft}}{2} \\
&= 168\text{ kip/ft}
\end{aligned}
$$

Tension from out-of-plane flexure:

$$
\begin{aligned}
T_{req.bp.M} &= \frac{M_{req.o}}{t_{sc}} \\
&= \frac{6{,}530\text{ kip-in./ft}}{56.0\text{ in.}} \\
&= 117\text{ kip/ft}
\end{aligned}
$$

Moment due to direct tension:

$$
\begin{aligned}
M_{req.bp.T} &= \frac{T_{req.bp.T} S_{an}}{4} \\
&= \frac{(168\text{ kip/ft})(8.50\text{ in.})}{4} \\
&= 356\text{ kip-in./ft}
\end{aligned}
$$

Moment from tension due to out-of-plane flexure:

$$
\begin{aligned}
M_{req.bp.M} &= \frac{T_{req.bp.M} S_{an}}{4} \\
&= \frac{(117\text{ kip/ft})(8.50\text{ in.})}{4} \\
&= 248\text{ kip-in./ft}
\end{aligned}
$$

Bearing pressure due to compression:

$$
\begin{aligned}
q_{req.bp} &= \frac{P_{req}}{B_{bp} N_{bp}} \\
&= \frac{804\text{ kip/ft}}{(12.0\text{ in.})(78.0\text{ in.})} \\
&= 0.859\text{ ksi/ft}
\end{aligned}
$$

Moment due to bearing:

$$
\begin{aligned}
M_{req.bp.C} &= \frac{q_{req.bp} B_{bp} l_{can}^2}{2} \\
&= \frac{(0.859\text{ ksi/ft})(12.0\text{ in.})(12.4\text{ in.})^2}{2} \\
&= 792\text{ kip-in./ft}
\end{aligned}
$$

The greater of the tension and compression moments is considered and added to the moment due to out-of-plane flexure.

$$
\begin{aligned}
DCR_{bp} &= \frac{\max\left(M_{req.bp.T}, M_{req.bp.C}\right) + M_{req.bp.M}}{\phi M_{bp}} \\
&= \frac{\max\left(356\text{ kip-in./ft},\ 729\text{ kip-in./ft}\right) + 248\text{ kip-in./ft}}{1{,}220\text{ kip-in./ft}} \\
&= 0.855 < 1.0
\end{aligned}
$$

Therefore, the base plate is adequate for the combination of demands.

The resulting compression force due to out-of-plane flexure is an order of magnitude less than the direct compression demand from the SC wall. Therefore, the base plate area provided considering compression bearing due to combination of demands is adequate.

Step 14. Connection Detailing

Connection detailing based on the design of the connection in Steps 12 and 13 is presented in Figure A-20.

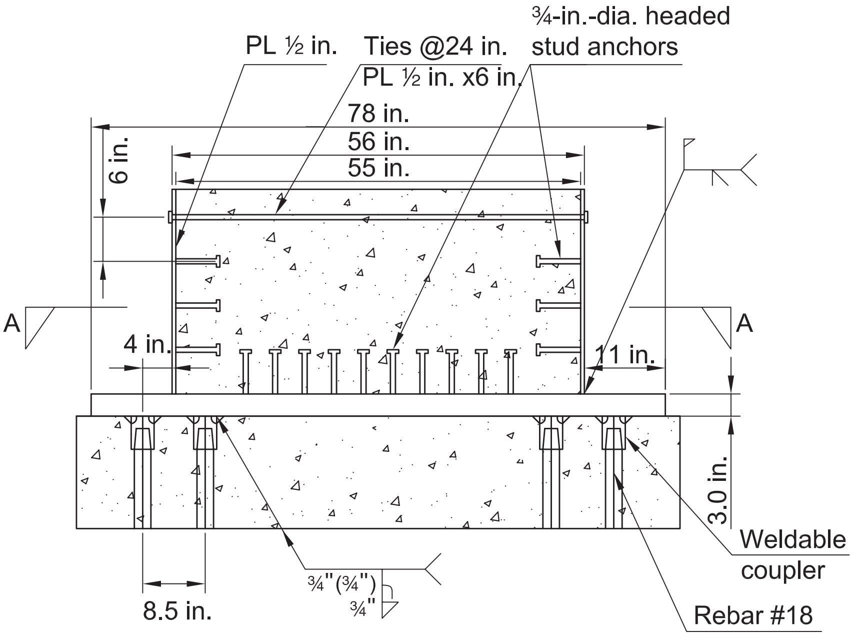

¾-in.-dia. headed
stud anchors
PL ½ in.
Ties @24 in.
PL ½ in. x6 in.
78 in.
56 in.
55 in.
6 in.
A
A
4 in.
11 in.
3.0 in.
Weldable
coupler
Rebar #18
8.5 in.
¾"(¾")
¾"

(a) Connection profile

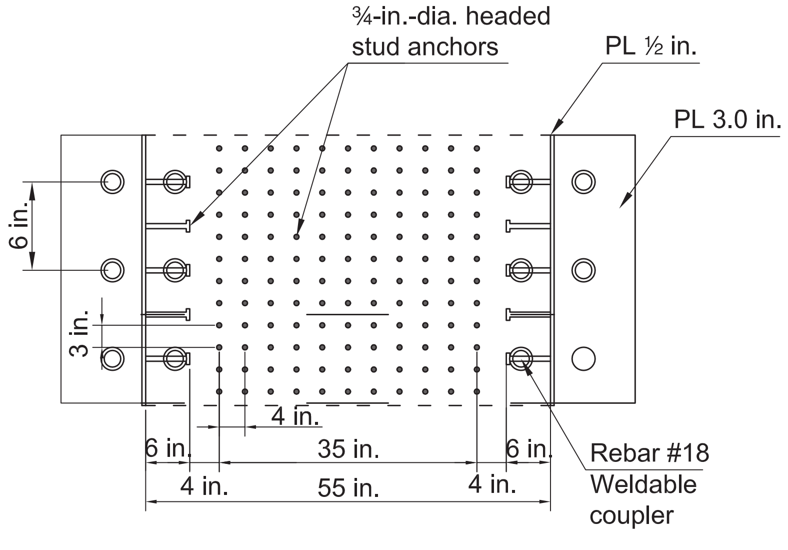

¾-in.-dia. headed
stud anchors
PL ½ in.
PL 3.0 in.
6 in.
3 in.
4 in.
6 in.
35 in.
6 in.
4 in.
55 in.
4 in.
Rebar #18
Weldable
coupler

(b) Section A-A

Fig. A-20 SC wall-to-basemat connection detailing.

Step 15. Design Optimization

This example presents the design of a sample SC wall. The intent was to illustrate the application of the provisions of AISC N690. Design optimization was not the focus of this example; however, it should be an important consideration for all projects. Some of the steps listed below can be considered for optimizing the design.

(a) The shear reinforcement for the SC wall can be optimized. Currently the tie area is 3 in.^{2} The tie area can be optimized to 2.5 in.^{2} The tie dimensions (0.5-in. × 6-in. flat bars) can be optimized to provide better welding between the tie and the faceplates. Reducing the out-of-plane shear reinforcement will reduce the available out-of-shear strength, which currently governs the stud spacing, as shown in Step 7(e). After optimizing the tie area to 2.5 in.^{2}, the steel headed stud anchor spacing can be optimized to 8 in. from 6 in. currently. The interaction check for out-of-plane shear demands and interfacial demands, as shown in Step 8, currently does not consider the interfacial shear contribution of the ties. This contribution of the ties can be included, but experimental studies would be needed to determine the interfacial shear strength of the ties. This would provide an additional margin of safety in the DCR calculation for interaction of demands.

(b) The current design does not satisfy the interaction requirement for in-plane forces and out-of-plane moments. However, the design example does not consider averaging of the demands. The required strengths are determined for individual elements—here for an element size of 24 in. AISC N690 permits averaging of demands for ductile limit states for panel sections up to $2t_{sc}$—112 in. for this example—for interior regions and t_{sc} for connection regions. The averaging of demands can be performed based on project documents. This averaging of demands will reduce the DCRs for individual demands and for a combination of demands.

SYMBOLS

A_{an}	Gross area of each anchor, in.^{2} (mm^2)
$A_{an.tot}$	Total anchor area, in.^{2} (mm^2)
$A_{BP.req}$	Area of base plate required, in.^{2} (mm^2)
$A_{BP.sum}$	Area of base plate provided, in.^{2} (mm^2)
A_c	Area of concrete infill per unit width, in.^{2}/ft (mm^2/m)
$A_{e.w}$	Area of weld resisting tensile force, in.^{2} (mm^2)
$A_{e.w.anc}$	Area of coupler weld, in.^{2} (mm^2)
A_s	Gross area of faceplates per unit width, in.^{2}/ft (mm^2/m)
A_s^F	Gross cross-sectional area of faceplates in tension due to flexure per unit width, in.^{2}/ft (mm^2/m)
A_{tie}	Area of ties, in.^{2} (mm^2)
B_{bp}	Base plate unit width, in. (mm)
B_{rc}	Length of Lenton weldable coupler for #18 rebar, in. (mm)
D_{rc}	Bottom diameter of Lenton weldable coupler for #18 rebar, in. (mm)
D_s	Displacement due to static loads, in. (mm)
D_y	Effective yield displacement, in. (mm)
DCR	Demand capacity ratio
DCR_{an}	Demand capacity ratio for steel headed stud anchors
DCR_{cb}	Demand capacity ratio for coupled bars
DCR_{bp}	Demand capacity ratio for base plate
DCR_{NH1}	Demand capacity ratio for notional half 1
DCR_{NH2}	Demand capacity ratio for notional half 2
DCR_{ops}	Demand capacity ratio for out-of-plane shear
DCR_w	Demand capacity ratio for faceplate weld
$(EI)_{cr\text{-}tr}$	Flexural stiffness per unit width
E_s	Modulus of elasticity of steel
	= 29,000 ksi (200 000 MPa) for carbon steel
	= 28,000 ksi (193 000 MPa) for stainless steel
E_m	Model elastic modulus, ksi
$E_{m.acc}$	Model elastic modulus for accident thermal condition, ksi
$E_{m.op}$	Model elastic modulus for operating thermal condition, ksi
EI_{eff}	Effective flexural stiffness for analysis of SC walls per unit width, kip-in.^{2}/ft (N-mm^2/m)
$EI_{eff.acc}$	Effective flexural stiffness per unit width for accident thermal condition, kip-in.^{2}/ft (N-mm^2/m)
$EI_{eff.buck}$	Effective stiffness for buckling evaluation of SC walls per unit width, kip-in.^{2}/ft (N-mm^2/m)
$EI_{eff.op}$	Effective flexural stiffness per unit width for operating thermal condition, kip-in.^{2}/ft (N-mm^2/m)
F_{EXX}	Filler metal classification strength, ksi (MPa)
F_{ny}	Nominal yield strength of the tie, kips (N)
F_{nr}	Nominal rupture strength of tie or nominal strength of associated connection, whichever is smaller, kips (N)
F_{req}	Required tensile strength for individual ties, kips (N)
F_{req}^n	Tie force required to resist the overturning moments, kips (N)
F_{steel}	Compression force carried in faceplate normalized with respect to its yield strength, kips (N)
F_t	Nominal tensile strength of ties, kips (N)
F_u	Specified minimum tensile stress, ksi (MPa)
$F_{u.an}$	Specified minimum tensile strength of anchors, ksi (MPa)
$F_{u.sc}$	Specified minimum tensile strength of shear connector, ksi (MPa)
F_y	Steel minimum yield stress, ksi (MPa)
$F_{y.an}$	Specified minimum yield strength of anchors, ksi (MPa)
G	Shear modulus of elasticity of steel = 11,200 ksi (77 200 MPa) for carbon steel = 10,800 ksi (74 500 MPa) for stainless steel
GA_{eff}	Effective in-plane shear stiffness per unit width, kip/ft (N/m)
GA_{uncr}	In-plane shear stiffness of uncracked composite SC panel section per unit width, kip/ft (N/m)
G_c	Shear modulus of concrete, ksi (MPa)
G_{rc}	Top diameter of Lenton weldable coupler for #18 rebar, in. (mm)

I_c	Moment of inertia of concrete infill per unit width, in.^{4}/ft (mm^4/m)
I_s	Moment of inertia of faceplates per unit width (corresponding to the condition when concrete is fully cracked), in.^{4}/ft (mm^4/m)
K_c	Stiffness of concrete
K_s	Stiffness of steel
K_{xy}^{cr}	Cracked stiffness
K_{xy}^{sec}	Secant stiffness
K_{xy}^{uncr}	Uncracked stiffness
L_{anc}	Total length of coupler welds, in. (mm)
L_d	Development length, in. (mm)
L_{TR}	Transfer length, in. (mm)
L_v	Length of shear span, in. (mm)
M	Out-of-plane bending moment, kip-in. (N-mm)
M_{bp}	Nominal base plate flexural resistance, kip-in. (N-mm)
M_n	Nominal flexural strength per unit width, kip-in./ft (N-mm/m)
M_o	Eccentric moment, kip-in. (N-mm)
M_{op}	Out-of-plane moment, kip-in./ft (N-mm/m)
M_p^{exp-c}	Expected plastic flexural strength of continuous SC wall, kip-in./ft (N-mm/m)
M_p^{exp-dc}	Expected out-of-plane flexural strength of discontinuous SC wall, kip-in./ft (N-mm/m)
M_R	Resisting moment, kip-in. (N-mm)
$M_{req.o}$	Out-of-plane flexural demand for SC wall-to-basemat connection, kip-in./ft (N-mm/m)
$M_{req.bp.C}$	Moment on base plate due to bearing, kip-in./ft (N-mm/m)
$M_{req.bp.M}$	Moment on base plate due to out-of-plane flexural tension, kip-in./ft (N-mm/m)
$M_{req.bp.T}$	Moment on base plate due to direct tension, kip-in./ft (N-mm/m)
$M_{r\text{-}th}$	Theoretical maximum out-of-plane moment per unit width induced due to thermal gradient, kip-in./ft (N-mm/m)
M_{rx},M_{ry}	Required out-of-plane flexural strength per unit width, kip-in./ft (N-m/m)
M_{rxy}	Required twisting moment strength per unit width, kip-in./ft (N-mm/m)
$M_{t.bp}$	Moment in base plate due to tension, kip-in. (N-mm)
M_{th}	Thermal moment, kip-in. (N-mm)
M_u	Out-of-plane bending moment, kip-in. (N-mm)
N_{anc}	Number of anchors needed per faceplate per foot
N_{bp}	Length of base plate, in. (mm)
$N_{bp.ex}$	Required base plate extension, in. (mm)
$N_{bp.req}$	Required width of base plate based on upper limit of shear friction from ACI 349, in. (mm)
N_r	Required membrane axial force, kips (N)
N_r	Maximum axial tension that can be transferred through the joint, kips (N)
$N_{SC.c}$	Required number of anchors per foot at SC wall-to-basemat connection
N_u	Membrane axial force, kips (N)
P_{ci}	Available compressive strength per unit width for each notional half of SC panel section, kip/ft (N/m)
P_e	Elastic critical buckling load per unit width, kip/ft (N/m)
$P_{n\,.com}$	Nominal compressive strength per unit width, kip/ft (N/m)
P_{no}	Nominal compressive strength per unit width, kip/ft (N/m)
$P_{n\,.ten}$	Nominal tensile strength per unit width, kip/ft (N/m)
P_{req}	Compression demand for SC wall-to-basemat connection, kip/ft (N/m)
Q_{cv}	Available shear strength of steel anchor, kips (N)
Q_{cv}^{avg}	Weighted average of available interfacial shear strength of ties and steel anchors while accounting for their respective tributary areas and numbers, kips (N)
Q_{cv}^{tie}	Available interfacial shear strength of tie, kips (N)
$R_{n.w}$	Nominal weld strength, kips (N)
$R_{n.w.anc}$	Nominal coupler weld strength, kips (N)
R_u	Total required strength, kips (N)
S_{an}	Transverse spacing of rebar anchors, in. (mm)
S_{cr}	In-plane shear force per unit width at concrete cracking threshold, kip/ft (N/m)

$S_{r.c.con}$	Required uniaxial compression strength at SC wall-to-basemat connection, kip/ft (N/m)
$S_{r.flex.con}$	Required out-of-plane flexural strength at SC wall-to-basemat connection, kip-in./ft (N-mm/m)
$S_{r.is.con}$	In-plane shear force at SC wall-to-basemat connection, kip/ft (N/m)
$S_{r,max}$	Maximum required principal in-plane strength per unit width for notional half of SC panel section, kip/ft (N/m)
$S_{r,min}$	Minimum required principal in-plane strength per unit width for notional half of SC panel section, kip/ft (N/m)
$S_{r.t.con}$	Required uniaxial tensile strength at SC wall-to-basemat connection, kip/ft (N/m)
$S_{r.vi.con}$	Required in-plane shear strength at SC wall-to-basemat connection, kip/ft (N/m)
$S_{r.vo.con}$	Required out-of-plane shear strength at SC wall-to-basemat connection, kip/ft (N/m)
S_{rx}	Required membrane axial strength per unit width in direction x, kip/ft (N/m)
S_{ry}	Required membrane axial strength per unit width in direction y, kip/ft (N/m)
S_{rxy}	Required membrane in-plane shear strength per unit width, kip/ft (N/m)
$S_{rxy.as}$	Required average membrane in-plane shear strength per unit width, kip/ft (N/m)
S'_{rx}	Required membrane axial strength per unit width in direction x for each notional half of SC panel section, kip/ft (N/m)
S'_{ry}	Required membrane axial strength per unit width in direction y for each notional half of SC panel section, kip/ft (N/m)
S'_{rxy}	Required membrane in-plane shear strength per unit width for each notional half of SC panel section, kip/ft (N/m)
T_{amb}	Ambient temperature, ºF (ºC)
$T_{anc.T}$	Tensile force per rebar, kips (N)
T_{ci}	Available tensile strength per unit width for each notional half of SC panel section, kip/ft (N/m)
T_{Mop}	Tensile demand due to out-of-plane moment, kip/ft (N/mm)
T_{ni}	Nominal tensile strength per unit width for each notional half of SC panel section, kip/ft (N/m)
T_{op}	Operating temperature, °F (°C)
T_{req}	Tensile demand for SC wall-to-basemat connection, kip/ft (N/m)
$T_{req.bp.T}$	Direct tensile demand on base plate, kip/ft (N/m)
$T_{req.bp.M}$	Tensile demand on base plate due to out-of-plane moment, kip/ft (N/m)
$T_{req.cb.T}$	Direct tensile demand on coupled bars, kip/ft (N/m)
$T_{req.cb.M}$	Tensile demand on coupled bars due to out-of-plane moment, kip/ft (N/m)
$T_{req.w.M}$	Tensile demand on faceplate weld due to out-of-plane moment, kip/ft (N/m)
$T_{req.w.T}$	Direct tensile demand on faceplate weld, kip/ft (N/m)
$T_{SC.con}$	Connection design tension force, kip/ft (N/mm)
V_{exp}	Experimental out-of-plane shear strength, kips (N)
V_c	Available out-plane shear strength of SC walls, kips (N)
V	Out-plane shear strength, kips (N)
V_{anc}	Anchor shear, kips (N)
V_c	Available out-of-plane shear strengths per unit width of SC panel section in local x (V_{cx}) and y (V_{cy}) directions, kip/ft (N/m)
$V_{c\ conc}$	Available out-of-plane shear strength provided by concrete per unit width of SC panel section, kip/ft (N/m)
V_{ci}	Available in-plane shear strength per unit width for each notional half of SC panel section, kip/ft (N/m)
V_{conc}	Nominal out-of-plane shear strength provided by concrete per unit width of SC panel section, kip/ft (N/m)
V_{exp}	Experimental out-of-plane shear strength, kips (N)
V_{fr}	Friction shear under baseplate, kips (N)
V_{jnp}	In-plane shear at SC wall-to-basemat connection, kip/ft (N/mm)
V_{js}	Joint shear, kips (N)
$V_{n.ACI}$	Nominal out-of-plane shear strength calculated using ACI 349 code equations, kips (N)
$V_n^{i\text{-}exp\text{-}dc}$	Expected in-plane shear strength, kips (N)
$V_n^{o\text{-}exp\text{-}dc}$	Expected out-of-plane shear strength, kips (N)

V_{ni}	Nominal in-plane shear strength per unit width of SC panel section, kip/ft (N/m)
V_{no}	Nominal out-of-plane shear strength per unit width of SC panel section, kip/ft (N/m)
$V_{n.sf}$	Nominal shear friction strength, kips (N)
V_r^{in}	Required membrane in-plane shear force, kips (N)
V_r^{out}	Required membrane out-of-plane shear force, kips (N)
$V_{req.an}$	Resultant shear demand on steel headed stud anchor, kip/ft (N/m)
$V_{req.an.is}$	In-plane shear demand on steel headed stud anchor, kip/ft (N/m)
$V_{req.an.os}$	Out-of-plane shear demand on steel headed stud anchor, kip/ft (N/m)
$V_{req.cb}$	Resultant shear demand on coupled bars, kip/ft (N/m)
$V_{req.cb.is}$	In-plane shear demand on coupled bars, kip/ft (N/m)
$V_{req.cb.os}$	Out-of-plane shear demand on coupled bars, kip/ft (N/m)
$V_{req.is}$	In-plane shear demand at SC wall-to-basemat connection, kip/ft (N/m)
$V_{req.os}$	Out-of-plane shear demand at SC wall-to-basemat connection, kip/ft (N/m)
V_{rx}	Required out-of-plane shear strength per unit width along edge parallel to direction x, kip/ft (N/m)
V_{ry}	Required out-of-plane shear strength per unit width along edge parallel to direction y, kip/ft (N/m)
V_s	Contribution of steel shear reinforcement (ties) to nominal out-of-plane shear strength per unit width of the SC panel section , kip/ft (N/m)
V_u^{in}	Membrane in-plane shear force, kips (N)
V_u^{out}	Membrane out-of-plane shear force, kips (N)
b	Largest unsupported length of faceplate between rows of steel anchors or ties, in. (mm)
c	Distance to the neutral axis, in. (mm)
c_1	Factor used to determine spacing of steel anchors (depends on whether the steel anchor is the yielding or nonyielding type)
c_c	Specific heat of concrete, Btu/lb-°F (J/kg-°C)
c_m	Specific heat used in elastic finite element analysis of SC panel section, Btu/lb-°F (J/kg-°C)
d_{an}	Distance from anchor to faceplate, in. (mm)
d_{anc}	Anchor diameter, in. (mm)
d_{ed}	Distance from anchor to edge of base plate, in. (mm)
d_s	Shear connection diameter, in. (mm)
d_1	Distance from faceplate to edge of base plate, in. (mm)
e_c	Top plate strain
f'_c	Concrete minimum compressive strength, ksi (MPa)
f'_t	Tensile stress, ksi (MPa)
h_{wall}	Unsupported height of SC wall, ft (m)
j_x, j_y	Parameter for distributing required flexural strength into force couple acting on each notional half of SC panel section
j_{xy}	Parameter for distributing required twisting moment strength into force couple acting on each notional half of SC panel section
l	Unit width, 12 in./ft (1000 mm/m)
l_{can}	Critical base plate cantilever dimension, in. (mm)
l_s	Shear connector length, in. (mm)
n	Number of ties in transfer length region
n	Concrete-to-steel modular ratio, E_c/E_s
n_{et}	Effective number of ties contributing to a unit cell
n_{es}	Effective number of shear connectors contributing to a unit cell
$q_{req.bp}$	Bearing pressure on base plate due to compression, ksi/ft (MPa/m)
s	Spacing of steel anchors, in. (mm)
s_{tl}	Spacing of shear reinforcement along direction of one-way shear, in. (mm)
s_{tt}	Spacing of shear reinforcement transverse to direction of shear, in. (mm)
s_L	Longitudinal spacing of stud anchors, in. (mm)
s_T	Transverse spacing of stud anchors, in. (mm)
t_{bp}	Thickness of base plate for compression loading, in. (mm)
t_c	Concrete wall thickness, in. (mm)

t_m	Model thickness, in. (mm)
$t_{m.acc}$	Model thickness for accident thermal conditions, in. (mm)
$t_{m.op}$	Model thickness for operating thermal conditions, in. (mm)
t_p	Thickness of faceplate, in. (mm)
$t_{req.m}$	Required thickness of base plate due to bending moment, in. (mm)
t_{sc}	SC section thickness, in. (mm)
t_{wanc}	Effective fillet weld throat at anchor, in. (mm)
$t_{wanc.f}$	Fillet weld throat at anchor, in. (mm)
t_{we}	Fillet weld thickness, in. (mm)
ΔT_{savg}	Average of maximum surface temperature increases for faceplates due to accident thermal conditions, °F (°C)
ΔT_{sg}	Maximum temperature difference in °F (°C) between faceplates due to accident thermal conditions, °F (°C)
ψ	Constant used to determine available interfacial shear strength
α	Ratio of available in-plane shear strength to available tensile strength for each notional half of SC panel section
α_c	Thermal expansion coefficient of concrete, °F^{-1} (°C^{-1})
α_s	Thermal expansion coefficient of steel, °F^{-1} (°C^{-1})
γ_m	Material density, lb/ft^3 (kg/m^3)
$\gamma_{m.acc}$	Material density for accident thermal condition, lb/ft^3 (kg/m^3)
$\gamma_{m.op}$	Material density for operating thermal condition, lb/ft^3 (kg/m^3)
γ_s	Density of steel used for SC panel section, lb/ft^3 (kg/m^3)
ξ	Factor used to calculate shear reinforcement contribution to out-of-plane shear strength (depends on whether shear reinforcement is yielding or nonyielding type)
κ	Calibration constant for determining in-plane shear strength
ε_{cr}	Buckling strain
ε_{sh}	Shrinking strain
ε_y	Strain corresponding to yield stress
σ_{req}^{i}	Tie stress, ksi (MPa)
μ	Ductility factor
μ_{dd}	Ductility ratio demand
μ_f	Shear friction coefficient from ACI 349
ν_c	Poisson’s ratio for concrete
ν_m	Poisson’s ratio used in elastic finite element analysis of SC panel section
ρ	Reinforcement ratio
$\overline{\rho}$	Strength-adjusted reinforcement ratio
ϕ_b	Resistance factor for flexure
ϕ_{bea}	Resistance factor for direct bearing
ϕ_c	Resistance factor for compression
ϕ_S	Alternate shear strength reduction factor from ACI 349
$\phi_{S.r}$	Alternate shear strength reduction factor from AISC *Specification* Section G1
ϕ_{th}	Thermal curvature
$\phi_{t.r}$	Resistance factor for tensile rupture
$\phi_{t.y}$	Resistance factor for tensile yielding
ϕ_{vo}	Resistance factor for out-of-plane shear
ϕ_w	Resistance factor for welds

ACRONYMS AND ABBREVIATIONS

ABWR	advanced boiling water reactor
ACI	American Concrete Institute
ASCE	American Society of Civil Engineers
APR	advanced pressurized water reactor
ASME	American Society of Mechanical Engineers
AWS	American Welding Society
BDB	beyond design basis
CIS	containment internal structure
COS	Committee on Specifications
DCR	demand capacity ratio
DIF	dynamic increase factors
DOE	Department of Energy
EFE	elastic finite element
FE	finite element
HCLPF	high confidence of low probability of failure
ISRS	in-structure response spectra
KHNP	Korea Hydro Nuclear Power
LIF	load increase factor
MBM	mechanics-based model
MHI	Mitsubishi Heavy Industries
NRC	Nuclear Regulatory Commission
OBE	operating basis earthquake
PT	post-tensioned
QA	quality assurance
QC	quality control
RC	reinforced concrete
SC	steel-plate composite
SMR	small modular reactors
SRP	standard review plan
SSE	safe-shutdown earthquake
SSI	soil structure interaction
TEPCO	Tokyo Electric Power Company
WEC	Westinghouse Electric Corporation

REFERENCES

ACI (2001), *Code for Concrete Containments*, ACI 359-01, American Concrete Institute, Farmington Hills, MI.

ACI (2006), *Code Requirements for Nuclear Safety-Related Concrete Structures and Commentary,* ACI 349-06, American Concrete Institute, Farmington Hills, MI.

ACI (2008), *Building Code Requirements for Structural Concrete*, ACI 318-08 and ACI 318M-08, American Concrete Institute, Farmington Hills, MI.

ACI (2010), *Specification for Tolerances for Concrete Construction and Materials*, ACI 117-10, American Concrete Institute, Farmington Hills, MI.

Adams, P.F. and Zimmerman, T.J.E. (1987), "Design and Behavior of Composite Ice-Resisting Walls, Steel/Composite Structural Systems, C-FER Publication No. 1," *Proceedings of a Special Symposium held in Conjunction with POAC '87*, 9th International Conference on Port and Ocean Engineering under Arctic Conditions, Fairbanks, Alaska.

AISC (2010a), *Prequalified Connections for Special and Intermediate Steel Moment Frames for Seismic Applications*, ANSI/AISC 358-10, American Institute of Steel Construction, Chicago, IL.

AISC (2010b), *Specification for Structural Steel Buildings*, ANSI/AISC 360-10, American Institute of Steel Construction, Chicago, IL.

AISC (2015), *Specification for Safety-Related Steel Structures for Nuclear Facilities*, including Supplement No. 1, ANSI/AISC N690-12 and ANSI/AISC N690s1-15, American Institute of Steel Construction, Chicago, IL.

AISC (2016a), *Code of Standard Practice for Steel Buildings and Bridges,* ANSI/AISC 303-16, American Institute of Steel Construction, Chicago, IL.

AISC (2016b), *Seismic Provisions for Structural Steel Buildings*, ANSI/AISC 341-16, American Institute of Steel Construction, Chicago, IL.

Akiyama, H., Sekimoto, H., Tanaka, M., Inoue, K., Fukihara, M. and Okuta, Y. (1989), "1/l0th Scale Model Test of Inner Concrete Structure Composed of Concrete Filled Steel Bearing Wall," *Transactions of the 10th International Conference on Structural Mechanics in Reactor Technology*, *SMiRT-10*, IASMIRT, Div. H03, North Carolina State University, Raleigh, NC.

Akiyama, H. and Sekimoto, H. (1991), "A Compression and Shear Loading Tests of Concrete Filled Steel Bearing Wall," *Transaction of the 11th Structural Mechanics in Reactor Technology*, *SMiRT-11*, IASMIRT, Div. H03, North Carolina State University, Raleigh, NC, pp. 323–328.

ASCE (1980), *Structural Analysis and Design of Nuclear Plant Facilities Manual*, Report No. 58, American Society of Civil Engineers, Committee on Nuclear Structures and Materials, Reston, VA.

ASCE (1998), *Seismic Analysis of Safety-Related Nuclear Structures,* ASCE 4-98, American Society of Civil Engineers, Reston, VA.

ASCE (2013), *Seismic Rehabilitation of Existing Buildings*, ASCE/SEI 41-13, American Society of Civil Engineers, Reston, VA.

ASME (2013), *Boiler and Pressure Vessel Code,* American Society of Mechanical Engineers, New York, NY.

AWS (2007), *Structural Welding Code—Stainless Steel,* AWS D1.6/D1.6M, American Welding Society, Miami, FL.

AWS (2010), *Structural Welding Code—Steel*, AWS D1.1/D1.1M, American Welding Society, Miami, FL.

Bhardwaj, S.R., Kurt, E.G., Terranova, B., Varma, A.H., Whittaker, A.S. and Orbovic, N. (2015a), "Preliminary Investigation of the Effects of Out-of-Plane Loading on the In-Plane Behavior of SC Walls," *Transactions of the 23rd Structural Mechanics in Reactor Technology*, *SMiRT-23,* Paper ID 712, Manchester, UK, IASMIRT, North Carolina State University, Raleigh, NC, pp. 1–10.

Bhardwaj, S.R., Varma, A.H. and Al-Shawaf, T. (2015b), "Outline of Specification for Composite SC Walls in Nuclear Facilities," *Proceedings of the SEI Structures Congress*, ASCE, Portland, OR, pp. 1,021–1,031.

Bhardwaj, S.R. and Varma, A.H. (2016), "Effect of Imperfections on the Compression Behavior of SC Walls," *Proceedings of the Annual Stability Conference*, Structural Stability Research Council, Orlando, FL, April 12–15.

Bhardwaj, S.R., Varma, A.H. and Malushte, S.R. (2017), "Minimum Requirements and Section Detailing Provisions for Steel-Plate Composite (SC) Walls in Nuclear Power Plants," *Engineering Journal*, AISC, Vol. 54, No. 2.

Biggs, J. (1964), *Introduction to Structural Dynamics*, McGraw-Hill, Inc., New York, NY.

Booth, P.N., Varma, A.H., Malushte, S.R. and Johnson, W.H. (2007), "Response of Modular Composite Walls to Combined Thermal & Mechanical Loads," *Transactions of the 19th International Association for Structural Mechanics in Reactor Technology Conference, SMiRT-19*, Paper No. H01/4, Toronto, Canada, IASMIRT, North Carolina State University, Raleigh, NC, pp. 1–10.

Booth, P.N., Varma, A.H. and Mitsubishi Heavy Industries Ltd. (2013), "Seismic Behavior and Design of Primary Shield Structure Consisting of SC Walls," *Transactions of the 22nd International Conference on Structural Mechanics in Reactor Technology, SMiRT-22*, San Francisco, CA, IASMIRT, North Carolina State University, Raleigh, NC, pp. 1–10.

Booth, P.N., Varma, A.H., Sener, K. and Malushte, S. (2015a), "Flexural Behavior and Design of Steel-Plate Composite (SC) Walls for Accident Thermal Loading," *Nuclear Engineering and Design*, Vol. 295, pp. 817–828.

Booth, P.N., Varma, A.H., Sener, K. and Mori., K. (2015b), "Seismic Behavior and Design of a Primary Shield Structure Consisting of Steel-Plate Composite (SC) Walls," *Nuclear Engineering and Design*, Vol. 295, pp. 829–842.

Booth, P., Varma, A.H. and Seo, J. (2015c), "Lateral Load Capacity of Steel Plate Composite Wall Structures," *Transactions of the 23rd International Conference on Structural Mechanics in Reactor Technology*, *SMiRT-23*, Paper ID 791, Manchester, UK, IASMIRT, North Carolina State University, Raleigh, NC, pp. 1–10.

Børvik, T., Forrestal, M.J., Hopperstad, O.S., Warren, T.L. and Langseth, M. (2009), "Perforation of AA5083-H116 Aluminum Plates with Conical-Nose Steel Projectiles—Calculations," *International Journal of Impact Engineering*, Vol. 36, No. 3, pp. 426–437.

Bruhl, J.C. and Varma, A.H. (2015), "Summary of Blast Tests on Steel-Plate Reinforced Concrete Walls," *Proceedings of the SEI Structures Congress*, ASCE, Portland, OR, pp. 151–159.

Bruhl, J.C. and Varma, A.H. (2016), "Experimentally-Validated Analysis Methods for Steel-Plate Composite Walls Subjected to Blast and Impact Loads*," Proceedings of the Geotechnical and SEI Congress*, ASCE, Phoenix, AZ, pp. 25–34.

Bruhl, J.C., Varma, A.H. and Johnson, W.H. (2015a), "Design of Composite SC Walls to Prevent Perforation from Missile Impact," *International Journal of Impact Engineering,* Vol. 75, pp. 75–87.

Bruhl, J.C., Varma, A.H. and Kim, J.M. (2015b), "Static Resistance Function for Steel-Plate Composite (SC) Walls Subjected to Impactive Loading," *Nuclear Engineering and Design*, Vol. 295, pp. 843–859.

CEN (2009), *Eurocode 4: Design of Composite Steel and Concrete Structures*, Comite Européen de Normalisation, Brussels, Belgium.

Choi, B.J. and Han, H.S. (2009), "An Experiment on Compressive Profile of the Unstiffened Steel Plate-Concrete Structures under Compression Loading," *Steel and Composite Structures*, Vol. 9, No. 6, pp. 519–534.

Dai, X.X. and Liew, J.Y.R. (2006), "Steel-Concrete-Steel Sandwich System for Ship Hull Construction," *Proceedings of the International Colloquium on Stability and Ductility of Steel Structures,* Lisbon, Portugal, pp. 877–884.

Darwin, D. (1990), *Design of Steel and Composite Beams with Web Openings*, Design Guide 2, AISC, Chicago, IL.

DCD (2011), Design Control Document for the AP1000, *U.S. Nuclear Regulatory Commission*, Washington, DC.

DOE (2006), "Accident Analysis for Aircraft Crash into Hazardous Facilities," *DOE-STD-3014*, U.S. Department of Energy, Washington, DC.

Epackachi, S., Nguyen, N., Kurt, E., Whittaker, A. and Varma, A. (2015), "In-Plane Seismic Behavior of Rectangular Steel-Plate Composite Wall Piers," *Journal of Structural Engineering*, ASCE, Vol. 141, No. 7.

Fisher, J.M. and Kloiber, L.A. (2006), *Base Plate and Anchor Rod Design,* Design Guide 1, 2nd Ed., AISC, Chicago, IL.

Hong, S. and Varma, A.H. (2009), "Analytical Modeling of the Standard Fire Behavior of Loaded CFT Columns," *Journal of Constructional Steel Research*, Vol. 65, pp. 54–69.

Hong, S., Kim, W., Lee, K., Hong, N.K. and Lee, D. (2009), "Out-of-Plane Shear Strength of Steel Plate Concrete Walls Dependent on Bond Behavior," *Transactions of the 20th International Conference on Structural Mechanics in Reactor Technology, SMiRT-20*, Div-6: Paper 1,855, Espoo, Finland, IASMIRT, North Carolina State University, Raleigh, NC, pp. 1–10.

JEAG (2005), *Technical Guidelines for Seismic Design of Nuclear Power Plants*, JEA (Japan Electric Association), JEAG 4601, Japan.

Kanchi, M. (1996), "Experimental Study on a Concrete Filled Steel Structure: Part 2 Compressive Tests (1)," *Summary of Technical Papers of Annual Meeting*, Architectural Institute of Japan*,* Structures, pp. 1,071–1,072.

Kato, M., Watanabe, Y., Takeda, T., Yamaguchi, T., Ito, M. and Furuya, N. (1987), "Horizontal Loading Tests on 1/10 Scale Model of Inner Concrete Structure for PWR-Type Nuclear Power Plant," *Transactions of the 9th International Conference on Structural Mechanics in Reactor Technology*, *SMiRT-9*, IASMIRT, North Carolina State University, Raleigh, NC, pp. 133–142.

Kim, W.B. and Kim, W.K. (2008), "Status and Background in Developing SC Structure Specifications for Nuclear Power Plants," *Journal of the Korean Society of Steel Construction* (in Korean), Vol. 20, No. 2, pp. 9–13.

KSSC (2010), *Specification for Safety-Related Steel Plate Concrete Structures for Nuclear Facilities*, KEPIC-SNG, Board of KEPIC Policy, Structural Committee, Korea Electric Association.

Kurt, E.G., Varma, A.H., Booth, P.N. and Whittaker, A. (2016a), "In-plane Behavior and Design of Rectangular SC Wall Piers Without Boundary Elements," *Journal of Structural Engineering*, ASCE, Vol. 142, No. 6.

Kurt, E.G., Varma, A.H. and Sohn, Y.M. (2016b), "Direct Shear Strength of Reinforcement Bar-Coupler Anchor Systems for Steel-Plate Composite (SC) Walls," *International Journal of Steel Structures*, Vol. 16, No. 4, pp. 1,397–1,409.

Lee, U.W., Kim, K.K., Mun, T.Y. and Sun, W.S. (2008), "Nuclear Power Plant Construction and SC Structures," *Journal of the Korean Society of Steel Construction* (in Korean), Vol. 20, No. 2.

Lee, S.J., Choi, B.J. and Kim, T.K. (2009), "An Experimental Study on the Behavior of Steel Plate Concrete Wall with Vertical Ribs," *Journal of the Korean Society of Steel Construction* (in Korean), Vol. 21, No. 3, pp. 277–287.

Leng, Y.-B., Song, X.-B., Chu, M. and Ge, H.-H. (2015a), "Experimental Study and Theoretical Analysis of Resistance of Steel-Concrete-Steel Sandwich Beams," *Journal of Structural Engineering,* ASCE, Vol. 141, No. 2.

Leng, Y.-B., Song, X.-B. and Wang, H.-L. (2015b), "Failure Mechanism and Shear Strength of Steel-Concrete-Steel Sandwich Deep Beams," *Journal of Constructional Steel Research*, Vol. 106, pp. 89–98.

Malushte, S.R. and Varma, A.H. (2015), "Rethinking Steel-Plate Composite (SC) Construction for Improved Sustainability and Resiliency of Nuclear Power Plants," *Nuclear Power International*, Vol. 8, Issue 4.

Mizuno, J., Tanaka, E., Nishimura, I., Koshika, N., Suzuki, A. and Mihara, Y. (2005), "Investigation on Impact Resistance of Steel Plate Reinforced Concrete Barriers Against Aircraft Impact Part 3: Analyses of Full-Scale Aircraft Impact," *Transactions of the 18th International Conference on Structural Mechanics in Reactor Technology, SMiRT-18*, Beijing, China, IASMIRT, North Carolina State University, Raleigh, NC, pp. 2,591–2,603.

Moon, I.H., Kim, S.M., Kim, W.B. and Kim, W.K. (2007), "The Use of Steel Plate Concrete for Structural Module of NPP Structures," *Journal of the Korean Society of Steel Construction* (in Korean), Vol. 19, No. 2, pp 740–745.

Moon, I.H., Kim, T.Y. and You, S.T. (2008), "Nuclear Power Plant Structure and SC Structure Design," *Journal of the Korean Society of Steel Construction* (in Korean), Vol. 20, No. 2, pp. 14–23.

Narayanan, R., Wright, H.D., Evans, H.R. and Francis, R.W. (1987), "Double-Skin Composite Construction for Submerged Tube Tunnels," *Steel Construction Today*, Vol. 2, pp. 185–189.

NRC (2001), "Safety-Related Concrete Structures for Nuclear Power Plants (Other than Reactor Vessels and Containments)," *Regulatory Guide 1.142, Revision 2*, U.S. Nuclear Regulatory Commission, Washington, DC.

NRC (2007), "Barrier Design Procedures," Standard Review Plan 3.5.3, *Report NUREG-0800, Revision 3,* U.S. Nuclear Regulatory Commission, Washington, DC.

NRC (2011), "Methodology for Performing Aircraft Impact Assessments for New Plant Designs," *NEI 07-13, Revision 8P,* U.S. Nuclear Regulatory Commission, Washington, DC.

Ollgaard, J.G., Slutter, R.G. and Fisher, J.W. (1971), "Shear Strength of Stud Shear Connections in Lightweight and Normal Weight Concrete," *Engineering Journal*, AISC, Vol. 8, No. 2, pp. 55–64.

Ozaki, M., Akita, S., Takeuchi, M., Oosuga, H., Nakayama, T. and Niwa, H. (2000), "Experimental Study on Steel-Plate-Reinforced Concrete Structure Part 41: Heating Tests (Outline of Experimental Program and Results)," *Annual Conference of Architectural Institute of Japan*, Part 41-43, pp. 1,127–1,132.

Ozaki, M., Akita, S., Niwa, N., Matsuo, I. and Usami, S. (2001), "Study on Steel Plate Reinforced Concrete Bearing Wall for Nuclear Power Plants Part 1: Shear and Bending Loading Tests of SC Walls," *Transactions of the 16th International Conference on Structural Mechanics in Reactor Technology, SMiRT-16*, Washington, DC, Paper ID 1554, IASMART, North Carolina State University, Raleigh, NC.

Ozaki, M., Akita, S., Oosuga, H., Nakayama, T. and Adachi, N. (2004), "Study on Steel Plate Reinforced Concrete Panels Subjected to Cyclic In-Plane Shear," *Nuclear Engineering and Design*, Vol. 228, pp. 225–244.

Ravindra, M.K. and Galambos, T.V. (1978), "Load and Resistance Factor Design for Steel," *Journal of the Structural Division*, ASCE, Vol. 104, No. ST9, pp. 1,337–1,353.

Schlaseman, S. and Russell, J. (2004), "Application of Advanced Construction Technologies to New Nuclear Power Plants," Prepared Report for U.S. Department of Energy, under contract for DE-AT01-02NE23476, *Report MPR-2610*, *Revision 2*.

Selden, K., Varma, A.H. and Mujagic, J. (2015), "Consideration of Shear Stud Slip in the Design of Partially Composite Beams," *Proceedings of the SEI Structures Congress*, ASCE, Portland, OR, pp. 889–899.

Sener, K.C. and Varma, A.H. (2014), "Steel-Plate Composite Walls: Experimental Database and Design for Out-of-Plane Shear," *Journal of Constructional Steel Research*, Vol. 100, pp. 197–210.

Sener, K.C., Varma, A.H., Booth, P.N. and Fujimoto, R. (2015a), “Seismic Behavior of a Containment Internal Structure Consisting of Composite SC Walls,” *Nuclear Engineering and Design*, Vol. 295, pp. 804–816.

Sener K.C., Varma, A.H. and Deniz, A. (2015b), “Steel-Plate Composite SC Walls: Out-of-Plane Flexural Behavior, Database and Design,” *Journal of Constructional Steel Research*, Vol. 108, pp. 46–59.

Sener, K.C., Varma, A.H. and Seo, J. (2016), “Experimental and Numerical Investigation of the Shear Behavior of Steel-Plate Composite (SC) Beams without Shear Reinforcement,” *Engineering Structures*, Vol. 127, pp. 495–509.

Seo, J., Varma, A.H. and Winkler, D. (2013), “Preliminary Investigations of the Joint Shear Strength of SC Wall-to-Wall T-Joints,” *Transactions of the 22nd International Association for Structural Mechanics in Reactor Technology Conference, SMiRT-22*, San Francisco, CA, IASMART, North Carolina State University, Raleigh, NC, pp. 1–10.

Seo, J. (2014), “Design of Steel Concrete Composite Wall-to-Wall Joints for Safety-Related Nuclear Facilities,” Ph.D. Dissertation, Purdue University, West Lafayette, IN.

Seo, J. and Varma, A.H. (2015), “Behaviour and Design of Corner or L-Joints in SC Walls,” *Transactions of the 23rd International Association for Structural Mechanics in Reactor Technology Conference, SMiRT-23,* Paper ID 695, Manchester, UK, IASMIRT, North Carolina State University, Raleigh, NC.

Seo, J., Varma, A.H., Sener, K. and Ayhan, D. (2016), “Steel-Plate Composite (SC) Walls: In-Plane Shear Behavior, Database, and Design,” *Journal of Constructional Steel Research*, Vol. 119, pp. 202–215.

Seo, J. and Varma, A.H. (2017), “Experimental Behavior and Design of SC-to-RC Lap Splice Connections,” *Journal of Structural Engineering*, ASCE, Vol. 143, No. 5.

Song, X., Chu, M., Ge, H. and Wang, H. (2014), “A Failure Criterion for Steel-Concrete Composite Walls,” *Sustainable Development of Critical Infrastructure*, ASCE, pp. 324–331.

Takeuchi, M., Narikawa, M., Matsuo, I., Hara, K. and Usami, S. (1998), “Study on a Concrete Filled Structure for Nuclear Power Plants,” *Nuclear Engineering and Design*, Vol. 179, No. 2, pp. 209–223.

Takeuchi, M., Fujita, F., Funakoshi, A., Shohara, R., Akira, S. and Matsumoto, R. (1999), “Experimental Study on Steel Plate Reinforced Concrete Structure, Part 2: Response of SC Members Subjected to Out-of-Plane Load (Outline of the Experimental Program and the Results),” *Proceedings of the Annual Conference of Architectural Institute of Japan, (in Japanese)*, pp. 1,037–1,038.

Usami, S., Akiyama, H., Narikawa, M., Hara, K., Takeuchi, M. and Sasaki, N. (1995), “Study on a Concrete Filled Steel Structure for Nuclear Plants (Part 2). Compressive Loading Tests on Wall Members,” *Transactions of the 13th International Structural Mechanics in Reactor Technology Conference, SMiRT-13*, Porto Alegre, Brazil, IASMART, North Carolina State University, Raleigh, NC, pp. 21–26.

Varma, A.H. (2000), “Seismic Behavior, Analysis and Design of High Strength Square Concrete Filled Tube (CFT) Columns,” Ph.D. Dissertation, Lehigh University, Bethlehem, PA.

Varma, A.H., Malushte, S.R., Sener, K.C. and Booth, P.N. (2009), “Analysis and Design of Modular Composite Walls for Combined Thermal and Mechanical Loadings,” *Transactions of the 20th International Association for Structural Mechanics in Reactor Technology Conference*, *SMiRT-20*, Div. TS 6 Paper 1820, Espoo, Finland, IASMART, North Carolina State University, Raleigh, NC.

Varma, A.H., Malushte, S.R., Sener, K.C., Booth, P.N. and Coogler, K. (2011a), “Steel-Plate Composite (SC) Walls: Analysis and Design including Thermal Effects,” *Transactions of the 21st International Association for Structural Mechanics in Reactor Technology Conference*, *SMiRT-21*, Div. X, Paper 761, New Delhi, India, IASMART, North Carolina State University, Raleigh, NC.

Varma, A.H., Malushte, S.R., Sener, K. and Lai, Z. (2011b), “Steel-Plate Composite Walls for Safety Related Nuclear Facilities: Design for Combined In-Plane and Out-of-Plane Demands,” *Transactions of the 21st International Association for Structural Mechanics in Reactor Technology Conference, SMiRT-21*, Paper ID 760, New Delhi, India, IASMART, North Carolina State University, Raleigh, NC.

Varma, A.H., Sener, K.C., Zhang, K., Coogler, K. and Malushte, S.R. (2011c), “Out-of-Plane Shear Behavior of SC Composite Structures,” *Transactions of the 21st International Association for Structural Mechanics in Reactor Technology Conference, SMiRT-21,* New Delhi, India, IASMART, North Carolina State University, Raleigh, NC.

Varma, A.H., Seo, J., Chi, H. and Baker, T. (2011d), “Behavior of SC Wall Lap Splice Anchorages,” *Transactions of the 21st International Association for Structural Mechanics in Reactor Technology Conference, SMiRT-21*, Paper ID 765, New Delhi, India, IASMART, North Carolina State University, Raleigh, NC.

Varma, A.H., Zhang, K., Chi, H., Booth, P.N. and Baker, T. (2011e), "In-Plane Shear Behavior of SC Walls: Theory vs. Experiment," *Transactions of the 21st International Association for Structural Mechanics in Reactor Technology Conference*, *SMiRT-21*, Div. X, Paper 761, New Delhi, India, IASMART, North Carolina State University, Raleigh, NC.

Varma, A.H., Zhang, K. and Malushte, S.R. (2013), "Local Buckling of SC Composite Walls at Ambient and Elevated Temperatures," *Transactions of the 22nd International Conference on Structural Mechanics in Reactor Technology, SMiRT-22*, San Francisco, CA, IASMART, North Carolina State University, Raleigh, NC.

Varma, A.H., Malushte, S.R., Sener, K.C. and Lai, Z. (2014), "Steel-Plate Composite (SC) Walls for Safety Related Nuclear Facilities: Design for In-Plane Forces and Out-of-Plane Moments," *Nuclear Engineering and Design*, Special Issue on SMiRT-21 Conference, Vol. 269, pp. 240–249.

Varma, A.H., Malushte, S.R. and Lai, Z. (2015), "Modularity and Innovation Using Steel-Plate Composite (SC) Walls for Nuclear and Commercial Construction," *Proceedings of the 11th International Conference on Advances in Steel-Concrete Composite Structures (ASCCS)*, Beijing, China.

Yan J.B., Liew J.Y.R., Qian, X.D. and Wang J.Y. (2015), "Ultimate Strength Behavior of Curved Steel-Concrete-Steel Sandwich Composite Beams," *Journal of Constructional Steel Research*, Vol. 115, pp. 316–328.

Yan, J.B., Xiong, M., Qian, X.D. and Liew, J.Y.R. (2016), "Numerical and Parametric Study of Curved Steel-Concrete-Steel Sandwich Composite Beams under Concentrated Loading," *Materials and Structures*, Vol. 49, Issue 10, pp. 3,981–4,001.

Zhang, K. (2014), "Axial Compression Behavior and Partial Composite Action of SC Walls in Safety-Related Nuclear Facilities," Ph.D. Dissertation, Purdue University, West Lafayette, IN.

Zhang, K., Varma, A.H., Malushte, S.R. and Gallocher, S. (2014), "Effect of Shear Connectors on Local Buckling and Composite Action in Steel Concrete Composite Walls," *Journal of Nuclear Engineering and Design*, Special Issue on SmiRT-21 Conference, Vol. 269, pp. 231–239.

There’s always a solution in steel.

American Institute of Steel Construction

312.670.2400 www.aisc.org